UNIVERSITY OF SOUTHAMPTON

FACULTY OF NATURAL AND ENVIRONMENTAL SCIENCES

Ocean and Earth Science

Volume 1 of 1

Coupling of the Cryosphere and Ocean During Intervals of Rapid Climate Change in the Palaeo Record: A Multi-Proxy Study of the Heinrich Events of the Last Glacial from the Northeast Atlantic

by

Anya Jane Crocker

Thesis for the Doctor of Philosophy

August 2013

UNIVERSITY OF SOUTHAMPTON

ABSTRACT

FACULTY OF NATURAL AND ENVIRONMENTAL SCIENCES
Ocean and Earth Science

Doctor of Philosophy

COUPLING OF THE CRYOSPHERE AND OCEAN DURING INTERVALS OF RAPID CLIMATE CHANGE IN THE PALAEO RECORD: A MULTI-PROXY STUDY OF THE HEINRICH EVENTS OF THE LAST GLACIAL FROM THE NORTHEAST ATLANTIC

by Anya Jane Crocker

Determining the response of the global thermohaline circulation to freshwater perturbations is of vital importance for future climate modelling efforts. The Heinrich events of the last glacial provide classic case studies, with major episodic inputs of freshwater associated with large numbers of icebergs flooding the North Atlantic Ocean. Climate modelling experiments and proxy reconstructions have both indicated a significant decrease in the strength of the meridional overturning circulation in response to this fresh water input to the ocean during each Heinrich event. Here, I present high resolution, multi-proxy reconstructions of cryospheric and surface and deep ocean behaviour over the last 40,000 years from Ocean Drilling Project (ODP) Site 980 in the northeast Atlantic, incorporating Heinrich events 1 to 4. Oxygen, carbon and neodymium isotope reconstructions of bottom water chemistry show a unique signature at this site for every Heinrich event, indicating the influence of a different water mass during each event. Bulk sediment leachate neodymium isotope values are strongly offset towards more radiogenic values than both planktonic foraminifera and fish debris throughout the Holocene, however, the agreement between the substrates is much closer under glacial conditions. This observed offset is attributed to modification of the leachate signal by fine material transported by strengthened bottom current activity in the Holocene, suggesting that bulk sediment leachates may not always record bottom water chemistry faithfully at sediment drift sites. Rare earth element profiles suggest that foraminifera without their ferromanganese coatings removed do not undergo significant diagenetic modification in the sediment, making these a better choice for reconstructions of bottom water neodymium isotope signatures. Each Heinrich event shows a different sequence of changes in the lithologies of ice-rafted debris, which argues against a simple repeating pattern of ice sheet destabilisation at each Heinrich event. The high degree of spatial variability in IRD patterns between sites in close proximity, however, suggests that surface ocean properties and circulation likely exerted a strong control over the IRD flux records, and hence the phasing of the circum-Atlantic ice sheets cannot be simply deduced from any single sedimentary record. Evidence of perturbation in bottom water properties can be seen prior to the deposition of the main ice-rafted debris layer during some of the Heinrich events at Site 980, suggesting that circulation changes may have played a role in the destabilisation of ice sheets, though the nature of these precursor changes differs between events. These findings show that Heinrich events are not simple, repeating events. Instead, differences in fresh water input and in surface ocean properties and circulation between Heinrich events likely give rise to different patterns of mid-depth North Atlantic circulation. The observed contrasts in bottom water chemistry at Site 980 between different Heinrich events highlights the sensitivity of the overturning circulation to fresh water inputs and argues against a simplistic model of thermohaline circulation cessation at each Heinrich event.

Contents

List of tables

List of figures

Chapter 1

Chapter 2

DECLARATION OF AUTHORSHIP

I, Anya Jane Crocker

declare that the thesis entitled

Coupling of the Cryosphere and Ocean During Intervals of Rapid Climate Change in the Palaeo Record: A Multi-Proxy Study of the Heinrich Events of the Last Glacial from the Northeast Atlantic

and the work presented in the thesis are both my own, and have been generated by me as the result of my own original research. I confirm that:

- this work was done wholly or mainly while in candidature for a research degree at this University;
- where any part of this thesis has previously been submitted for a degree or any other qualification at this University or any other institution, this has been clearly stated;
- where I have consulted the published work of others, this is always clearly attributed;
- where I have quoted from the work of others, the source is always given. With the exception of such quotations, this thesis is entirely my own work;
- I have acknowledged all main sources of help;
- where the thesis is based on work done by myself jointly with others, I have made clear exactly what was done by others and what I have contributed myself;
- none of this work has been published before submission,

Signed: ……..

Date:…….

Acknowledgements

I would like to thank my supervisor Prof. Heiko Pälike and for this guidance and support, and for giving me the freedom to pursue my research in whatever direction it took me. I owe a huge debt of gratitude to Prof. Paul Wilson and Dr. Ian Bailey for giving me the opportunity to work on this exciting project, and for many productive discussions and insightful comments. I would also like to thank Prof. Eelco Rohling for giving me the opportunity to begin my career in scientific research. Gratitude also goes to the Integrated Ocean Drilling Program and the captain, crew and scientists of ODP Leg 162 for the acquisition and provision of sample material.

This work would not have been possible without the help of a large number of people, to whom I am greatly indebted. Megan Spencer provided invaluable laboratory assistance and moral support. The expertise of Dr. Marcus Gutjahr gave me the opportunity to undertake the geochemical work presented here, which has greatly enriched this thesis. Many stimulating and fruitful discussions were had with Tom Chalk, who is also thanked for sharing his research findings as they developed. Critical laboratory assistance was provided by Mike Bolshaw, Dr. Matt Cooper, Dr. Andy Milton and Dave Spanner, without which this study would not have been possible.

My time in Southampton has been greatly enriched by many of the people I have met here. I would like to thank the members of the palaeoceanography and palaeoclimate research group for many interesting and informative discussions, and for making the lab an enjoyable place to be. Special thanks go to my office mates Helen Griffin, Joe Stewart and Fred Le Moigne for providing support, inspiration and entertainment. I am also grateful to my housemates for their much valued friendship and encouragement, namely Catriona Menzies, Sarah Taws, Steve Hollis, Alex Webber, Grant Duffy, Michael Henehan, Jen Rutter, Gemma Smith and Mike Cassidy.

Finally, I would like to thank my family for all of their unconditional love and support. This thesis would not have been possible without them.

This studentship was funded by National Environment Research Council grant NE/D005728/2.

Commonly used abbreviations

AABW	Antarctic Bottom Water
AAIW	Antarctic Intermediate Water
AMOC	Atlantic Meridional Overturning Circulation
AMS	Accelerator Mass Spectrometry
B-A	Bølling-Allerød
BIIS	British and Irish Ice Sheet
CHUR	Chondritic Uniform Reservoir
D-O	Dansgaard-Oeschger
DC	Detrital Carbonate
DSOW	Denmark Strait Overflow Water
ENAW	Eastern North Atlantic Water
FMAZ	Faeroe Marine Ash Zone
FBC	Faeroe-Bank Channel
FSC	Faeroe-Shetland Channel
FIS	Fennoscandian Ice Sheet
GAABW	Glacial Antarctic Bottom Water
GAAIW	Glacial Antarctic Intermediate Water
GI	Greenland Interstadial
GIN	Greenland, Iceland and Norwegian
GIS	Greenland Ice Sheet
GNAIW	Glacial North Atlantic Intermediate Water
GRAPE	Gamma Ray Attenuation Porosity Evaluation
GS	Greenland Stadial
H-	Heinrich
HREE	Heavy Rare Earth Elements
IIS	Icelandic Ice Sheet
InIS	Innuitian Ice Sheet
IRD	Ice-Rafted Debris
ISOW	Iceland-Scotland Overflow Water

LIS	Laurentide Ice Sheet
LGM	Last Glacial Maximum
LREE	Light Rare Earth Elements
LSW	Labrador Sea Water
MAD	Moisture and Density
mbsf	Metres below seafloor
mcd	Metres composite depth
MIS	Marine Isotope Stage
MOW	Mediterranean Overflow Water
MREE	Middle Rare Earth Elements
NAC	North Atlantic Current
NADW	North Atlantic Deep Water
NEADW	North East Atlantic Deep Water
NGRIP	North Greenland Ice Core Project
Nps	*Neogloboquadrina pachyderma* (sinistral)
NSAIW	Norwegian Sea Intermediate Water
NSDW	Norwegian Sea Deep Water
NWEIS	North West European Ice Sheet
ODP	Ocean Drilling Program
PAAS	Post-Archean Australian Shale
pISOW	Pure Iceland-Scotland Overflow Water
REE	Rare Earth Element
rpm	Rotations per minute
SAIW	Subarctic Intermediate Water
SBIS	Svalbard-Barents Ice Sheet
SPMW	Subpolar Mode Water
SST	Sea Surface Temperature
WTOW	Wyville-Thomson Ridge Overflow Water
WTR	Wyville-Thomson Ridge
YD	Younger Dryas

This thesis is dedicated to my family
for their unwavering love and support

Chapter 1
Introduction

1.1 Patterns of past climate variability

In order to better understand how Earth's climate may change in the future in response to increasing anthropogenic greenhouse gas emissions, it is important to decipher how climate has varied in the past. In this way, we aim to improve our knowledge of what the Earth System is capable of naturally, the feedbacks within the system and the processes responsible for driving the observed variability. Targeting research towards specific intervals with relevance to predicted future climate, for example, intervals of rapid change, elevated carbon dioxide levels, or major ice sheet destabilisation can be particularly advantageous.

Beyond the instrumental records of the past few centuries, we do not have direct measurements of temperature changes and many other climatic variables. We turn, therefore, to proxy records to reconstruct parameters of interest instead. Numerous processes in the modern Earth System have been shown to vary in a predictable manner with climatic parameters. A range of biotic, geochemical and sedimentological techniques are among those proving successful for reconstructions. If it is assumed that the same relationship between the proxy variable and the climatic variable of interest persisted back in time, and the proxy signature is faithfully preserved, then these proxy records can be used to reconstruct past climate change.

Over the past few decades, the number of climatic proxy reconstructions has increased dramatically. A wide range of archives have been exploited, including marine and lacustrine sediments, ice cores, speleothems, tree rings and corals. These records have revealed a highly dynamic system, with distinct patterns of variability observed over different timescales (illustrated in figure 1.1). A wide range of processes have been invoked to explain the observed patterns in climate reconstructions, however, as yet, not all of these are fully understood.

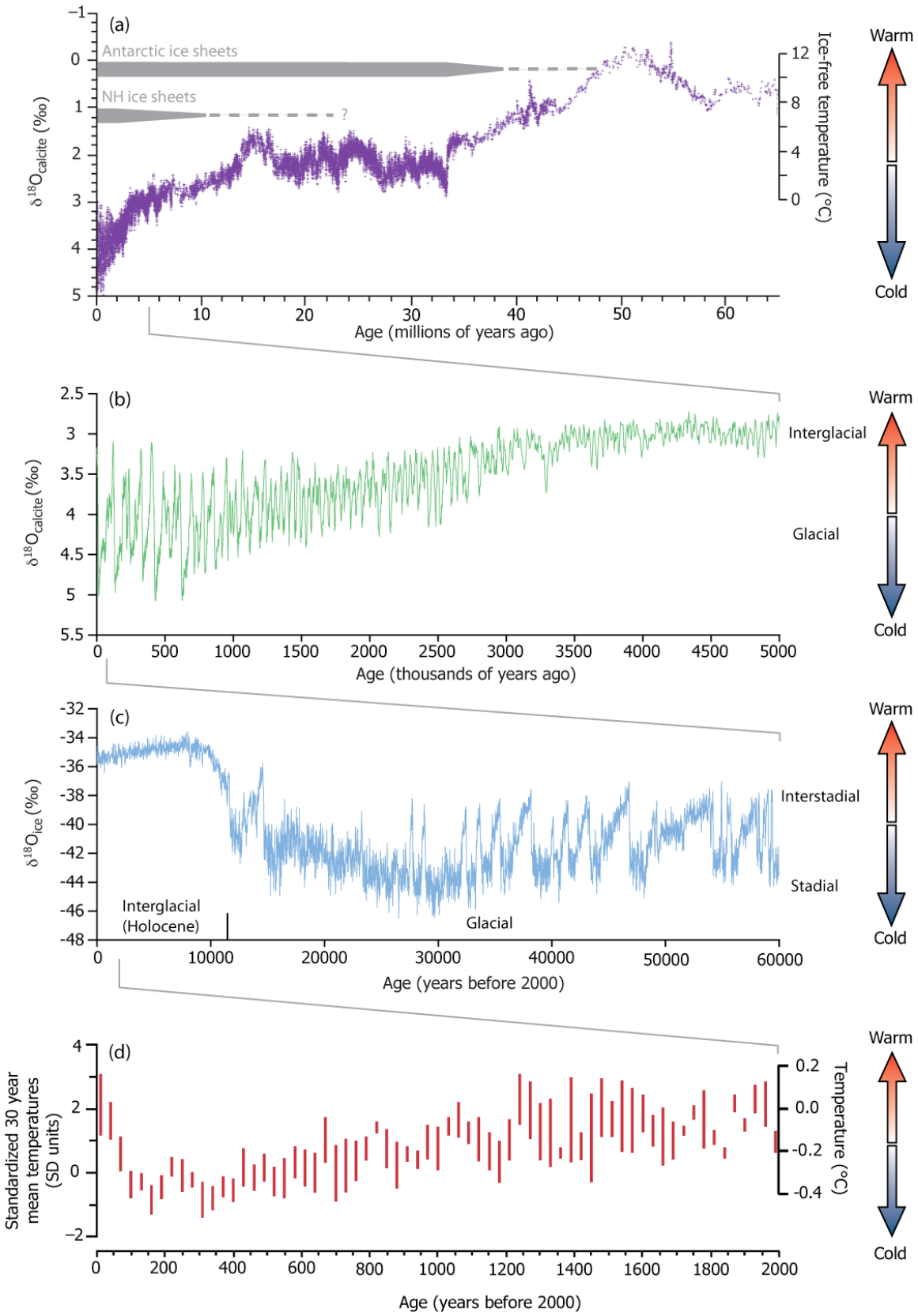
(a)
Antarctic ice sheets
NH ice sheets
?
δ18Ocalcite (‰)
Ice-free temperature (°C)
Age (millions of years ago)
Warm
Cold
(b)
δ18Ocalcite (‰)
Interglacial
Glacial
Age (thousands of years ago)
Warm
Cold
(c)
δ18Oice (‰)
Interstadial
Stadial
Interglacial (Holocene)
Glacial
Age (years before 2000)
Warm
Cold
(d)
Standardized 30 year mean temperatures (SD units)
Temperature (°C)
Age (years before 2000)
Warm
Cold

Figure 1.1: Proxy reconstructions of past climate variability over different timescales through the Cenozoic era. (a) Compilation of oxygen isotope signatures of benthic foraminiferal calcite over the past 65 Ma, from Zachos et al. [2008]. Low values indicate warmer bottom water temperatures and/or decreased global ice volume. Note that the temperature scale only applies for an ice-free world where variation in $\delta^{18}O$ is driven solely by temperature change. Grey bars indicate the growth of the Antarctic and Northern Hemisphere ice sheets, with narrower widths indicating partial or ephemeral ice sheets [Zachos et al. 2008]. (b) Compilation of measurements of the oxygen isotope composition of benthic foraminiferal calcite over the last 5 Ma, from Lisiecki and Raymo [2005]. The record is marked by higher frequency variation between cold glacial and warmer interglacial conditions, superimposed on a longer term cooling trend. (c) Oxygen isotopic signature of ice from the NGRIP ice core spanning the last 60 ka [North Greenland Ice Core Project Members et al. 2004]. Warmer atmospheric temperatures correlate with less negative $\delta^{18}O_{ice}$ values. Strong variability between cold stadial and milder interstadial conditions can be seen through much of the glacial interval, with significantly more stable temperatures in the Holocene. (d) Standardized 30-year-mean temperatures, expressed in standard deviation units through the last 2000 years, averaged across 7 continental-scale regions (bars show the twenty-fifth to seventy-fifth unweighted percentiles) [from PAGES 2k consortium 2013]. Temperature scale on the right axis is determined by comparison to the HadCRUT4 instrumental time series [Jones et al. 2012; PAGES 2k

Global temperatures have been dominated by a gradual cooling trend over the last 50 million years, with the progressive growth of polar ice sheets, first on Antarctica, and then in the northern hemisphere as temperatures decrease, illustrated in figure 1.1(a) [e.g. Emiliani 1954; Miller et al. 1987; Lear et al. 2000; Zachos et al. 2001]. Many of the processes suggested as drivers of these long-term trends are tectonic in origin, including opening and closing of oceanic gateways, volcanic and metamorphic outgassing and continental weathering [e.g. Walker et al. 1981; Berner et al. 1983; Berner 1992; Haug and Tiedemann 1998; Scher and Martin 2006]. Superimposed on these gradational, million year trends are strong oscillations. These have specific frequencies, with 400 kyr, 100 kyr, 41 kyr, 23 kyr and 19 kyr the most distinctive, and are attributed to subtle

variations in the Earth's orbit around the sun [Hays et al. 1976; Berger 1988; Laskar et al. 2004]. Evidence of this orbital-driven variability has been found across a range of timescales [e.g. Van Houten 1964; Olsen 1986; Crowley and Kim 1994; Lourens et al. 2005; Pälike et al. 2006], and can clearly be seen superimposed over the gradual cooling trend of the past 5 Ma in figure 1.1(b) [Lisiecki and Raymo 2005]. Climatic variability over the past 800,000 years is dominated by alternation of temperatures between cold (glacial) and warm (interglacial) states, with a periodicity of approximately 100 kyr. It has been suggested that glacial-interglacial variability in the latest Pleistocene is either paced or driven by the 100 kyr eccentricity cycle [e.g. Shackleton et al. 1988; Berger and Jansen 1994; Maslin and Ridgwell 2005], although pacing of the glacial terminations by the 41 kyr obliquity cycle has also been proposed [Huybers and Wunsch 2005].

Strong sub-orbital variability is visible in records of glacial climate, with surface temperatures alternating between two distinct states: mild interstadial and cold stadial intervals [Broecker et al. 1985; Bond et al. 1993; Dansgaard et al. 1993; Voelker 2002]. These two states are clearly expressed in the North Greenland Icecore Project (NGRIP) record of the last glacial interval, illustrated in figure 1.1(c) [North Greenland Ice Core Project Members et al. 2004]. Millennial scale climatic oscillations have been preserved in numerous archives, including ocean sediments [Heinrich 1988; Bond et al. 1992; Bond and Lotti 1995], Greenland ice cores [Johnsen et al. 1992; Dansgaard et al. 1993], pollen [Grimm et al. 1993; Sánchez-Goñi et al. 2000; Harrison and Sánchez-Goñi 2010] and speleothem records [Bar-Matthews et al. 1997; Genty et al. 2003]. Stadial-interstadial variability is best documented in the North Atlantic region, however similar variability has been observed at numerous locations across the globe [e.g. Broecker and Hemming 2001; Voelker 2002].

The transitions from stadial to interstadial conditions are extremely rapid, and are followed by a more gradual cooling into the next stadial interval. These cycles are known as Dansgaard-Oeschger events, and, in general, are spaced by a period of 1470 years ± 20%, or a multiple of this [Schulz 2002]. Greenland ice cores record warmings

of 10–15°C occur in over a period of decades [Grootes et al. 1993; Lang et al. 1999; Johnsen et al. 2001], with fluctuations in North Atlantic sea surface temperatures of 3–10°C believed to occur synchronously [Bond et al. 1993; Elliot et al. 2002; Hall et al. 2011]. Dansgaard-Oeschger events group into longer cooling cycles with asymmetrical saw-tooth shapes, known as Bond cycles, each typically spanning 10–15 kyr [Bond et al. 1993]. The end of each of these cycles is marked by a Heinrich event, with a dramatic increase in the amount of ice-rafted debris (IRD) deposited in the North Atlantic [Heinrich 1988; Bond et al. 1992; Broecker et al. 1992]. There is little to distinguish Heinrich events from non-Heinrich stadials in the ice core record [Rahmstorf 2002; Heinrich Events: Land Ice and Ocean Workshop 2012]. However, Heinrich events are much more distinctive in the sediments of the North Atlantic Ocean, with concentrations (and fluxes) of IRD significantly elevated above other stadial intervals, particularly in a distinctive band across the North Atlantic [Ruddiman 1977; Bond et al. 1992; Hemming 2004]. This IRD-rich horizon is known as a 'Heinrich layer'. A simplified illustration of climatic variability during Bond cycles, Dansgaard-Oeschger and Heinrich events is shown in figure 1.2.

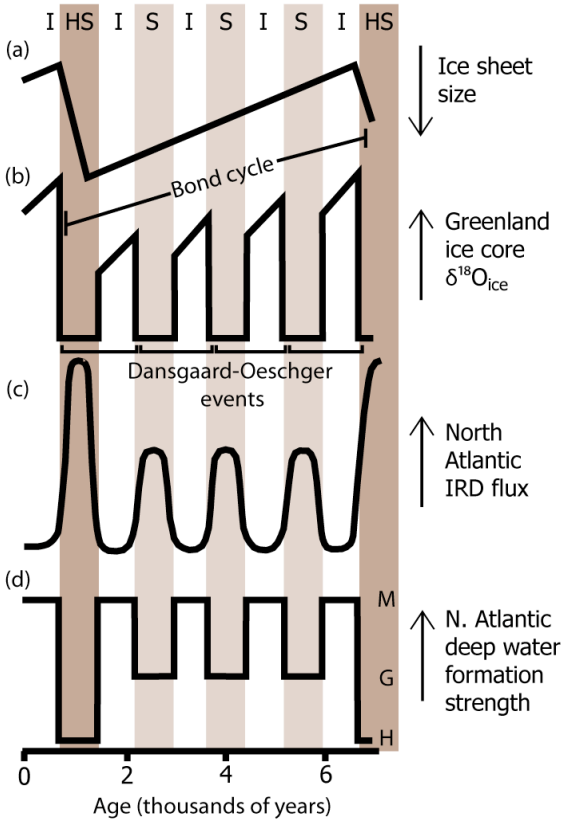

Figure 1.2: Simplified illustration of Dansgaard-Oeschger and Heinrich variability, showing typical interstadial (I), stadial (S) and Heinrich stadial (HS) conditions. (a) Northern hemisphere ice sheet size, from Alley [1998] (note inverted axis). (b) Idealised Greenland ice $\delta^{18}O$ values, with low values during stadials indicating cold atmospheric temperatures [based upon Grootes et al. 1993; Alley 1998; North Greenland Ice Core Project Members et al. 2004]. (c) Flux of ice-rafted debris recorded in North Atlantic sediment cores [e.g. Heinrich 1988; Bond and Lotti 1995; Elliot et al. 1998]. (d) Strength of overturning circulation in the North Atlantic, switching between three modes: M: modern/warm, G: glacial/cold, H: Heinrich/off [Alley et al. 1999; Rahmstorf 2002].

Many annual to centennial processes also act to modulate climate over regional to global scales. These include solar activity, internal climate oscillations (such as the El Niño Southern Oscillation and the North Atlantic Oscillation) and greenhouse gas emissions (including volcanic and anthropogenic sources) [e.g. Bray 1971; Rasmusson and Wallace 1983; Hurrell 1995; Tett et al. 1999; Bond et al. 2001; Moy et al. 2002; Hegerl et al. 2003; Solomon et al. 2007]. These shorter term processes contribute to the variability in the climate of the past 2,000 years observed in figure 1.1(d).

1.2 Project Rationale

Heinrich events provide excellent case studies to better understand the coupling between the ocean and cryosphere, in particular, the response of the Atlantic meridional overturning circulation (AMOC) to the addition of fresh water associated with rapid change in the cryosphere. This has become a crucial area of research, particularly in the context of the rapid, anthropogenically driven change already documented in the polar regions [Lemke et al. 2007, and references therein].

Ocean Drilling Program (ODP) Site 980 is a classic site in the study of North Atlantic climate evolution. Together with its partner site ODP Site 981, the recovered sediments provide an archive of climatic variability through the Pleistocene and into the Pliocene,

providing excellent records of centennial to orbital scale variability, spanning the growth and evolution of the ice sheets of the northern hemisphere [e.g. Oppo et al. 1998; Mc Intyre et al. 1999; McManus et al. 1999; Flower et al. 2000; Oppo et al. 2001; Draut et al. 2003; Raymo et al. 2004; Becker et al. 2006; Oppo et al. 2006; Marino et al. 2011]. Part of the reason why Site 980 has proven to be such a valuable climatic archive is its location within the Feni Drift sediment deposit [Jones et al. 1970; van Weering and de Rijk 1991]. Sediment drifts commonly have accumulation rates elevated above comparable sites at similar water depths [e.g. McCave and Tucholke 1986; Hollister 1993; Wold 1994; Knutz 2008], and therefore have the potential to provide palaeoclimatic records with high temporal resolution. These benefits were exploited in a classic study of climate evolution by McManus et al. [1999], who produced palaeoceanographic reconstructions of the last 500,000 years from Site 980 to demonstrate that millennial scale climatic variability increases dramatically when global ice volume exceeds a critical threshold. However, the published record of the last glacial is of relatively low resolution [McManus et al. 1999], and cannot clearly resolve suborbital climate variability. Revisiting this time interval, therefore, has the potential to provide significant new insights. Understanding the dynamics of the most recent glacial interval can have important implications for the interpretation of longer timescale climatic reconstructions, hence data generated from some of the youngest sediments recovered at Site 980 have the potential to aid research efforts over the Pleistocene and Pliocene.

Strong variability in bottom water properties has previously been inferred at Site 980 for the last glacial through the use of neodymium isotopes, and attributed to melt water release during Heinrich events [Crocket et al. 2011]. However, the stratigraphy of this section of the core is poor, with the position of the Heinrich IRD layers not yet established to prove that the two phenomena are linked. Site 980 is located at the edge of the belt of major ice-rafted debris deposition in the North Atlantic during the last glacial interval [Ruddiman 1977]. Therefore, distinctive peaks in IRD fluxes are expected at each Heinrich event (including the presence of Laurentide Ice Sheet derived detrital carbonate grains at H1, H2 and H4), making the identification of the Heinrich layer

much less ambiguous [Heinrich 1988; Bond et al. 1992; Hemming 2004]. This is particularly important, as the term 'Heinrich event' is not well defined. The IRD layer forms part of a longer, more complex event [e.g. Gutjahr and Lippold 2011; Stanford et al. 2011 etc.], so it is vital to clarify exactly which part of the event is referred to, particularly if comparing records from different locations. Identification of the Heinrich layer permits the relative phasing of changes in other components of the Earth System to be identified, increasing our understanding of both the mechanism responsible for Heinrich event generation and the response of the ocean to the addition of icebergs and associated fresh water release. The high sedimentation rate at Site 980 also results in a clearer expression of any temporal offsets between the proxy records.

The North Atlantic is one of the most significant sites globally for convection and deep water formation, hence changes in this region have a wide ranging influence. Labrador Sea Water, overflows from the Nordic Seas, recirculating North East Atlantic Deep Water and Antarctic Bottom Water are all found in the Rockall Trough today [Ellett and Martin 1973; McGrath et al. 2012] and all play a role in the formation of North Atlantic Deep Water [Lacan and Jeandel 2005]. Site 980 is sensitive to changes in the strengths and properties of each of these water masses, making the site an ideal target to monitor temporal variations in the vigour of deep water formation in the North Atlantic.

It has been suggested that a significant reduction in the vigour of the overturning thermohaline circulation of the ocean occurs as a result of fresh water addition during Heinrich events, with the cessation of regional deepwater formation in the North Atlantic reducing ocean ventilation and allowing southern sourced waters to penetrate further northwards and to shallower depths [e.g. Keigwin and Lehman 1994; Sarnthein et al. 1995; Seidov et al. 1996; Ganopolski and Rahmstorf 2001; McManus et al. 2004; Hall et al. 2006; Stanford et al. 2006]. Site 980 is located at a water depth close to the postulated glacial boundary between northern and southern sourced waters, estimated as 2 to 2.8 km water depth (figure 1.3) [e.g. Boyle and Keigwin 1987; Curry et al. 1988; Duplessy et al. 1988; Bertram et al. 1995; Curry and Oppo 2005; Marchitto and Broecker 2006; Meland et al. 2008; Yu et al. 2008]. The site is well situated, therefore,

to evaluate changes in the northwards extent of southern sourced waters and hence also assess the extent to which thermohaline circulation shutdown occurred at Heinrich events.

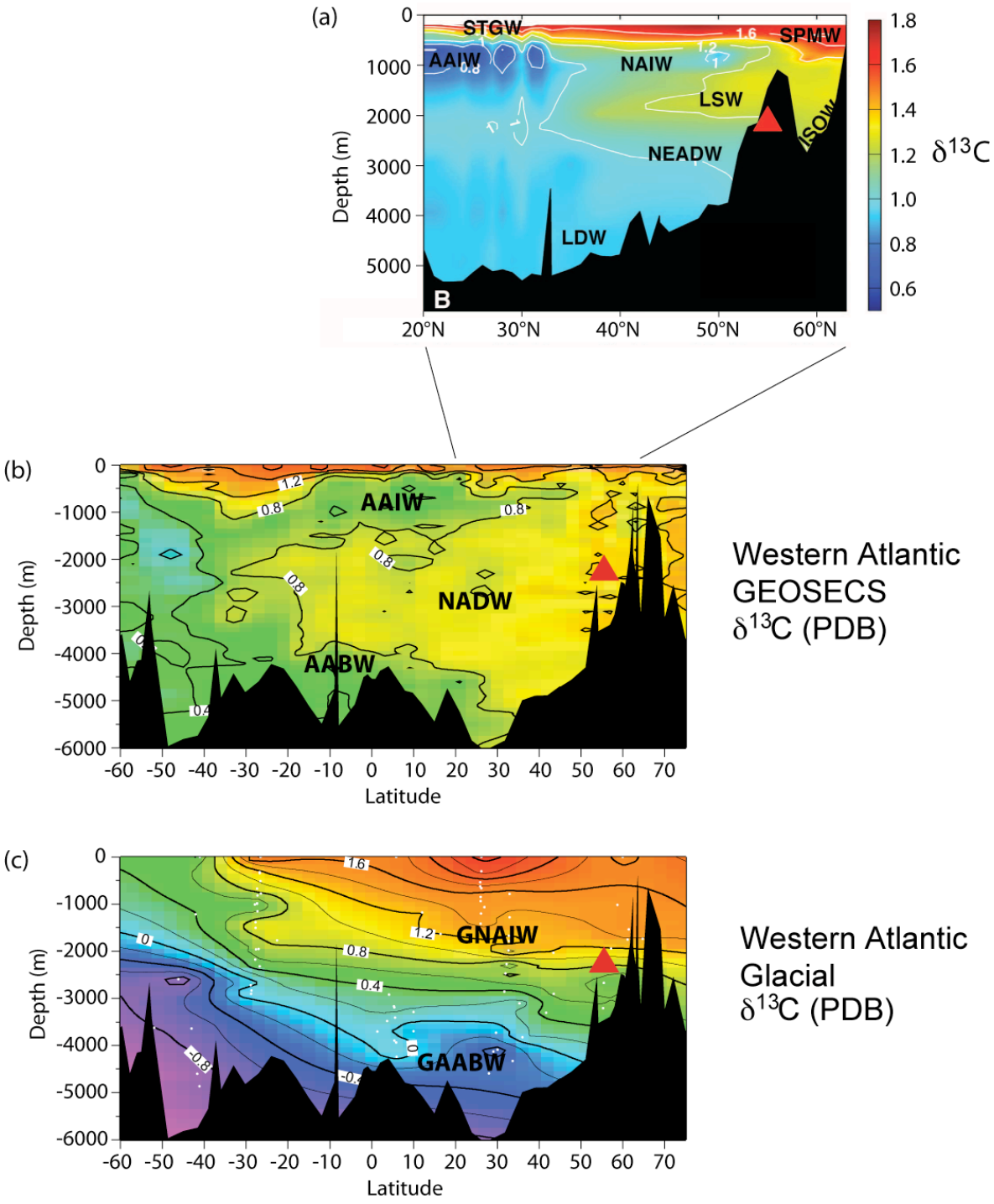

Figure 1.3: (a) Cross-section of the $\delta^{13}C$ of seawater total inorganic carbon in the pre-industrial North Atlantic, with modern values corrected for the Suess effect (the invasion of ^{12}C enriched anthropogenic carbon dioxide), from Olsen and Ninneman [2010]. (b) Modern western Atlantic ΣCO_2 $\delta^{13}C$ values from the GEOSECS expeditions [Kroopnick 1985], adapted from Curry and Oppo [2005]. (c) Western Atlantic glacial $\delta^{13}C$ values compiled from measurements on Cibicidoides and Planulina, adapted from Curry and Oppo [2005]. The position of ODP Site 980 is marked by a red triangle. Water mass abbreviations are STGW: Subtropical Gyre Water; SPMW: Subpolar Mode Water; AAIW: Antarctic Intermediate Water; NAIW: North Atlantic Intermediate Water; LSW: Labrador Sea Water; ISOW: Iceland-Scotland Overflow Water; NEADW: North East Atlantic Deep Water; LDW: Lower Deep Water; NADW: North Atlantic Deep Water; AABW: Antarctic Bottom Water, GNAIW: Glacial North Atlantic Intermediate Water; GAABW: Glacial Antarctic Bottom Water. Note the different colour scale of figure (a) compared to (b) and (c).

This thesis aims to investigate the sequence of changes in the cryosphere, surface and deep ocean occurring at Heinrich events in order to better understand both the mechanism responsible for their generation and the response of the system to the addition of fresh water. Reconstructing changes in water mass structure, including the presence or absence of southern sourced waters can help to understand the extent to which the vigour of the overturning circulation is reduced, and test the working hypothesis of a shutdown of the overturning circulation at Heinrich events. By producing a record spanning multiple Heinrich events at the same location, the natural repeatability of the Heinrich events can be assessed. Documenting and understanding the commonalities and distinguishing any differences among the Heinrich events will help to explore the sensitivity of the ocean system to the nature of the fresh water pulse and/or the pre-event conditions, thereby potentially shedding light on the key factors that determine the response of the ocean to a rapid input of fresh water.

1.3 Site location

ODP Site 980 is located at 55°29.1'N, 14°42.1'W in the Eastern North Atlantic, with a water depth of 2170 m [Shipboard Scientific Party 1996]. It is situated on the western edge of the Rockall Trough, which is located to the south of the Greenland-Scotland Ridge (illustrated in figure 1.4). The trough is bordered by the Irish continental margin to the east and the Rockall Plateau to the west. It deepens to the southwest, from a depth of ca. 1000 m in the north to >3000 m in the south as it connects to the main Atlantic basin. ODP Site 980 was drilled to recover sediments from the Feni Drift, which is a contourite deposit plastered against the eastern margin of the Rockall Plateau, with a development history strongly influenced by the activity of bottom currents [Jones et al. 1970; McCave and Tucholke 1986; van Weering and de Rijk 1991; Howe et al. 1994].

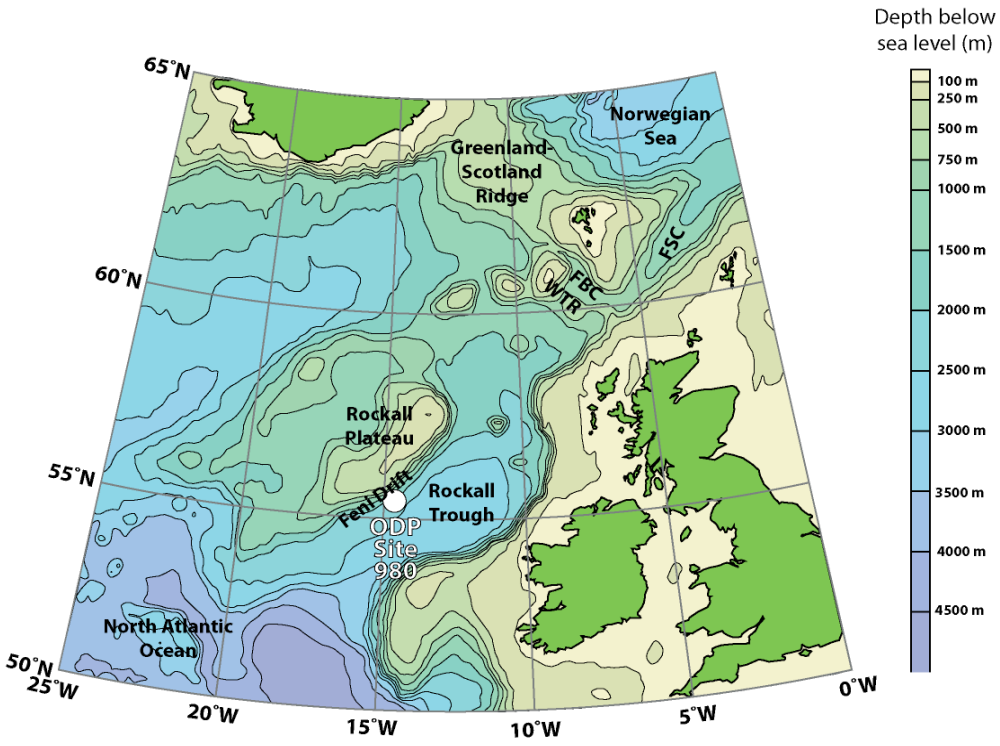

Figure 1.4: Location of ODP Site 980 (marked by a white circle). FSC: Faeroe-Shetland Channel, FBC: Faeroe-Bank Channel, WTR: Wyville-Thomson Ridge. Figure created using Ocean Data View [Schlitzer 2013].

Sediments recovered from ODP Site 980 form a continuous sequence dominated by clay and nannofossils, with smaller amounts of silt and foraminifera and including occasional coarser dropstones [Shipboard Scientific Party 1996]. Three holes (980A, 980B and 980C) were drilled at the site. This study uses samples from the top 10 metres composite depth (mcd), with a combination of samples from holes B (0.05–4.13 metres below seafloor, or mbsf) and A (0.32–4.08 mbsf) to produce a complete record spanning the last 40,000 years. Sedimentation rates through this section range from 0.06 to 0.84 m ka^{-1} and there are no known hiatuses in this section of the core.

1.4 Modern Oceanography

1.4.1 Major water masses of the Rockall Trough

Much of the upper water column (<1000 m depth) in the Rockall Trough consists of the relatively warm and saline Eastern North Atlantic Water (ENAW), a form of Subpolar Mode Water (SPMW). ENAW forms in the Bay of Biscay and travels northwards, becoming progressively fresher due to mixing from water masses from the west [Ellett and Martin 1973]. These waters are transported northwards into the Nordic Seas by branches of North Atlantic Current (NAC) [Hansen and Østerhus 2000]. Below this, small amounts of fresher Subarctic Intermediate Water (SAIW) and saline Mediterranean Overflow Water (MOW) are commonly documented in the southern parts of the Rockall Trough, at depths of approximately 600–1000 m and 800–1100 m respectively [Ullgren and White 2010; McGrath et al. 2012], although neither water mass is believed to directly influence ODP site 980 at the present day.

Labrador Sea Water (LSW) formed by deep winter mixing in the Labrador Basin circulates in the modern Rockall Trough at depths of 1500–2000 m [Ellett and Martin 1973]. The properties of this water mass strongly depend on the influence of local climate upon the convective regime where it is formed [Clarke and Gascard 1983; Yashayaev et al. 2007]. Below the LSW layer (at depths of 2500–3000 m) is the more saline North East Atlantic Deep Water (NEADW). This is formed from a combination of

waters overflowing the Iceland-Scotland Ridge, southern-sourced Lower Deep Water, Labrador Sea Water and the shallower Modified North Atlantic Water [Swift 1984; Lacan and Jeandel 2005]. Both LSW and NEADW enter the trough from the southeast before circulating in a cyclonic gyre [New and Smythe-Wright 2001]. In the deepest parts of the basin, Antarctic Bottom Water (AABW) has been identified by its high dissolved silicate content. It is typically found at depths below 3000 m in the modern ocean, although its exact strength and position varies between years [McGrath et al. 2012]. The circulation of these major water masses in the North Atlantic is illustrated in figure 1.5.

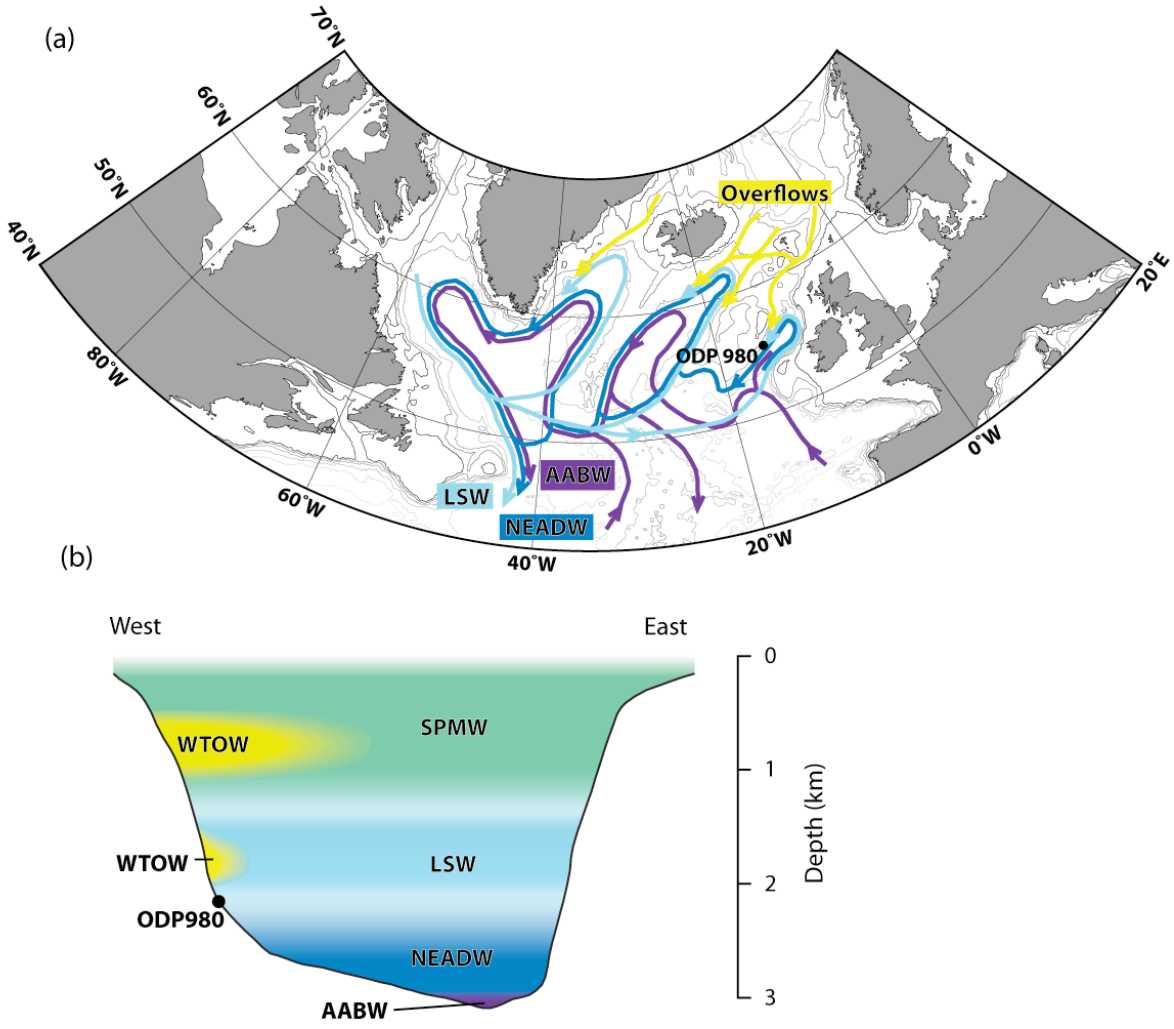

Figure 1.5: (a) Major intermediate and deep currents of the North Atlantic Ocean. (b) Schematic cross-section of the Rockall Trough indicating the major water masses at 55°N. Vertical exaggeration approximately x66. Based upon McCartney [1992], McCave et al. [1995], Hansen and Østerhus [2000], New and Smythe-Wright [2001] and Lacan and Jeandel [2005]. WTOW: Wyville-Thomson overflow water; SPMW: Subpolar mode water; LSW: Labrador Sea water; NEADW: Northeast Atlantic deep water; AABW: Antarctic bottom water.

1.4.2 Overflow waters from the Nordic Seas

The Greenland, Iceland and Norwegian (GIN) Seas are a major site of formation of cold, dense water in the modern ocean, as warmer surface waters are cooled by cold atmospheric temperatures and sink to greater depths via a variety of mechanisms in both the open ocean and along continental margins [e.g. Aagaard et al. 1985; Clarke et al. 1990; Mauritzen 1996; Marshall and Schott 1999]. These dense waters are separated from the main body of the Atlantic Ocean at depths below 840 m by the Greenland-Scotland Ridge. However, waters from the GIN Seas are able to flow southwards into the main Atlantic basin over the deeper parts of the ridge. Once on the southern side of the ridge, the high density of the overflow waters compared to the North Atlantic surface and intermediate water masses leads them to sink to greater depths and become a major contributor to North Atlantic Deep Water [e.g. Swift 1984].

There are several different pathways by which subsurface water masses from the GIN Seas are able to cross the Greenland-Scotland Ridge. The Denmark Strait, between Iceland and Greenland has a sill depth of approximately 620 m and east of Iceland, the sill depth is generally less than 500 m. Of the total flux of water entering the North Atlantic from the Nordic Seas, just over half (of a total of 5.6 Sv) passes through the Denmark Strait and into the Irminger Basin, with approximately 1 Sv directly overflowing the Iceland-Scotland Ridge. The remaining 1.5–2.4 Sv flows through the Faeroe-Shetland Channel to the west of the Faeroe Islands, where water depths exceed 800 m (overflow pathways shown in figure 1.5) [Hansen and Østerhus 2000; Olsen et al.

2008]. Most of the water flowing along this channel continues into the Faeroe Bank Channel and eventually drains into the Iceland Basin, however a small amount of water (approximately 0.3 Sv) overflows the Wyville-Thomson Ridge (which bounds the channel to the south) into the Rockall Trough [Sherwin and Turrell 2005; Olsen et al. 2008].

Pure overflow waters crossing the Wyville-Thomson Ridge are thought to consist of Norwegian Sea Arctic Intermediate Water (NSAIW) and/or Norwegian Sea Deep Water (NSDW) [Hansen and Østerhus 2000; Sherwin and Turrell 2005]. As these dense waters descend on the southern side of the Wyville-Thomson Ridge, they entrain the surrounding Eastern North Atlantic Water, increasing the total volume of the overflow waters from >0.2 Sv to a maximum estimate of 0.8–0.9 Sv [Sherwin et al. 2008]. The water mass formed by this process is known as Wyville-Thomson Overflow Water (WTOW) [Ellett and Roberts 1973], and travels southwards, flowing along the eastern edge of the Rockall Plateau, with WTOW traced to at least 55^{o}N in the North Atlantic, and sometimes beyond [Johnson et al. 2010].

Recent oceanographic transects place the main core of Wyville-Thompson Overflow Water in the Northern Rockall Trough at intermediate depths (600–1200 m), based upon its temperature, salinity and chemical properties [Johnson et al. 2010; McGrath et al. 2012]. The development of the Feni sediment drift has previously been attributed to rapidly flowing overflow waters [Jones et al. 1970; van Weering and de Rijk 1991], however, with a maximum crest height approximately 2100 m below sea level, the Feni Drift is located significantly below the core of modern WTOW. One possible explanation for this discrepancy is that the depth of the overflow waters has changed over time. Temporal variation in overflow behaviour has been observed over time scales from days to seasons to years [Dickson and Kidd 1986; Sherwin and Turrell 2005; Sherwin et al. 2008; Johnson et al. 2010]. Also, the strength of overflow water export is very likely to vary with regional climate over longer timescales for example, over glacial-interglacial cycles [e.g. Raymo et al. 2004; Yu et al. 2008] or linked to the development of the northern hemisphere ice sheets [e.g. Raymo et al. 1992; Henrich et

al. 2002]. Changes in the height of the Greenland-Scotland Ridge would also have had an impact on overflow strength [Wright and Miller 1996; Poore et al. 2006; Poore et al. 2011]. The Feni Drift formed over millions of years, with its inception in the Late Palaeogene or Early Neogene [Jones et al. 1970; Masson and Kidd 1986], therefore, the relief of the Feni Drift today may not necessarily be indicative of the modern circulation patterns.

Alternatively, the Feni Ridge may be shaped by extreme events, as proposed by Dickson and Kidd [1986]. A denser component of WTOW at depths below 1500 m has been identified in 12 of the 31 years between 1976 and 2006, in years both with and without the shallower WTOW core present [Johnson et al. 2010]. The deeper component is only found on the extreme west of the Rockall Trough, as a slope current, and may indicate a different pathway for WTOW, potentially associated with large overflow events [Johnson et al. 2010]. Such an event was documented by Sherwin and Turrell [2005], with WTOW forming as NSDW cascaded down the southern side of the Wyville-Thomson Ridge at a rate of 1.5–2.1 Sv and entrained ENAW, increasing the volume of the overflow water mass by a factor of three as it descended.

1.5 Thesis outline

Chapter 2 investigates changes in the surface ocean and deposition of ice-rafted debris in the northeast Atlantic during the last glacial interval. A new stratigraphy for ODP Site 980 is established by correlation of the percentages of the polar planktonic foraminiferal species *N. pachyderma* (s.) to a regional stratotype, supplemented by recalibrated, previously published radiocarbon ages of planktonic foraminifera. Fluxes of ice-rafted detrital carbonate grains provides a clear identification of the Heinrich IRD layers. Variability in the lithology of IRD both within and between Heinrich events and the ability of these changes to reconstruct phasing between ice sheets is considered. The implications of the sequence of changes in the flux and assemblage of both planktonic foraminifera and IRD for the mechanism by which Heinrich events are generated is also discussed.

Chapter 3 explores the use of neodymium isotopes as a proxy to reconstruct the provenance of water masses. New reconstructions of the neodymium isotope composition of planktonic foraminifera and fish debris at ODP Site 980 are presented and compared to previously published sediment leachates records from the same core [Crocket et al. 2011]. The fidelity of each of these substrates as a record of seawater neodymium isotopic composition is compared, with rare earth element distributions used to shed further light on the acquisition of the neodymium isotopic signature and its stability as samples become more deeply buried over time.

Chapter 4 investigates the changes in bottom water chemistry through the Heinrich events at ODP Site 980. The neodymium isotope data are combined with high resolution benthic carbon and oxygen isotope records to disentangle the influences of changing properties and/or provenance of the bottom waters. Comparison with the records of ice-rafted debris and *N. pachyderma* (s.) presented in chapter 2 allows the phasing between the different components of the Earth System at Heinrich events to be reconstructed. The sequence of changes in the cryosphere, and surface and deep ocean is used to evaluate the plausibility of some of the mechanisms responsible for Heinrich event generation, and assess the extent of thermohaline shutdown.

Finally, in chapter 5, the main conclusions of this thesis are summarised, and several suggestions for future research directions presented.

1.6 References

Aagaard, K., Swift, J. H., and Carmack, E. C., 1985, Thermohaline circulation in the Arctic Mediterranean Seas: Journal of Geophysical Research: Oceans, v. 90, p. 4833-4846.

Alley, R. B., 1998, Palaeoclimatology: Icing the North Atlantic: Nature, v. 392, p. 335-337.

Alley, R. B., Clark, P. U., Keigwin, L. D., and Webb, R. S., 1999, Making sense of millennial-scale climate change: Geophysical Monograph - American Geophysical Union, v. 112, p. 385-394.

Bar-Matthews, M., Ayalon, A., and Kaufman, A., 1997, Late Quaternary Paleoclimate in the Eastern Mediterranean Region from Stable Isotope Analysis of Speleothems at Soreq Cave, Israel: Quaternary Research, v. 47, p. 155-168.

Becker, J., Lourens, L. J., and Raymo, M. E., 2006, High-frequency climate linkages between the North Atlantic and the Mediterranean during marine oxygen isotope stage 100 (MIS100): Paleoceanography, v. 21, p. PA3002.

Berger, A., 1988, Milankovitch Theory and climate: Reviews of Geophysics, v. 26, p. 624-657.

Berger, W. H., and Jansen, E., 1994, Mid-Pleistocene climate shift - The Nansen connection, The Polar Oceans and Their Role in Shaping the Global Environment: Geophys. Monogr. Ser., Washington, DC, AGU, p. 295-311.

Berner, R. A., 1992, Weathering, plants, and the long-term carbon cycle: Geochimica et Cosmochimica Acta, v. 56, p. 3225-3231.

Berner, R. A., Lasaga, A. C., and Garrels, R. M., 1983, The carbonate-silicate geochemical cycle and its effect on atmospheric carbon dioxide over the past 100 million years: American Journal of Science, v. 283, p. 641-683.

Bertram, C. J., Elderfield, H., Shackleton, N. J., and MacDonald, J. A., 1995, Cadmium/Calcium and Carbon Isotope Reconstructions of the Glacial Northeast Atlantic Ocean: Paleoceanography, v. 10, p. 563-578.

Bond, G., Broecker, W., Johnsen, S., McManus, J., Labeyrie, L., Jouzel, J., and Bonani, G., 1993, Correlations between climate records from North Atlantic sediments and Greenland ice: Nature, v. 365, p. 143-147.

Bond, G., Heinrich, H., Broecker, W., Labeyrie, L., McManus, J., Andrews, J., Huon, S., Jantschik, R., Clasen, S., and Simet, C., 1992, Evidence for massive discharges of icebergs into the North Atlantic ocean during the last glacial period: Nature, v. 360, p. 245-249.

Bond, G., Kromer, B., Beer, J., Muscheler, R., Evans, M. N., Showers, W., Hoffmann, S., Lotti-Bond, R., Hajdas, I., and Bonani, G., 2001, Persistent Solar Influence on North Atlantic Climate During the Holocene: Science, v. 294, p. 2130-2136.

Bond, G. C., and Lotti, R., 1995, Iceberg Discharges into the North Atlantic on Millennial Time Scales During the Last Glaciation: Science, v. 267, p. 1005-1010.

Boyle, E. A., and Keigwin, L., 1987, North Atlantic thermohaline circulation during the past 20,000 years linked to high-latitude surface temperature: Nature, v. 330, p. 35-40.

Bray, J. R., 1971, Solar-Climate Relationships in the Post-Pleistocene: Science, v. 171, p. 1242-1243.

Broecker, W., Bond, G., Klas, M., Clark, E., and McManus, J., 1992, Origin of the northern Atlantic's Heinrich events: Climate Dynamics, v. 6, p. 265-273.

Broecker, W. S., and Hemming, S., 2001, Climate Swings Come into Focus: Science, v. 294, p. 2308-2309.

Broecker, W. S., Peteet, D. M., and Rind, D., 1985, Does the ocean-atmosphere system have more than one stable mode of operation?: Nature, v. 315, p. 21-26.

Clarke, R. A., and Gascard, J.-C., 1983, The Formation of Labrador Sea Water. Part I: Large-Scale Processes: Journal of Physical Oceanography, v. 13, p. 1764-1778.

Clarke, R. A., Swift, J. H., Reid, J. L., and Koltermann, K. P., 1990, The formation of Greenland Sea Deep Water: double diffusion or deep convection?: Deep Sea Research Part A. Oceanographic Research Papers, v. 37, p. 1385-1424.

Crocket, K. C., Vance, D., Gutjahr, M., Foster, G. L., and Richards, D. A., 2011, Persistent Nordic deep-water overflow to the glacial North Atlantic: Geology, v. 39, p. 515-518.

Crowley, T. J., and Kim, K.-Y., 1994, Milankovitch Forcing of the Last Interglacial Sea Level: Science, v. 265, p. 1566-1568.

Curry, W. B., Duplessy, J. C., Labeyrie, L. D., and Shackleton, N. J., 1988, Changes in the distribution of δ13C of deep water ΣCO2 between the Last Glaciation and the Holocene: Paleoceanography, v. 3, p. 317-341.

Curry, W. B., and Oppo, D. W., 2005, Glacial water mass geometry and the distribution of δ13C of ΣCO2 in the western Atlantic Ocean: Paleoceanography, v. 20, p. PA1017.

Dansgaard, W., Johnsen, S. J., Clausen, H. B., Dahl-Jensen, D., Gundestrup, N. S., Hammer, C. U., Hvidberg, C. S., Steffensen, J. P., Sveinbjörnsdottir, A. E., Jouzel, J., and Bond, G., 1993, Evidence for general instability of past climate from a 250-kyr ice-core record: Nature, v. 364, p. 218-220.

Dickson, R. R., and Kidd, R. B., 1986, Deep Circulation in the Southern Rockall Trough – The Oceanographic Setting of Site 610: Initial Reports of the Deep-Sea Drilling Project, v. 94, p. 1061-1074.

Draut, A. E., Raymo, M. E., McManus, J. F., and Oppo, D. W., 2003, Climate stability during the Pliocene warm period: Paleoceanography, v. 18, p. 1078.

Duplessy, J. C., Shackleton, N. J., Fairbanks, R. G., Labeyrie, L., Oppo, D., and Kallel, N., 1988, Deepwater source variations during the last climatic cycle and their impact on the global deepwater circulation: Paleoceanography, v. 3, p. 343-360.

Ellett, D. J., and Martin, J. H. A., 1973, The physical and chemical oceanography of the Rockall channel: Deep Sea Research and Oceanographic Abstracts, v. 20, p. 585-625.

Ellett, D. J., and Roberts, D. G., 1973, The overflow of Norwegian Sea Deep Water across the Wyville-Thomson Ridge: Deep Sea Research and Oceanographic Abstracts, v. 20, p. 819-835.

Elliot, M., Labeyrie, L., Bond, G., Cortijo, E., Turon, J.-L., Tisnerat, N., and Duplessy, J.-C., 1998, Millennial-Scale Iceberg Discharges in the Irminger Basin During the Last Glacial Period: Relationship with the Heinrich Events and Environmental Settings: Paleoceanography, v. 13, p. 433-446.

Elliot, M., Labeyrie, L., and Duplessy, J.-C., 2002, Changes in North Atlantic deep-water formation associated with the Dansgaard-Oeschger temperature oscillations (60-10 ka): Quaternary Science Reviews, v. 21, p. 1153-1165.

Emiliani, C., 1954, Temperatures of Pacific Bottom Waters and Polar Superficial Waters during the Tertiary: Science, v. 119, p. 853-855.

Flower, B. P., Oppo, D. W., McManus, J. F., Venz, K. A., Hodell, D. A., and Cullen, J. L., 2000, North Atlantic Intermediate to Deep Water Circulation and Chemical Stratification During the Past 1 Myr: Paleoceanography, v. 15, p. 388-403.

Ganopolski, A., and Rahmstorf, S., 2001, Rapid changes of glacial climate simulated in a coupled climate model: Nature, v. 409, p. 153-158.

Genty, D., Blamart, D., Ouahdi, R., Gilmour, M., Baker, A., Jouzel, J., and Van-Exter, S., 2003, Precise dating of Dansgaard-Oeschger climate oscillations in western Europe from stalagmite data: Nature, v. 421, p. 833-837.

Grimm, E. C., Jacobson, G. L., Watts, W. A., Hansen, B. C. S., and Maasch, K. A., 1993, A 50,000-Year Record of Climate Oscillations from Florida and Its Temporal Correlation with the Heinrich Events: Science, v. 261, p. 198-200.

Grootes, P. M., Stuiver, M., White, J. W. C., Johnsen, S., and Jouzel, J., 1993, Comparison of oxygen isotope records from the GISP2 and GRIP Greenland ice cores: Nature, v. 366, p. 552-554.

Gutjahr, M., and Lippold, J., 2011, Early arrival of Southern Source Water in the deep North Atlantic prior to Heinrich event 2: Paleoceanography, v. 26, p. PA2101.

Hall, I. R., Colmenero-Hidalgo, E., Zahn, R., Peck, V. L., and Hemming, S. R., 2011, Centennial- to millennial-scale ice-ocean interactions in the subpolar northeast Atlantic 18-41 kyr ago: Paleoceanography, v. 26, p. PA2224.

Hall, I. R., Moran, S. B., Zahn, R., Knutz, P. C., Shen, C. C., and Edwards, R. L., 2006, Accelerated drawdown of meridional overturning in the late-glacial Atlantic triggered by transient pre-H event freshwater perturbation: Geophysical Research Letters, v. 33, p. L16616.

Hansen, B., and Østerhus, S., 2000, North Atlantic-Nordic Seas exchanges: Progress In Oceanography, v. 45, p. 109-208.

Harrison, S. P., and Sánchez-Goñi, M. F., 2010, Global patterns of vegetation response to millennial-scale variability and rapid climate change during the last glacial period: Quaternary Science Reviews, v. 29, p. 2957-2980.

Haug, G. H., and Tiedemann, R., 1998, Effect of the formation of the Isthmus of Panama on Atlantic Ocean thermohaline circulation: Nature, v. 393, p. 673-676.

Hays, J. D., Imbrie, J., and Shackleton, N. J., 1976, Variations in the Earth's orbit: pacemaker of the ice ages: Science, v. 194, p. 1121-1132.

Hegerl, G. C., Crowley, T. J., Baum, S. K., Kim, K.-Y., and Hyde, W. T., 2003, Detection of volcanic, solar and greenhouse gas signals in paleo-reconstructions of Northern Hemispheric temperature: Geophysical Research Letters, v. 30, p. 1242.

Heinrich Events: Land Ice and Ocean Workshop, 2012: National Oceanography Centre, Southampton.

Heinrich, H., 1988, Origin and consequences of cyclic ice rafting in the Northeast Atlantic Ocean during the past 130,000 years: Quaternary Research, v. 29, p. 142-152.

Hemming, S. R., 2004, Heinrich events: Massive late Pleistocene detritus layers of the North Atlantic and their global climate imprint: Rev. Geophys., v. 42, p. RG1005.

Henrich, R., Baumann, K.-H., Huber, R., and Meggers, H., 2002, Carbonate preservation records of the past 3 Myr in the Norwegian–Greenland Sea and the northern North Atlantic: implications for the history of NADW production: Marine Geology, v. 184, p. 17-39.

Hollister, C. D., 1993, The concept of deep-sea contourites: Sedimentary Geology, v. 82, p. 5-11.

Howe, J. A., Stoker, M. S., and Stow, D. A. V., 1994, Late Cenozoic Sediment Drift Complex, Northeast Rockall Trough, North Atlantic: Paleoceanography, v. 9, p. 989-999.

Hurrell, J. W., 1995, Decadal Trends in the North Atlantic Oscillation: Regional Temperatures and Precipitation: Science, v. 269, p. 676-679.

Huybers, P., and Wunsch, C., 2005, Obliquity pacing of the late Pleistocene glacial terminations: Nature, v. 434, p. 491-494.

Johnsen, S. J., Clausen, H. B., Dansgaard, W., Fuhrer, K., Gundestrup, N., Hammer, C. U., Iversen, P., Jouzel, J., Stauffer, B., and Steffensen, J. P., 1992, Irregular glacial interstadials recorded in a new Greenland ice core: Nature, v. 359, p. 311-313.

Johnsen, S. J., Dahl-Jensen, D., Gundestrup, N., Steffensen, J. P., Clausen, H. B., Miller, H., Masson-Delmotte, V., Sveinbjörnsdottir, A. E., and White, J., 2001, Oxygen isotope and palaeotemperature records from six Greenland ice-core stations: Camp Century, Dye-3, GRIP, GISP2, Renland and NorthGRIP: Journal of Quaternary Science, v. 16, p. 299-307.

Johnson, C., Sherwin, T., Smythe-Wright, D., Shimmield, T., and Turrell, W., 2010, Wyville Thomson Ridge Overflow Water: Spatial and temporal distribution in the Rockall Trough: Deep Sea Research Part I: Oceanographic Research Papers, v. 57, p. 1153-1162.

Jones, E. J. W., Ewing, M., Ewing, J. I., and Eittreim, S. L., 1970, Influences of Norwegian Sea Overflow Water on Sedimentation in the Northern North Atlantic and Labrador Sea: J. Geophys. Res., v. 75, p. 1655-1680.

Jones, P. D., Lister, D. H., Osborn, T. J., Harpham, C., Salmon, M., and Morice, C. P., 2012, Hemispheric and large-scale land-surface air temperature variations: An extensive revision and an update to 2010: Journal of Geophysical Research: Atmospheres, v. 117, p. D05127.

Keigwin, L. D., and Lehman, S. J., 1994, Deep Circulation Change Linked to HEINRICH Event 1 and Younger Dryas in a Middepth North Atlantic Core: Paleoceanography, v. 9, p. 185-194.

Knutz, P. C., 2008, Chapter 24 Palaeoceanographic Significance of Contourite Drifts, *in* Rebesco, M., and Camerlenghi, A., eds., Developments in Sedimentology, Elsevier, p. 511-535.

Kroopnick, P. M., 1985, The distribution of 13C of ΣCO2 in the world oceans: Deep Sea Research Part A. Oceanographic Research Papers, v. 32, p. 57-84.

Lacan, F., and Jeandel, C., 2005, Acquisition of the neodymium isotopic composition of the North Atlantic Deep Water: Geochem. Geophys. Geosyst., v. 6, p. Q12008.

Lang, C., Leuenberger, M., Schwander, J., and Johnsen, S., 1999, 16°C Rapid Temperature Variation in Central Greenland 70,000 Years Ago: Science, v. 286, p. 934-937.

Laskar, J., Robutel, P., Joutel, F., Gastineau, M., Correia, A. C. M., and Levrard, B., 2004, A long-term numerical solution for the insolation quantities of the Earth: Astronomy & Astrophysics, v. 428, p. 261-285.

Lear, C. H., Elderfield, H., and Wilson, P. A., 2000, Cenozoic Deep-Sea Temperatures and Global Ice Volumes from Mg/Ca in Benthic Foraminiferal Calcite: Science, v. 287, p. 269-272.

Lemke, P., Ren, J., Alley, R. B., Allison, I., Carrasco, J., Flato, G., Fujii, Y., Kaser, G., Mote, P., Thomas, R. H., and Zhang, T., 2007, Observations: Changes in snow, ice and frozen ground, *in* Solomon, S., Qin, D., Manning, M., Chen, Z., Marquis, M., Averyt, K. B., Tignor, M., and Miller, H. L., eds., Climate change 2007: The Physical Science Basis. Contribution of Working Group I to the Fourth Assessment Report of the Intergovernmental Panel on Climate Change, Cambridge University Press, Cambridge, United Kingdom and New York, NY, USA, p. 337-383.

Lisiecki, L. E., and Raymo, M. E., 2005, A Pliocene-Pleistocene stack of 57 globally distributed benthic $\delta^{18}O$ records: Paleoceanography, v. 20, p. PA1003.

Lourens, L. J., Sluijs, A., Kroon, D., Zachos, J. C., Thomas, E., Rohl, U., Bowles, J., and Raffi, I., 2005, Astronomical pacing of late Palaeocene to early Eocene global warming events: Nature, v. 435, p. 1083-1087.

Marchitto, T. M., and Broecker, W. S., 2006, Deep water mass geometry in the glacial Atlantic Ocean: A review of constraints from the paleonutrient proxy Cd/Ca: Geochemistry, Geophysics, Geosystems, v. 7, p. Q12003.

Marino, M., Maiorano, P., and Flower, B. P., 2011, Calcareous nannofossil changes during the Mid-Pleistocene Revolution: Paleoecologic and paleoceanographic evidence from North Atlantic Site 980/981: Palaeogeography, Palaeoclimatology, Palaeoecology, v. 306, p. 58-69.

Marshall, J., and Schott, F., 1999, Open-ocean convection: Observations, theory, and models: Reviews of Geophysics, v. 37, p. 1-64.

Maslin, M. A., and Ridgwell, A. J., 2005, Mid-Pleistocene revolution and the 'eccentricity myth': Geological Society, London, Special Publications, v. 247, p. 19-34.

Masson, D. G., and Kidd, R. B., 1986, Revised Tertiary seismic stratigraphy of the southern Rockall Trough: Initial Reports of the Deep Sea Drilling Project, v. 94, p. 1117-1126.

Mauritzen, C., 1996, Production of dense overflow waters feeding the North Atlantic across the Greenland-Scotland Ridge. Part 1: Evidence for a revised circulation scheme: Deep Sea Research Part I: Oceanographic Research Papers, v. 43, p. 769-806.

Mc Intyre, K., Ravelo, A. C., and Delaney, M. L., 1999, North Atlantic Intermediate Waters in the Late Pliocene to Early Pleistocene: Paleoceanography, v. 14, p. 324-335.

McCartney, M. S., 1992, Recirculating components to the deep boundary current of the northern North Atlantic: Progress In Oceanography, v. 29, p. 283-383.

McCave, I. N., Manighetti, B., and Beveridge, N. A. S., 1995, Circulation in the glacial North Atlantic inferred from grain-size measurements: Nature, v. 374, p. 149-152.

McCave, I. N., and Tucholke, B. E., 1986, Deep current-controlled sedimentation in the western North Atlantic: The Geology of North America, v. 1000, p. 451-468.

McGrath, T., Nolan, G., and McGovern, E., 2012, Chemical characteristics of water masses in the Rockall Trough: Deep Sea Research Part I: Oceanographic Research Papers.

McManus, J. F., Francois, R., Gherardi, J. M., Keigwin, L. D., and Brown-Leger, S., 2004, Collapse and rapid resumption of Atlantic meridional circulation linked to deglacial climate changes: Nature, v. 428, p. 834-837.

McManus, J. F., Oppo, D. W., and Cullen, J. L., 1999, A 0.5-Million-Year Record of Millennial-Scale Climate Variability in the North Atlantic: Science, v. 283, p. 971-975.

Meland, M. Y., Dokken, T. M., Jansen, E., and Hevrøy, K., 2008, Water mass properties and exchange between the Nordic seas and the northern North Atlantic during the period 23-6 ka: Benthic oxygen isotopic evidence: Paleoceanography, v. 23, p. PA1210.

Miller, K. G., Fairbanks, R. G., and Mountain, G. S., 1987, Tertiary Oxygen Isotope Synthesis, Sea Level History, and Continental Margin Erosion: Paleoceanography, v. 2.

Moy, C. M., Seltzer, G. O., Rodbell, D. T., and Anderson, D. M., 2002, Variability of El Niño/Southern Oscillation activity at millennial timescales during the Holocene epoch: Nature, v. 420, p. 162-165.

New, A. L., and Smythe-Wright, D., 2001, Aspects of the circulation in the Rockall Trough: Continental Shelf Research, v. 21, p. 777-810.

North Greenland Ice Core Project Members, Andersen, K. K., Azuma, N., Barnola, J.-M., Bigler, M., Biscaye, P., Caillon, N., Chappellaz, J., Clausen, H. B., Dahl-Jensen, D., Fischer, H., Flückiger, J., Fritzsche, D., Fujii, Y., Goto-Azuma, K., Grønvold, K., Gundestrup, N. S., Hansson, M., Huber, C., Hvidberg, C. S., Johnsen, S. J., Jonsell, U., Jouzel, J., Kipfstuhl, S., Landais, A., Leuenberger, M., Lorrain, R., Masson-Delmotte, V., Miller, H., Motoyama, H., Narita, H., Popp, T., Rasmussen, S. O., Raynaud, D., Rothlisberger, R., Ruth, U., Samyn, D., Schwander, J., Shoji, H., Siggard-Andersen, M.-L., Steffensen, J. P., Stocker, T., Sveinbjörnsdóttir, A. E., Svensson, A., Takata, M., Tison, J.-L., Thorsteinsson, T., Watanabe, O., Wilhelms, F., and White, J. W. C., 2004, High-resolution record of Northern Hemisphere climate extending into the last interglacial period: Nature, v. 431, p. 147-151.

Olsen, A., and Ninnemann, U., 2010, Large δ13C Gradients in the Preindustrial North Atlantic Revealed: Science, v. 330, p. 658-659.

Olsen, P. E., 1986, A 40-Million-Year Lake Record of Early Mesozoic Orbital Climatic Forcing: Science, v. 234, p. 842-848.

Olsen, S. M., Hansen, B., Quadfasel, D., and Osterhus, S., 2008, Observed and modelled stability of overflow across the Greenland-Scotland ridge: Nature, v. 455, p. 519-522.

Oppo, D. W., Keigwin, L. D., McManus, J. F., and Cullen, J. L., 2001, Persistent suborbital climate variability in marine isotope stage 5 and termination II: Paleoceanography, v. 16, p. 280-292.

Oppo, D. W., McManus, J. F., and Cullen, J. L., 1998, Abrupt Climate Events 500,000 to 340,000 Years Ago: Evidence from Subpolar North Atlantic Sediments: Science, v. 279, p. 1335-1338.

—, 2006, Evolution and demise of the Last Interglacial warmth in the subpolar North Atlantic: Quaternary Science Reviews, v. 25, p. 3268-3277.

PAGES 2k consortium, 2013, Continental-scale temperature variability during the past two millennia: Nature Geosci, v. 6, p. 339-346.

Pälike, H., Norris, R. D., Herrle, J. O., Wilson, P. A., Coxall, H. K., Lear, C. H., Shackleton, N. J., Tripati, A. K., and Wade, B. S., 2006, The Heartbeat of the Oligocene Climate System: Science, v. 314, p. 1894-1898.

Poore, H., White, N., and Maclennan, J., 2011, Ocean circulation and mantle melting controlled by radial flow of hot pulses in the Iceland plume: Nature Geosci, v. 4, p. 558-561.

Poore, H. R., Samworth, R., White, N. J., Jones, S. M., and McCave, I. N., 2006, Neogene overflow of Northern Component Water at the Greenland-Scotland Ridge: Geochem. Geophys. Geosyst., v. 7, p. Q06010.

Rahmstorf, S., 2002, Ocean circulation and climate during the past 120,000 years: Nature, v. 419, p. 207-214.

Rasmusson, E. M., and Wallace, J. M., 1983, Meteorological Aspects of the El Niño/Southern Oscillation: Science, v. 222, p. 1195-1202.

Raymo, M. E., Hodell, D., and Jansen, E., 1992, Response of deep ocean circulation to initiation of northern hemisphere glaciation (3–2 Ma): Paleoceanography, v. 7, p. 645-672.

Raymo, M. E., Oppo, D. W., Flower, B. P., Hodell, D. A., McManus, J. F., Venz, K. A., Kleiven, K. F., and McIntyre, K., 2004, Stability of North Atlantic water masses in face of pronounced climate variability during the Pleistocene: Paleoceanography, v. 19, p. PA2008.

Ruddiman, W. F., 1977, Late Quaternary deposition of ice-rafted sand in the subpolar North Atlantic (lat 40° to 65°N): Geological Society of America Bulletin, v. 88, p. 1813-1827.

Sánchez-Goñi, M. F., Turon, J.-L., Eynaud, F., and Gendreau, S., 2000, European Climatic Response to Millennial-Scale Changes in the Atmosphere-Ocean System during the Last Glacial Period: Quaternary Research, v. 54, p. 394-403.

Sarnthein, M., Jansen, E., Weinelt, M., Arnold, M., Duplessy, J. C., Erlenkeuser, H., Flatøy, A., Johannessen, G., Johannessen, T., Jung, S., Koc, N., Labeyrie, L., Maslin, M., Pflaumann, U., and Schulz, H., 1995, Variations in Atlantic Surface Ocean Paleoceanography, 50º-80ºN: A Time-Slice Record of the Last 30,000 Years: Paleoceanography, v. 10, p. 1063-1094.

Scher, H. D., and Martin, E. E., 2006, Timing and Climatic Consequences of the Opening of Drake Passage: Science, v. 312, p. 428-430.

Schlitzer, R., 2013, Ocean Data View, http://odv.awi.de.

Schulz, M., 2002, On the 1470-year pacing of Dansgaard-Oeschger warm events: Paleoceanography, v. 17, p. 1014.

Seidov, D., Sarnthein, M., Stattegger, K., Prien, R., and Weinelt, M., 1996, North Atlantic ocean circulation during the last glacial maximum and subsequent meltwater event: A numerical model: J. Geophys. Res., v. 101, p. 16305-16332.

Shackleton, N. J., Imbrie, J., Pisias, N. G., and Rose, J., 1988, The Evolution of Oceanic Oxygen-Isotope Variability in the North Atlantic Over the Past Three Million Years: Philosophical Transactions of the Royal Society of London. B, Biological Sciences, v. 318, p. 679-688.

Sherwin, T. J., Griffiths, C. R., Inall, M. E., and Turrell, W. R., 2008, Quantifying the overflow across the Wyville Thomson Ridge into the Rockall Trough: Deep Sea Research Part I: Oceanographic Research Papers, v. 55, p. 396-404.

Sherwin, T. J., and Turrell, W. R., 2005, Mixing and advection of a cold water cascade over the Wyville Thomson Ridge: Deep Sea Research Part I: Oceanographic Research Papers, v. 52, p. 1392-1413.

Shipboard Scientific Party, 1996, Explanatory Notes, *in* Jansen, E., Raymo, M. E., and Blum P. et al., eds., Proceedings of the Ocean Drilling Program, Initial Reports, College station, TX, p. 21-45.

Solomon, S., Qin, D., Manning, M., Chen, Z., Marquis, M., Averyt, K. B., Tignor, M., and Miller, H. L., (eds.), 2007, Contribution of Working Group I to the Fourth

Assessment Report of the Intergovernmental Panel on Climate Change, 2007, Cambridge University Press, Cambridge, United Kingdom and New York, NY, USA.

Stanford, J. D., Rohling, E. J., Bacon, S., Roberts, A. P., Grousset, F. E., and Bolshaw, M., 2011, A new concept for the paleoceanographic evolution of Heinrich event 1 in the North Atlantic: Quaternary Science Reviews, v. 30, p. 1047-1066.

Stanford, J. D., Rohling, E. J., Hunter, S. E., Roberts, A. P., Rasmussen, S. O., Bard, E., McManus, J., and Fairbanks, R. G., 2006, Timing of meltwater pulse 1a and climate responses to meltwater injections: Paleoceanography, v. 21, p. PA4103.

Swift, J. H., 1984, The circulation of the Denmark Strait and Iceland-Scotland overflow waters in the North Atlantic: Deep Sea Research Part A. Oceanographic Research Papers, v. 31, p. 1339-1355.

Tett, S. F. B., Stott, P. A., Allen, M. R., Ingram, W. J., and Mitchell, J. F. B., 1999, Causes of twentieth-century temperature change near the Earth's surface: Nature, v. 399, p. 569-572.

Ullgren, J. E., and White, M., 2010, Water mass interaction at intermediate depths in the southern Rockall Trough, northeastern North Atlantic: Deep Sea Research Part I: Oceanographic Research Papers, v. 57, p. 248-257.

Van Houten, F. B., 1964, Cyclic lacustrine sedimentation, upper Triassic Lockatong formation, central New Jersey and adjacent Pennsylvania: Symposium on cyclic sedimentation: Kansas Geological Survey Bulletin, p. 497-531.

van Weering, T. C. E., and de Rijk, S., 1991, Sedimentation and climate-induced sediments on Feni Ridge, Northeast Atlantic Ocean: Marine Geology, v. 101, p. 49-69.

Voelker, A. H. L., 2002, Global distribution of centennial-scale records for Marine Isotope Stage (MIS) 3: a database: Quaternary Science Reviews, v. 21, p. 1185-1212.

Walker, J. C. G., Hays, P. B., and Kasting, J. F., 1981, A negative feedback mechanism for the long-term stabilization of Earth's surface temperature: Journal of Geophysical Research: Oceans, v. 86, p. 9776-9782.

Wold, C. N., 1994, Cenozoic Sediment Accumulation on Drifts in the Northern North Atlantic: Paleoceanography, v. 9, p. 917-941.

Wright, J. D., and Miller, K. G., 1996, Control of North Atlantic Deep Water Circulation by the Greenland-Scotland Ridge: Paleoceanography, v. 11, p. 157-170.

Yashayaev, I., Bersch, M., and van Aken, H. M., 2007, Spreading of the Labrador Sea Water to the Irminger and Iceland basins: Geophys. Res. Lett., v. 34, p. L10602.

Yu, J., Elderfield, H., and Piotrowski, A. M., 2008, Seawater carbonate ion-δ13C systematics and application to glacial-interglacial North Atlantic ocean circulation: Earth and Planetary Science Letters, v. 271, p. 209-220.

Zachos, J., Pagani, M., Sloan, L., Thomas, E., and Billups, K., 2001, Trends, Rhythms, and Aberrations in Global Climate 65 Ma to Present: Science, v. 292, p. 686-693.

Zachos, J. C., Dickens, G. R., and Zeebe, R. E., 2008, An early Cenozoic perspective on greenhouse warming and carbon-cycle dynamics: Nature, v. 451, p. 279-283.

Chapter 2

Millennial Scale Variability in Surface Ocean Conditions during the Last Glacial Interval: Spatial and Temporal Variability in the Northeast Atlantic

2.1 Abstract

The last glacial interval and deglaciation were marked by dramatic, high frequency variability in the global climate, most noticeably in the North Atlantic region. Large armadas of icebergs flooded the North Atlantic Ocean as a result of destabilisation of the Laurentide Ice Sheet (LIS) and other circum-Atlantic ice sheets, adding large amounts of fresh water to the ocean and disrupting the Atlantic meridional overturning circulation. The mechanisms responsible for generating these Heinrich events are still debated. Proxy reconstructions of upper ocean temperature variations at Ocean Drilling Project (ODP) Site 980 in the northeast Atlantic show excellent agreement with the millennial scale variability captured by the geochemistry of ice cores from Greenland, although their expression in the sedimentary record is modified by a combination of variable sedimentation rates, bioturbation and bottom current activity. Variations in the flux of planktonic foraminifera deposited may be linked to highly variable sea ice extent, with the bulk magnetic susceptibility of the sediment illustrating how the marine sedimentary record is strongly influenced by both the deposition of ice-rafted debris (IRD) and bottom current activity. Spatial variability in the composition of IRD across the Northeast Atlantic illustrates the fact that changing patterns in grain lithologies in open ocean settings cannot be interpreted simply as a function of large-scale ice-sheet behaviour. Instead, IRD deposition is also influenced by surface ocean properties and circulation, and the mass balance of both major ice sheets and their smaller, less stable ice streams. Differences in the sequence of lithologies deposited between Heinrich events suggests that they are not simple, repeating events, with local factors and internal ice sheet instabilities potentially playing a role in the observed patterns of IRD deposition in marine sediments. Evidence of European sourced IRD preceding detrital

carbonate deposition at multiple Heinrich events, however, suggests that melt water input to the ocean from smaller ice sheets could have played a role in the destabilisation of the LIS at Heinrich events.

2.2 Introduction

Current predictions of global climate over the coming centuries suggest that future warming will be extremely rapid, unlike anything observed over the relatively stable conditions of the Holocene [Solomon et al. 2007]. The climate of the last glacial interval was much more unstable than the Holocene, with strong fluctuations between mild (interstadial) and cold (stadial) conditions [e.g. Bond et al. 1993; Dansgaard et al. 1993; Alley et al. 1999; Broecker and Hemming 2001; Rahmstorf 2002; Voelker 2002]. Certain stadials are marked by a significant increase in the input of icebergs to the North Atlantic, and have been christened "Heinrich events" [e.g. Heinrich 1988; Bond et al. 1992; Grousset et al. 1993; Bond and Lotti 1995; Hemming 2004]. Large inputs of freshwater to the ocean at high latitudes severely disrupted the meridional overturning circulation during Heinrich events [e.g. Stommel 1961; Broecker et al. 1985; Maslin et al. 1995; Oppo and Lehman 1995; Vidal et al. 1997; Ganopolski and Rahmstorf 2001]. Understanding the links between the locations and mechanisms of fresh water addition to the oceans and the resulting changes in overturning circulation helps to develop our understanding of the oceanic response to future freshwater inputs as a result of anthropogenic ice sheet destabilisation.

Despite being the focus of many investigations, the mechanism responsible for generating millennial scale Dansgaard-Oeschger variability is still much debated. For responses to be seen over a hemispheric, and perhaps even global scale, it is thought that interactions between the global thermohaline circulation, sea ice feedbacks and tropical ocean-atmosphere processes must all play a part [Clement and Peterson 2008].

Many of the hypotheses put forward to explain why Heinrich (H-) events have a greater impact on both the North Atlantic sedimentary record and the oceanic thermohaline

circulation than Dansgaard-Oeschger (D-O) variability focus on internal instability of ice sheets [Hemming 2004]. MacAyeal [1993] proposed that periodic purging of the Laurentide ice sheet occurred when its volume reached a threshold, at which point basal melting lubricated the ice sheet, triggering a rapid collapse. Alternative mechanisms have since been suggested including jökulhlaup activity (the catastrophic release of meltwater previously trapped behind a dam) [Johnson and Lauritzen 1995], episodic activity of a Hudson Strait ice stream [Marshall and Clarke 1997] and ice shelf collapse as a result of warming of surface [Hulbe 1997; Hulbe et al. 2004] or subsurface [Marcott et al. 2011] waters.

Synchronous or near-synchronous release of icebergs from multiple ice sheets during Heinrich events would imply either some form of coupling between the ice sheets or an external forcing acting across the region. Sea level [Bond and Lotti 1995; Flückiger et al. 2006] and thermohaline circulation changes [Zahn et al. 1997; Moros et al. 2002; Alvarez-Solas et al. 2010; Gutjahr and Lippold 2011] have both been invoked as potential triggers for Heinrich events, with surges from one ice sheet also being proposed as destabilising agents for other ice sheets [e.g. Bond and Lotti 1995; Snoeckx et al. 1999; Scourse et al. 2000; Darby et al. 2002]. The importance of solar forcing is also currently debated [e.g. Bond et al. 2001; Braun et al. 2005; Muscheler and Beer 2006; Darby et al. 2012; Obrochta et al. 2012].

Icebergs transport the terrigenous products of glacial erosion from their source area out into the open ocean, where this ice-rafted debris (IRD) is deposited as drifting icebergs melt and/or break up due to the physical abrasive action of waves [Andrews 2000]. In certain cases, it is possible to identify the provenance of the IRD on the basis of its composition, chemistry or age. Therefore, marine sediments can provide an insight into the dynamics of major ice-sheets.

Deciphering the source(s) of IRD and meltwater input has important implications for understanding the resulting changes in ocean thermohaline circulation [Bigg et al. 2011]. A number of different IRD provenance indicators have been used to explore this further.

These include grain lithologies [e.g. Darby et al. 2002; Peck et al. 2007], lead isotopes [e.g. Gwiazda et al. 1996a; Gwiazda et al. 1996b; Hemming et al. 1998; Bailey et al. 2012; Crocket et al. 2012], neodymium and strontium isotopes [e.g. Grousset et al. 1993; Revel et al. 1996; Farmer et al. 2003], K/Ar [e.g.Jantschik and Huon 1992], $^{40}Ar/^{39}Ar$ [e.g. Gwiazda et al. 1996c; Hemming et al. 2002; Hemming and Hajdas 2003], Rb-Sr [e.g. Huon and Jantschik 1993], magnetic properties [e.g. Robinson et al. 1995; Walden et al. 2007; Watkins et al. 2007], organic geochemical footprints [Naafs et al. 2013] and the presence of reworked late Tertiary and early Cenozoic nannofossils [e.g. Rahman 1995; Scourse et al. 2000].

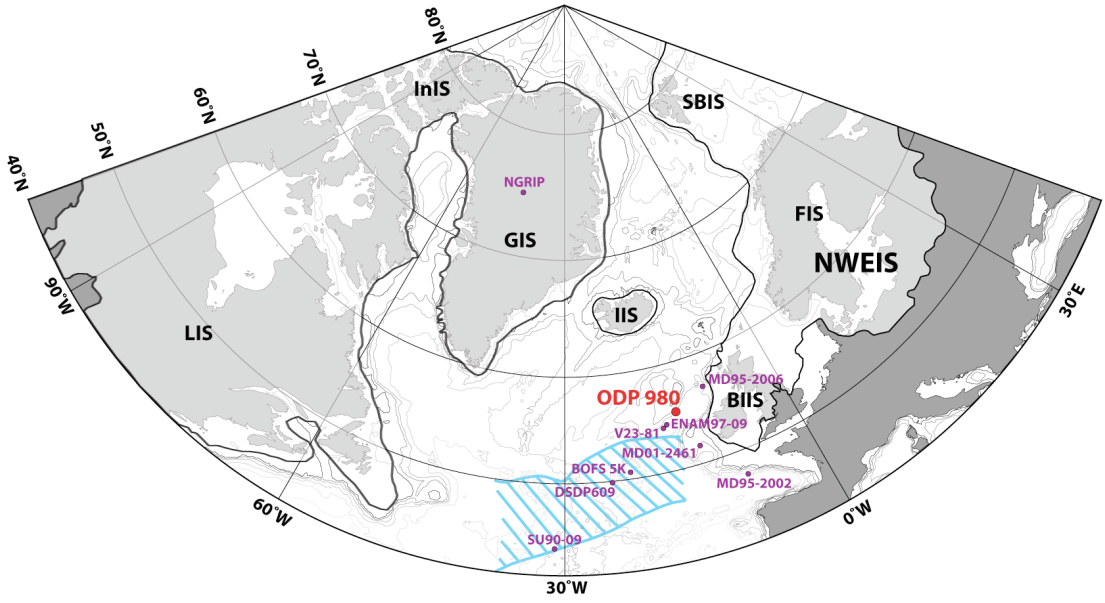

Figure 2.1: Reconstructed extent of ice at the Last Glacial Maximum (LGM) based upon Funder and Hansen [1996], Landvik et al. [1998], Svendsen et al. [1999], Clark and Mix [2002], Dyke et al. [2002; Naafs et al. 2013], Huybrechts [2002], Marshall et al. [2002], Peltier [2004], Sejrup et al. [2005] and Clark et al. [2012]. Blue hashed region marks the location of the main N. Atlantic IRD belt, with the 25–13 ka 250 mg cm^{-2} kyr^{-1} IRD flux line of Ruddiman [1977] shown, redrawn from Hemming [2004]. Location of ODP Site 980, with the positions of other cores referred to in the text also shown, plotted on an orthographic (North Polar) projection. LIS: Laurentide Ice Sheet; InIS: Innuitian Ice Sheet; GIS: Greenland Ice Sheet; IIS: Icelandic Ice Sheet; BIIS: British and Irish Ice Sheet; FIS: Fennoscandian Ice Sheet; SBIS: Svalbard-Barents Ice Sheet; NWEIS: North West European Ice Sheet.

Detrital carbonate clasts sourced from the Hudson Bay area beneath the Laurentide Ice Sheet which covered much of North America (shown in figure 2.1) are found in many of the Heinrich layers of the last glacial across the North Atlantic (including Heinrich (H) events 1, 2, 4 and 5) [Heinrich 1988; Andrews and Tedesco 1992; Broecker et al. 1992], but may be absent in others (e.g. H3 and H6) [Gwiazda et al. 1996a; Hemming 2004]. This suggests that the magnitude of iceberg release from each of the circum-Atlantic ice sheets may have differed between Heinrich events [Grousset et al. 1993; Snoeckx et al. 1999]. Evidence of variability in IRD provenance within Heinrich events has added support to suggestions that precursory change in the European ice sheets lead to the destabilisation of the Laurentide Ice Sheet [e.g. Bond and Lotti 1995; Snoeckx et al. 1999; Grousset et al. 2000; Scourse et al. 2000], although recent studies have painted a more complex picture [e.g. Walden et al. 2007; Scourse et al. 2009; Haapaniemi et al. 2010].

In order to distinguish between the different mechanisms proposed to explain Heinrich and Dansgaard-Oeschger variability, it is vital to know the phasing between the different components of the ocean and Earth system. Leads and lags between changes in the surface and deep ocean, sea ice cover and instabilities of different ice sheets can convey crucial information. High resolution, multi-proxy records from a single sediment section allow offsets between different proxy records to be distinguished, avoiding the uncertainties associated with comparing records with different chronologies. A time series spanning multiple rapid climatic events also has the advantage of highlighting any differences between events, which may have important implications for the mechanism by which they are generated. ODP Site 980 is well situated to reconstruct variability in the surface ocean and cryosphere, as it has a high sedimentation rate due to its position in a major sediment drift (discussed in section 1.2), increasing the probability that any offsets between proxy records can be resolved. The site is also located on the periphery of the main North Atlantic IRD belt [Ruddiman 1977], and hence is expected to record a signal from the Laurentide Ice Sheet, however, due to its location in the Northeast Atlantic, an influence of the major European ice sheets may also be detected. Site 980

therefore provides an excellent opportunity to study the interactions between the ocean and cryosphere during the last 40,000 years.

2.3 Aims

The key aims of this chapter are to:

- Provide a clear and unambiguous identification of the depth of the Heinrich layers in the last glacial stratigraphy of ODP Site 980.
- Update and improve the age model for Site 980, making use of new reference stratigraphies and recommended stratigraphic procedures.
- Deduce changes in the temperature and productivity of the upper ocean using changes in the species and fluxes of planktonic foraminifera.
- Reconstruct the lithology and flux of sand-sized lithic grains transported to the site by ice-rafting and discuss the links to ice-sheet dynamics.
- Compare new, high-resolution data generated from Site 980 with other climate archives from the North Atlantic to better understand spatial variability in proxy records.
- Improve the understanding between the mechanisms responsible for generating the changes documented in the North Atlantic during Heinrich events by comparing records of change in the surface ocean and cryosphere.
- Provide a framework for interpreting the data generated in later chapters, by permitting interpretation of the phasing between the changes in the cryosphere, surface and deep ocean.

2.4 Methods

2.4.1 Sediment preparation

All sediment samples used in this study are from ODP Site 980 with a combination of samples from Hole B (0.05–4.13 metres below seafloor, or mbsf) and Hole A (0.32–4.08 mbsf), as shown in figure 2.2. In order to be able to place samples from the different

holes onto a single age scale, the depth scale for each hole was converted from metres below seafloor (mbsf) to metres composite depth (mcd). This procedure is documented in appendix 1. Sample volumes were approximately 20 cm^3. Bulk sediment samples were weighed, oven dried at 50°C for 3–7 days and their dry mass was recorded. They were then washed with deionised water over a 63 µm mesh. The coarse fraction (>63 µm) was oven dried, weighed and stored in a glass vial. The fine fraction of each sample (<63 µm) was allowed to settle, then freeze-dried and stored for future use.

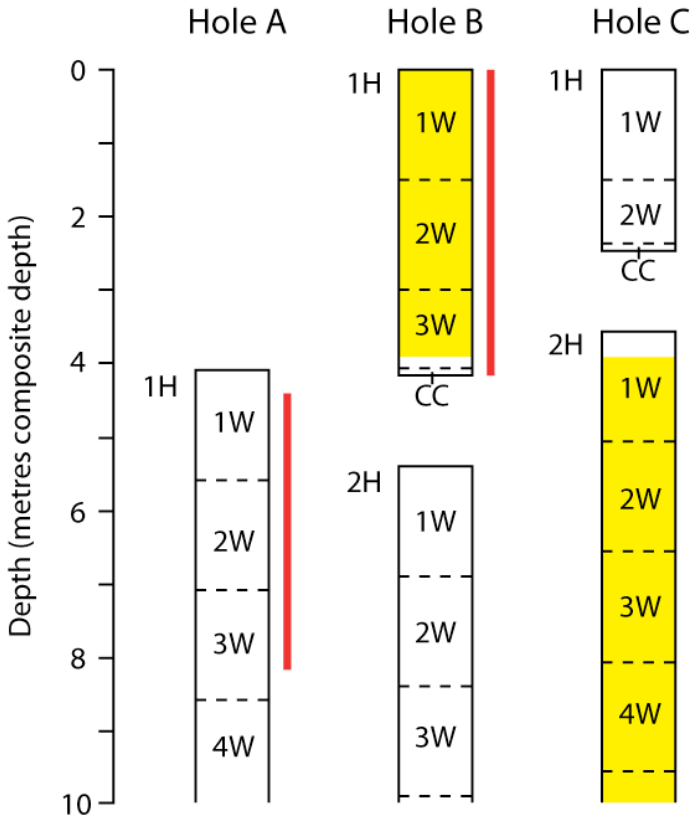

Figure 2.2: Schematic of the uppermost core sections recovered from ODP Site 980, displaying all three holes (A, B and C). Core numbers are followed by H, indicating that the core is an advanced piston core (1H, 2H etc.), while section numbers are followed by W, as they are from the working half of the core (1W, 2W etc.). Depths plotted as metres composite depth, using the values given in the Leg 162 Initial Report [Shipboard Scientific Party 1996b]. Red lines mark the positions of the samples used in this study. Yellow shading marks the sections used to construct the splice record [Shipboard Scientific Party 1996b].

2.4.2 Ice-rafted debris and foraminifera counts

Samples were dry sieved at the 150–500 μm size fraction, and the total number of *C. wuellerstorfi* (a species of benthic foraminifera typically associated with high bottom current velocities [Linke and Lutze 1993; Wollenburg and Mackensen 1998; Gupta and Thomas 2003]) were counted. Sediment samples were then repeatedly divided into two equal halves using a sediment splitter until approximately 300 lithic grains remained. These grains were then identified and counted, using the categorisations of Hall et al. [2011], with reproducibility of counts estimated as ±1 %. The samples were then split again until approximately 300 planktonic foraminifera remained. The number of specimens of the polar species of planktonic foraminifera *Neogloboquadrina pachyderma* (sinistral) (Ehrenberg, 1861) was counted as a proportion of the total number of planktonic foraminifera in the samples using an optical microscope, allowing the percentage of *N. pachyderma* (s.) to be calculated. Repeat counts gave values within 3 % of original counts. The number of planktonic foraminifera per gram of sediment was estimated as follows:

$$\text{Foraminifera per gram sediment} = \left(\frac{\text{Foraminifera counted}}{\text{Fraction of sample counted}}\right) \times \text{Sediment dry bulk mass}$$

Equation 2.1

2.4.3 Ice-rafted debris lithologies

Although it is very difficult to assign a geographical origin to any single lithic grain purely based upon lithology, large scale shifts in the proportions of different lithologies may indicate changes in the significance of different source regions of IRD. The attributions used in this study are based upon the arguements of Peck et al. [2007] and Scourse et al. [2009], and are shown in table 2.1.

2.4.4 Flux estimates

In order to convert estimated concentrations of IRD and planktonic foraminifera into

fluxes, bulk sediment density estimates are needed. Unfortunately the shipboard estimates of gamma-ray attenuation porosity evaluator (GRAPE) wet bulk density data from ODP Leg 162 contained a systematic error of ca. 10 % due to a misalignment of the GRAPE source-sensor apparatus [Carter and Raymo 1999]. Two alternative techniques were therefore applied to estimate the sediment density: cross-plotting the GRAPE density estimates from Hole 980A with estimates of the wet bulk density of discrete samples from the same depth (data from the Leg 162 initial report [Jansen et al. 1996]), and using the wet and dry bulk masses of each sample (based upon the same principles as the moisture and density (MAD) estimates outlined in the explanatory notes of the Leg 162 Initial Reports [Shipboard Scientific Party 1996a]). These techniques are detailed in appendix 2.

Ice sheet	**Lithologies**
Laurentide ice sheet (LIS)	Cream coloured detrital carbonate
British and Irish ice sheet (BIIS)	Sedimentary grains Metamorphic grains Dark carbonate
Icelandic ice sheet (IIS)	Mafic volcanic glass[1] Felsic volcanic glass[1]
Unatributable origin	Transparent quartz Yellow quartz Basalt[2] Haematite coated grains[3] Haematite coated grains[3] Feldspars Pumice[4]

Table 2.1: Classification of IRD lithologies for provenance allocation.

[1]Volcanic glasses may also have been transported to the site through the atmosphere as ash particles.

[2]Basalt was likely sourced from both the BIS and IIS. Two very different volcanic assemblages have been documented on the British margin. At the Barra Fan, in the NE part of the Rockall Trough (MD95-2006 [Knutz et al. 2001]), the volcanic assemblage is dominated by basalt, thought to originate from the Tertiary volcanic provinces of the NW British Isles. The very low content of volcanic glass is used to rule out a dominant Icelandic source at this site. In contrast, at site MD01-2461 (Porcupine Seabight, SE Rockall Trough [Peck et al. 2007]), volcanic glass fluxes are much higher than basalt, an assemblage more typical of the IIS. The assemblage at Site 980 is much more similar to that described at MD01-2461, however, this still does not allow us to determine the source of the basaltic grains with certainty. Another possible source for the basaltic grains is the Rockall Plateau itself (particularly at times of lowered sea level) [Hibbert et al. 2010; Naafs et al. 2013].

[3]Haematite coated grains have been attributed to both E. Greenland, Svalbard and the Arctic [Bond et al. 1997; van Kreveld et al. 2000] and the Gulf of St. Lawrence [Bond and Lotti 1995].

[4]Pumice has previously been attributed to both the Icelandic [Lacasse et al. 1996; Lackschewitz and Wallrabe-Adams 1997; Scourse et al. 2009] and British [Peck et al. 2007] ice sheets. The highly sporadic occurrence of pumice in Site 980 could also indicate the presence of ash layers.

A comparison of IRD fluxes estimated by each of these methods is illustrated in figure 2.3. Estimates calculated from the wet and dry masses of the samples were consistently higher than those from GRAPE density, most likely as a result of the sediment partially drying out since recovery. There is a large offset between the densities estimated from MAD data for Holes A and B. This discrepancy may be due to the fact that samples from Hole B had dried out to a much greater extent because they had been subjected to additional handling by another investigator, while the samples from Hole A came directly from the Bremen Core Repository.

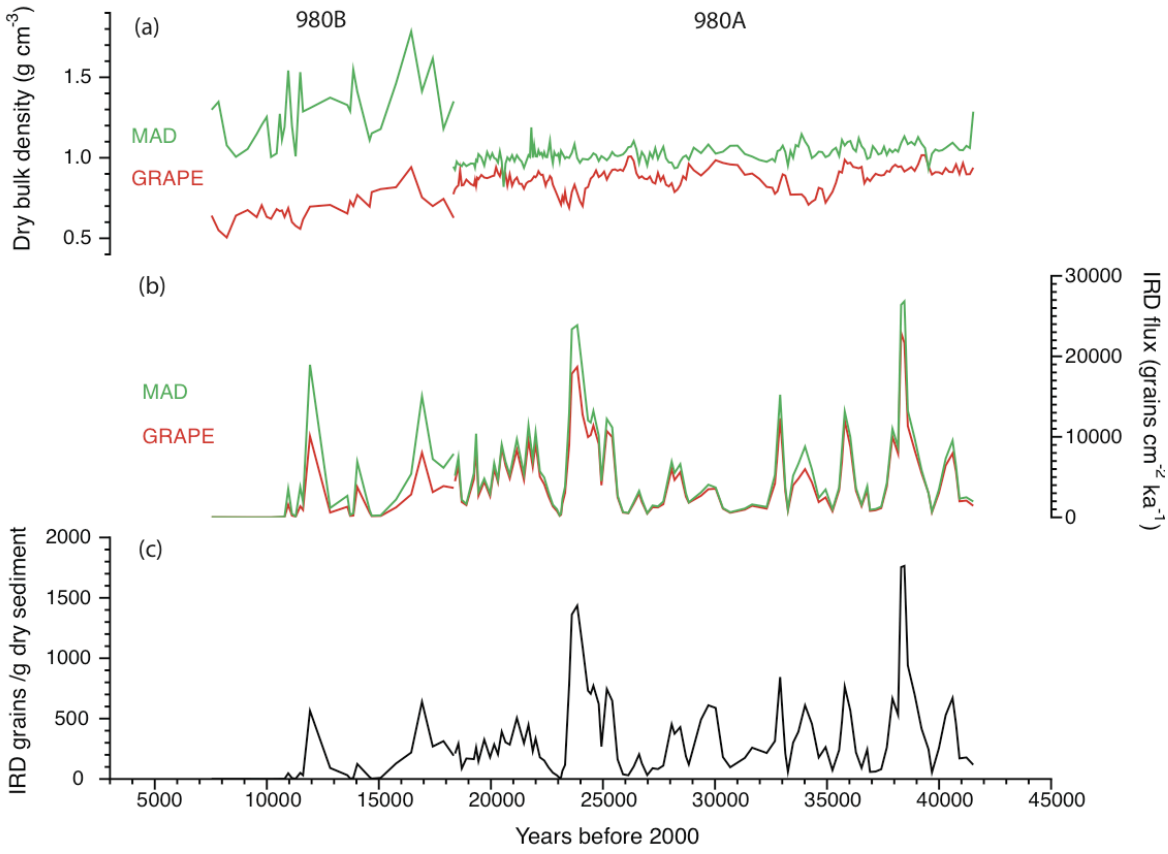

Figure 2.3: Comparison of density and flux estimates for (a) sediment dry bulk density and (b) IRD flux calculated using GRAPE (red) and MAD properties (green). (c) IRD concentration in grains >150 µm / g dry bulk sediment mass. GRAPE data from Jansen et al. [1996].

The choice of density correction does not significantly affect the conclusions of this work, with the only major difference being that the fluxes estimated using GRAPE data in Hole 980B samples are approximately halved when compared to the MAD-derived estimates (figure 2.3). Both show excellent agreement with the concentration data illustrated in figure 2.3(c), showing that the choice of density correction does not significantly alter the observed pattern of variability. Due to the uncertain degree of drying affecting the MAD-derived estimates, however, GRAPE-derived estimates will be used to calculate fluxes in the remainder of this chapter.

2.5 Age model generation

The published age model for ODP Site 980 of McManus et al. [1999] was created by graphically tuning the benthic oxygen isotopes from Site 980 to previously published sediment core chronologies (where stratigraphies had been developed by orbital tuning of benthic oxygen isotope records) [Martinson et al. 1987; Shackleton et al. 1990]. Suborbital variations in benthic $\delta^{18}O$ within the last glacial interval are, however, relatively small, hence it is not possible to resolve and correlate millennial-scale variations to fine-tune an age model. Moreover, the signal at any one site may be influenced by local variations in bottom water $\delta^{18}O$. This is particularly true at times and in regions where there may have been either significant bottom water generation associated with sea ice formation, large melt water inputs or the influence of multiple bottom water masses with different $\delta^{18}O$ signatures. All of these issues have been previously documented in the vicinity of the core site during the last glacial interval [e.g. Dokken and Jansen 1999; Thornalley et al. 2010; Crocket et al. 2011; Waelbroeck et al. 2011], hence there are multiple reasons to suspect that the benthic $\delta^{18}O$ record at Site 980 may not correlate well with globally representative stacks [e.g. Lisiecki and Raymo 2005].

In light of these limitations, a new age model is developed here, following the procedures suggested in Austin and Hibbert [2012]. Their recommended method for developing stratigraphies for North Atlantic sediment cores advocates the creation of a local event stratigraphy for the site using a proxy sensitive to sea surface temperatures, and then correlating the mid-points of rapid warming intervals to a regional stratotype (ideally the NGRIP $\delta^{18}O_{ice}$ record [North Greenland Ice Core Project Members et al. 2004; Lowe et al. 2008]). This allows the transfer of the GICC05 chronology [Andersen et al. 2006; Rasmussen et al. 2006; Svensson et al. 2006; Vinther et al. 2006; Svensson et al. 2008] to the marine realm. Where possible, this should be constrained by additional evidence, for example, IRD-rich horizons, radiocarbon dates and independently tested the presence of ash layers.

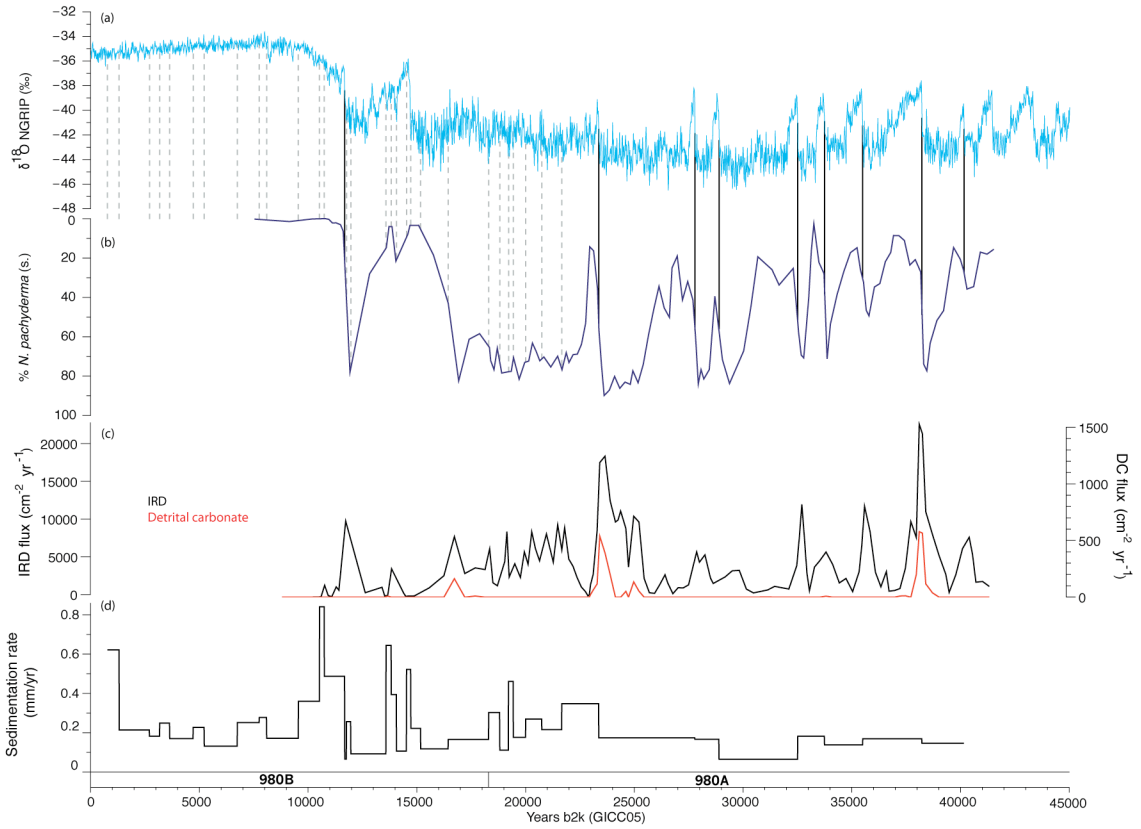

Figure 2.4: (a,b) Tuning of % N. pachyderma (s.) from Site 980 (b) to the $\delta^{18}O_{ice}$ record of the NGRIP ice core (a) [North Greenland Ice Core Project Members et al. 2004], with both records plotted on the GICC05 chronology [Andersen et al. 2006; Rasmussen et al. 2006; Svensson et al. 2006; Vinther et al. 2006; Svensson et al. 2008]. Tie-points at intervals of rapid warming (inferred from sharp reductions in % N. pachyderma (s.)) are shown by solid black lines, with dotted grey lines marking the position of the recalibrated radiocarbon dates of Oppo et al. [2003] and Benway et al. [2010] (listed in table 2.2). No % N. pachyderma (s.) data was generated for much of the Holocene, as conditions were too warm for N. pachyderma (s.) to thrive (>10 °C) [Darling et al. 2006]. (c) IRD (black) and detrital carbonate (red) fluxes at Site 980. (d) Site 980 sedimentation rate calculated using new age model presented here.

The % *N. pachyderma* (s.) record generated at Site 980 (a proxy for upper ocean temperature when sea surface temperatures are between 4 °C and 10 °C [Darling et al. 2006]) was tuned to North Greenland Ice Core Project (NGRIP) $\delta^{18}O_{ice}$, a proxy record for atmospheric temperatures [North Greenland Ice Core Project Members et al. 2004],

on the GICC05 chronology [Andersen et al. 2006; Rasmussen et al. 2006; Svensson et al. 2006; Vinther et al. 2006; Svensson et al. 2008]. Intervals of rapid warming were chosen as tie-points, as the age uncertainty in identifying the midpoint of a shift is smallest when the change is most rapid. Visual correlation of the two records carried out using the Analyseries software of Paillard et al. [1996] (results shown in figure 2.4). Tuning of sea surface temperatures to the NGRIP $\delta^{18}O_{ice}$ record assumes that changes in North Atlantic are synchronous with air temperatures over Greenland. Although numerous studies support this idea [e.g. Lehman and Keigwin 1992; Bond et al. 1993; Shackleton et al. 2000], records correlated in this way are not independent, therefore great care must be taken when inferring differences in phasing [Blaauw 2012]. Linear sedimentation rates were assumed between each tie-point.

Tuning of the % *N. pachyderma* (s.) from Site 980 to the NGRIP $\delta^{18}O_{ice}$ record was guided by the counts of detrital carbonate grains in the >150 μm size fraction. Three major peaks in detrital carbonate fluxes were identified as H1, H2 and H4 (figure 2.4), correlating to layers documented across much of the North Atlantic [Andrews and Tedesco 1992; Bond et al. 1992; Hemming 2004]. Each of these is also associated with high IRD fluxes and a dominance of polar species of planktonic foraminifera, and is in good agreement with expected ages from the age model of McManus et al. [1999]. This allows the shorter-term variations in % *N. pachyderma* (s.) between the Heinrich events to be correlated to the NGRIP $\delta^{18}O_{ice}$ record with increased confidence.

The lack of a detrital carbonate peak during H3 in the Site 980 record makes the event difficult to identify. As a result, two alternative age models are presented in figure 2.5 based upon different tie points between the Site 980 % *N. pachyderma* (s.) and $\delta^{18}O_{ice}$ NGRIP records.

Correlation of new % *N. pachyderma* (s.) data to the published NGRIP $\delta^{18}O_{ice}$ record [North Greenland Ice Core Project Members et al. 2004] allows the creation of a new chronology for Hole 980A (spanning 18.3–41.5 ka). However, this technique is much less suitable for generating a chronology for the uppermost part of Hole 980B (0.8–18.3

ka). This is attributable to a combination of factors: concentrations of *N. pachyderma* (s.) are very low in the Holocene meaning that fluctuations in sea surface temperature cannot be resolved, the sample resolution of Hole B is much lower than Hole A, and the amplitude of climatic millennial-scale variations are much smaller in the Holocene than during the glacial [e.g. Bond et al. 1997].

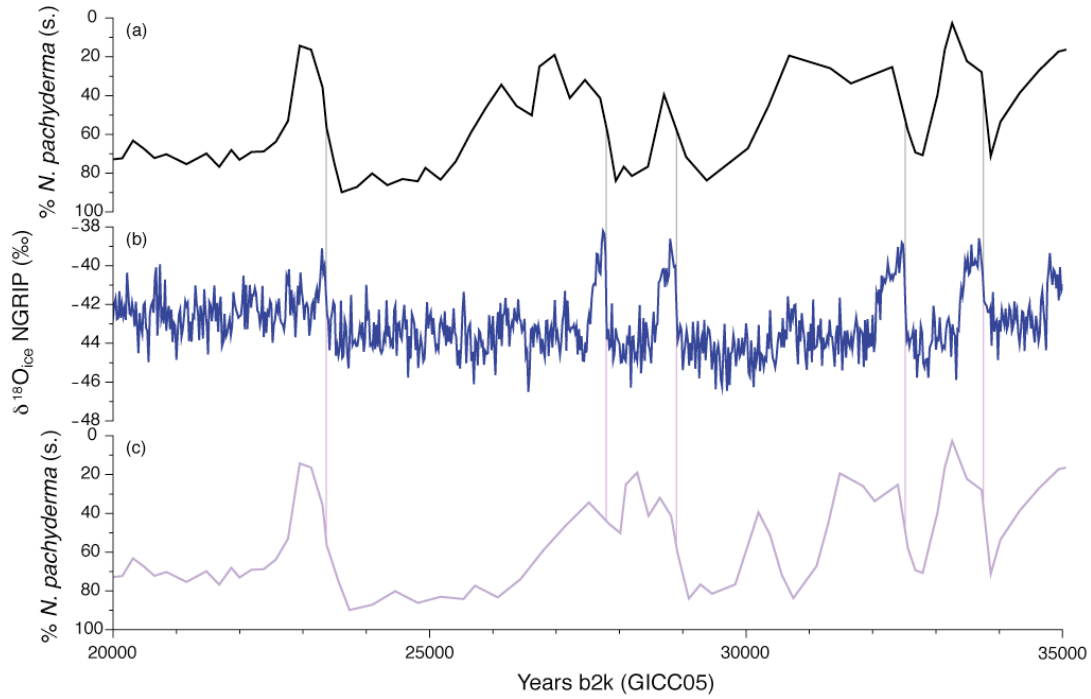

Figure 2.5: Comparison of potential age models for ODP Site 980 based upon correlations of the % N. pachyderma (s.) record to the NGRIP $\delta^{18}O_{ice}$ record. (a) Site 980 % N. pachyderma (s.) displayed on the main age model, (b) NGRIP [North Greenland Ice Core Project Members et al. 2004] (c) alternative Site 980 age model based upon different correlations for the rapid warmings into Greenland stadials 3 and 4.

Correlation of new % *N. pachyderma* (s.) data to the published NGRIP $\delta^{18}O_{ice}$ record [North Greenland Ice Core Project Members et al. 2004] allows the creation of a new chronology for Hole 980A (spanning 18.3–41.5 ka). However, this technique is much less suitable for generating a chronology for the uppermost part of Hole 980B (0.8–18.3

ka). This is attributable to a combination of factors: concentrations of *N. pachyderma* (s.) are very low in the Holocene meaning that fluctuations in sea surface temperature cannot be resolved, the sample resolution of Hole B is much lower than Hole A, and the amplitude of climatic millennial-scale variations are much smaller in the Holocene than during the glacial [e.g. Bond et al. 1997].

To circumvent these problems, the correlations with the NGRIP ice core record are supplemented with accelerator mass spectrometry radiocarbon dates of the planktonic foraminifera species *Globigerina bulloides*, *Neogloboquadrina pachyderma* (dextral) and *Neogloboquadrina pachyderma* (sinistral). These were originally published by Oppo et al. [2003] and Benway et al. [2010], but have been recalibrated to incorporate more recent refinements of the radiocarbon calibration curve since the original publication of Oppo et al. [2003]. Here, the Marine09 calibration curve of Reimer et al. [2009] is used in conjunction with the Calib 6.0 software [Stuiver and Reimer 1993; Stuiver et al. 2005] to calibrate the raw radiocarbon ages. A constant reservoir age of 400 ± 100 years is assumed for the majority of samples [Bard 1988; Reimer and Reimer 2001; Waelbroeck et al. 2001]. The exceptions to this are the Younger Dryas (800 ± 300 years) and Heinrich event 1 (1600 ± 1000 years) [Bard et al. 1994; Austin et al. 1995; Waelbroeck et al. 2001; Bondevik et al. 2006; Peck et al. 2006; Cao et al. 2007; Thornalley et al. 2011b; Stern and Lisiecki 2013], which were identified from the ice-rafted debris, detrital carbonate and % *N. pachyderma* (s.) records, at depths in excellent agreement with previous work at Site 980 [McManus et al. 1999; Benway et al. 2010]. A sample age span of 40 years per cm of depth was applied, estimated from previously published core chronologies of Site 980 [McManus et al. 1999; Oppo et al. 2003]. The median value for each calculated probability function has been quoted as the calibrated radiocarbon age in table 2.2, with errors of ± 1 sigma stated. Sample ages were converted from ‘years before 1950’ to ‘years before 2000’ by the addition of 50 years to place them onto the GICC05 chronology [Andersen et al. 2006; Rasmussen et al. 2006; Svensson et al. 2006; Vinther et al. 2006; Svensson et al. 2008].

Hole	Core	Section	Depth range (cm)	Midpoint depth (mcd)	Species	Radiocarbon age (^{14}C years)	Reservoir age (^{14}C years)	Calibrated age (years b2k)
980B	1H	1W	0-1	0.005	Gb	1060±25	400±100	630±100
980B	1H	1W	0-2	0.010	Npd	1190±35	400±100	750±100
980B	1H	1W	2-3	0.025	Gb	1330±35	400±100	870±130
980B	1H	1W	5-7	0.060	Npd	1060±30	400±100	630±100
980B	1H	1W	35-37	0.360	Npd	1710±55	400±100	1260±130
980B	1H	1W	57-58	0.575	Npd	3090±30	400±100	2890±140
980B	1H	1W	65-67	0.660	Npd	2910±35	400±100	2660±150
980B	1H	1W	74-75	0.745	Gb	3290±35	400±100	3120±150
980B	1H	1W	85-87	0.860	Npd	3670±40	400±100	3590±150
980B	1H	1W	104-105	1.045	Gb	4490±25	400±100	4670±140
980B	1H	1W	115-117	1.160	Gb	4880±50	400±100	5170±170
980B	1H	1W	135-137	1.360	Npd	6240±65	400±100	6690±150
980B	1H	2W	11-12	1.615	Gb	7230±70	400±100	7700±130
980B	1H	2W	20-22	1.710	Npd	7580±50	400±100	8050±120
980B	1H	2W	45-47	1.960	Gb	8830±45	400±100	9500±130
980B	1H	2W	65-67	2.160	Gb	9640±45	400±100	10490±140
980B	1H	2W	80-82	2.310	Npd	9620±50	400±100	10470±140
980B	1H	2W	99-100	2.495	Gb	9780±70	400±100	10690±180
980B	1H	2W	145-147	2.960	Gb	10900±55	800±300	11720±510
980B	1H	3W	0-2	3.010	Nps	11050±50	800±300	11920±450
980B	1H	3W	15-17	3.160	Nps	12050±75	400±100	13510±150
980B	1H	3W	15-17	3.160	Npd	12100±60	400±100	13550±140
980B	1H	3W	31-32	3.315	Nps	12200±55	400±100	13640±150
980B	1H	3W	31-32	3.315	Npd	12450±60	400±100	13910±140
980B	1H	3W	40-42	3.410	Nps	12550±50	400±100	14010±170
980B	1H	3W	45-47	3.460	Nps	12800±70	400±100	14480±350
980B	1H	3W	55-57	3.560	Nps	13100±55	400±100	15010±360
980B	1H	3W	55-57	3.560	Npd	12700±90	400±100	14330±360
980B	1H	3W	65-67	3.660	Nps	13250±55	400±100	15370±350
980B	1H	3W	65-67	3.660	Npd	13050±100	400±100	14880±340
980B	1H	3W	80-82	3.810	Nps	15300±80	1600±1000	16390±1490
980C	2H	1W	44-46	4.020	Nps	15350±80	1600±1000	16470±1450
980C	2H	1W	54-56	4.120	Nps	15450±55	400±100	18260±200
980C	2H	1W	70-71	4.275	Nps	16000±75	400±100	18770±120
980C	2H	1W	74-76	4.320	Nps	16450±75	400±100	19170±230
980C	2H	1W	84-86	4.420	Nps	16650±95	400±100	19390±180
980C	2H	1W	94-96	4.520	Nps	17200±85	400±100	19950±230
980C	2H	1W	114-116	4.720	Nps	17750±80	400±100	20690±270
980C	2H	1W	134-136	4.920	Nps	18500±65	400±100	21620±230

Table 2.2: Accelerator mass spectrometry (AMS) radiocarbon ages of planktonic foraminifera from Site 980 [Oppo et al. 2003; Benway et al. 2010], recalibrated using Calib6.0 [Stuiver and Reimer 1993; Stuiver et al. 2005]. Samples in red have been excluded from the age model, while those in green have been averaged,

as described in the text. Gb = Globigerina bulloides*, Npd* = Neogloboquadrina pachyderma *(dextral), Nps* – Neogloboquadrina pachyderma *(sinistral). All ages rounded to the nearest 10 years, except the errors in the radiocarbon ages, which have been rounded to the nearest 5 years.*

Mean calibrated ages have also been used where multiple measurements were taken at the same age horizon. The samples with unclaibrated radiocarbon ages of 3090 and 9640 years have been excluded due to age reversals, following the suggestion of Oppo et al. [2003]. The data point at 4.02 mcd has also been excluded, as it has a very similar age to the date 21 cm above it (at 3.81 mcd), giving an interval of unusually rapid sedimentation.

There is very good agreement between the calibrated radiocarbon ages and those generated by correlation to the NGRIP record, with only 85 years difference between estimates taken 1 cm apart at the Younger Dryas (which is well within error). However, there are greater discrepancies at Heinrich event 1. This may be a result of the greater uncertainty in estimating temporal changes in the surface ocean reservoir radiocarbon age. The radiocarbon age of the modern surface ocean is offset from the atmosphere, and varies spatially as a result of variable rates of air-sea exchange, ocean circulation, and the rate of atmospheric ^{14}C production [e.g. Mangerud 1972; Stuiver et al. 1986; Bard 1988; Stocker and Wright 1996]. A correction needs to be applied for this offset if the radiocarbon age of planktonic foraminifera is to be eventually converted into a calendar age estimate.

Unlike the Younger Dryas, published estimates of the reservoir age changes during H1 are almost entirely based upon the assumption that changes in surface ocean temperature in the North Atlantic are synchronous with the Greenland ice core records [Waelbroeck et al. 2001; Peck et al. 2006; Thornalley et al. 2011b]. However, many of the records from the northeast Atlantic (including the data presented in this chapter, figure 2.6) show evidence of warming concurrent with or only just above the H1 detrital carbonate layer [e.g. Lagerklint and Wright 1999; Cortijo et al. 2005; Peck et al. 2008; Scourse et al. 2009; Benway et al. 2010; Thornalley et al. 2011a]. This suggests either that there was

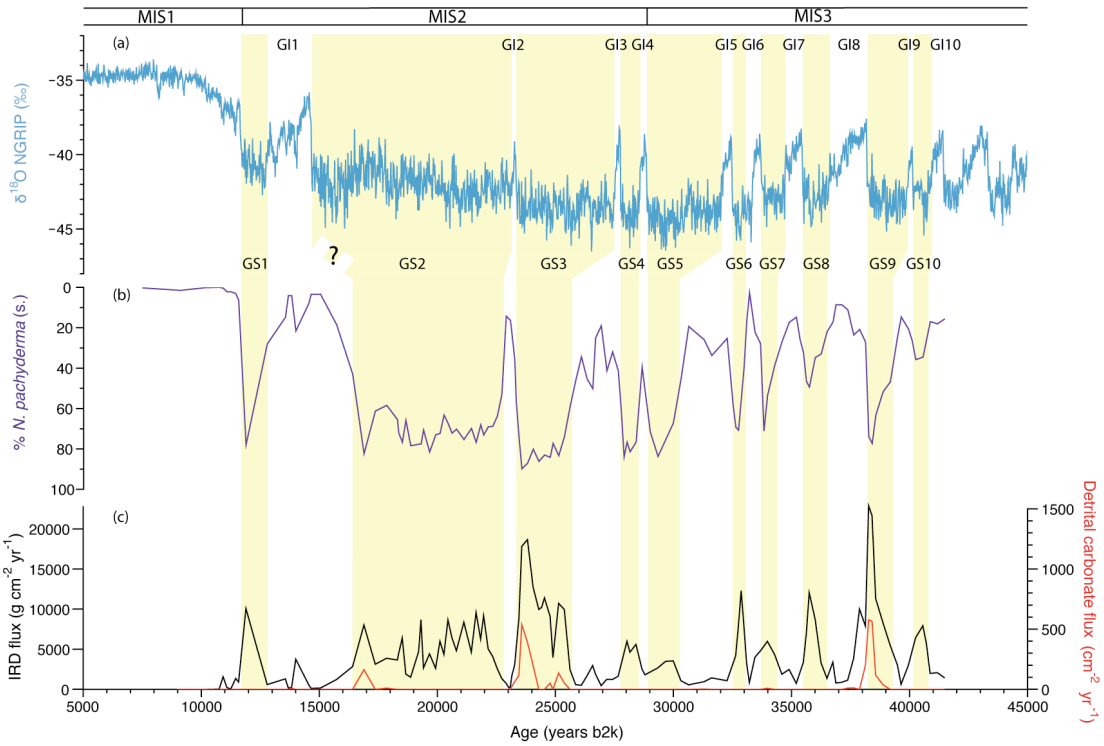

Figure 2.6: Dansgaard-Oeschger variability shown in (a) $\delta^{18}O_{ice}$ record of the NGRIP ice core [North Greenland Ice Core Project Members et al. 2004], (b) Site 980 % N. pachyderma *(s.), (c) fluxes of ice-rafted debris >150 µm (black) and detrital carbonate (red) from Site 980. All records plotted on the GICC05 chronology [Andersen et al. 2006; Rasmussen et al. 2006; Svensson et al. 2006; Vinther et al. 2006; Svensson et al. 2008]. MIS1, 2 and 3 indicate marine isotope stages (after Hays et al. [1976]). Stadial (GS) intervals are shaded in yellow with interstadials (GI) in white. Nomenclature for Greenland stadial and interstadial intervals from Björck et al. [1998] and Walker et al. [1999]. Question mark indicates uncertain correlation of the GS2-GI1 transition.*

an interval of very low sedimentation immediately after H1, high levels of bioturbation spread the warming signal preserved in the planktonic foraminifera down core or that there was some warming of the upper ocean prior to the Bølling warming (onset recorded in the NGRIP record at 14.69 ± 0.19 ka [Rasmussen et al. 2006]) in this region. If the shift in % *N. pachyderma* (s.) identified at 3.81 mcd in the Site 980 record predates the Bølling warming, it could explain why there is a large offset between the ages derived by the two different techniques at this point in the record. Estimates of changes in the surface reservoir age through H1 which are not based upon the

assumption of synchronous warming of the whole of the North Atlantic with Greenland are therefore urgently needed to test this supposition [e.g. Waelbroeck et al. 2001; Bondevik et al. 2006].

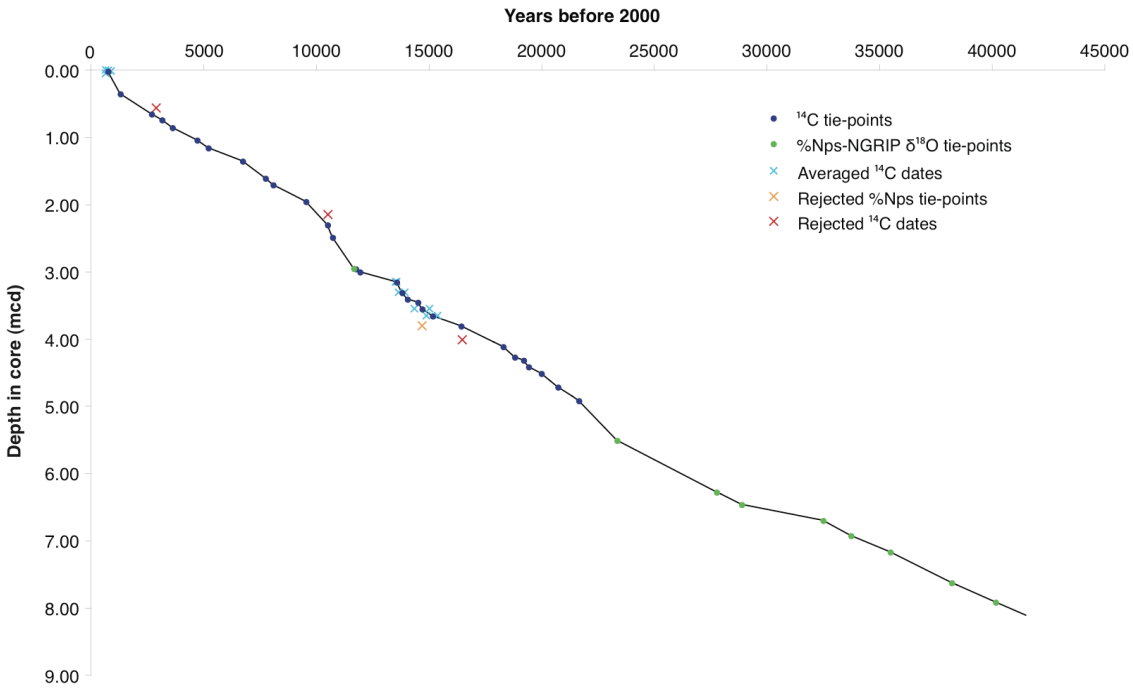

Figure 2.7: Age-depth relationship of combined Hole 980A and Hole 980B record on main new age model described here. Dots indicate tie-points used in the construction of the age model, with crosses representing rejected tie-points (reasoning explained in the text). All radiocarbon dates originally from Oppo et al. [2003] and Benway et al. [2010]. Errors in radiocarbon dates are too small to show on this plot (but are given in table 2.2). Uncertainty in positioning of NGRIP-Nps tie points estimated as a maximum of ± 750 years.

An alternative age model for the deglaciation can be created by assuming synchronous warming between the northeast Atlantic (Site 980 % *N. pachyderma* (s.)) and over Greenland (NGRIP $\delta^{18}O_{ice}$). If this scenario is valid, the offset to the radiocarbon dates in this section of the core can be explained by uncertainty in the surface reservoir age of the North Atlantic. The difference in the resulting age models is illustrated in figure 2.8. The original, radiocarbon-based age model gives an estimate of the age of the detrital carbonate layer which is in better agreement with previously published estimates [e.g. Hemming 2004; Stanford et al. 2011], hence this will be used for the rest of this study.

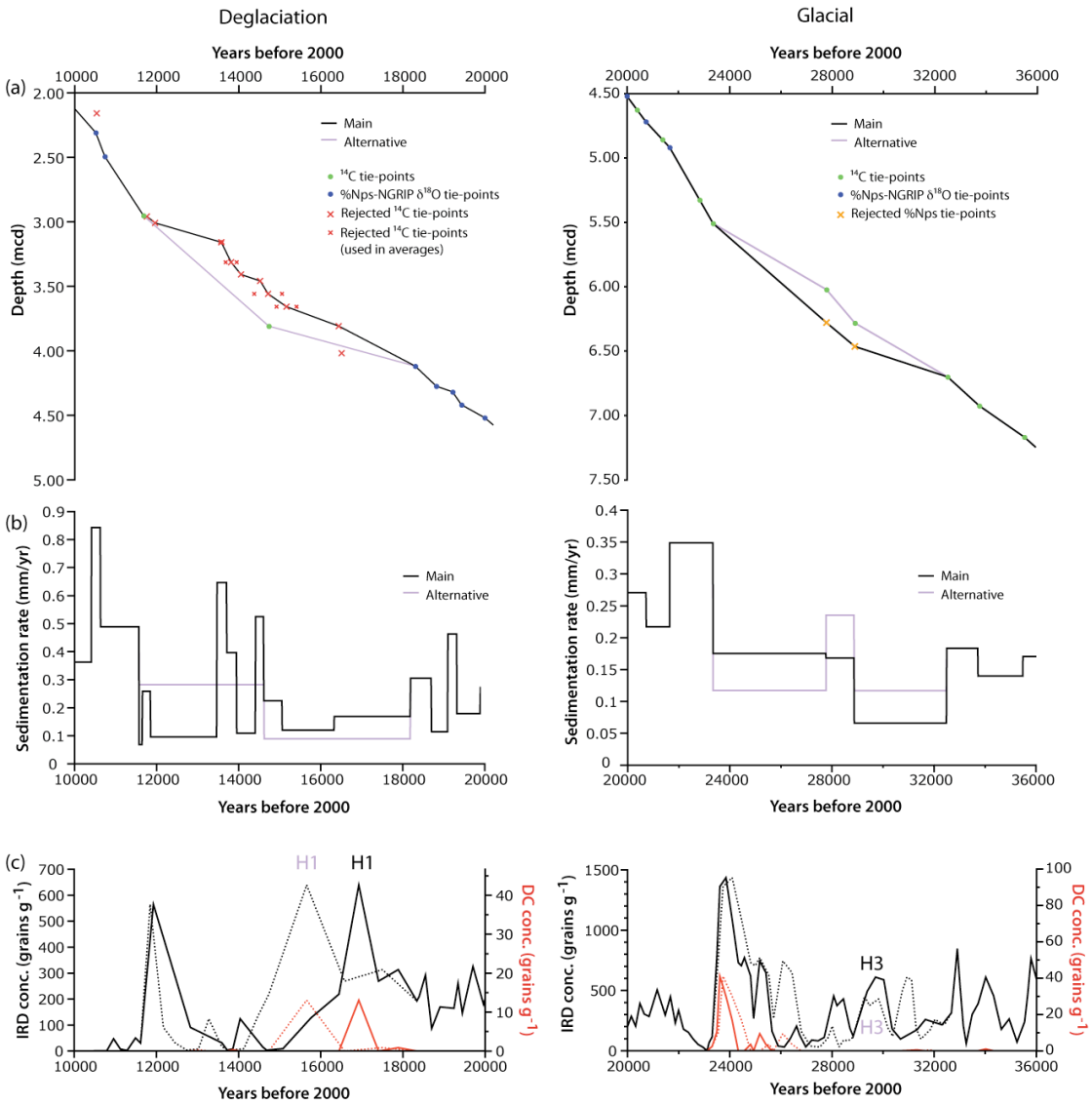

Figure 2.8: Comparison of main new age model (black/solid lines) with alternatives (purple/dotted) for the deglaciation (left) and glacial (right). (a) Age-depth models, with the position and nature of tie-points indicated. (b) Sedimentation rates calculated based upon each of the two models. (c) Concentrations of ice-rafted debris (black) and detrital carbonate (red) grains at Site 980, plotted on both age

The choice of age model through the deglaciation, however, does not alter the conclusions of this work, as the focus is on the phasing of components within a single record rather than comparison of ages between archives, and the high concentration of

detrital carbonate clearly marks the position of the H1 IRD layer. In contrast, the choice of tie-points in the glacial (shown in figure 2.5) affects the identification of the depth of H3 within the core (illustrated in figure 2.8). Both models give reasonable sedimentation rates, hence additional information is required to strengthen the chronology through this interval.

Hole	Midpoint depth (mbsf)	Depth (mcd)	Age (years before 2000)	Description
980B	0.025	0.025	772	Mean of top 4 recalibrated ^{14}C dates (1)
980B	0.360	0.360	1311	Recalibrated ^{14}C date (1)
980B	0.660	0.660	2710	Recalibrated ^{14}C date (1)
980B	0.745	0.745	3175	Recalibrated ^{14}C date (1)
980B	0.860	0.860	3636	Recalibrated ^{14}C date (1)
980B	1.045	1.045	4720	Recalibrated ^{14}C date (1)
980B	1.160	1.160	5225	Recalibrated ^{14}C date (1)
980B	1.360	1.360	6742	Recalibrated ^{14}C date (1)
980B	1.615	1.615	7755	Recalibrated ^{14}C date (1)
980B	1.710	1.710	8097	Recalibrated ^{14}C date (1)
980B	1.960	1.960	9551	Recalibrated ^{14}C date (1)
980B	2.310	2.310	10522	Recalibrated ^{14}C date (1)
980B	2.495	2.495	10742	Recalibrated ^{14}C date (1)
980B	2.954	2.954	11685	Correlated warming out of YD
980B	2.960	2.960	11770	Recalibrated ^{14}C date (1)
980B	3.010	3.010	11965	Recalibrated ^{14}C date (2)
980B	3.160	3.160	13581	Mean of 2 recalibrated ^{14}C dates (2)
980B	3.315	3.315	13821	Mean of 2 recalibrated ^{14}C dates (2)
980B	3.410	3.410	14062	Recalibrated ^{14}C date (2)
980B	3.460	3.460	14530	Recalibrated ^{14}C date (2)
980B	3.560	3.560	14722	Mean of 2 recalibrated ^{14}C dates (2)
980B	3.660	3.660	15171	Mean of 2 recalibrated ^{14}C dates (2)
980B	3.810	3.810	16444	Recalibrated ^{14}C date (2)
980C	4.120	4.120	18306	Recalibrated ^{14}C date (2)
980C	4.275	4.275	18818	Recalibrated ^{14}C date (2)
980C	4.320	4.320	19220	Recalibrated ^{14}C date (2)
980C	4.420	4.420	19437	Recalibrated ^{14}C date (2)
980C	4.520	4.520	20002	Recalibrated ^{14}C date (2)
980C	4.720	4.720	20744	Recalibrated ^{14}C date (2)
980C	4.920	4.920	21670	Recalibrated ^{14}C date (2)
980A	1.629	5.510	23367	Correlated warming out of H2/into GI-2
980A	2.366	6.281	27789	Correlated warming into GI-3
980A	2.541	6.467	28898	Correlated warming out of H3/into GI-4
980A	2.763	6.702	32515	Correlated warming into GI-5
980A	2.975	6.927	33749	Correlated warming into GI-6
980A	3.204	7.170	35500	Correlated warming into GI-7
980A	3.639	7.632	38225	Correlated warming out of H4/ into GI-8
980A	3.893	7.916	40166	Correlated warming into GI-9

Table 3.3: Tie points used in the construction of the main new ODP Site 980 age model. Radiocarbon dates all originally from (1) Oppo et al. [2003] and (2) Benway et al. [2010]. Correlated points based upon matching Site 980 % N. pachyderma (s.) record to the NGRIP $\delta^{18}O_{ice}$ record [North Greenland Ice Core Project Members et al. 2004].

The presence of several ash layers, widely documented across the North Atlantic, can be used to provide an independent test of the new chronology for ODP Site 980 presented here. It is very difficult to differentiate between grains transported by ice-rafting and ash particles purely on the basis of lithic counts (discussed more in section 2.7.4.1). However, peaks in lithic grains of volcanic origin not in proportion to the total IRD flux can be seen at 28.1 ka and 37.7 ka (figure 2.9), which approximately correlate with the Fugloyarbanki/Faeroe Marine Ash Zone II and Faeroe Marine Ash Zone III, reported at 26.7 ± 0.4 ka [Svensson et al. 2006; Davies et al. 2008; Lowe et al. 2008] and 38.1 ± 0.7 ka [Svensson et al. 2006; Davies et al. 2010]. The presence of an ash peak at 28.1 ka supports the use of the main chronology over the alternative correlation presented in figure 2.5 (which gives the ash peak an estimated age of 29.3 ka) as it is closer to the published Fugloyarbanki/Faeroe Marine Ash Zone II age estimates. Therefore, the main chronology will be used throughout the remainder of this study.

The greatest fluxes of volcanic grains in the Site 980 record occur during the Younger Dryas (11.9 ka), most likely corresponding to the Vedde Ash (reported at 12.1 ± 0.1 ka [Mangerud et al. 1984; Rasmussen et al. 2006]). The geochemistry of ash layers can be used to trace their provenance, increasing confidence in site-to-site correlations [e.g. Mangerud et al. 1984; Grönvold et al. 1995; Lacasse et al. 1995; Wastegård et al. 2006; Thornalley et al. 2011b], however, there is no geochemical data for the volcanic grains identified at Site 980. Therefore, the published ages of these ash layers have not been incorporated into the new age model, however their presence at the expected ages within the core adds confidence to the new chronology presented here.

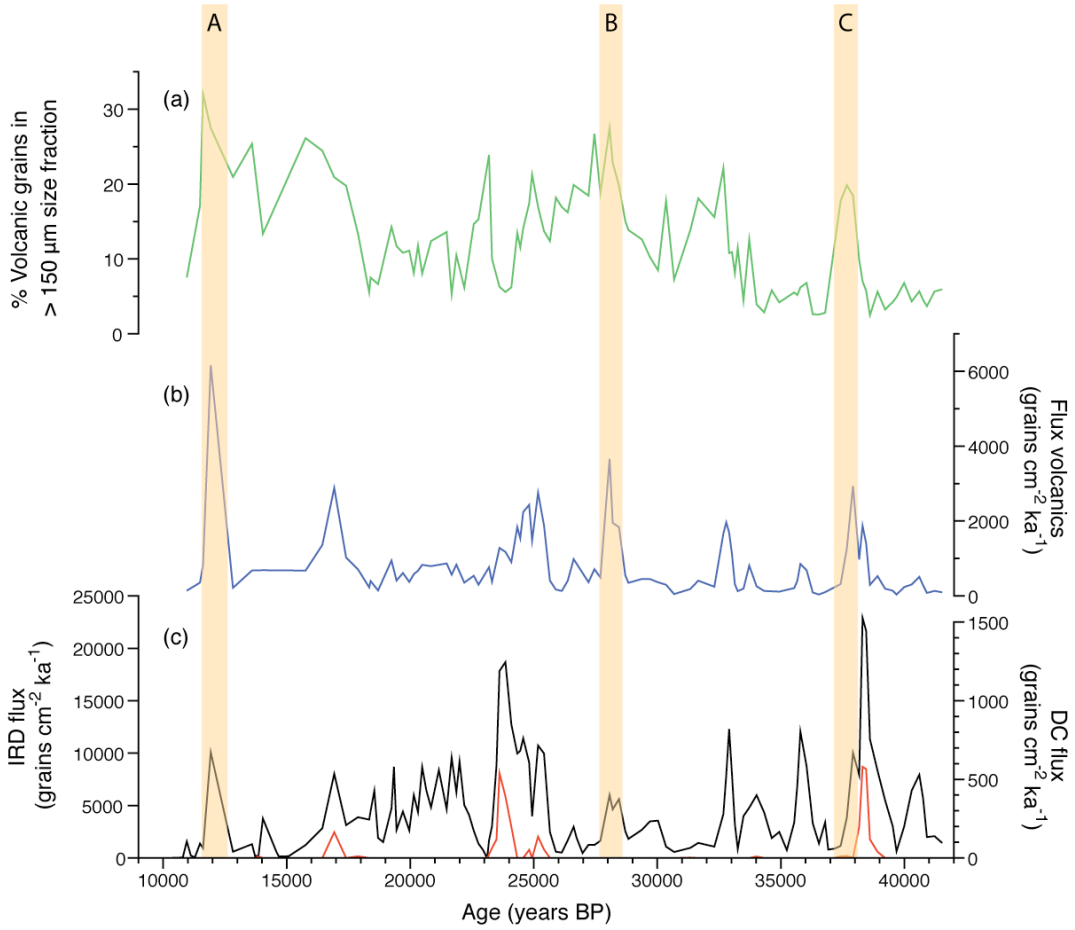

Figure 2.9: Identification of ash layers at Site 980. (a) Proportion of the total lithic grains >150 µm size fraction that are volcanic in origin, (b) flux of volcanic grains >150 µm, (c) total flux of IRD (black) and detrital carbonate grains (red) (both >150 µm). Ash layers are shaded in orange with probable identifications: (A) Vedde Ash, (B) Fugloyarbanki/Faeroe Marine Ash Zone II and (C) Faeroe Marine Ash Zone III. Ash layer identification is complicated by the fact that volcanic grains can also be transported by ice-rafting, hence they were identified by an increased volcanic grain flux not in proportion to the total IRD flux, and an increase in the proportion of volcanic grains in the > 150 µm size fraction (although an increase in the proportion of icebergs from volcanic-dominated areas cannot be ruled out as a contributing factor).

2.6 Results

Down core records of the fluxes of ice-rafted debris (including detrital carbonate and groups of lithologies attributed to input from Britain and Iceland), planktonic foraminifera, *C. wuellerstorfi* and the percentages of *N. pachyderma* (s.) from ODP Site 980 are all illustrated in figure 2.10. Data is plotted on the new age model for Site 980 (as described in section 2.5), with the NGRIP $\delta^{18}O_{ice}$ record [North Greenland Ice Core Project Members et al. 2004; Andersen et al. 2006; Rasmussen et al. 2006; Svensson et al. 2006; Vinther et al. 2006; Svensson et al. 2008] and Site 980 bulk core magnetic susceptibility [Jansen et al. 1996] included for comparison.

2.6.1 % *N. pachyderma* (s.)

Throughout the glacial part of the record (980A), the percentage of the planktonic foraminifera *N. pachyderma* (s.) (% Nps) oscillates between very low (typically <20 %) and very high (>70 %) percentages (figure 2.10(b)). This is likely to be an underestimate of the original variability, due to attenuation of the original signal in the stratigraphic record by bioturbation [Anderson 2001]. A longer interval of dominance of the planktonic faunal record by *N. pachyderma* (s.) is found at the last glacial maximum (LGM), with cold sea surface temperatures dominating the study site from 22.7 ka to 16.9 ka. A longer term shift towards increasing % Nps values during both stadial and interstadial conditions can be seen through MIS3 and 2, approaching the LGM. Typical stadial values increase from 50 % to >80 %, with interstadial values increasing from 15 % to 35 %. Not all stadials are characterized by the same magnitude increase in % Nps. Heinrich event 4 is much more pronounced than the preceding and subsequent stadial periods, and the highest proportions of *N. pachyderma* (s.) in the whole record are recorded during H2. However, cooling of surface waters (as indicated by the % Nps record) is no more pronounced during H1 or H3 than the adjacent stadial intervals.

In contrast, the percentages of *N. pachyderma* (s.) are very low in the majority of samples examined from Hole 980B (<3 %), indicating the persistence of warm upper ocean temperatures in the northeast Atlantic during the Holocene. High % Nps values around 17 ka correspond with a peak in detrital carbonate abundance, indicating that sea

surface temperatures were cold at H1, but warmed rapidly afterwards, with % Nps values of 3–5 %. This warming may have predated the warming into the Bølling interval/Greenland Interstadial 1e, as documented in the Greenland ice core records [Dansgaard et al. 1993; Björck et al. 1998]. A brief interruption in this warm interval is found at 14.0 ka with % Nps reaching 22 %, with the timing suggesting that this event may correspond to the Older Dryas (GI-1d), although the low sample resolution here makes identification uncertain. A more dramatic increase in % Nps at 11.9 ka is identified as the Younger Dryas (GS1). Percentages of *N. pachyderma* (s.) are very low in the Holocene, with values below 3 %. This suggests that the specimens identified as *N. pachyderma* (s.) may instead be left-coiling morphotypes of the warmer water species *Neogloboquadrina incompta,* which is typically right-coiling. Genetic studies have demonstrated that both *N. pachyderma* and *N. incompta* have specimens with aberrant coiling directions, which cannot easily be distinguished visually from tests of the other species exhibiting typical coiling directions [Bauch et al. 2003; Darling et al. 2006]. Sea surface temperature fluctuations therefore cannot be resolved by % Nps in the Holocene as sea surface temperatures were too warm for the species to thrive (>10 ^{o}C) [Darling et al. 2006], in agreement with previous estimates by McManus et al. [1999].

2.6.2 Ice-rafted debris

The total flux of ice-rafted debris (IRD) in the uppermost part of the core (the Holocene) is minimal, showing a very similar trend to the % Nps data (illustrated in figure 2.10(c)). In contrast, IRD fluxes show very strong variability from the base of the record at 42,000 years BP to 10,000 years BP, oscillating between high (stadial) and low (interstadial) coarse lithic inputs, in very good agreement with the Dansgaard-Oeschger variability documented in Greenland ice cores [Dansgaard et al. 1993] and the Site 980 % Nps data (figure 2.10).

Maximum IRD fluxes of >18,000 grains cm^{-2} ka^{-1} are identified during Heinrich events 4 and 2, well above the typical stadial fluxes of 5,000–12,500 grains cm^{-2} ka^{-1} (figure 2.10(c)). H3, H1 and the Younger Dryas can also be distinguished on the basis of

elevated IRD fluxes, although these are much less distinctive, and more typical of the non-Heinrich stadial intervals.

The detrital carbonate (DC) record clearly indicates the position of H1, 2 and 4 in the record, with peak fluxes for each event of 160–580 grains cm^{-2} ka^{-1}. Detrital carbonate fluxes are either zero or negligible throughout the rest of the record. At Heinrich events, the peaks in total IRD flux typically longer in duration than the detrital carbonate peaks, with increases in detrital carbonate generally appearing slightly delayed compared to the total IRD flux.

The IRD peak during Heinrich event 2 occurs in two phases. An increase in the IRD flux to 10,000 grains cm^{-2} ka^{-1} (approximately equal to that at some of the larger preceding stadials) occurs at 25.4 ka, with values remaining roughly constant until 24.3 ka when the flux increases further to 18,000 grains cm^{-2} ka^{-1}, before dropping to very low values by 23.2 ka. The detrital carbonate record shows a first peak concurrent with the initial IRD flux increase at 25.4 ka. Values then drop back to zero for ca. 250 years before reaching a second (much larger) maximum, coincident the IRD maximum at 23.6 ka.

2.6.3 Flux of foraminifera

Fluxes and variability in the fluxes of both planktonic foraminifera and the benthic species *C. wuellerstorfi* are much greater during MIS3 than MIS2 (with the exception of the deglaciation), with the Holocene and deglacial transition marked by high fluxes of planktonic foraminifera. Increased stadial fluxes of *C. wuellerstorfi* during MIS3 are not as clearly expressed in the planktonic foraminiferal fluxes.

There is no simple pattern in the fluxes of either total planktonic foraminifera or *C. wuellerstorfi* at Heinrich events. Both are relatively high during H4 and during at H3 (but with neither event standing out above background variability). There is a strong decrease in fluxes of both planktonic foraminifera and *C. wuellerstorfi* through H2, from relatively high values at the start of the IRD increase to very low values concurrent with

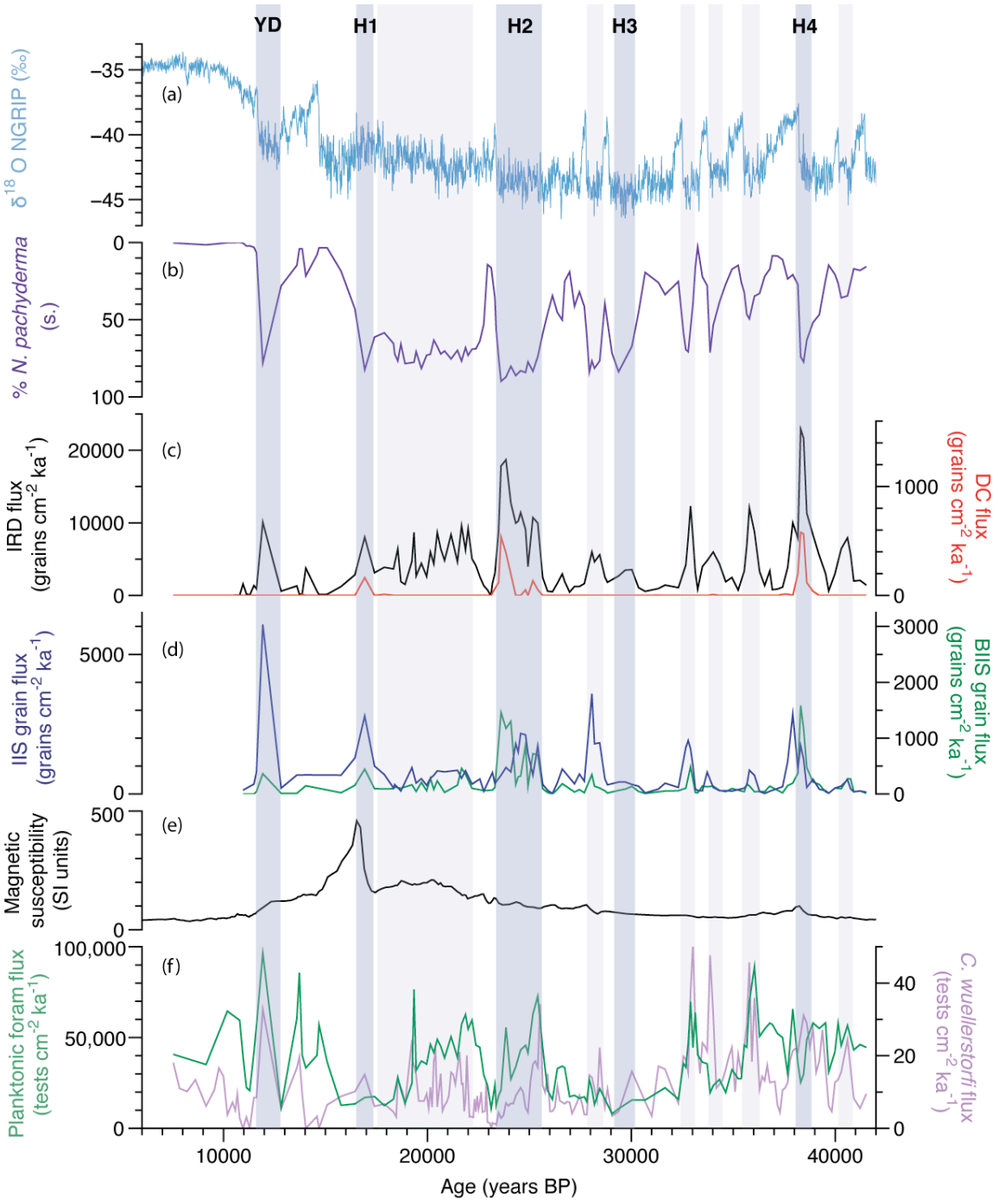

Figure 2.10: Comparison of IRD and foraminiferal records from Site 980, plotted on the new age model. (a) $\delta^{18}O_{ice}$ record of the NGRIP ice core [North Greenland Ice Core Project Members et al. 2004], (b) % N. pachyderma (s.), (c) Flux of ice-rafted debris >150 µm (black) and detrital carbonate (red), (d) Flux of ice-rafted debris >150 µm with lithologies attributed to the Icelandic Ice Sheet (IIS, navy) and British

and Irish Ice Sheet (BIIS, green), (e) Magnetic susceptibility of the spliced Site 980 record [Shipboard Scientific Party 1996b], (f) Flux of planktonic foraminifera (green) and C. wuellerstorfi (purple). Dark shading marks the position of Heinrich events 1-4, with the stadials in a lighter colour.

the drop in IRD after the event. Both records show increases up to and through H1 before dropping again (although peak *C. wuellerstorfi* fluxes are reached before peak planktonic foraminifera).

In general, fluxes of total planktonic foraminifera and the benthic species *Cibicides wuellerstorfi* show good agreement throughout the whole record (illustrated in figure 2.10(f)). *C. wuellerstorfi* is an epifaunal species, typically associated with high bottom current velocities [Linke and Lutze 1993; Wollenburg and Mackensen 1998; Gupta and Thomas 2003]. However, fluxes of organic matter from the surface have also been proposed to control its distribution [Belanger and Streeter 1980; Mackensen et al. 1985]. The correspondence between the fluxes of planktonic foraminifera and *C. wuellerstorfi* adds support to the suggestion that the temporal distribution of *C. wuellerstorfi* at Site 980 is strongly influenced by surface productivity, although bottom current circulation is believed to be generally most vigorous at times when surface conditions are warm and planktonic foraminiferal fluxes are high, making the dominant factor difficult to ascertain [Rahmstorf 1994; Sarnthein et al. 1994; van Kreveld 1996; Alley et al. 1999]. Increased *C. wuellerstorfi* fluxes during the stadial intervals therefore suggest either that the relationship between sea surface temperature, productivity and benthic foraminiferal assemblages is complex [e.g. Wollenburg and Mackensen 1998; Murray 2006] or that bottom currents at Site 980 were stronger during stadial intervals than interstadials. The influence of variable dilution on the concentrations of both types of foraminifera also cannot be ruled out.

2.7 Discussion

2.7.1 Decoupling of sea surface temperatures and flux of ice-rafted debris

The records of ice-rafted debris flux and % *N. pachyderma* (s.) (a proxy for sea surface temperature) are generally very closely coupled throughout the last 40,000 years, with both proxies illustrating strong synchronous variation over millennial time scales (illustrated in figure 2.10). However, the two proxy records show different longer-term trends. Both the stadial and interstadial planktonic foraminiferal fauna (illustrated by % Nps) show a gradual progression towards colder temperatures through marine isotope stages (MIS) 3 and 2, approaching the LGM. However, with the exception of Heinrich events 2 and 4, neither the stadial nor interstadial IRD flux changes significantly through this interval.

Decreasing sea surface temperatures during stadial intervals approaching the LGM therefore seem to have little impact on the flux of IRD to the sediments. This suggests that iceberg survivability is not the dominant control on the IRD flux to Site 980 through the last glacial, as originally suggested by Bond and Lotti [1995], unless temperature changes along the path of iceberg transport were the main determining factor and showed a different trend to that at our site. However, the long term cooling trend approaching the last glacial maximum has been well documented at numerous localities [Sancetta et al. 1973; Broecker et al. 1992; Bond et al. 1993; Oppo and Lehman 1995; van Kreveld 1996; Elliot et al. 1998]. It therefore seems likely that variability in the flux of IRD to ODP Site 980 is a result of changes in the surface ocean circulation patterns, iceberg production and/or iceberg sediment load.

2.7.2 Atypical nature of ODP Site 980

Despite being located at the edge of the well-documented North Atlantic Heinrich IRD belt (illustrated in figure 2.1) [Ruddiman 1977; Hemming 2004], ODP Site 980 does not show some of the classic features associated with Heinrich events. One example of this is the flux of planktonic foraminifera, suggested as a useful approximation of primary productivity (particularly with asymbiotic species) in regions with low organic carbon and potential contamination by terrestrial organic matter [Thunell and Reynolds 1984; van Kreveld 1996; Žarić et al. 2005]. In the main IRD belt, fluxes of foraminiferal tests

drop to very low numbers during Heinrich events as a result of a decreased production rate of foraminifera and dilution driven by an increased flux of IRD [Bond et al. 1992; Broecker et al. 1992; van Kreveld 1996]. This productivity drop is also seen in dinocyst assemblages [Radi and de Vernal 2008], coccolith and biogenic carbonate mass accumulation rates [van Kreveld et al. 1996] and benthic foraminiferal assemblages [Thomas et al. 1995]. Low productivity is attributed to melt water and turbidity from melting icebergs [van Kreveld 1996], which is supported by pronounced shifts to lighter planktonic oxygen isotope values between 43°N and 50°N [Cortijo et al. 1997]. In contrast, some North Atlantic sites instead show increases in planktonic foraminiferal concentration with increased lithic content, including the Irminger Basin [Elliot et al. 1998] and Faeroe-Shetland Channel [Rasmussen et al. 1996]. Increases in productivity are also supported by diatom assemblages [Sancetta 1992], attributed to high productivity at the sea ice edge when it is located over the site [Carstens et al. 1997; Elliot et al. 1998]. Polynya formation, increased nutrient supplies and mixing by deep-keeled icebergs may also play a role in increasing productivity [Sancetta 1992; Carlson et al. 1998; Sweeney et al. 2000].

Heinrich events are not prominent in the record of foraminiferal fluxes at ODP Site 980 (figure 2.10(f)), despite evidence of melt waters reaching the nearby site BOFS 5K during each of H1 to 4 [Maslin et al. 1995]. During the LGM, it has been proposed that Site 980 was located either just to the north of the summer sea ice limit [de Vernal et al. 2005; Hillaire-Marcel and de Vernal 2008] or close to the winter sea ice limit [Sarnthein et al. 2003], depending on the reconstruction technique used. Sea ice cover reduces the flux of planktonic foraminifera by approximately an order of magnitude in the Fram Strait today when compared to ice-free areas [Carstens et al. 1997]. Maximum fluxes occur along the ice margin, attributed to a high food supply due to increased primary production [Smith Jr. et al. 1987; Carstens et al. 1997], however, an unstable ice margin can result in much lower productivity [Carstens et al. 1997]. Therefore, the variable foraminiferal fluxes observed at Site 980 may be a result of a combination of increased accumulation when there is a stable ice edge close to the site and reduced accumulation when icebergs are particularly abundant, the ice margin is unstable or when there is a

permanent sea ice cover. Each sample is an integration of the surface ocean conditions over tens or hundreds of years, and hence, seasonal and annual fluctuations in sea ice extent are smoothed in the sedimentary record.

A further illustration of the complex relationship between surface ocean conditions and foraminiferal flux occurs during H2. An increased flux of both planktonic foraminifera and *C. wuellerstorfi* occurs in the early part of the event where IRD fluxes are moderate, but then decreases as the IRD flux increases (figure 2.10). This observation could be a result of increasing iceberg melting over the site in the later stages of H2, leading to low salinities and high turbidities and creating inhospitable conditions (although dilution by increased IRD fluxes also likely plays a role). However, foraminiferal fluxes reach their lowest values as the flux of IRD drops to very low levels just above the H2 detrital carbonate layer (figure 2.10). If the low foraminiferal flux is a result of extremely low productivity, this suggests either highly unstable surface conditions or a permanent sea ice cover, however, a low proportion of *N. pachyderma* (s.) in the planktonic foraminiferal assemblage suggests that sea surfaces are relatively warm, arguing against a permanent sea ice cover. The observed decrease in % Nps cannot be explained by salinity changes, as *N. pachyderma* (s.) is more tolerant of low salinities than other high latitude species [Volkmann 2000]. In addition, species outside their optimum conditions often exhibit smaller tests, which would bias the assemblage in the 150–500 μm size fraction towards the larger *N. pachyderma* (s.) [Boltovskoy and Wright 1976; Bijma et al. 1990]. Sediment layers of low foraminiferal concentration are also particularly susceptible to the effects of bioturbation, as particles are moved from regions of high concentrations to low [Manighetti et al. 1995; Hodell et al. 2010]. However, because the low % *N. pachyderma* (s.) values do not extend significantly beyond the interval of low foraminifera accumulation, bioturbation cannot easily explain the apparent warm sea surface temperatures.

An alternative explanation for the low foraminiferal and IRD fluxes is dilution by fine grained, sediment-laden melt water plumes, as has been observed along the Nordic margins and northwest Atlantic [e.g. Bout-Roumazeilles et al. 1999; Lekens et al. 2005; Jessen et al. 2010]. The lack of a benthic oxygen isotope excursion would argue against

the influence of hyperpycnal plumes as invoked by Stanford et al. [2011] and instead suggest the settling of fine material from surface waters, linked to ice sheet disintegration and meltwater release, as proposed by Lekens et al. [2005]. A large input of freshwater to the surface ocean occurring after the deposition of the H2 IRD layer is supported by an excursion of almost 2 ‰ in the $\delta^{18}O$ of the surface-dwelling planktonic foraminifera *G. bulloides* at nearby Porcupine Bank site MD01-2461 [Peck et al. 2006], with a drop in sea surface salinity around this time identified in MD95-2002 [Auffret et al. 2002]. Low salinity, sediment-laden surface waters would also likely dampen productivity, hence the low fluxes of foraminifera may be attributable to a combination of dilution and reduced production.

Prominent magnetic susceptibility anomalies during Heinrich events have been widely documented across the North Atlantic, however (with the exception of H1), no major anomalies are seen at Site 980 (figure 2.10). "Classic" North Atlantic Heinrich layers (as expressed in cores within the IRD belt of Ruddiman [1977]) show an increase in magnetic susceptibility to more than double background values [e.g. Grousset et al. 1993; Robinson et al. 1995; Hemming 2004], which has been attributed to an increase in titanomagnetite transported in the IRD fraction from lower Palaeozoic basic and ultrabasic volcanics from the Gulf of St. Lawrence region, and lower Tertiary basalts from Baffin Island and West Greenland, with additional potential sources in Iceland, Scotland and East Greenland [Robinson et al. 1995; Stoner et al. 1996; Thouveny et al. 2000; Walden et al. 2007; Watkins et al. 2007]. However, the trend of increased magnetic susceptibility is not seen in all parts of the North Atlantic. Reduced magnetic susceptibility at Heinrich events (and to a lesser extent, stadials) has been observed in the Nordic Seas and areas directly in the path of overflow waters from the Nordic Seas (see figure 2.11). This drop in susceptibility has been attributed to reduced bottom water circulation transporting less titanomagnetite from the Greenland-Scotland Ridge [Moros et al. 1997; Kissel et al. 1999; Ballini et al. 2006]. Heinrich events at these sites are marked by decreased mean grain sizes in the < 20 μm size fraction [Moros et al. 1997], a decrease in the magnetic grain size [Rasmussen et al. 1996; Kissel et al. 1999], and a

shift in the clay mineralogy, with a drop in the proportion of smectite [Gehrke et al. 1996; Ballini et al. 2006].

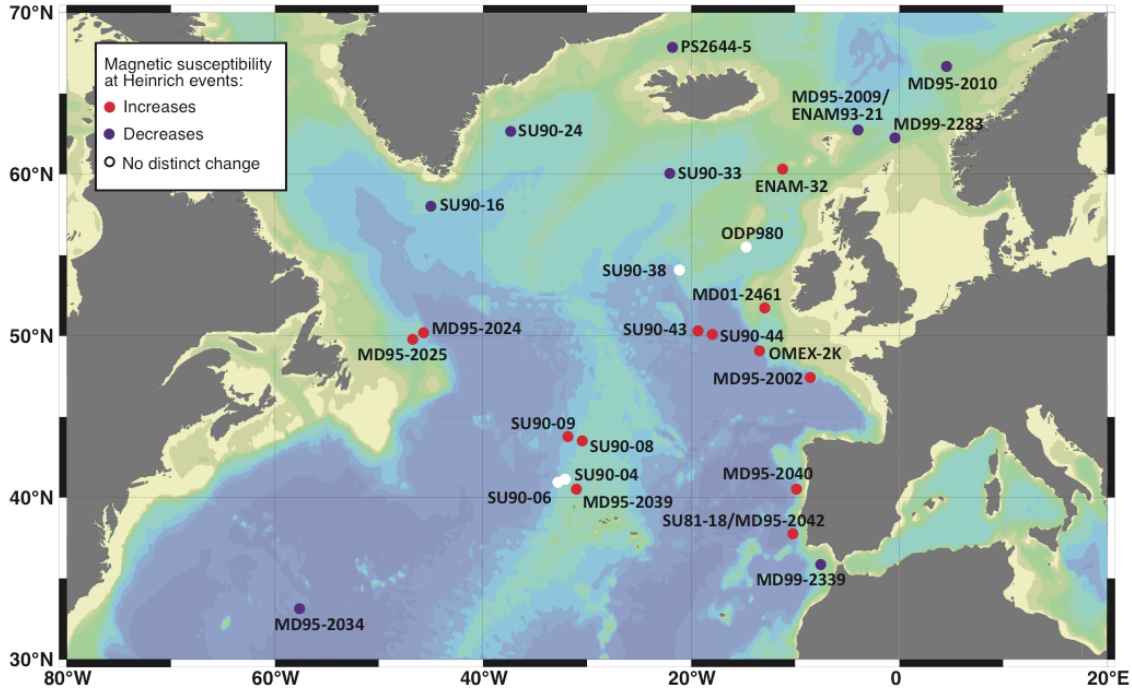

Figure 2.11: Generalised spatial patterns of magnetic susceptibility variation across the North Atlantic for H1–6. None of the sites show a switch between positive and negative magnetic susceptibility anomalies between events, suggesting that the drivers of variability in sediment magnetic susceptibility in the North Atlantic do not vary significantly between events. Dots show location of previously published records [Ruddiman 1977; Grousset et al. 1993; Rasmussen et al. 1996; Kissel et al. 1998; Kuijpers et al. 1998; Cayre et al. 1999; Dokken and Jansen 1999; Kissel et al. 1999; Grousset et al. 2000; Scourse et al. 2000; Thouveny et al. 2000; Weber et al. 2001; de Abreu et al. 2003; Lekens et al. 2006; Voelker et al. 2006; Peck et al. 2007; Walden et al. 2007]. Map created using Ocean Data View, and plotted using linear scales of latitude and longitude [Schlitzer 2013].

ODP Site 980 is geographically located between the two magnetic susceptibility regimes described above, with increased magnetic susceptibility during Heinrich events to the south and mostly decreased magnetic susceptibility to the north and west [Kissel 2005]. The strong detrital carbonate signal seen at Site 980 suggests that the site is influenced by icebergs sourced from the Laurentide Ice Sheet, hence the transport of titanomagnetite from nearby rock formations might also be expected. However, the proportion of detrital carbonate in the IRD fraction is much lower at Site 980 (2–3 % of the total IRD flux at H1, H2 and H4) when compared to sites within the main IRD belt, such as SU90-08 (8–20 %) [Grousset et al. 1993], hence the flux of titanomagnetite transported from the northwest Atlantic in the IRD fraction is also likely to be significantly reduced at Site 980.

The location of ODP Site 980 in one of the major sediment drifts of the North Atlantic (the Feni Drift) highlights the sensitivity of the site to bottom water velocities. Intermediate and deep currents bathing the site today are travelling southwards, with a combination of overflowing waters from the Nordic Seas and recirculating Atlantic waters flowing anticlockwise around the Rockall Trough [e.g. Ellett and Roberts 1973; New and Smythe-Wright 2001]. Assuming that the anticlockwise direction of deep water circulation was maintained during the last glacial interval, fine titanomagnetite particles could be transported from the Greenland-Scotland Ridge to the Feni Drift. A reduction in current velocity (as proposed at Heinrich events [e.g. Keigwin and Lehman 1994; Manighetti and McCave 1995; McManus et al. 2004]) would result in a decrease in the size of grains that could be transported by bottom currents (and possibly also a decrease in erosion), resulting in fewer high magnetic susceptibility grains being transported to the site [Manighetti et al. 1995; McCave et al. 1995a; McCave et al. 1995b]. Therefore, absence of an distinctive shift in magnetic susceptibility during Heinrich events at ODP Site 980 could be explained by a combination of the opposing influences of a small increase in the flux of titanomagnetite transported from the northwest Atlantic in the IRD fraction, and a reduction in the strength of bottom currents, resulting in a drop in transport of titanomagnetite from the Greenland-Scotland Ridge [Kissel 2005; Kissel et al. 2009].

The only Heinrich event to show a clear excursion in the Site 980 magnetic susceptibility record is H1, with values approximately double glacial background values. There is little indication that a more vigorous current flow was maintained than during the other Heinrich events [e.g. McManus et al. 2004; Praetorius et al. 2008], which would have resulted in an increased transport of titanomagnetite from the Greenland-Scotland Ridge (see chapter 4 for further discussion of bottom water circulation). There is no drop in the flux of planktonic foraminifera at H1 to suggest a greater fall in productivity than during other Heinrich events, which would concentrate the magnetic particles (although a drop in the accumulation rate of the fine fraction significantly greater than the other Heinrich events cannot be ruled out). It seems that the most likely explanation, therefore, is an increase in the delivery of titanomagnetite to the Rockall Trough from the northwest Atlantic at this time, either attributable to greater iceberg production, a higher iceberg sediment content or favourable patterns of sea surface temperatures and/or currents.

The magnetic susceptibility record provides a perfect illustration of the sensitivity of the sediments recovered at ODP Site 980 to changes in both the surface and deep ocean. This makes the site an ideal location to study links and phasings between the different components of the ocean system. The differences in the magnetic susceptibility patterns at Heinrich events between sediment cores also highlights the danger of using susceptibility records to correlate between sites over long distances in the North Atlantic region, where the patterns of bottom current circulation and transport and sources of ice-rafted material under glacial conditions are complex.

2.7.3 Expression of Dansgaard-Oeschger events in ice core and sediment records

The Dansgaard-Oeschger events in the NGRIP $\delta^{18}O_{ice}$ record exhibit a strong saw-tooth shape with a rapid warming followed by a gradual cooling. This distinctive profile is not as clear for the corresponding events in the sedimentary record from Site 980 (figure 2.6). The most notable discrepancy between the two climatic archives is a difference in the proportion of the record illustrating stadial versus interstadial conditions during

MIS2 and 3. The sedimentary record suggests that similar proportions of time are spent under stadial and interstadial conditions until the longer stadial GS2. The ice core record shows a much higher proportion of time under stadial conditions. The difference between the two archives is most notable during the longer stadials, particularly GS5 and GS3. One possible explanation for this difference is that the signal in the sediment core is smoothed by bioturbation, which results in signal smoothing, attenuation and possibly a shift in the position of the peak of any excursion, and hence could result in the attrition of a saw-tooth pattern [Anderson 2001]. However, it seems unlikely that bioturbation alone can explain the proportions of the record recording stadial and interstadial conditions

An alternative explanation for this difference between the NGRIP and Site 980 records is that the sedimentation rate is much higher during the warmer interstadial conditions. As only one tie-point is used in the age control per stadial-interstadial cycle (as can be seen in figure 2.4), major fluctuations in sedimentation rate between stadials and interstadials cannot be resolved by the age model presented here. IRD fluxes are higher under stadial conditions and there is no clear trend in the planktonic foraminiferal fluxes to suggest that these were responsible for an increase in sedimentation rate (figure 2.10(f)). However, the coarse size fraction (>63 μm) only forms a small proportion of the bulk sediment (1–14 % by mass), so changes in the fluxes of fine grained material are likely to be the dominant factor in the overall sedimentation rate. Any increase in sediment flux under interstadial conditions would therefore most likely be attributable to increased accumulation of either coccoliths (which are more abundant under interglacial conditions both at this site [Stolz and Baumann 2010; Marino et al. 2011] and in nearby locations [van Kreveld et al. 1996]) or other fine material. Carbonate fluxes in cores from this region are higher during interglacials than glacials [van Weering and de Rijk 1991; Cremer et al. 1993], supporting the idea that an increase in coccolith accumulation rate during interstadials is responsible for a higher sedimentation rate.

Another possibility is that increased seafloor erosion could explain the relative lack of sediment accumulation during stadial conditions [Dowling and McCave 1993]. Bottom

current-induced winnowing has been observed in the western Rockall Trough, with ODP Site 980 located just to the south of the main area of winnowing of the Feni Drift (identified north of 55°30'N) [van Weering and de Rijk 1991; Øvrebø et al. 2005]. However, bottom currents were strongest (and hence erosion most likely) during the warmer intervals (interstadials and the early Holocene) [Øvrebø et al. 2005]. This would lead to a relative increase in the amount of sediment preserved from the stadial periods rather than the interstadials, hence erosion does not seem a likely explanation for apparent differences between the sediment and ice core records.

Alternatively, increased remobilisation of finer material upstream, which is later deposited at the Feni Drift could increase the sedimentation rate under more vigorous bottom current regimes. This is supported by well-expressed millennial scale variability in magnetic susceptibility attributed to variable fine titanomagnetite transport from the Greenland-Scotland Ridge at a number of bottom water influenced sites across the North Atlantic [Kissel 2005]. These processes may influence Site 980, although the lack of Dansgaard-Oeschger variability in magnetic susceptibility suggests not to the same extent as documented at other sites with a strong overflow signature (see section 2.7.2 and Cremer et al. [1993]).

The alternative to these scenarios is that a large difference in the patterns of air/sea surface temperatures between Greenland and the North East Atlantic repeatedly persisted during the last glacial period. Although this scenario cannot be ruled out entirely, there is little support for this hypothesis in the published literature, with the coherence between the two regions widely considered to be very good [e.g. Bond and Lotti 1995; Alley and Clark 1999; van Kreveld et al. 2000; Voelker 2002; Clement and Peterson 2008]. Therefore, it seems likely that a combination of increased coccolith accumulation and greater current-induced winnowing upstream of the site were responsible for increased sedimentation rates during interstadials, leading to different expressions of Dansgaard-Oeschger variability in the Site 980 sediment record and NGRIP ice core.

2.7.4 IRD provenance through Heinrich events

Although Heinrich events are now very well documented (particularly in the North Atlantic region), their underlying causal mechanisms are still widely debated [e.g. Hemming 2004; Clement and Peterson 2008]. Many attempts to decipher the relative importance of internal ice sheet instabilities and external forcings have focused on the synchroneity of response of the different circum-Atlantic ice sheets. A lag of the Laurentide Ice Sheet derived detrital carbonates behind basaltic glass and haematite-coated clasts was noted by Bond and Lotti [1995] and Grousset et al. [2001], and attributed to smaller ice-rafting events originating in Iceland and the Gulf of St Lawrence/Greenland/Scandinavia which occurred before the main Laurentide Ice Sheet destabilization, and may have played a causal role. Geochemical records also show evidence of precursor intervals [Grousset et al. 2000; Vance and Archer 2002], with early iceberg release from the British and Irish Ice Sheet [Scourse et al. 2000] and Innuitian Ice Sheet [Darby et al. 2002].

There has been some debate about whether some of the documented "precursor" events are instead either previous stadial intervals or background variability [Grousset et al. 2000; Jullien et al. 2006; Haapaniemi et al. 2010], resulting in the suggestion that the term should be discontinued [Scourse et al. 2009]. The well-expressed Dansgaard-Oeschger variability and high sedimentation rate at ODP Site 980 allows non-Heinrich stadials to be clearly distinguished from intra-Heinrich variability. Heinrich IRD layers are also well defined by the presence of significant detrital carbonate grains sourced from the Laurentide Ice Sheet allowing the phasing of other sediment components to be described in relation to these layers.

2.7.4.1 Heinrich event 4

During Heinrich event 4, peaks in LIS sourced detrital carbonates, and sedimentary and metamorphic grains attributed to the British and Irish Ice Sheet (BIIS) are approximately synchronous with peaks in the total IRD flux (figure 2.10). However, a strong

contribution from other European ice sheets prior to the detrital carbonate layer has been documented at other locations, with several sites from the European margin suggesting a European source for the early part of H4, with contributions from Iceland and Greenland [Bond and Lotti 1995; Snoeckx et al. 1999; Knutz et al. 2001]. In contrast, at Site 980, maximum fluxes of detrital carbonate, and sedimentary/metamorphic clasts (most likely sourced from the British and Irish or Fennoscandian ice sheets) are synchronous with the main IRD peak. The absence of early European sourced IRD at Site 980 may be a result of the smaller size of the BIIS at this time [e.g. Sejrup et al. 2009]. Peak fluxes in volcanic glasses (generally attributed to an Icelandic Ice Sheet source) are not reached for approximately another 500 years. It seems probable, however, that at least some of the volcanic glass identified at Site 980 in this horizon was sourced from Icelandic eruptions, and hence, does not necessarily reflect an increased in icebergs sourced from Iceland or East Greenland occurring after the main LIS event. A basaltic tephra horizon known as the Faeroe Marine Ash Zone III (FMAZIII) has been identified in the NGRIP ice core at 38,122 ± 723 yr b2k, synchronous with the rapid warming event into Greenland Interstadial 8 [Davies et al. 2010]. This horizon has been well documented in the sediments of the northern North Atlantic [e.g. Austin and Hibbert 2012; Davies et al. 2012], and closely matches the age of our volcanic glass peak (38.5–37.7 ka), shown in figure 2.9.

2.7.4.2 Heinrich event 3

No detrital carbonate grains are identified during Heinrich event 3 in the Site 980 record. The absence of detrital carbonate is a common feature of many sites across the North Atlantic with the exception of locations close to the Labrador Sea and, to a lesser extent, in the main IRD belt [compare Bond et al. 1992; Hillaire-Marcel et al. 1994; Bond and Lotti 1995; Andrews et al. 1998; Rasmussen et al. 2003; Jullien et al. 2006; Hodell and Curtis 2008]. The smaller extent of H3 is also illustrated by the total IRD flux, which does not exceed that found during non-Heinrich stadials (in contrast to H2 and H4, which are much more distinctive). Peak values in lithologies with a likely BIIS origin

are found in the early part of the event, with volcanic glasses then reaching a maximum as BIIS-sourced grains decrease.

A dominance of Icelandic-sourced lithics during H3 has been documented by Peters et al. [2008], and is supported by high fluxes of volcanic glass at Site 980, at an age not corresponding to the previously documented major ash layers [e.g. Wastegård et al. 2006; Svensson et al. 2008; Davies et al. 2010; Davies et al. 2012]. Modelling results suggest a significant iceberg release from the northern Fennoscandian Ice Sheet [Bigg et al. 2011], with concurrent melt water pulses observed in the Nordic Seas [Lekens et al. 2006]. Involvement of iceberg and melt water releases from the Arctic has also been postulated at this time [Darby et al. 2002; Howe et al. 2008; Bigg et al. 2012]. This is not easily discernible in the northeast Atlantic on the basis of grain lithologies alone, particularly as few icebergs released are expected to survive to the main Atlantic basin [Bigg et al. 2011]. It therefore seems most likely that a complex combination of source areas were responsible for the pattern of IRD observed across the North Atlantic during H3 [e.g. Snoeckx et al. 1999; Jullien et al. 2006].

2.7.4.3 Heinrich event 2

The IRD record from ODP Site 980 shows two distinct phases during H2. The early part of the event (from 25.7–24.3 ka) is marked by moderate IRD fluxes, comparable to typical stadial values. Volcanic glass fluxes reach a peak and fluxes of grains attributed to the BIIS and LIS are elevated above stadial values. At 24.3 ka, there is a sharp increase in the fluxes of detrital carbonate, sedimentary/metamorphic lithics and total IRD fluxes, while volcanic glass fluxes decrease. These high total IRD fluxes persist until 23.5 ka, when fluxes of total IRD and all individual components drop to very low values. A very similar pattern of IRD deposition at H2 is recorded at site V23-81 [Bond et al. 1992; Bond and Lotti 1995; Elliot et al. 1998].

The strontium and lead isotopic signatures of bulk sediment suggests a dominance of lithic input from an Icelandic source at the start of H2 at DSDP Site 609 [Vance and

Archer 2002], which is supported by the large amounts of volcanic glass found in ODP Site 980 at this time. Peck et al. [2006] find a strong influence of material from both Iceland and NW Europe in core MD01-2461, with the Icelandic signal becoming weaker and European dominance stronger prior to the deposition of LIS-sourced carbonates, in good agreement with Grousset et al. [2001]. A two-phase H2 event has also been documented by Walden et al. [2007] and Scourse et al. [2000], but with BIIS-sourced grains leading the detrital carbonate peak. Evidence of the arrival of European-sourced icebergs before the main LIS IRD event has even been documented in the eastern Labrador Sea [Rahman 1995]. Some studies also find evidence of a high European input occurring after the main detrital carbonate deposition has stopped [Grousset et al. 2000; Auffret et al. 2002; Peck et al. 2007; Walden et al. 2007; Peters et al. 2008]. Although there is no evidence of European sourced IRD deposited after the detrital carbonate, collapse of northwest European ice sheets is supported by the identification of deposition from sediment-laden meltwater plumes at this time (as described in section 2.7.2).

2.7.4.4 Heinrich event 1

All defined groups of grain lithologies appear to show synchronous variability at Heinrich event 1 in the records from ODP Site 980, although the lack of intra-event variability may be an artefact of the increased sample spacing in this part of the record, with a resolution too poor to resolve offsets of less than 400 years. H1 occurred during the most recent deglaciation, an interval of major global climate change, resulting in a complex pattern of IRD deposition preserved at other localities. Records from the Goban Spur show a complex structure to H1, including a double detrital carbonate peak with different sediment compositions before and after, likely representing the activity of different BIIS or FIS lobes [Scourse et al. 2000; Walden et al. 2007; Haapaniemi et al. 2010]. IRD of European origin is widely documented prior to detrital carbonate deposition [Rasmussen et al. 1997; Grousset et al. 2001; Knutz et al. 2007; Hall et al. 2011]. A major collapse of the NWEIS occurred after the LIS [Bigg et al. 2012],

however, retreat of the BIIS means that its signal is only seen at more northerly sites along the Irish continental margin [Scourse et al. 2009].

2.7.4.5 Factors influencing IRD distribution

Comparison of the new data from ODP Site 980 presented here with other published records from the North Atlantic highlights the spatially variability in the composition and patterns of IRD deposition at Heinrich events. Differences can be seen between the temporal IRD distributions in the BIIS-dominated sites of the eastern Rockall Trough [e.g. Scourse et al. 2000; Knutz et al. 2001; Peck et al. 2007; Scourse et al. 2009] and the open ocean sites further to the west. An example of this is the absence of evidence of a European precursor to H4 and H1 at Site 980, despite indications elsewhere [e.g. Bond and Lotti 1995; Rasmussen et al. 1997; Snoeckx et al. 1999; Grousset et al. 2001; Knutz et al. 2001; Knutz et al. 2007; Hall et al. 2011]. Increased distance from the BIIS and a location raised above the deeper parts of the trough to the east are probably responsible for the weaker record of BIIS fluctuations and increased prominence of Heinrich events at Site 980, with fewer icebergs and no mass transport deposits reaching the site from the British/Irish continental margin. This suggests that Site 980 provides a more integrated record of North Atlantic variability than the continental margin sites along the eastern margin of the Rockall Trough. However, the differences between records from Site 980 and core ENAM 97-09 (located on the western margin of the Rockall Trough, shown on figure 2.1) are less easy to explain. IRD lithologies are dominated by Irish Carboniferous carbonates at ENAM 97-07 [Richter et al. 2001], in strong contrast to Site 980, where these grains are almost absent. Therefore, there must be other factors influencing the supply of IRD to these two closely spaced sites.

The complex pattern of IRD deposition in the North Atlantic can partially be attributed to the spatially heterogeneous nature of ice sheet behaviour. Ice sheets have highly complex geometries with fast-flowing streams prone to rapid collapses interspersed with much more stable areas, and ice behaviour can be highly spatially and temporally variable [e.g. Anandakrishnan and Alley 1997; Bindschadler and Vornberger 1998; Dowdeswell et al. 1999; Stokes and Clark 2001; Joughin et al. 2004; Alley et al. 2005b].

In addition, most of the circum-Atlantic landmasses have complex geologies, hence different ice streams of the same ice sheet may carry a different combination of lithologies, resulting in a different composition of the lithic grains transported as IRD.

An increase in the number of clasts attributed to a particular source region does not necessarily indicate an increase in iceberg production at that site. Surface ocean circulation patterns also play a key role in determining the patterns of IRD preserved in sediment cores, as these are responsible for the transport of icebergs from their release

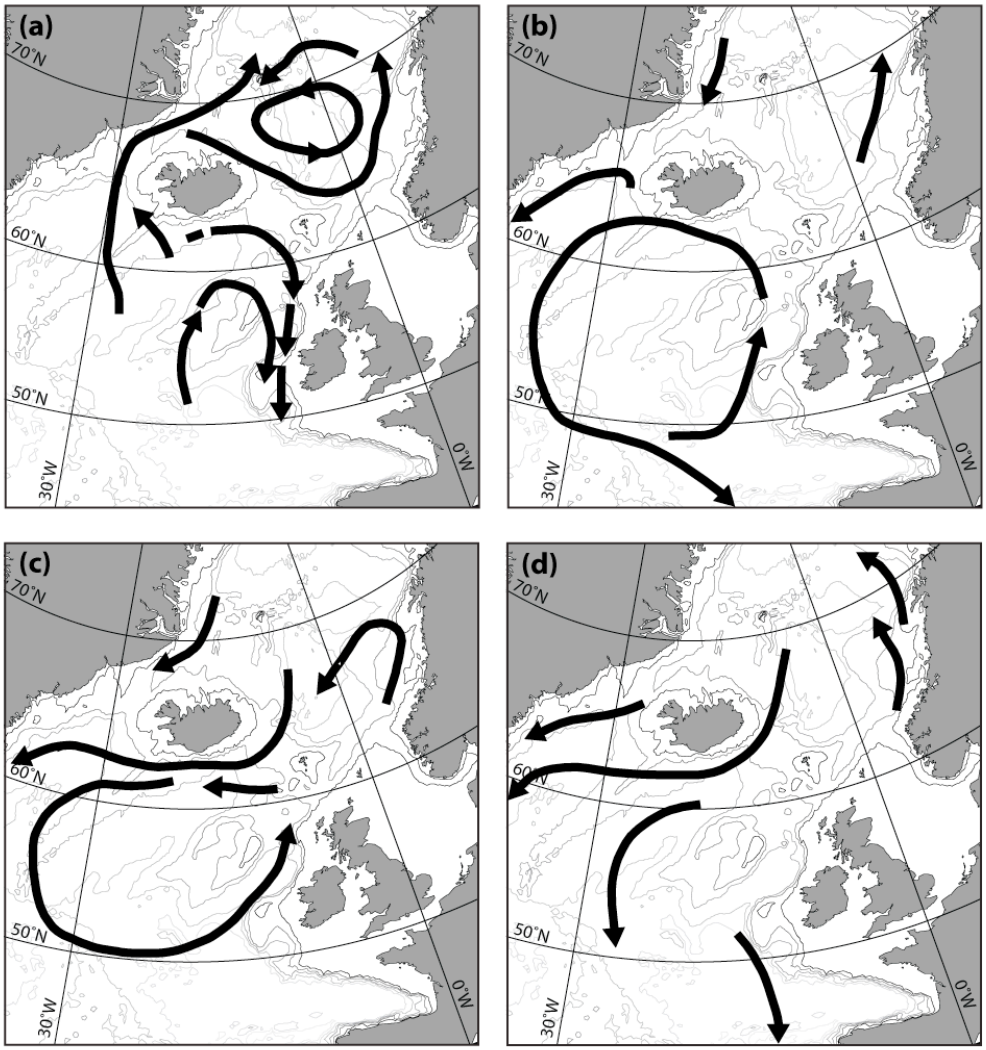

Figure 2.12: Simplified reconstructions of the surface or near surface ocean circulation at the LGM from (a) Sarnthein et al. [1995], (b) Seidov et al. [1996], (c) Death et al. [2006] and (d) Bigg et al. [2010].

sites to the open ocean. There is currently much uncertainty in the major current pathways during the last glacial interval, with four different reconstructions of surface or near surface circulation in the North Atlantic at the LGM illustrated in figure 2.12 [Sarnthein et al. 1995; Seidov et al. 1996; Death et al. 2006; Bigg et al. 2010].

Short term surface circulation variations at Heinrich events (triggered by localized melt water inputs or changes in surface water properties) would have resulted in very different depositional patterns to background glacial/stadial conditions [Sarnthein et al. 1995; Seidov et al. 1996; Bigg et al. 2012]. A small shift in the position or strength of the subpolar gyre could have resulted in vastly different patterns of IRD deposition in the North Atlantic, even if the flux of icebergs produced by each ice sheet remained constant. Surface water properties not only influence the direction that icebergs travel, but also the distance that they cover and the rate at which any transported lithics are deposited. High sea surface temperatures melt icebergs more rapidly, while sluggish currents would result in icebergs melting at shorter distances from their source areas. It is probable that the colder sea surface temperatures widely documented across the N. Atlantic region during Heinrich events [e.g. Broecker et al. 1992; van Kreveld 1996; Rosell-Melé et al. 1997; Grousset et al. 2000; Elliot et al. 2002; de Abreu et al. 2003] would have increased iceberg survivability, allowing greater numbers of them to survive to more far-field localities.

As the iceberg production signal from any source location is highly modified by the transport pathway of the iceberg to the site, care must be taken in drawing any firm conclusions about ice sheet phasing from any single sedimentary record. This is illustrated by the contrast in IRD lithologies between Site 980 and ENAM 97-09, and the absence of European-derived IRD input prior to detrital carbonate deposition documented at other sites in the region during both H4 and H1 at Site 980. It is therefore vital to combine data from as many locations as possible to start to separate out the influence of surface ocean properties and circulation and variable lithologies transported by different ice strea on IRD fluxes if conclusions are to be drawn about ice sheet behaviour from ocean sediments [Rashid et al. 2012]. It may be possible to use patterns of IRD deposition to deduce patterns and/or changes in surface ocean circulation [e.g.

Robinson et al. 1995; Watkins et al. 2007], particularly if open ocean sites are compared to records located close to the outlet of major ice streams.

2.7.6 Implications for the mechanism of Heinrich event generation

An increase in European-sourced IRD prior to the deposition of detrital carbonate identified at many of the Heinrich events in the North Atlantic has led to the suggestion either that the behaviour of the European ice sheets was responsible for the destabilisation of the Laurentide Ice Sheet [Snoeckx et al. 1999; Grousset et al. 2000], or that ice sheets on opposite sides of the Atlantic were responding to the same external trigger, albeit with a longer response time for the larger LIS [Heinrich 1988; Scourse et al. 2000]. Both of these hypotheses argue against the suggestion that Heinrich events were driven by internal ice sheet instabilities [MacAyeal 1993; Alley and MacAyeal 1994].

A wide array of North Atlantic IRD records generated over the past couple of decades (including the data presented here from Site 980) have enabled these hypotheses to be more closely examined. Reconstructions from Site 980 show changes in lithologies within Heinrich events (particularly H2), which cannot be attributed to previous stadials. Evidence of "precursor" changes in the circum-Atlantic ice sheets is supported by other reconstructions, which clearly show either phases just before the Heinrich layer deposition with ice-rafting indicators distinct from the preceding stadial intervals [e.g. Rahman 1995], or variability within the Heinrich event itself [e.g. Walden et al. 2007]. Lithological and geochemical evidence of increased IRD deposition prior to the classic LIS-derived detrital carbonate Heinrich layer has therefore been documented at numerous sites and with multiple proxies. This pattern of deposition is spatially complex, with different ice sheet signals more prominent in different parts of the Atlantic basin, for example, with a much stronger NWEIS signal seen along the European continental margin than at more open ocean sites (including Site 980). However, certain features, such as the presence of European-sourced IRD preceding major LIS destabilization have been recorded in multiple records at H4, H2 and H1. This

lends support to the suggestion that destabilization of smaller ice sheets may have played a role in the release of icebergs from the LIS.

Reconstructions from ODP Site 980 suggest that there are also distinct differences between Heinrich events 1 to 4. No clear repeating sequence of ice sheet instabilities is observed as might be expected if each Heinrich event was a response to the same external trigger [Scourse et al. 2000], although it should be noted that changes in the extent and geometries of ice sheets through MIS3 and 2 would likely alter the response times of each ice sheet. Melt water releases from the various circum-Atlantic ice sheets (or lobes/streams/sections of these) may well have played a role in preconditioning the overturning circulation for the shift to a weaker "Heinrich mode" [e.g. Sarnthein et al. 1994; Alley and Clark 1999; Rahmstorf 2002], and started a sea level rise contributing to the destabilization of the remaining ice sheets [Snoeckx et al. 1999], but the pattern and magnitude of these releases likely varied between events. Therefore, the phasing between ice sheets observed at multiple sites across the North Atlantic could be a result of either differing response times of the different ice sheets (and ice streams within them) to the same triggers [Scourse et al. 2000], each ice sheet responding to different, local or internal factors [Rashid et al. 2012], or a combination of these two scenarios.

An alternative hypothesis to explain ice shelf destabilisation at Heinrich events suggests that melting as a result of high summer air temperatures was the key trigger [Hulbe 1997; Hulbe et al. 2004]. Increasing percentages of *N. pachyderma* (s.) at Site 980 can clearly be seen predating detrital carbonate deposition during Heinrich events 4 and 2, with upper ocean warming occurring only after significant IRD deposition (figure 2.10). Although the percentage of *N. pachyderma* (s.) is not a perfect proxy for summer air surface temperatures, the two are likely to be highly correlated [e.g. Bé and Tolderlund 1971; Schröder-Ritzrau et al. 2001; Darling et al. 2006; Jonkers et al. 2010; Jonkers et al. 2013]. Therefore, there is no indication of ice sheet destabilisation occurring as a result of surface warming from Site 980, in agreement the findings of Alley et al. [2005a].

The role of sea ice as a feedback mechanism [e.g. Clement and Peterson 2008] cannot be easily resolved from the records presented here. Highly fluctuating fluxes of foraminifera observed at Site 980 may well be the result of a variable sea ice extent, and if so, there is no clear link with IRD deposition. Excursions in the $\delta^{18}O$ signature of surface waters associated with a drop in surface ocean salinity have been widely documented across the North Atlantic at Heinrich events, but have been attributed to a combination of iceberg melting, continental input and sea ice formation [Maslin et al. 1995; Cortijo et al. 1997; Dokken and Jansen 1999; Cortijo et al. 2005; Lekens et al. 2006; Hillaire-Marcel and de Vernal 2008; Eynaud et al. 2012]. This highlights the need for independent reconstructions of sea ice extent to understand the significance of this feedback, with a range of proxies including diatoms [Koç et al. 1993], dinocyst assemblages [de Vernal et al. 1997; de Vernal and Hillaire-Marcel 2000] and the biomarker-based proxy IP_{25} [Belt et al. 2007; Massé et al. 2008; Müller et al. 2011; Weckström et al. 2013] all showing promise in this regard.

It has also been suggested that variations in the strength of the overturning circulation may play a role in the generation of Heinrich events [e.g. Gutjahr and Lippold 2011]. This hypothesis will be examined further in the following chapters.

2.8 Summary and conclusions

North Atlantic ODP Site 980 provides a high-resolution record of rapid changes in surface ocean conditions spanning the last 40,000 years. Laurentide Ice Sheet (LIS) derived detrital carbonate grains transported to the site by ice-rafting are found at H1, H2 and H4, allowing clear identification of the classic Heinrich layers, and hence permitting detailed comparison of phasing of different components within the records at this site, and aiding comparison with other sites. Higher frequency variability in sea surface temperature and ice-rafted debris (IRD) fluxes corresponds very well with the Dansgaard-Oeschger events, although their expression in the sedimentary record has been modified by bioturbation, changes in the fluxes of individual components of the sediment fine fraction and potentially also bottom current variability.

Assuming synchroneity of these millennial-scale events with the Greenland ice cores, a new age model is developed for ODP Site 980, placing it on the GICC05 chronology [Andersen et al. 2006; Rasmussen et al. 2006; Svensson et al. 2006; Vinther et al. 2006; Svensson et al. 2008]. Low fluxes of IRD and the polar planktonic foraminifera *N. pachyderma* (s.) make correlation with the ice core data much more difficult in the deglaciation and Holocene, hence recalibrated previously published radiocarbon dates from planktonic foraminifera [Oppo et al. 2003; Benway et al. 2010] were used to further constrain the chronology here.

Although Site 980 is located on the fringes of the well-documented IRD belt of Ruddiman et al. [1977], the down core records presented here do not show some of the typical features associated with North Atlantic Heinrich events. Comparing the data from Site 980 with other localities across the North Atlantic highlights a sharp contrast in conditions between the IRD belt and the surrounding area, expressed here both in the magnetic susceptibility of the sediments and in the flux of planktonic foraminifera. The magnetic susceptibility of the Site 980 sediments is determined by the interplay between the flux of ice-rafted debris and the strength of bottom water currents, while the high variability in planktonic foraminiferal flux is likely attributable to the complex relationship between ice cover and productivity.

Comparison of the records presented here with data from other sites across the North Atlantic region suggests a degree of spatial heterogeneity, with surface circulation patterns and difficulties in identifying source terrains likely contributing to the observed local differences. The results of this study therefore cautions against using any single sediment core record to infer changes in ice sheet phasing, and instead highlights the importance of combining evidence from multiple sites before drawing any conclusions about basin-wide changes.

The variable patterns of IRD lithologies through Heinrich events at Site 980 are not suggestive of a simple repeating sequence of ice sheet destabilisations at each event.

However, evidence of change in the smaller circum-Atlantic ice sheets has been documented in multiple records (including this study) prior to major iceberg release from the Laurentide Ice Sheet. This supports the hypothesis that a rise in sea level resulting from these early melt water inputs could play a role in the destabilisation of the LIS [e.g. Snoeckx et al. 1999; Grousset et al. 2000]. An absence of any warming of sea surface temperatures prior to the increase in IRD fluxes at Site 980 argues against surface melt playing a role in ice sheet destabilisation [Hulbe 1997], though subsurface warming may play a role [Alvarez-Solas et al. 2010; Marcott et al. 2011]. However, the differences recorded between the Heinrich events suggests that internal ice sheet dynamics could also play a role in generating the observed patterns of IRD deposition at Heinrich events [MacAyeal 1993].

2.9 Acknowledgements

Megan Spencer was responsible for generating the IRD data, plus approximately half of the % *N. pachyderma* data points, and washed approximately 60 % of the sediment samples. Paul Wilson, Ian Bailey, Heiko Pälike, Fiona Hibbert and Megan Spencer are thanked for fruitful discussions and comments on this work. Gratitude goes to all of the shipboard staff and scientists aboard Ocean Drilling Project Leg 162. Sediment samples were kindly provided by the Bremen Core Repository, with additional material donated by Kirsty Crocket.

2.10 References

Alley, R. B., Andrews, J. T., Barber, D. C., and Clark, P. U., 2005a, Comment on "Catastrophic ice shelf breakup as the source of Heinrich event icebergs" by C. L. Hulbe et al: Paleoceanography, v. 20, p. PA1009.

Alley, R. B., and Clark, P. U., 1999, The deglaciation of the northern hemisphere: a global perspective: Annual Review of Earth and Planetary Sciences, v. 27, p. 149-182.

Alley, R. B., Clark, P. U., Huybrechts, P., and Joughin, I., 2005b, Ice-Sheet and Sea-Level Changes: Science, v. 310, p. 456-460.

Alley, R. B., Clark, P. U., Keigwin, L. D., and Webb, R. S., 1999, Making sense of millennial-scale climate change: Geophysical Monograph - American Geophysical Union, v. 112, p. 385-394.

Alley, R. B., and MacAyeal, D. R., 1994, Ice-rafted debris associated with binge/purge oscillations of the Laurentide Ice Sheet: Paleoceanography, v. 9, p. 503-511.

Alvarez-Solas, J., Charbit, S., Ritz, C., Paillard, D., Ramstein, G., and Dumas, C., 2010, Links between ocean temperature and iceberg discharge during Heinrich events: Nature Geosci, v. 3, p. 122-126.

Anandakrishnan, S., and Alley, R. B., 1997, Stagnation of Ice Stream C, West Antarctica by water piracy: Geophysical Research Letters, v. 24, p. 265-268.

Andersen, K. K., Svensson, A., Johnsen, S. J., Rasmussen, S. O., Bigler, M., Röthlisberger, R., Ruth, U., Siggaard-Andersen, M.-L., Steffensen, J. P., Dahl-Jensen, D., Vinther, B. M., and Clausen, H. B., 2006, The Greenland Ice Core Chronology 2005, 15-42 ka. Part 1: constructing the time scale: Quaternary Science Reviews, v. 25, p. 3246-3257.

Anderson, D. M., 2001, Attenuation of Millennial-Scale Events by Bioturbation in Marine Sediments: Paleoceanography, v. 16, p. 352-357.

Andrews, J. T., 2000, Icebergs and iceberg rafted detritus (IRD) in the North Atlantic: facts and assumptions: Oceanography, v. 13, p. 100-108.

Andrews, J. T., Kirby, M., Jennings, A. E., and Barber, D. C., 1998, Late Quaternary stratigraphy, chronology, and depositional processes on the slope of SE Baffin Island, detrital carbonate and Heinrich events: Implications for onshore glacial history: Geographie physique et Quaternaire, v. 52.

Andrews, J. T., and Tedesco, K., 1992, Detrital carbonate-rich sediments, northwestern Labrador Sea: Implications for ice-sheet dynamics and iceberg rafting (Heinrich) events in the North Atlantic: Geology, v. 20, p. 1087-1090.

Auffret, G., Zaragosi, S., Dennielou, B., Cortijo, E., Van Rooij, D., Grousset, F., Pujol, C., Eynaud, F., and Siegert, M., 2002, Terrigenous fluxes at the Celtic margin during the last glacial cycle: Marine Geology, v. 188, p. 79-108.

Austin, W. E. N., and Hibbert, F. D., 2012, Tracing time in the ocean: a brief review of chronological constraints (60-8 kyr) on North Atlantic marine event-based stratigraphies: Quaternary Science Reviews, v. 36, p. 28-37.

Austin, W. N., Hunt, J. B., Kroon, D., and Peacock, J. D., 1995, The 14C age of the Icelandic Vedde Ash: implications for Younger Dryas marine reservoir age corrections: Radiocarbon, v. 37, p. 53-62.

Bailey, I., Foster, G. L., Wilson, P. A., Jovane, L., Storey, C. D., Trueman, C. N., and Becker, J., 2012, Flux and provenance of ice-rafted debris in the earliest Pleistocene sub-polar North Atlantic Ocean comparable to the last glacial maximum: Earth and Planetary Science Letters, v. 341-344, p. 222-233.

Ballini, M., Kissel, C., Colin, C., and Richter, T., 2006, Deep-water mass source and dynamic associated with rapid climatic variations during the last glacial stage in the North Atlantic: A multiproxy investigation of the detrital fraction of deep-sea sediments: Geochem. Geophys. Geosyst., v. 7, p. Q02N01.

Bard, E., 1988, Correction of Accelerator Mass Spectrometry ^{14}C Ages Measured in Planktonic Foraminifera: Paleoceanographic Implications: Paleoceanography, v. 3, p. 635-645.

Bard, E., Arnold, M., Mangerud, J., Paterne, M., Labeyrie, L., Duprat, J., Mélières, M.-A., Sønstegaard, E., and Duplessy, J.-C., 1994, The North Atlantic atmosphere-sea surface 14C gradient during the Younger Dryas climatic event: Earth and Planetary Science Letters, v. 126, p. 275-287.

Bauch, D., Darling, K., Simstich, J., Bauch, H. A., Erlenkeuser, H., and Kroon, D., 2003, Palaeoceanographic implications of genetic variation in living North Atlantic Neogloboquadrina pachyderma: Nature, v. 424, p. 299-302.

Bé, A. W. H., and Tolderlund, D. S., 1971, Distribution and ecology of living planktonic foraminifera in surface waters of the Atlantic and Indian Oceans, *in* Funnell, B. M., and Riedel, W. R., eds., The Micropaleontology of Oceans, Cambridge University Press, p. 105-149.

Belanger, P. E., and Streeter, S. S., 1980, Distribution and ecology of benthic foraminifera in the Norwegian-Greenland Sea: Marine Micropaleontology, v. 5, p. 401-428.

Belt, S. T., Massé, G., Rowland, S. J., Poulin, M., Michel, C., and LeBlanc, B., 2007, A novel chemical fossil of palaeo sea ice: IP25: Organic Geochemistry, v. 38, p. 16-27.

Benway, H. M., McManus, J. F., Oppo, D. W., and Cullen, J. L., 2010, Hydrographic changes in the eastern subpolar North Atlantic during the last deglaciation: Quaternary Science Reviews, v. 29, p. 3336-3345.

Bigg, G. R., Clark, C. D., Greenwood, S. L., Haflidason, H., Hughes, A. L. C., Levine, R. C., Nygård, A., and Sejrup, H. P., 2012, Sensitivity of the North Atlantic circulation to break-up of the marine sectors of the NW European ice sheets during the last Glacial: A synthesis of modelling and palaeoceanography: Global and Planetary Change, v. 98-99, p. 153-65.

Bigg, G. R., Levine, R. C., Clark, C. D., Greenwood, S. L., Haflidason, H., Hughes, A. L. C., Nygård, A., and Sejrup, H. P., 2010, Last glacial ice-rafted debris off southwestern Europe: the role of the British–Irish Ice Sheet: Journal of Quaternary Science, v. 25, p. 689-699.

Bigg, G. R., Levine, R. C., and Green, C. L., 2011, Modelling abrupt glacial North Atlantic freshening: Rates of change and their implications for Heinrich events: Global and Planetary Change, v. 79, p. 176-192.

Bijma, J., Faber, W. W., and Hemleben, C., 1990, Temperature and salinity limits for growth and survival of some planktonic foraminifers in laboratory cultures: The Journal of Foraminiferal Research, v. 20, p. 95-116.

Bindschadler, R., and Vornberger, P., 1998, Changes in the West Antarctic Ice Sheet Since 1963 from Declassified Satellite Photography: Science, v. 279, p. 689-692.

Björck, S., Walker, M. J. C., Cwynar, L. C., Johnsen, S., Knudsen, K.-L., Lowe, J. J., and Wohlfarth, B., 1998, An event stratigraphy for the Last Termination in the North Atlantic region based on the Greenland ice-core record: a proposal by the INTIMATE group: Journal of Quaternary Science, v. 13, p. 283-292.

Blaauw, M., 2012, Out of tune: the dangers of aligning proxy archives: Quaternary Science Reviews, v. 36, p. 38-49.

Boltovskoy, E., and Wright, R. C., 1976, Recent foraminifera, Junk, The Hague.

Bond, G., Broecker, W., Johnsen, S., McManus, J., Labeyrie, L., Jouzel, J., and Bonani, G., 1993, Correlations between climate records from North Atlantic sediments and Greenland ice: Nature, v. 365, p. 143-147.

Bond, G., Heinrich, H., Broecker, W., Labeyrie, L., McManus, J., Andrews, J., Huon, S., Jantschik, R., Clasen, S., and Simet, C., 1992, Evidence for massive discharges of icebergs into the North Atlantic ocean during the last glacial period: Nature, v. 360, p. 245-249.

Bond, G., Kromer, B., Beer, J., Muscheler, R., Evans, M. N., Showers, W., Hoffmann, S., Lotti-Bond, R., Hajdas, I., and Bonani, G., 2001, Persistent Solar Influence on North Atlantic Climate During the Holocene: Science, v. 294, p. 2130-2136.

Bond, G., Showers, W., Cheseby, M., Lotti, R., Almasi, P., deMenocal, P., Priore, P., Cullen, H., Hajdas, I., and Bonani, G., 1997, A Pervasive Millennial-Scale Cycle in North Atlantic Holocene and Glacial Climates: Science, v. 278, p. 1257-1266.

Bond, G. C., and Lotti, R., 1995, Iceberg Discharges into the North Atlantic on Millennial Time Scales During the Last Glaciation: Science, v. 267, p. 1005-1010.

Bondevik, S., Mangerud, J., Birks, H. H., Gulliksen, S., and Reimer, P., 2006, Changes in North Atlantic Radiocarbon Reservoir Ages During the Allerod and Younger Dryas: Science, v. 312, p. 1514-1517.

Bout-Roumazeilles, V., Cortijo, E., Labeyrie, L., and Debrabant, P., 1999, Clay mineral evidence of nepheloid layer contributions to the Heinrich layers in the northwest Atlantic: Palaeogeography, Palaeoclimatology, Palaeoecology, v. 146, p. 211-228.

Braun, H., Christl, M., Rahmstorf, S., Ganopolski, A., Mangini, A., Kubatzki, C., Roth, K., and Kromer, B., 2005, Possible solar origin of the 1,470-year glacial climate cycle demonstrated in a coupled model: Nature, v. 438, p. 208-211.

Broecker, W., Bond, G., Klas, M., Clark, E., and McManus, J., 1992, Origin of the northern Atlantic's Heinrich events: Climate Dynamics, v. 6, p. 265-273.

Broecker, W. S., and Hemming, S., 2001, Climate Swings Come into Focus: Science, v. 294, p. 2308-2309.

Broecker, W. S., Peteet, D. M., and Rind, D., 1985, Does the ocean-atmosphere system have more than one stable mode of operation?: Nature, v. 315, p. 21-26.

Cao, L., Fairbanks, R. G., Mortlock, R. A., and Risk, M. J., 2007, Radiocarbon reservoir age of high latitude North Atlantic surface water during the last deglacial: Quaternary Science Reviews, v. 26, p. 732-742.

Carlson, C. A., Ducklow, H. W., Hansell, D. A., and Smith, W. O., Jr., 1998, Organic Carbon Partitioning During Spring Phytoplankton Blooms in the Ross Sea Polynya and the Sargasso Sea: Limnology and Oceanography, v. 43, p. 375-386.

Carstens, J., Hebbeln, D., and Wefer, G., 1997, Distribution of planktic foraminifera at the ice margin in the Arctic (Fram Strait): Marine Micropaleontology, v. 29, p. 257-269.

Carter, S. J., and Raymo, M. E., 1999, Sedimentological and Mineralogical control of Multisensor Track Data at Sites 981 and 984, *in* Raymo, M. E., Jansen, E., Blum, P., and Herbert, T. D., eds., Proceedings of the Ocean Drilling Program, Scientific Results.

Cayre, O., Lancelot, Y., Vincent, E., and Hall, M. A., 1999, Paleoceanographic Reconstructions from Planktonic Foraminifera off the Iberian Margin: Temperature, Salinity, and Heinrich Events: Paleoceanography, v. 14, p. 384-396.

Clark, C. D., Hughes, A. L. C., Greenwood, S. L., Jordan, C., and Sejrup, H. P., 2012, Pattern and timing of retreat of the last British-Irish Ice Sheet: Quaternary Science Reviews, v. 44, p. 112-146.

Clark, P. U., and Mix, A. C., 2002, Ice sheets and sea level of the Last Glacial Maximum: Quaternary Science Reviews, v. 21, p. 1-7.

Clement, A. C., and Peterson, L. C., 2008, Mechanisms of abrupt climate change of the last glacial period: Rev. Geophys., v. 46, p. RG4002.

Cortijo, E., Duplessy, J.-C., Labeyrie, L., Duprat, J., and Paillard, D., 2005, Heinrich events: hydrological impact: Comptes Rendus Geoscience, v. 337, p. 897-907.

Cortijo, E., Labeyrie, L., Vidal, L., Vautravers, M., Chapman, M., Duplessy, J.-C., Elliot, M., Arnold, M., Turon, J.-L., and Auffret, G., 1997, Changes in sea surface hydrology associated with Heinrich event 4 in the North Atlantic Ocean between 40˚ and 60˚N: Earth and Planetary Science Letters, v. 146, p. 29-45.

Cremer, M., Faugères, J.-C., Grousset, F., and Gonthier, E., 1993, Late Quaternary sediment flux on sedimentary drifts in the Northeast Atlantic: Sedimentary Geology, v. 82, p. 89-101.

Crocket, K. C., Vance, D., Foster, G. L., Richards, D. A., and Tranter, M., 2012, Continental weathering fluxes during the last glacial/interglacial cycle: insights from the marine sedimentary Pb isotope record at Orphan Knoll, NW Atlantic: Quaternary Science Reviews, v. 38, p. 89-99.

Crocket, K. C., Vance, D., Gutjahr, M., Foster, G. L., and Richards, D. A., 2011, Persistent Nordic deep-water overflow to the glacial North Atlantic: Geology, v. 39, p. 515-518.

Dansgaard, W., Johnsen, S. J., Clausen, H. B., Dahl-Jensen, D., Gundestrup, N. S., Hammer, C. U., Hvidberg, C. S., Steffensen, J. P., Sveinbjörnsdottir, A. E., Jouzel, J., and Bond, G., 1993, Evidence for general instability of past climate from a 250-kyr ice-core record: Nature, v. 364, p. 218-220.

Darby, D. A., Bischof, J. F., Spielhagen, R. F., Marshall, S. A., and Herman, S. W., 2002, Arctic ice export events and their potential impact on global climate during the late Pleistocene: Paleoceanography, v. 17, p. 1025.

Darby, D. A., Ortiz, J. D., Grosch, C. E., and Lund, S. P., 2012, 1,500-year cycle in the Arctic Oscillation identified in Holocene Arctic sea-ice drift: Nature Geosci, v. 5, p. 897-900.

Darling, K. F., Kucera, M., Kroon, D., and Wade, C. M., 2006, A resolution for the coiling direction paradox in Neogloboquadrina pachyderma: Paleoceanography, v. 21, p. PA2011.

Davies, S. M., Abbott, P. M., Pearce, N. J. G., Wastegård, S., and Blockley, S. P. E., 2012, Integrating the INTIMATE records using tephrochronology: rising to the challenge: Quaternary Science Reviews, v. 36, p. 11-27.

Davies, S. M., Wastegård, S., Abbott, P. M., Barbante, C., Bigler, M., Johnsen, S. J., Rasmussen, T. L., Steffensen, J. P., and Svensson, A., 2010, Tracing volcanic events in the NGRIP

ice-core and synchronising North Atlantic marine records during the last glacial period: Earth and Planetary Science Letters, v. 294, p. 69-79.

Davies, S. M., Wastegård, S., Rasmussen, T. L., Svensson, A., Johnsen, S. J., Steffensen, J. P., and Andersen, K. K., 2008, Identification of the Fugloyarbanki tephra in the NGRIP ice core: a key tie-point for marine and ice-core sequences during the last glacial period: Journal of Quaternary Science, v. 23, p. 409-414.

de Abreu, L., Shackleton, N. J., Schönfeld, J., Hall, M., and Chapman, M., 2003, Millennial-scale oceanic climate variability off the Western Iberian margin during the last two glacial periods: Marine Geology, v. 196, p. 1-20.

de Vernal, A., Eynaud, F., Henry, M., Hillaire-Marcel, C., Londeix, L., Mangin, S., Matthiessen, J., Marret, F., Radi, T., Rochon, A., Solignac, S., and Turon, J. L., 2005, Reconstruction of sea-surface conditions at middle to high latitudes of the Northern Hemisphere during the Last Glacial Maximum (LGM) based on dinoflagellate cyst assemblages: Quaternary Science Reviews, v. 24, p. 897-924.

de Vernal, A., and Hillaire-Marcel, C., 2000, Sea-ice cover, sea-surface salinity and halo-/thermocline structure of the northwest North Atlantic: modern versus full glacial conditions: Quaternary Science Reviews, v. 19, p. 65-85.

de Vernal, A., Rochon, A., Turon, J.-L., and Matthiessen, J., 1997, Organic-walled dinoflagellate cysts: Palynological tracers of sea-surface conditions in middle to high latitude marine environments: Geobios, v. 30, p. 905-920.

Death, R., Siegert, M. J., Bigg, G. R., and Wadley, M. R., 2006, Modelling iceberg trajectories, sedimentation rates and meltwater input to the ocean from the Eurasian Ice Sheet at the Last Glacial Maximum: Palaeogeography, Palaeoclimatology, Palaeoecology, v. 236, p. 135-150.

Dokken, T. M., and Jansen, E., 1999, Rapid changes in the mechanism of ocean convection during the last glacial period: Nature, v. 401, p. 458-461.

Dowdeswell, J. A., Elverhoi, A., Andrews, J. T., and Hebbeln, D., 1999, Asynchronous deposition of ice-rafted layers in the Nordic seas and North Atlantic Ocean: Nature, v. 400, p. 348-351.

Dowling, L. M., and McCave, I. N., 1993, Sedimentation on the Feni Drift and late Glacial bottom water production in the northern Rockall Trough: Sedimentary Geology, v. 82, p. 79-87.

Dyke, A. S., Andrews, J. T., Clark, P. U., England, J. H., Miller, G. H., Shaw, J., and Veillette, J. J., 2002, The Laurentide and Innuitian ice sheets during the Last Glacial Maximum: Quaternary Science Reviews, v. 21, p. 9-31.

Ellett, D. J., and Roberts, D. G., 1973, The overflow of Norwegian Sea Deep Water across the Wyville-Thomson Ridge: Deep Sea Research and Oceanographic Abstracts, v. 20, p. 819-835.

Elliot, M., Labeyrie, L., Bond, G., Cortijo, E., Turon, J.-L., Tisnerat, N., and Duplessy, J.-C., 1998, Millennial-Scale Iceberg Discharges in the Irminger Basin During the Last Glacial Period: Relationship with the Heinrich Events and Environmental Settings: Paleoceanography, v. 13, p. 433-446.

Elliot, M., Labeyrie, L., and Duplessy, J.-C., 2002, Changes in North Atlantic deep-water formation associated with the Dansgaard-Oeschger temperature oscillations (60-10 ka): Quaternary Science Reviews, v. 21, p. 1153-1165.

Eynaud, F., Malaizé, B., Zaragosi, S., de Vernal, A., Scourse, J., Pujol, C., Cortijo, E., Grousset, F. E., Penaud, A., Toucanne, S., Turon, J.-L., and Auffret, G., 2012, New constraints on European glacial freshwater releases to the North Atlantic Ocean: Geophys. Res. Lett., v. 39, p. L15601.

Farmer, G. L., Barber, D., and Andrews, J., 2003, Provenance of Late Quaternary ice-proximal sediments in the North Atlantic: Nd, Sr and Pb isotopic evidence: Earth and Planetary Science Letters, v. 209, p. 227-243.

Flückiger, J., Knutti, R., and White, J. W. C., 2006, Oceanic processes as potential trigger and amplifying mechanisms for Heinrich events: Paleoceanography, v. 21, p. PA2014.

Funder, S., and Hansen, L., 1996, The Greenland ice sheet - a model for its culmination and decay during and after the last glacial maximum: Bulletin of the Geological Society of Denmark, v. 42, p. 137-152.

Ganopolski, A., and Rahmstorf, S., 2001, Rapid changes of glacial climate simulated in a coupled climate model: Nature, v. 409, p. 153-158.

Gehrke, B., Lackschewitz, K., and Wallrabe-Adams, H., 1996, Late Quaternary sedimentation on the Mid-Atlantic Reykjanes Ridge: clay mineral assemblages and depositional environment: Geologische Rundschau, v. 85, p. 525-535.

Grönvold, K., Óskarsson, N., Johnsen, S. J., Clausen, H. B., Hammer, C. U., Bond, G., and Bard, E., 1995, Ash layers from Iceland in the Greenland GRIP ice core correlated with oceanic and land sediments: Earth and Planetary Science Letters, v. 135, p. 149-155.

Grousset, F. E., Cortijo, E., Huon, S., Hervé, L., Richter, T., Burdloff, D., Duprat, J., and Weber, O., 2001, Zooming in on Heinrich Layers: Paleoceanography, v. 16, p. 240-259.

Grousset, F. E., Labeyrie, L., Sinko, J. A., Cremer, M., Bond, G., Duprat, J., Cortijo, E., and Huon, S., 1993, Patterns of Ice-Rafted Detritus in the Glacial North Atlantic (40-55°N): Paleoceanography, v. 8, p. 175-192.

Grousset, F. E., Pujol, C., Labeyrie, L., Auffret, G., and Boelaert, A., 2000, Were the North Atlantic Heinrich events triggered by the behavior of the European ice sheets?: Geology, v. 28, p. 123-126.

Gupta, A. K., and Thomas, E., 2003, Initiation of Northern Hemisphere glaciation and strengthening of the northeast Indian monsoon: Ocean Drilling Program Site 758, eastern equatorial Indian Ocean: Geology, v. 31, p. 47-50.

Gutjahr, M., and Lippold, J., 2011, Early arrival of Southern Source Water in the deep North Atlantic prior to Heinrich event 2: Paleoceanography, v. 26, p. PA2101.

Gwiazda, R. H., Hemming, S. R., and Broecker, W. S., 1996a, Provenance of Icebergs During Heinrich Event 3 and the Contrast to their Sources During Other Heinrich Episodes: Paleoceanography, v. 11, p. 371-378.

—, 1996b, Tracking the Sources of Icebergs with Lead Isotopes: The Provenance of Ice-rafted Debris in Heinrich Layer 2: Paleoceanography, v. 11, p. 77-93.

Gwiazda, R. H., Hemming, S. R., Broecker, W. S., Onsttot, T., and Mueller, C., 1996c, Evidence from 40Ar/39Ar ages for a Churchill province source of ice-rafted amphiboles in Heinrich layer 2: Journal of Glaciology, v. 42, p. 440-446.

Haapaniemi, A. I., Scourse, J. D., Peck, V. L., Kennedy, H., Kennedy, P., Hemming, S. R., Furze, M. F. A., Pieńkowski, A. J., Austin, W. E. N., Walden, J., Wadsworth, E., and Hall, I. R., 2010, Source, timing, frequency and flux of ice-rafted detritus to the Northeast Atlantic margin, 30–12 ka: testing the Heinrich precursor hypothesis: Boreas, v. 39, p. 576-591.

Hall, I. R., Colmenero-Hidalgo, E., Zahn, R., Peck, V. L., and Hemming, S. R., 2011, Centennial- to millennial-scale ice-ocean interactions in the subpolar northeast Atlantic 18-41 kyr ago: Paleoceanography, v. 26, p. PA2224.

Hays, J. D., Imbrie, J., and Shackleton, N. J., 1976, Variations in the Earth's orbit: pacemaker of the ice ages: Science, v. 194, p. 1121-1132.

Heinrich, H., 1988, Origin and consequences of cyclic ice rafting in the Northeast Atlantic Ocean during the past 130,000 years: Quaternary Research, v. 29, p. 142-152.

Hemming, S. R., 2004, Heinrich events: Massive late Pleistocene detritus layers of the North Atlantic and their global climate imprint: Rev. Geophys., v. 42, p. RG1005.

Hemming, S. R., Broecker, W. S., Sharp, W. D., Bond, G. C., Gwiazda, R. H., McManus, J. F., Klas, M., and Hajdas, I., 1998, Provenance of Heinrich layers in core V28-82, northeastern Atlantic: $^{40}Ar/^{39}Ar$ ages of ice-rafted hornblende, Pb isotopes in feldspar grains, and Nd-Sr-Pb isotopes in the fine sediment fraction: Earth and Planetary Science Letters, v. 164, p. 317-333.

Hemming, S. R., and Hajdas, I., 2003, Ice-rafted detritus evidence from $^{40}Ar/^{39}Ar$ ages of individual hornblende grains for evolution of the eastern margin of the Laurentide ice sheet since 43 ^{14}C ky: Quaternary International, v. 99-100, p. 29-43.

Hemming, S. R., Hall, C. M., Biscaye, P. E., Higgins, S. M., Bond, G. C., McManus, J. F., Barber, D. C., Andrews, J. T., and Broecker, W. S., 2002, 40Ar/39Ar ages and 40Ar* concentrations of fine-grained sediment fractions from North Atlantic Heinrich layers: Chemical Geology, v. 182, p. 583-603.

Hibbert, F. D., Austin, W. E. N., Leng, M. J., and Gatliff, R. W., 2010, British Ice Sheet dynamics inferred from North Atlantic ice-rafted debris records spanning the last 175 000 years: Journal of Quaternary Science, v. 25, p. 461-482.

Hillaire-Marcel, C., and de Vernal, A., 2008, Stable isotope clue to episodic sea ice formation in the glacial North Atlantic: Earth and Planetary Science Letters, v. 268, p. 143-150.

Hillaire-Marcel, C., De Vernal, A., Bilodeau, G., and Wu, G., 1994, Isotope stratigraphy, sedimentation rates, deep circulation, and carbonate events in the Labrador Sea during the last ~ 200 ka: Canadian Journal of Earth Sciences, v. 31, p. 63-89.

Hodell, D. A., and Curtis, J. H., 2008, Oxygen and carbon isotopes of detrital carbonate in North Atlantic Heinrich Events: Marine Geology, v. 256, p. 30-35.

Hodell, D. A., Evans, H. F., Channell, J. E. T., and Curtis, J. H., 2010, Phase relationships of North Atlantic ice-rafted debris and surface-deep climate proxies during the last glacial period: Quaternary Science Reviews, v. 29, p. 3875-3886.

Howe, J. A., Tracy M, S., and Rex, H., 2008, Late Quaternary contourites and glaciomarine sedimentation in the Fram Strait: Sedimentology, v. 55, p. 179-200.

Hulbe, C. L., 1997, An Ice Shelf Mechanism for Heinrich Layer Production: Paleoceanography, v. 12, p. 711-717.

Hulbe, C. L., MacAyeal, D. R., Denton, G. H., Kleman, J., and Lowell, T. V., 2004, Catastrophic ice shelf breakup as the source of Heinrich event icebergs: Paleoceanography, v. 19, p. PA1004.

Huon, S., and Jantschik, R., 1993, Detrital silicates in Northeast Atlantic deep-sea sediments during the Late Quaternary: major element, REE and Rb-Sr isotopic data: Eclogae Geologicae Helvetiae, v. 86, p. 195-218.

Huybrechts, P., 2002, Sea-level changes at the LGM from ice-dynamic reconstructions of the Greenland and Antarctic ice sheets during the glacial cycles: Quaternary Science Reviews, v. 21, p. 203-231.

Jansen, E., Raymo, M. E., and Blum P. et al., 1996, Proceedings of the Ocean Drilling Program, Initial Reports, Volume 162, College station, TX.

Jantschik, R., and Huon, S., 1992, Detrital silicates in Northeast Atlantic deep-sea sediments during the Late Quaternary: Mineralogical and K-Ar isotopic data: Eclogae Geologicae Helvetiae, v. 85, p. 195-212.

Jessen, S. P., Rasmussen, T. L., Nielsen, T., and Solheim, A., 2010, A new Late Weichselian and Holocene marine chronology for the western Svalbard slope 30,000-0 cal years BP: Quaternary Science Reviews, v. 29, p. 1301-1312.

Johnson, R. G., and Lauritzen, S. E., 1995, Hudson Bay-Hudson Strait jökulhlaups and Heinrich events: a hypothesis: Palaeogeography, Palaeoclimatology, Palaeoecology, v. 117, p. 123-137.

Jonkers, L., Brummer, G.-J. A., Peeters, F. J. C., van Aken, H. M., and De Jong, M. F., 2010, Seasonal stratification, shell flux, and oxygen isotope dynamics of left-coiling N. pachyderma and T. quinqueloba in the western subpolar North Atlantic: Paleoceanography, v. 25, p. PA2204.

Jonkers, L., van Heuven, S., Zahn, R., and Peeters, F. J. C., 2013, Seasonal patterns of shell flux, δ18O and δ13C of small and large N. pachyderma (s.) and G. bulloides in the subpolar North Atlantic: Paleoceanography, v. 28, p. 164-174.

Joughin, I., Abdalati, W., and Fahnestock, M., 2004, Large fluctuations in speed on Greenland's Jakobshavn Isbrae glacier: Nature, v. 432, p. 608-610.

Jullien, E., Grousset, F. E., Hemming, S. R., Peck, V. L., Hall, I. R., Jeantet, C., and Billy, I., 2006, Contrasting conditions preceding MIS3 and MIS2 Heinrich events: Global and Planetary Change, v. 54, p. 225-238.

Keigwin, L. D., and Lehman, S. J., 1994, Deep Circulation Change Linked to HEINRICH Event 1 and Younger Dryas in a Middepth North Atlantic Core: Paleoceanography, v. 9, p. 185-194.

Kissel, C., 2005, Magnetic signature of rapid climatic variations in glacial North Atlantic, a review: Comptes Rendus Geoscience, v. 337, p. 908-918.

Kissel, C., Laj, C., Labeyrie, L., Dokken, T., Voelker, A., and Blamart, D., 1999, Rapid climatic variations during marine isotopic stage 3: magnetic analysis of sediments from Nordic Seas and North Atlantic: Earth and Planetary Science Letters, v. 171, p. 489-502.

Kissel, C., Laj, C., Mazaud, A., and Dokken, T., 1998, Magnetic anisotropy and environmental changes in two sedimentary cores from the Norwegian Sea and the North Atlantic: Earth and Planetary Science Letters, v. 164, p. 617-626.

Kissel, C., Laj, C., Mulder, T., Wandres, C., and Cremer, M., 2009, The magnetic fraction: A tracer of deep water circulation in the North Atlantic: Earth and Planetary Science Letters, v. 288, p. 444-454.

Knutz, P. C., Austin, W. E. N., and Jones, E. J. W., 2001, Millennial-scale depositional cycles related to British Ice Sheet variability and North Atlantic paleocirculation since 45 kyr B.P., Barra Fan, U.K. margin: Paleoceanography, v. 16, p. 53-64.

Knutz, P. C., Zahn, R., and Hall, I. R., 2007, Centennial-scale variability of the British Ice Sheet: Implications for climate forcing and Atlantic meridional overturning circulation during the last deglaciation: Paleoceanography, v. 22, p. PA1207.

Koç, N., Jansen, E., and Haflidason, H., 1993, Paleoceanographic reconstructions of surface ocean conditions in the Greenland, Iceland and Norwegian seas through the last 14 ka based on diatoms: Quaternary Science Reviews, v. 12, p. 115-140.

Kuijpers, A., Troelstra, S. R., Wisse, M., Heier Nielsen, S., and van Weering, T. C. E., 1998, Norwegian Sea overflow variability and NE Atlantic surface hydrography during the past 150,000 years: Marine Geology, v. 152, p. 75-99.

Lacasse, C., Sigurdsson, H., Carey, S., Paterne, M., and Guichard, F., 1996, North Atlantic deep-sea sedimentation of Late Quaternary tephra from the Iceland hotspot: Marine Geology, v. 129, p. 207-235.

Lacasse, C., Sigurdsson, H., Jóhannesson, H., Paterne, M., and Carey, S., 1995, Source of Ash Zone 1 in the North Atlantic: Bulletin of Volcanology, v. 57, p. 18-32.

Lackschewitz, K. S., and Wallrabe-Adams, H.-J., 1997, Composition and origin of volcanic ash zones in Late Quaternary sediments from the Reykjanes Ridge: evidence for ash fallout and ice-rafting: Marine Geology, v. 136, p. 209-224.

Lagerklint, I. M., and Wright, J. D., 1999, Late glacial warming prior to Heinrich event 1: The influence of ice rafting and large ice sheets on the timing of initial warming: Geology, v. 27, p. 1099-1102.

Landvik, J. Y., Bondevik, S., Elverhøi, A., Fjeldskaar, W., Mangerud, J. A. N., Salvigsen, O., Siegert, M. J., Svendsen, J.-I., and Vorren, T. O., 1998, The Last Glacial Maximum of

Svalbard and the Barents Sea Area: Ice Sheet Extent and Configuration: Quaternary Science Reviews, v. 17, p. 43-75.

Lehman, S. J., and Keigwin, L. D., 1992, Sudden changes in North Atlantic circulation during the last deglaciation: Nature, v. 356, p. 757-762.

Lekens, W. A. H., Sejrup, H. P., Haflidason, H., Knies, J., and Richter, T., 2006, Meltwater and ice rafting in the southern Norwegian Sea between 20 and 40 calendar kyr B.P.: Implications for Fennoscandian Heinrich events: Paleoceanography, v. 21, p. PA3013.

Lekens, W. A. H., Sejrup, H. P., Haflidason, H., Petersen, G. Ø., Hjelstuen, B., and Knorr, G., 2005, Laminated sediments preceding Heinrich event 1 in the Northern North Sea and Southern Norwegian Sea: Origin, processes and regional linkage: Marine Geology, v. 216, p. 27-50.

Linke, P., and Lutze, G. F., 1993, Microhabitat preferences of benthic foraminifera—a static concept or a dynamic adaptation to optimize food acquisition?: Marine Micropaleontology, v. 20, p. 215-234.

Lisiecki, L. E., and Raymo, M. E., 2005, A Pliocene-Pleistocene stack of 57 globally distributed benthic $\delta^{18}O$ records: Paleoceanography, v. 20, p. PA1003.

Lowe, J. J., Rasmussen, S. O., Björck, S., Hoek, W. Z., Steffensen, J. P., Walker, M. J. C., and Yu, Z. C., 2008, Synchronisation of palaeoenvironmental events in the North Atlantic region during the Last Termination: a revised protocol recommended by the INTIMATE group: Quaternary Science Reviews, v. 27, p. 6-17.

MacAyeal, D. R., 1993, Binge/Purge Oscillations of the Laurentide Ice Sheet as a Cause of the North Atlantic's Heinrich Events: Paleoceanography, v. 8, p. 775-784.

Mackensen, A., Sejrup, H. P., and Jansen, E., 1985, The distribution of living benthic foraminifera on the continental slope and rise off southwest Norway: Marine Micropaleontology, v. 9, p. 275-306.

Mangerud, J., 1972, Radiocarbon dating of marine shells, including a discussion of apparent age of Recent shells from Norway: Boreas, v. 1, p. 143-172.

Mangerud, J., Lie, S. E., Furnes, H., Kristiansen, I. L., and Lømo, L., 1984, A Younger Dryas Ash Bed in western Norway, and its possible correlations with tephra in cores from the Norwegian Sea and the North Atlantic: Quaternary Research, v. 21, p. 85-104.

Manighetti, B., and McCave, I. N., 1995, Late Glacial and Holocene Palaeocurrents Around Rockall Bank, NE Atlantic Ocean: Paleoceanography, v. 10, p. 611-626.

Manighetti, B., McCave, I. N., Maslin, M., and Shackleton, N. J., 1995, Chronology for climate change: Developing age models for the biogeochemical ocean flux study cores: Paleoceanography, v. 10, p. 513-525.

Marcott, S. A., Clark, P. U., Padman, L., Klinkhammer, G. P., Springer, S. R., Liu, Z., Otto-Bliesner, B. L., Carlson, A. E., Ungerer, A., Padman, J., He, F., Cheng, J., and Schmittner, A., 2011, Ice-shelf collapse from subsurface warming as a trigger for Heinrich events: Proceedings of the National Academy of Sciences, v. 108, p. 13415-13419.

Marino, M., Maiorano, P., and Flower, B. P., 2011, Calcareous nannofossil changes during the Mid-Pleistocene Revolution: Paleoecologic and paleoceanographic evidence from North Atlantic Site 980/981: Palaeogeography, Palaeoclimatology, Palaeoecology, v. 306, p. 58-69.

Marshall, S. J., and Clarke, G. K. C., 1997, A continuum mixture model of ice stream thermomechanics in the Laurentide Ice Sheet 2. Application to the Hudson Strait Ice Stream: J. Geophys. Res., v. 102, p. 20615-20637.

Marshall, S. J., James, T. S., and Clarke, G. K. C., 2002, North American Ice Sheet reconstructions at the Last Glacial Maximum: Quaternary Science Reviews, v. 21, p. 175-192.

Martinson, D. G., Pisias, N. G., Hays, J. D., Imbrie, J., Moore Jr, T. C., and Shackleton, N. J., 1987, Age dating and the orbital theory of the ice ages: Development of a high-resolution 0 to 300,000-year chronostratigraphy: Quaternary Research, v. 27, p. 1-29.

Maslin, M. A., Shackleton, N. J., and Pflaumann, U., 1995, Surface Water Temperature, Salinity, and Density Changes in the Northeast Atlantic During the Last 45,000 Years: Heinrich Events, Deep Water Formation, and Climatic Rebounds: Paleoceanography, v. 10, p. 527-544.

Massé, G., Rowland, S. J., Sicre, M.-A., Jacob, J., Jansen, E., and Belt, S. T., 2008, Abrupt climate changes for Iceland during the last millennium: Evidence from high resolution sea ice reconstructions: Earth and Planetary Science Letters, v. 269, p. 565-569.

McCave, I. N., Manighetti, B., and Beveridge, N. A. S., 1995a, Circulation in the glacial North Atlantic inferred from grain-size measurements: Nature, v. 374, p. 149-152.

McCave, I. N., Manighetti, B., and Robinson, S. G., 1995b, Sortable silt and fine sediment size/composition slicing: Parameters for palaeocurrent speed and palaeoceanography: Paleoceanography, v. 10, p. 593-610.

McManus, J. F., Francois, R., Gherardi, J. M., Keigwin, L. D., and Brown-Leger, S., 2004, Collapse and rapid resumption of Atlantic meridional circulation linked to deglacial climate changes: Nature, v. 428, p. 834-837.

McManus, J. F., Oppo, D. W., and Cullen, J. L., 1999, A 0.5-Million-Year Record of Millennial-Scale Climate Variability in the North Atlantic: Science, v. 283, p. 971-975.

Moros, M., Endler, R., Lackschewitz, K. S., Wallrabe-Adams, H. J., Mienert, J., and Lemke, W., 1997, Physical Properties of Reykjanes Ridge Sediments and their Linkage to High-Resolution Greenland Ice Sheet Project 2 Ice Core Data: Paleoceanography, v. 12, p. 687-695.

Moros, M., Kuijpers, A., Snowball, I., Lassen, S., Bäckström, D., Gingele, F., and McManus, J., 2002, Were glacial iceberg surges in the North Atlantic triggered by climatic warming?: Marine Geology, v. 192, p. 393-417.

Müller, J., Wagner, A., Fahl, K., Stein, R., Prange, M., and Lohmann, G., 2011, Towards quantitative sea ice reconstructions in the northern North Atlantic: A combined biomarker and numerical modelling approach: Earth and Planetary Science Letters, v. 306, p. 137-148.

Murray, J. W., 2006, Ecology and applications of benthic foraminifera, Cambridge University Press.

Muscheler, R., and Beer, J., 2006, Solar forced Dansgaard/Oeschger events?: Geophysical Research Letters, v. 33, p. L20706.

Naafs, B. D. A., Hefter, J., and Stein, R., 2013, Millennial-scale ice rafting events and Hudson Strait Heinrich(-like) Events during the late Pliocene and Pleistocene: a review: Quaternary Science Reviews, v. 80, p. 1-28.

New, A. L., and Smythe-Wright, D., 2001, Aspects of the circulation in the Rockall Trough: Continental Shelf Research, v. 21, p. 777-810.

North Greenland Ice Core Project Members, Andersen, K. K., Azuma, N., Barnola, J.-M., Bigler, M., Biscaye, P., Caillon, N., Chappellaz, J., Clausen, H. B., Dahl-Jensen, D., Fischer, H., Flückiger, J., Fritzsche, D., Fujii, Y., Goto-Azuma, K., Grønvold, K., Gundestrup, N. S., Hansson, M., Huber, C., Hvidberg, C. S., Johnsen, S. J., Jonsell, U., Jouzel, J., Kipfstuhl, S., Landais, A., Leuenberger, M., Lorrain, R., Masson-Delmotte, V., Miller, H., Motoyama, H., Narita, H., Popp, T., Rasmussen, S. O., Raynaud, D., Rothlisberger, R., Ruth, U., Samyn, D., Schwander, J., Shoji, H., Siggard-Andersen, M.-L., Steffensen, J. P., Stocker, T., Sveinbjörnsdóttir, A. E., Svensson, A., Takata, M., Tison, J.-L., Thorsteinsson, T., Watanabe, O., Wilhelms, F., and White, J. W. C., 2004,

High-resolution record of Northern Hemisphere climate extending into the last interglacial period: Nature, v. 431, p. 147-151.

Obrochta, S. P., Miyahara, H., Yokoyama, Y., and Crowley, T. J., 2012, A re-examination of evidence for the North Atlantic "1500-year cycle" at Site 609: Quaternary Science Reviews, v. 55, p. 23-33.

Oppo, D. W., and Lehman, S. J., 1995, Suborbital Timescale Variability of North Atlantic Deep Water During the Past 200,000 Years: Paleoceanography, v. 10, p. 901-910.

Oppo, D. W., McManus, J. F., and Cullen, J. L., 2003, Palaeo-oceanography: Deepwater variability in the Holocene epoch: Nature, v. 422, p. 277-277.

Øvrebø, L. K., Haughton, P. D. W., and Shannon, P. M., 2005, Temporal and spatial variations in Late Quaternary slope sedimentation along the undersupplied margins of the Rockall Trough, offshore west Ireland: Norsk Geologisk Tiddsskrift, v. 85, p. 279-294.

Paillard, D., Labeyrie, L., and Yiou, P., 1996, Macintosh program performs time-series analysis: Eos. Trans. AGU, v. 77.

Peck, V. L., Hall, I. R., Zahn, R., and Elderfield, H., 2008, Millennial-scale surface and subsurface paleothermometry from the northeast Atlantic, 55-8 ka BP: Paleoceanography, v. 23, p. PA3221.

Peck, V. L., Hall, I. R., Zahn, R., Elderfield, H., Grousset, F., Hemming, S. R., and Scourse, J. D., 2006, High resolution evidence for linkages between NW European ice sheet instability and Atlantic Meridional Overturning Circulation: Earth and Planetary Science Letters, v. 243, p. 476-488.

Peck, V. L., Hall, I. R., Zahn, R., Grousset, F., Hemming, S. R., and Scourse, J. D., 2007, The relationship of Heinrich events and their European precursors over the past 60 ka BP: a multi-proxy ice-rafted debris provenance study in the North East Atlantic: Quaternary Science Reviews, v. 26, p. 862-875.

Peltier, W. R., 2004, Global Glacial Isostasy and the Surface of the Ice-Age Earth: The ICE-5G (VM2) Model and GRACE: Annual Review of Earth and Planetary Sciences, v. 32, p. 111-149.

Peters, C., Walden, J., and Austin, W. E. N., 2008, Magnetic signature of European margin sediments: Provenance of ice-rafted debris and the climatic response of the British ice sheet during Marine Isotope Stages 2 and 3: J. Geophys. Res., v. 113, p. F03007.

Praetorius, S. K., McManus, J. F., Oppo, D. W., and Curry, W. B., 2008, Episodic reductions in bottom-water currents since the last ice age: Nature Geosci, v. 1, p. 449-452.

Radi, T., and de Vernal, A., 2008, Dinocysts as proxy of primary productivity in mid-high latitudes of the Northern Hemisphere: Marine Micropaleontology, v. 68, p. 84-114.

Rahman, A., 1995, Reworked nannofossils in the North Atlantic Ocean and subpolar basins: Implications for Heinrich events and ocean circulation: Geology, v. 23, p. 487-490.

Rahmstorf, S., 1994, Rapid climate transitions in a coupled ocean-atmosphere model: Nature, v. 372, p. 82-85.

—, 2002, Ocean circulation and climate during the past 120,000 years: Nature, v. 419, p. 207-214.

Rashid, H., Saint-Ange, F., Barber, D. C., Smith, M. E., and Devalia, N., 2012, Fine scale sediment structure and geochemical signature between eastern and western North Atlantic during Heinrich events 1 and 2: Quaternary Science Reviews, v. 46, p. 136-150.

Rasmussen, S. O., Andersen, K. K., Svensson, A. M., Steffensen, J. P., Vinther, B. M., Clausen, H. B., Siggaard-Andersen, M. L., Johnsen, S. J., Larsen, L. B., Dahl-Jensen, D., Bigler, M., Röthlisberger, R., Fischer, H., Goto-Azuma, K., Hansson, M. E., and Ruth, U., 2006, A new Greenland ice core chronology for the last glacial termination: J. Geophys. Res., v. 111, p. D06102.

Rasmussen, T. L., Oppo, D. W., Thomsen, E., and Lehman, S. J., 2003, Deep sea records from the southeast Labrador Sea: Ocean circulation changes and ice-rafting events during the last 160,000 years: Paleoceanography, v. 18, p. 1018.

Rasmussen, T. L., Thomsen, E., van Weering, T. C. E., and Labeyrie, L., 1996, Rapid Changes in Surface and Deep Water Conditions at the Faeroe Margin During the Last 58,000 Years: Paleoceanography, v. 11, p. 757-771.

Rasmussen, T. L., van Weering, T. C. E., and Labeyrie, L., 1997, Climatic instability, ice sheets and ocean dynamics at high northern latitudes during the last glacial period (58-10 ka BP): Quaternary Science Reviews, v. 16, p. 71-80.

Reimer, P. J., Baillie, M. G. L., Bard, E., Bayliss, A., Beck, J. W., Blackwell, P. G., Ramsey, C. B., Buck, C. E., Burr, G. S., and Edwards, R. L., 2009, IntCal09 and Marine09 radiocarbon age calibration curves, 0-50,000 years cal BP: Radiocarbon, v. 51, p. 1111-1150.

Reimer, P. J., and Reimer, R. W., 2001, A marine reservoir correction database and on-line interface: Radiocarbon, v. 43, p. 461-463.

Revel, M., Sinko, J. A., Grousset, F. E., and Biscaye, P. E., 1996, Sr and Nd isotopes as tracers of North Atlantic lithic particles: Paleoclimatic implications: Paleoceanography, v. 11, p. 95-113.

Richter, T. O., Lassen, S., van Weering, T. C. E., and de Haas, H., 2001, Magnetic susceptibility patterns and provenance of ice-rafted material at Feni Drift, Rockall Trough: implications for the history of the British-Irish ice sheet: Marine Geology, v. 173, p. 37-54.

Robinson, S. G., Maslin, M. A., and McCave, I. N., 1995, Magnetic Susceptibility Variations in Upper Pleistocene Deep-Sea Sediments of the NE Atlantic: Implications for Ice Rafting and Paleocirculation at the Last Glacial Maximum: Paleoceanography, v. 10, p. 221-250.

Rosell-Melé, A., Maslin, M. A., Maxwell, J. R., and Schaeffer, P., 1997, Biomarker evidence for "Heinrich" events: Geochimica et Cosmochimica Acta, v. 61, p. 1671-1678.

Ruddiman, W. F., 1977, Late Quaternary deposition of ice-rafted sand in the subpolar North Atlantic (lat 40° to 65°N): Geological Society of America Bulletin, v. 88, p. 1813-1827.

Sancetta, C., 1992, Primary production in the glacial North Atlantic and North Pacific oceans: Nature, v. 360, p. 249-251.

Sancetta, C., Imbrie, J., and Kipp, N. G., 1973, Climatic record of the past 130,000 years in North Atlantic deep-sea core V23-82: Correlation with the terrestrial record: Quaternary Research, v. 3, p. 110-116.

Sarnthein, M., Jansen, E., Weinelt, M., Arnold, M., Duplessy, J. C., Erlenkeuser, H., Flatøy, A., Johannessen, G., Johannessen, T., Jung, S., Koc, N., Labeyrie, L., Maslin, M., Pflaumann, U., and Schulz, H., 1995, Variations in Atlantic Surface Ocean Paleoceanography, 50º-80ºN: A Time-Slice Record of the Last 30,000 Years: Paleoceanography, v. 10, p. 1063-1094.

Sarnthein, M., Pflaumann, U., and Weinelt, M., 2003, Past extent of sea ice in the northern North Atlantic inferred from foraminiferal paleotemperature estimates: Paleoceanography, v. 18, p. 1047.

Sarnthein, M., Winn, K., Jung, S. J. A., Duplessy, J.-C., Labeyrie, L., Erlenkeuser, H., and Ganssen, G., 1994, Changes in East Atlantic Deepwater Circulation Over the Last 30,000 years: Eight Time Slice Reconstructions: Paleoceanography, v. 9, p. 209-267.

Schlitzer, R., 2013, Ocean Data View, http://odv.awi.de.

Schröder-Ritzrau, A., Andruleit, H., Jensen, S., Samtleben, C., Schäfer, P., Matthiessen, J., Hass, H. C., Kohly, A., and Thiede, J., 2001, Distribution, Export and Alteration of Fossilizable Plankton in the Nordic Seas, *in* Schäfer, P., Ritzrau, W., Schlüter, M., and Thiede, J., eds., The Northern North Atlantic, Springer Berlin Heidelberg, p. 81-104.

Scourse, J. D., Haapaniemi, A. I., Colmenero-Hidalgo, E., Peck, V. L., Hall, I. R., Austin, W. E. N., Knutz, P. C., and Zahn, R., 2009, Growth, dynamics and deglaciation of the last

British-Irish ice sheet: the deep-sea ice-rafted detritus record: Quaternary Science Reviews, v. 28, p. 3066-3084.

Scourse, J. D., Hall, I. R., McCave, I. N., Young, J. R., and Sugdon, C., 2000, The origin of Heinrich layers: evidence from H2 for European precursor events: Earth and Planetary Science Letters, v. 182, p. 187-195.

Seidov, D., Sarnthein, M., Stattegger, K., Prien, R., and Weinelt, M., 1996, North Atlantic ocean circulation during the last glacial maximum and subsequent meltwater event: A numerical model: J. Geophys. Res., v. 101, p. 16305-16332.

Sejrup, H. P., Hjelstuen, B. O., Torbjørn Dahlgren, K. I., Haflidason, H., Kuijpers, A., Nygård, A., Praeg, D., Stoker, M. S., and Vorren, T. O., 2005, Pleistocene glacial history of the NW European continental margin: Marine and Petroleum Geology, v. 22, p. 1111-1129.

Sejrup, H. P., Nygård, A., Hall, A. M., and Haflidason, H., 2009, Middle and Late Weichselian (Devensian) glaciation history of south-western Norway, North Sea and eastern UK: Quaternary Science Reviews, v. 28, p. 370-380.

Shackleton, N. J., Berger, A., and Peltier, W. R., 1990, An alternative astronomical calibration of the lower Pleistocene timescale based on ODP Site 677: Earth and Environmental Science Transactions of the Royal Society of Edinburgh, v. 81, p. 251-261.

Shackleton, N. J., Hall, M. A., and Vincent, E., 2000, Phase Relationships Between Millennial-Scale Events 64,000-24,000 Years Ago: Paleoceanography, v. 15, p. 565-569.

Shipboard Scientific Party, 1996a, Explanatory Notes, *in* Jansen, E., Raymo, M. E., and Blum P. et al., eds., Proceedings of the Ocean Drilling Program, Initial Reports, College station, TX, p. 21-45.

—, 1996b, Sites 980/981, *in* Jansen, E., Raymo, M. E., and Blum P. et al., eds., Proceedings of the Ocean Drilling Program, Initial Reports, College station, TX, p. 49-90.

Smith Jr., W. O., Baumann, M. E. M., Wilson, D. L., and Aletsee, L., 1987, Phytoplankton Biomass and Productivity in the Marginal Ice Zone of the Fram Strait During Summer 1984: J. Geophys. Res., v. 92, p. 6777-6786.

Snoeckx, H., Grousset, F., Revel, M., and Boelaert, A., 1999, European contribution of ice-rafted sand to Heinrich layers H3 and H4: Marine Geology, v. 158, p. 197-208.

Solomon, S., Qin, D., Manning, M., Chen, Z., Marquis, M., Averyt, K. B., Tignor, M., and Miller, H. L., (eds.), 2007, Contribution of Working Group I to the Fourth Assessment Report of the Intergovernmental Panel on Climate Change, 2007, Cambridge University Press, Cambridge, United Kingdom and New York, NY, USA.

Stanford, J. D., Rohling, E. J., Bacon, S., Roberts, A. P., Grousset, F. E., and Bolshaw, M., 2011, A new concept for the paleoceanographic evolution of Heinrich event 1 in the North Atlantic: Quaternary Science Reviews, v. 30, p. 1047-1066.

Stern, J. V., and Lisiecki, L. E., 2013, North Atlantic circulation and reservoir age changes over the past 41,000 years: Geophysical Research Letters, v. 40, p. 3693-3697.

Stocker, T. F., and Wright, D. G., 1996, Rapid changes in ocean circulation and atmospheric radiocarbon: Paleoceanography, v. 11, p. 773-795.

Stokes, C. R., and Clark, C. D., 2001, Palaeo-ice streams: Quaternary Science Reviews, v. 20, p. 1437-1457.

Stolz, K., and Baumann, K.-H., 2010, Changes in palaeoceanography and palaeoecology during Marine Isotope Stage (MIS) 5 in the eastern North Atlantic (ODP Site 980) deduced from calcareous nannoplankton observations: Palaeogeography, Palaeoclimatology, Palaeoecology, v. 292, p. 295-305.

Stommel, H., 1961, Thermohaline Convection with Two Stable Regimes of Flow: Tellus, v. 13, p. 224-230.

Stoner, J. S., Channell, J. E. T., and Hillaire-Marcel, C., 1996, The Magnetic Signature of Rapidly Deposited Detrital Layers From the Deep Labrador Sea: Relationship to North Atlantic Heinrich Layers: Paleoceanography, v. 11, p. 309-325.

Stuiver, M., Pearson, G. W., and Braziunas, T. F., 1986, Radiocarbon age calibration of marine samples back to 9000 cal yr BP: Radiocarbon, v. 28, p. 980-1021.

Stuiver, M., and Reimer, P. J., 1993, Extended ^{14}C database and revised CALIB radiocarbon calibration program: Radiocarbon, v. 35, p. 215-230.

Stuiver, M., Reimer, P. J., and Reimer, R. W., 2005, CALIB 5.0.

Svendsen, J. I., Astakhov, V. I., Bolshiyanov, D. Y., Demidov, I., Dowdeswell, J. A., Gataullin, V., Hjort, C., Hubberten, H. W., Larsen, E., Mangerud, J. A. N., Melles, M., Möller, P. E. R., Saarnisto, M., and Siegert, M. J., 1999, Maximum extent of the Eurasian ice sheets in the Barents and Kara Sea region during the Weichselian: Boreas, v. 28, p. 234-242.

Svensson, A., Andersen, K. K., Bigler, M., Clausen, H. B., Dahl-Jensen, D., Davies, S. M., Johnsen, S. J., Muscheler, R., Parrenin, F., Rasmussen, S. O., Röthlisberger, R., Seierstad, I., Steffensen, J. P., and Vinther, B. M., 2008, A 60 000 year Greenland stratigraphic ice core chronology: Clim. Past, v. 4, p. 47-57.

Svensson, A., Andersen, K. K., Bigler, M., Clausen, H. B., Dahl-Jensen, D., Davies, S. M., Johnsen, S. J., Muscheler, R., Rasmussen, S. O., Röthlisberger, R., Steffensen, J. P., and

Vinther, B. M., 2006, The Greenland Ice Core Chronology 2005, 15-42 ka. Part 2: comparison to other records: Quaternary Science Reviews, v. 25, p. 3258-3267.

Sweeney, C., Hansell, D. A., Carlson, C. A., Codispoti, L. A., Gordon, L. I., Marra, J., Millero, F. J., Smith, W. O., and Takahashi, T., 2000, Biogeochemical regimes, net community production and carbon export in the Ross Sea, Antarctica: Deep Sea Research Part II: Topical Studies in Oceanography, v. 47, p. 3369-3394.

Thomas, E., Booth, L., Maslin, M., and Shackleton, N. J., 1995, Northeastern Atlantic benthic foraminifera during the last 45,000 years: Changes in productivity seen from the bottom up: Paleoceanography, v. 10, p. 545-562.

Thornalley, D. J. R., Elderfield, H., and McCave, I. N., 2010, Intermediate and deep water paleoceanography of the northern North Atlantic over the past 21,000 years: Paleoceanography, v. 25, p. PA1211.

—, 2011a, Reconstructing North Atlantic deglacial surface hydrography and its link to the Atlantic overturning circulation: Global and Planetary Change, v. 79, p. 163-175.

Thornalley, D. J. R., McCave, I. N., and Elderfield, H., 2011b, Tephra in deglacial ocean sediments south of Iceland: Stratigraphy, geochemistry and oceanic reservoir ages: Journal of Quaternary Science, v. 26, p. 190-198.

Thouveny, N., Moreno, E., Delanghe, D., Candon, L., Lancelot, Y., and Shackleton, N. J., 2000, Rock magnetic detection of distal ice-rafted debries: clue for the identification of Heinrich layers on the Portuguese margin: Earth and Planetary Science Letters, v. 180, p. 61-75.

Thunell, R. C., and Reynolds, L. A., 1984, Sedimentation of planktonic foraminifera: Seasonal changes in species flux in the Panama Basin: Micropaleontology, v. 30, p. 243-262.

van Kreveld, S., Sarnthein, M., Erlenkeuser, H., Grootes, P., Jung, S., Nadeau, M. J., Pflaumann, U., and Voelker, A., 2000, Potential Links Between Surging Ice Sheets, Circulation Changes, and the Dansgaard-Oeschger Cycles in the Irminger Sea, 60-18 Kyr: Paleoceanography, v. 15, p. 425-442.

van Kreveld, S. A., 1996, Northeast Atlantic Late Quaternary planktic Foraminifera as primary productivity and water mass indicators: Scripta Geologica, v. 113, p. 23-91.

van Kreveld, S. A., Knappertsbusch, M., Ottens, J., Ganssen, G. M., and van Hinte, J. E., 1996, Biogenic carbonate and ice-rafted debris (Heinrich layer) accumulation in deep-sea sediments from a Northeast Atlantic piston core: Marine Geology, v. 131, p. 21-46.

van Weering, T. C. E., and de Rijk, S., 1991, Sedimentation and climate-induced sediments on Feni Ridge, Northeast Atlantic Ocean: Marine Geology, v. 101, p. 49-69.

Vance, D., and Archer, C., 2002, Isotopic constraints on the origin of Heinrich event precursors, Goldschmidt Conference Abstract.

Vidal, L., Labeyrie, L., Cortijo, E., Arnold, M., Duplessy, J. C., Michel, E., Becqué, S., and van Weering, T. C. E., 1997, Evidence for changes in the North Atlantic Deep Water linked to meltwater surges during the Heinrich events: Earth and Planetary Science Letters, v. 146, p. 13-27.

Vinther, B. M., Clausen, H. B., Johnsen, S. J., Rasmussen, S. O., Andersen, K. K., Buchardt, S. L., Dahl-Jensen, D., Seierstad, I. K., Siggaard-Andersen, M. L., Steffensen, J. P., Svensson, A., Olsen, J., and Heinemeier, J., 2006, A synchronized dating of three Greenland ice cores throughout the Holocene: J. Geophys. Res., v. 111, p. D13102.

Voelker, A. H. L., 2002, Global distribution of centennial-scale records for Marine Isotope Stage (MIS) 3: a database: Quaternary Science Reviews, v. 21, p. 1185-1212.

Voelker, A. H. L., Lebreiro, S. M., Schönfeld, J., Cacho, I., Erlenkeuser, H., and Abrantes, F., 2006, Mediterranean outflow strengthening during northern hemisphere coolings: A salt source for the glacial Atlantic?: Earth and Planetary Science Letters, v. 245, p. 39-55.

Volkmann, R., 2000, Planktic foraminifer ecology and stable isotope geochemistry in the Arctic Ocean: implications from water column and sediment surface studies for quantitative reconstructions of oceanic parameters: Berichte zur Polarforschung (Reports on Polar Research), v. 361.

Waelbroeck, C., Duplessy, J.-C., Michel, E., Labeyrie, L., Paillard, D., and Duprat, J., 2001, The timing of the last deglaciation in North Atlantic climate records: Nature, v. 412, p. 724-727.

Waelbroeck, C., Skinner, L. C., Labeyrie, L., Duplessy, J. C., Michel, E., Vazquez Riveiros, N., Gherardi, J. M., and Dewilde, F., 2011, The timing of deglacial circulation changes in the Atlantic: Paleoceanography, v. 26, p. PA3213.

Walden, J., Wadsworth, E., Austin, W. E. N., Peters, C., Scourse, J. D., and Hall, I. R., 2007, Compositional variability of ice-rafted debris in Heinrich layers 1 and 2 on the northwest European continental slope identified by environmental magnetic analyses: Journal of Quaternary Science, v. 22, p. 163-172.

Walker, M. J. C., Björck, S., Lowe, J. J., Cwynar, L. C., Johnsen, S., Knudsen, K. L., Wohlfarth, B., and group, I., 1999, Isotopic 'events' in the GRIP ice core: a stratotype for the Late Pleistocene: Quaternary Science Reviews, v. 18, p. 1143-1150.

Wastegård, S., Rasmussen, T. L., Kuijpers, A., Nielsen, T., and van Weering, T. C. E., 2006, Composition and origin of ash zones from Marine Isotope Stages 3 and 2 in the North Atlantic: Quaternary Science Reviews, v. 25, p. 2409-2419.

Watkins, S. J., Maher, B. A., and Bigg, G. R., 2007, Ocean circulation at the Last Glacial Maximum: A combined modeling and magnetic proxy-based study: Paleoceanography, v. 22, p. PA2204.

Weber, M. E., Mayer, L. A., Hillaire-Marcel, C., Bilodeau, G., Rack, F., Hiscott, R. N., and Aksu, A. E., 2001, Derivation of δ18O from Sediment Core Log Data: Implications for Millennial-Scale Climate Change in the Labrador Sea: Paleoceanography, v. 16, p. 503-514.

Weckström, K., Massé, G., Collins, L. G., Hanhijärvi, S., Bouloubassi, I., Sicre, M.-A., Seidenkrantz, M.-S., Schmidt, S., Andersen, T. J., Andersen, M. L., Hill, B., and Kuijpers, A., 2013, Evaluation of the sea ice proxy IP25 against observational and diatom proxy data in the SW Labrador Sea: Quaternary Science Reviews.

Wollenburg, J. E., and Mackensen, A., 1998, Living benthic foraminifers from the central Arctic Ocean: faunal composition, standing stock and diversity: Marine Micropaleontology, v. 34, p. 153-185.

Zahn, R., Schönfeld, J., Kudrass, H.-R., Park, M.-H., Erlenkeuser, H., and Grootes, P., 1997, Thermohaline Instability in the North Atlantic During Meltwater Events: Stable Isotope and Ice-Rafted Detritus Records from Core SO75-26KL, Portuguese Margin: Paleoceanography, v. 12, p. 696-710.

Žarić, S., Donner, B., Fischer, G., Mulitza, S., and Wefer, G., 2005, Sensitivity of planktic foraminifera to sea surface temperature and export production as derived from sediment trap data: Marine Micropaleontology, v. 55, p. 75-105.

Chapter 3

Multi-substrate Neodymium Isotopic Reconstructions: How Faithfully is a Bottom Water Signature Preserved in Sediments?

3.1 Abstract

Neodymium isotopes are becoming an increasingly widely used tool in the palaeoceanographic community, as the neodymium isotopic composition of bottom water masses is dependent upon their source region and transport history, and hence can be used to reconstruct changes in ocean circulation patterns. Fish debris, planktonic foraminifera and leached iron-manganese oxyhydroxide coatings from bulk sediment have all been used to reconstruct changes in bottom water properties in the palaeo realm. However, the accuracy with which these substrates preserve the bottom water signature as they become buried over time has not yet been fully established. This is explored here by combining multi-substrate neodymium isotopic reconstructions from ODP Site 980 with rare earth element distributions of planktonic foraminifera to better understand how rare earth elements (REEs) become associated with foraminifera, and the extent to which the signal is modified with increasing depth in the sediment. Rare earth element distributions suggest that foraminifera and fish debris acquire their signature in the in the shallow sediment pore water, and are not significantly modified by diagenetic processes during deeper burial. Differences in REE profiles between the upper and lower section of the sedimentary record presented here are attributed to decreased oxygen content of the shallow pore waters during the last glacial compared to the Holocene. A significant offset between the neodymium isotopic signatures of sediment leachates and those of fish debris and planktonic foraminifera is recorded throughout the Holocene, with agreement between the substrates under glacial conditions. These differences are attributed to increased transport of fine, radiogenic material by bottom water currents during the Holocene influencing the leachate record, which is too radiogenic to accurately record bottom water chemistry.

3.2 Introduction

3.2.1 Neodymium isotopes as a water mass tracer

Over the last few decades, neodymium isotopes have become an important part of the palaeoceanography toolkit. This is mainly because neodymium isotopes are not significantly influenced by biological processes, unlike many of the most commonly used proxies for water mass chemistry. This means that they have the potential to be more reliable tracers of water mass provenance and transport history than some of the more widely used proxies including thecarbon isotope and cadmium/calcium ratios of benthic foraminifera.

Neodymium isotopic compositions are commonly expressed in epsilon notation:

$$\varepsilon_{Nd} = \left(\frac{\left({}^{143}Nd/{}^{144}Nd \right)_{sample}}{\left({}^{143}Nd/{}^{144}Nd \right)_{CHUR}} - 1 \right) x10^{4} \qquad \text{Equation 3.1}$$

where CHUR is the CHondritic Uniform Reservoir, an estimate of a present day mean Earth value [Jacobsen and Wasserburg 1980]:

$$({}^{143}Nd/{}^{144}Nd)_{CHUR} = 0.512638 \qquad \text{Equation 3.2}$$

Rocks exhibit a wide range of neodymium isotopic compositions, depending upon both their age and initial Sm/Nd ratios, with values ranging from $\varepsilon_{Nd} = -56$ for old granitic cratons to +12 for young mid-ocean ridge basalts [Jeandel et al. 2007; Sarbas and Nohl 2008; Lacan et al. 2012, and references therein]. A global compilation of rock neodymium isotope signatures can be seen in figure 3.1 (a) [Jeandel et al. 2007]. Neodymium from this range of sources is transferred from the continents to the ocean via both riverine and aeolian inputs, resulting in different water masses acquiring distinct neodymium isotopic signatures [Goldstein et al. 1984; Mearns 1988; Grousset et al. 1992; Tachikawa et al. 1999]. Removal of neodymium from the water column occurs by

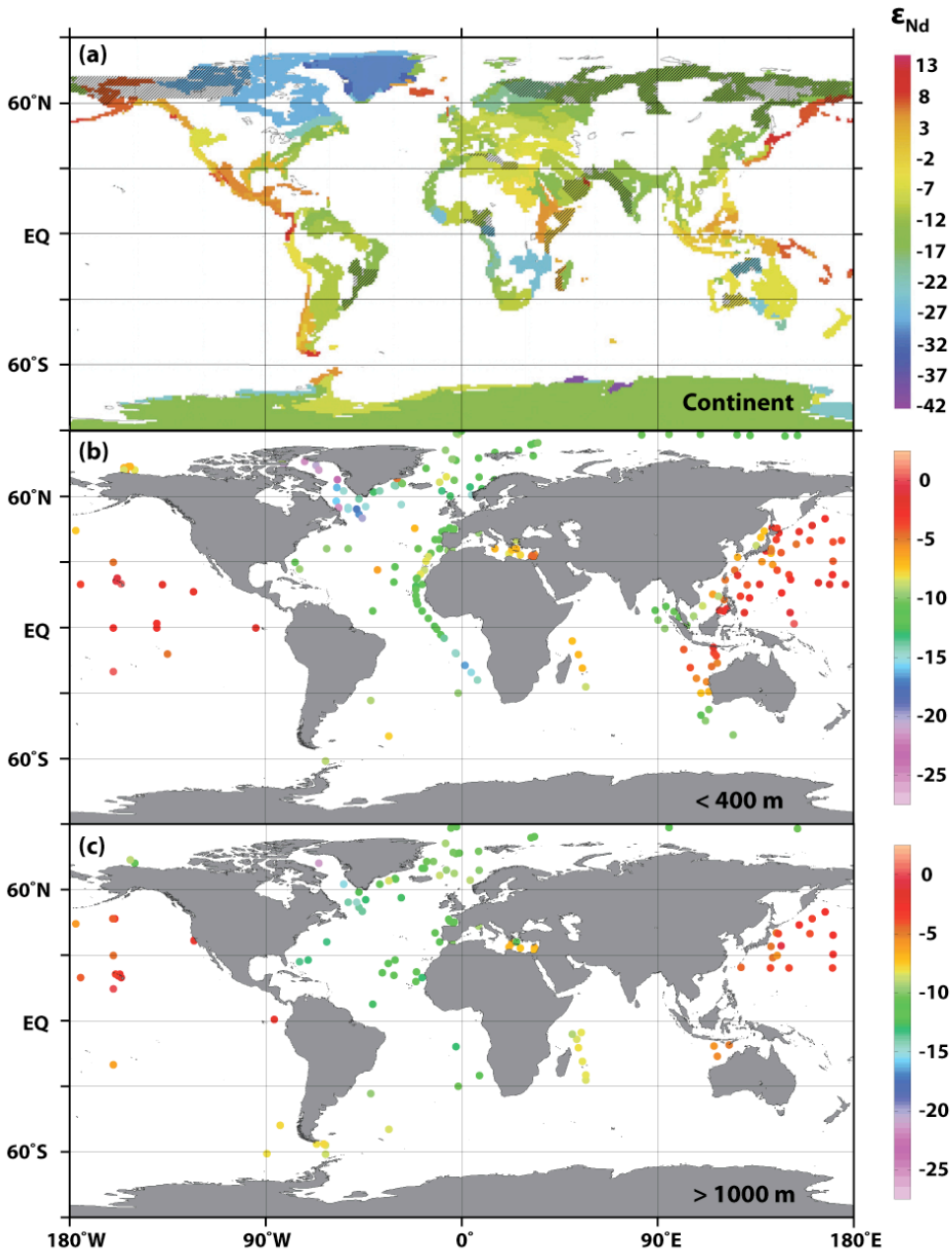

Figure 3.1: Global compilations of neodymium isotope data. (a) Continental ε_{Nd} signatures, with estimates extrapolated between sample data using lithology, from Jeandel et al. [2007]. (b) Seawater ε_{Nd} measurements from <400 m depth, with the mean values displayed where multiple measurements taken at a site. Replotted from Lacan et al. [2012]. (c) As (b), but from water depths >1000 m. All data sources are listed in Jeandel et al. [2007] and Lacan et al. [2012]. Note the wider range of continental values compared to oceanographic measurements.

adsorption to settling particles, including both organic matter and ferromanganese coatings [Sholkovitz et al. 1994; Haley et al. 2004].

The residence time of neodymium in the ocean is estimated to be approximately 200–1000 years [Tachikawa et al. 1999; Tachikawa et al. 2003; Arsouze et al. 2009], which is shorter than the modern oceanic mixing time of 1000–1600 years [e.g. Broecker and Peng 1982; Sarmiento and Gruber 2004; Garrison 2011]. This means that the neodymium isotopic composition of seawater varies spatially (illustrated in figure 3.1 (b)), allowing the signature of a water mass to be used as a tracer of its provenance [Piepgras and Wasserburg 1987; Innocent et al. 1997]. Surface waters in the Labrador Sea show the least radiogenic values, reaching as low as $\varepsilon_{Nd} = -26.6$, as a result of very old crustal material on the nearby continents [Stordal and Wasserburg 1986]. The abundance of young mantle-derived rocks leads to the most radiogenic values reported in the surface waters of the North Pacific, with values reaching $\varepsilon_{Nd} = +0.4$ [Vance et al. 2004]. There is a large amount of spatial variability between these two end members, with a global mean value of $\varepsilon_{Nd} = -8.8$ [Lacan et al. 2012]. In general, surface and deep waters show very similar neodymium isotope distributions (figure 3.1 (b) and (c)), although depth gradients depend strongly on water mass distributions and increase with deep water age [Siddall et al. 2008; Lacan et al. 2012]. The signal of a water mass may also be modified by mixing with other water masses, and by boundary exchange processes [e.g. Jeandel et al. 1998; Lacan and Jeandel 2004a; Lacan and Jeandel 2005b; Wilson et al. 2012; Pearce et al. 2013].

3.2.2 Substrates for neodymium isotope reconstructions

The first neodymium isotope reconstructions of past ocean chemistry used ferromanganese nodules and crusts to reconstruct changes in seawater composition [e.g. O'Nions et al. 1978; Piepgras et al. 1979; Goldstein and O'Nions 1981]. Their use is, however, limited by low temporal resolution. More recently, a wider suite of substrates have been exploited including leached ferromanganese coatings from bulk sediments [e.g. Rutberg et al. 2000; Bayon et al. 2002; Piotrowski et al. 2004; Gutjahr et al. 2007;

Martin et al. 2010], fish teeth and debris [e.g. Staudigel et al. 1985; Grandjean et al. 1987; Stille and Fischer 1990; Stille 1992; Martin and Haley 2000], corals [e.g. van de Flierdt et al. 2006; Robinson and van de Flierdt 2009; Colin et al. 2010; Copard et al. 2010] and foraminifera both with and without authigenic coatings [e.g. Palmer and Elderfield 1985; Vance and Burton 1999; Vance et al. 2004; Roberts et al. 2010; Elmore et al. 2011].

Fish teeth and other debris are very rich in neodymium and their use as a recorder of the neodymium isotope signal of bottom waters is well documented [DePaolo and Wasserburg 1977; Shaw and Wasserburg 1985; Staudigel et al. 1985; Martin and Haley 2000; Thomas et al. 2003], however their occurrence in the Pleistocene sediments recovered at ODP 980 is sporadic, precluding high resolution reconstructions. Bulk sediment leachates have the advantage that sample material is plentiful and high-resolution records can therefore be produced comparatively quickly and from all environments. However, several concerns have been raised about the fidelity of seawater chemistry reconstructions produced by this technique. Horizontal advection of fine sediments can transport material from upstream to the study site, particularly at sediment drifts sites such as the Feni Drift [Kidd and Hill 1986; McCave 2002]. Contamination of the leachate signal by ash or other fine material has also been documented, potentially occurring during acid-reductive leaching in the laboratory [Wilson et al. 2009; Roberts et al. 2010; Elmore et al. 2011]. Planktonic foraminifera are abundant in many ocean sediments, hence they can be used to produce high resolution records of neodymium isotope variation [Roberts et al. 2010]. They show less susceptibility to contamination by radiogenic volcanic material or fine unradiogenic sediments than bulk sediment leachates [Elmore et al. 2011], and hence provide a compromise between the fidelity of fish debris signature and the high resolution achievable through the use of sediment leachates. However, the mechanism by which neodymium and the other rare earth elements become incorporated into the tests of foraminifera is still debated.

3.2.3 Rare earth element association with foraminifera

The rare earth elements (REEs) are a subset of the transition metals, composing the lanthanides, scandium and yttrium (with the actinides sometimes also included), and are often found together in nature. This study focuses on the naturally occurring lanthanide elements (from lanthanum to lutetium). In general, these elements all show similar behaviour, existing in a 3+ oxidation state, although subtle fractionation between them occurs as the ionic radius decreases with increasing atomic number, as a result of a stronger nucleic charge. This results in differences in their speciation in seawater, with the heavy rare earth elements (HREE) more likely to form complexes, most commonly with carbonate ions, while the light rare earth elements (LREE) are more readily scavenged onto organic matter [Goldberg et al. 1963; Elderfield and Greaves 1982; Cantrell and Byrne 1987; Elderfield et al. 1988; Byrne and Kim 1990; Bertram and Elderfield 1993; Sholkovitz et al. 1994; Dubinin 2004]. However, both cerium and europium exhibit behaviour distinct from the main REE trends. This is because they have multiple oxidation states: in addition to the 3+ state, Ce can exist as 4+ while Eu can be reduced to 2+ [Frank 2002, and references therein]. While Eu exists only in its 3+ oxidation state under normal marine conditions, Ce is much more sensitive and can be easily converted between the soluble Ce (III) and insoluble Ce (IV) states in the water column [Elderfield et al. 1988]. Therefore, the relative abundance of Ce compared to the other REEs is controlled by the degree of anoxia.

Rare earth elements are not readily incorporated into biogenic calcite, resulting in very low concentrations within the calcite lattice of foraminifera [Palmer 1985; Palmer and Elderfield 1986]. Instead, a number of alternate mechanisms have been proposed for the association of rare earth elements with planktonic foraminifera. In the upper water column, rare earth elements associate with foraminifera by binding to organic material, and can then transfer the REEs to the test upon oxidation of the organic matter [Vance et al. 2004; Haley et al. 2005; Martìnez-Botì et al. 2009]. Organic layers between the layers of calcite of the test may also play a key role in the accumulation of REEs [Roberts et al. 2012], while other studies suggest that barite formed in the upper water column is a significant Nd-carrier [Haley and Klinkhammer 2002; Vance et al. 2004]. Ferromanganese coatings also contain high concentrations of REEs, with some

precipitation in the water column, but the majority of the coating added either at the sediment-water interface or at shallow depths in the sediment [Palmer 1985; Sholkovitz et al. 1994; Pomiès et al. 2002; Tachikawa et al. 2013]. In core top foraminifera, it is estimated that 80–90% of the total neodymium is contained within the coatings [Palmer 1985; Roberts et al. 2012]. Foraminifera which have not undergone reductive cleaning to remove these authigenic coatings are therefore commonly interpreted as representative of bottom water chemistry, although they may be modified to a pore water signal under sub-oxic conditions [Palmer and Elderfield 1985; Palmer and Elderfield 1986; Roberts et al. 2012]. Attempts have been made to reconstruct a surface water signal by completely removing the ferromanganese coatings from planktonic foraminifera [Vance and Burton 1999; Burton and Vance 2000; Scrivner et al. 2004; Vance et al. 2004; Haley et al. 2005; Martìnez-Botì et al. 2009], however concerns have been raised regarding whether the coating signature can be fully removed, if reabsorption occurs during the cleaning process and whether the calcite lattice itself also records a bottom and/or pore water signature [Pomiès et al. 2002; Roberts et al. 2010].

The rare earth signature of foraminifera may be modified as burial depth within the sediment increases over time. Redox-sensitive elements typically undergo a sequence of reactions as pore water dissolved oxygen levels decrease with depth in the sediment linked to the oxidation of organic matter, with iron and manganese oxides and iron oxyhydroxides becoming soluble under reducing conditions, releasing Mn^{2+} and Fe^{2+} ions which diffuse upwards and then reprecipitate when they reach the oxic-anoxic front [e.g. Froelich et al. 1979; Thomson et al. 1996; Burdige 2006]. Although the same well-documented sequence of redox reactions has been identified across the globe, the depth at which these processes occur varies hugely between sites [e.g. Richards 1965; Hartmann et al. 1973; Froelich et al. 1979; Burdige 1993]. With the exception of cerium, the lanthanides do not undergo changes in oxidation state under shallow sediment conditions, however, the phases with which they associate often do (including iron and manganese) [Sholkovitz et al. 1992; Haley et al. 2004; Burdige 2006]. Under suboxic/anoxic conditions in the sediment, REEs may become associated with other phases which can precipitate onto foraminiferal calcite, particularly manganese

carbonates and iron sulphides [Boyle 1983; Pena et al. 2005; Chaillou et al. 2006; Pena et al. 2008; Roberts et al. 2012; Tachikawa et al. 2013].

3.3 Aims

The main aims of this chapter are:

- To compare the neodymium isotope records preserved by uncleaned foraminifera, bulk sediment leachates and fish debris from a sediment drift in an open ocean setting; a typical environment for palaeoceanographic reconstructions.
- To better understand the origin of the rare earth element signature recorded by the different substrates, including the degree of post-depositional signal modification.
- To assess the suitability of bulk sediment leachates, uncleaned foraminifera and fish debris as recorders of bottom water neodymium isotope compositions.

3.4 Methods

3.4.1 Sample preparation

Between 600–1600 mixed planktonic foraminifera were picked at the >212 μm size fraction from each sample for neodymium isotopic analysis. Ferromanganese coatings were not removed from the foraminiferal tests because the majority of the neodymium associated with fossilised foraminifera occurs in the ferromanganese coating [Palmer 1985] and both calcite and coatings have been shown to record bottom water neodymium isotope values in the North Atlantic [Roberts et al. 2010; Elmore et al. 2011].

Foraminifera were broken open between two glass plates and ultrasonicated in ELGA water for 10 seconds. The supernant was pippetted off the top, removing any suspended clays. The samples were then sonicated twice more in methanol, with the supernant

removed after both sonications. Once the supernant was clear, the sample was left to dry and then checked under a microscope to ensure no dirty or non-foraminiferal fragments remained. 500 µl of 1.75 M hydrochloric acid (HCl) was added to dissolve the foraminifera and each sample was centrifuged for 45 seconds at 13,000 rotations per minute (rpm).

One to fifteen pieces of fish debris were picked from the >125 µm size fraction of certain samples to provide an additional check on the fidelity of the foraminiferal record. Fish teeth were scarce in the samples, hence analyses were dominated by fragments of bone. Adhering clays were removed by sonication twice in methanol (for 1 minute each time) and then in ELGA water (4 times at 30 seconds). Samples were then oxidatively cleaned for 30 minutes in a 1% H_2O_2 – 0.1 M NH_4OH solution. Next, they were rinsed in ELGA water before being leached in 0.001 M nitric acid (HNO_3) for 1 minute in an ultrasonic bath. No reductive cleaning was used because it has been deemed unnecessary at a number of Atlantic locations, including nearby ODP Site 982 [Martin et al. 2010]. Each sample was rinsed twice in ELGA water before being transferred to a savillex vial and dissolved in 0.5 ml 1.75 M HCl, then dried down on a hotplate at 140 ^{o}C. After removal from the hotplate, samples were allowed to cool, and then redissolved in 0.5 ml 1.75M HCl.

3.4.2 REE and trace element analysis

An aliquot of 10 µl was extracted from each of the dissolved foraminifera and fish debris samples for rare earth (REE) and other trace element analysis. 2 ml of 3% HNO_3 spiked with In and Re (to a concentration of 5 ppb) and Be (concentration 20 ppb) was added to each sample. A further aliquot of 0.1 ml was removed from each of these diluted samples and diluted a second time with 4.9 ml of 3 % HNO_3 spiked with 5 ppb In, Re and 20 ppb Be. These samples were used to determine calcium and strontium concentrations, as calcium concentrations were too high to analyse concurrently with the REE. The Quadrupole ICP-MS: Thermo X-Series 2 at the Ocean and Earth Science department, University of Southampton was used to measure calcium and strontium

concentrations. The remaining sample solutions were analysed for REE and trace element concentrations using the High Resolution ICP-MS: Thermo ELEMENT 2XR at the Ocean and Earth Science department, University of Southampton. Strontium was measured using both the Element and the X-Series to allow the two runs to be directly compared, and hence REE/Ca ratios to be calculated. All samples were corrected for matrix effects and instrument drift using the beryllium, indium and rhenium standard incorporated into each sample. A blank correction was then applied, and rare earth element standards were used to correct samples for oxide formation. A suite of five standards with known concentrations bracketing those of the samples were then used to create a linear calibration to calculate sample element concentrations. External reproducibility is estimated as 4–5 %, with internal reproducibility much less than this for the majority of samples.

Rare earth element concentrations of the samples (REE_{sample}) were expressed relative to the REE signature of the Post-Archaen Australian Shale (REE_{PAAS}) which is thought to be a good approximation of upper continental crust [Taylor and McLennan 1985; McLennan 1989], with a composition in good agreement with published estimates of shale composites [Haskin and Haskin 1966; Gromet et al. 1984; de Baar et al. 1985]. Shale normalisation allows small changes in the relative proportions of two elements with very different abundances to be more clearly expressed. In order to better visualise changes within the normalised REE distribution, several ratios were used, after De Baar et al. [1988] and Martin et al. [2010] (equations 3.3–3.7). These have been modified slightly by replacing Tm with Er in calculating the HREEs due to the low concentrations of the rarer Tm in some samples and previously reported inter-REE molecular interference in the ICP-MS [Haley et al. 2005]. For these reasons, Tm measurements were not plotted in the rare earth profiles of the Site 980 samples.

$$LREE = La_n + Pr_n + Nd_n \quad \text{Equation 3.3}$$

$$MREE = Gd_n + Tb_n + Dy_n \quad \text{Equation 3.4}$$

$$HREE = Er_n + Yb_n + Lu_n \quad \text{Equation 3.5}$$

$$\frac{MREE}{MREE*} = \frac{MREE}{0.5(HREE + LREE)} \qquad \text{Equation 3.6}$$

$$\text{where } REE_n = \frac{REE_{sample}}{REE_{PAAS}} \qquad \text{Equation 3.7}$$

The multiple oxidation states of cerium mean that, under certain conditions, cerium behaves differently to the other rare earth elements (as discussed in section 3.2.3). This distinction is expressed in the cerium anomaly (Ce/Ce*), which is the difference in the shale-normalised abundance of cerium compared to the expected value calculated from the nearby LREE elements [de Baar et al. 1985]:

$$\frac{Ce}{Ce*} = \frac{3Ce_n}{2La_n + Nd_n} \qquad \text{Equation 3.8}$$

3.4.3 Neodymium isotope analysis

Neodymium was purified from the dissolved samples using standard procedure column chemistry, based upon the methods of Cohen et al. [1988]. Two series of columns were used. Firstly, cation columns were used to strip iron and titanium from the samples. The remaining material was then run through LN Spec™ columns to isolate neodymium (and samarium) as far as possible [Pin and Zalduegui 1997]. The detailed column procedure can be found in appendix 3.

To prepare for analysis, each purified sample was dissolved in 420 µl 0.5 M HNO_3. Autosampler vials were cleaned in 10% HNO_3, rinsed in MilliQ water and then dried. A calibration set of samples were prepared by adding 20 µl of the dissolved sample to an autosampler vial already containing 100 µl 0.5 M HNO_3. These were analysed in three separate runs by the Multi-collector ICP-MS: Thermo NEPTUNE at the School of Ocean and Earth Science, University of Southampton. ^{144}Nd and ^{140}Ce intensities were noted for each sample. This allowed samples to be diluted further with 0.5 M HNO_3 (if necessary) so that the intensities of the neodymium peaks in the main run were as constant as possible. Instrumental mass bias ratios were corrected using the procedure of

Vance and Thirlwall [2002], adjusting to a $^{146}Nd/^{144}Nd$ of 0.7219 and using cerium-doped standards to correct for interference of ^{142}Ce on ^{142}Nd. All values were normalised to the JNdi-1 Standard ($^{143}Nd/^{144}Nd = 0.512115 \pm 7$) [Tanaka et al. 2000]. Replicate measurements of this standard across the three runs gave an external reproducibility 2σ (2 standard deviations) = 0.2 ε_{Nd} units.

3.5 Results

3.5.1 Neodymium isotopes

The neodymium isotopic signature of planktonic foraminifera shows distinctive downcore variation, illustrated in figure 3.2 (a). Glacial age samples show a steady baseline value of $\varepsilon_{Nd} = -10$ (with a slight long-term shift towards more radiogenic values approaching the last glacial maximum). Superimposed on this are two distinct excursions: a negative excursion to values of $\varepsilon_{Nd} = -12$ at Heinrich event 4 and a positive excursion to $\varepsilon_{Nd} = -7$ at Heinrich event 2. A gradual shift towards less radiogenic values begins at 14 ka, with minimum values of $\varepsilon_{Nd} = -13.5$ occurring in the early Holocene. These then slowly increase towards a core top value of $\varepsilon_{Nd} = -11.7$. The oceanographic implications of these features will be discussed in chapter 4.

The neodymium isotope records of fish debris and uncleaned foraminifera show excellent agreement throughout the record, with samples from the same depth horizon either within error, or close to it. The record derived from bulk sediment leachates shows overall agreement in pattern but with substantial offsets to planktonic foraminifera and fish debris in several sections of the record. This is especially true during the Holocene (from approximately 12 ka BP), where there is a systematic offset of 1–2 ε_{Nd} units between the substrates, with the leachates giving a consistently more radiogenic signal. There are also several shorter intervals of more radiogenic leachate values at 16 ka, 20 ka and 32 ka.

3.5.2 REE and trace element concentrations

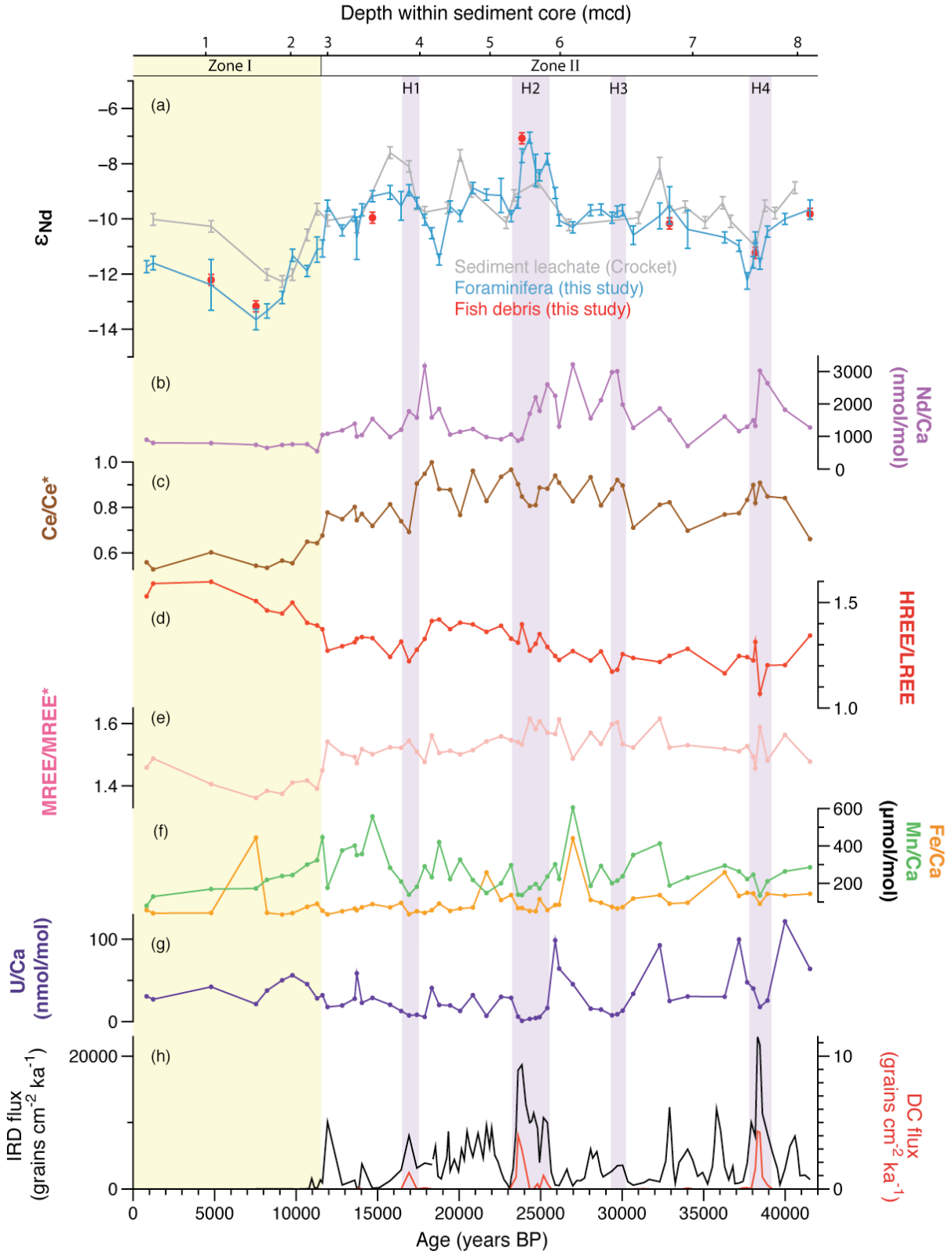
Depth within sediment core (mcd)
1
2
3
4
5
6
7
8
Zone I
Zone II
H1
H2
H3
H4
(a)
εNd
−6
−8
−10
−12
−14
Sediment leachate (Crocket)
Foraminifera (this study)
Fish debris (this study)
(b)
Nd/Ca (nmol/mol)
3000
2000
1000
0
(c)
Ce/Ce*
1.0
0.8
0.6
(d)
HREE/LREE
1.5
1.0
(e)
MREE/MREE*
1.6
1.4
(f)
Fe/Ca
Mn/Ca
(μmol/mol)
600
400
200
(g)
U/Ca (nmol/mol)
100
0
(h)
IRD flux (grains cm-2 ka-1)
20000
0
DC flux (grains cm-2 ka-1)
10
0
0
5000
10000
15000
20000
25000
30000
35000
40000
Age (years BP)

Figure 3.2: (a) Neodymium isotope composition of sediment leachates (grey, from Crocket et al. [2011]), mixed planktonic foraminifera (blue) and fish debris (red), all from ODP Site 980. Error bars show either internal or external error (whichever is larger). (b) Nd/Ca ratios of mixed planktonic foraminifera. (c), (d) and (e) Ratios of PAAS-normalised rare earth elements of mixed planktonic foraminifera (formulae given in equations 3.3–3.8). (f) and (g) Fe/Ca (orange), Mn/Ca (green) and U/Ca (purple) ratios of mixed planktonic foraminifera. (h) Fluxes of ice-rafted debris (black) and detrital carbonate (red) grains from the >150 μm size fraction of Site 980 samples. Purple shading marks position of Heinrich events (as identified from the IRD record) and yellow shading highlights the upper section of the core with an offset in the neodymium isotope ratios between the planktonic foramifera and fish debris sediment leachate values (zone I). Note that depth within sediment core (in metres composite depth) is a non-linear scale.

The downcore rare earth element data from Site 980 clearly show different behaviour in the upper and lower parts of the core (illustrated in figure 3.2), with a distinct transition at 2.9 m depth (11.5 ka). In the following discussions, the upper section of the core will be referred to as zone I, and the lower section, zone II. Nd/Ca values are relatively low and steady throughout zone I, at approximately 700–800 nmol/mol, with higher and more variable values (900–3000 nmol/mol) in zone II. The distribution of the rare earth elements also changes across this depth interval, with the enrichment of the heavy rare earth elements over the light rare earths higher in zone I (1.4–1.6) than zone II (1.2–1.4). The magnitude of the negative cerium anomaly shifts at the same depth, with anomaly values in zone I of 0.5–0.6 to compared to 0.75–1 in zone II (where 1 indicates no anomaly in cerium concentrations compared to the other rare earth elements). Cerium anomaly values never exceed 1, in agreement with pore waters measured across a range of environments [Haley et al. 2004]. There is also a small difference in MREE/MREE* values between zones I and II, most likely attributable to a decreased relative proportion of the HREE deeper within the core.

There is no clear correlation of the rare earth elements (represented by Nd) with any of the redox sensitive elements manganese, iron or uranium (shown in figure 3.3), in

contrast to the results presented from the Bermuda Rise by Roberts et al. [2012]. Neither the Fe/Ca nor U/Ca ratios of foraminifera show distinctive differences between zone I and zone II, while although Mn/Ca is more variable in zone II, it lacks the marked increase seen in the Nd/Ca record (figure 3.2).

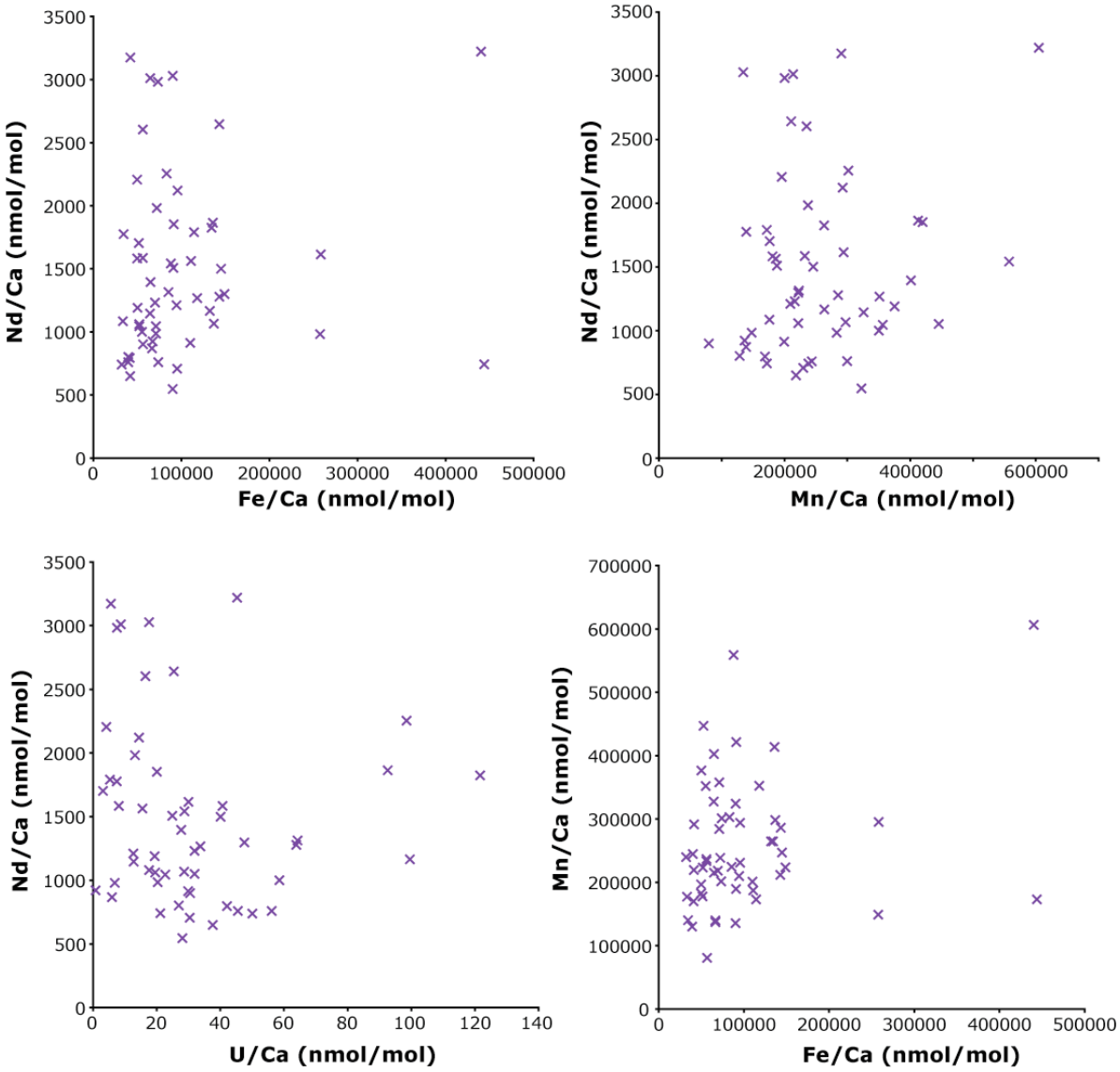

Figure 3.3: Cross plots of trace element concentrations of mixed planktonic foraminifera from ODP Site 980.

3.6 Discussion

3.6.1 Assessing potential sources of contamination

3.6.1.1 Detrital input

Before the neodymium isotope record generated here can be interpreted palaeoceanographically, it is important to determine the precise nature of signal recorded by the samples (as far as possible). The extent to which contaminating clays influence the samples is assessed through Al/Ca ratios, which are generally low (< 100 μmol/mol). A few samples contain higher Al/Ca ratios, however, these are all associated with low Nd/Ca values (illustrated in figure 3.4). This suggests that clays are not a significant source of neodymium to the samples, and hence no samples have been excluded from the data set on the basis of their Al/Ca values.

Sediments from ODP Site 980 contain a high proportion of lithic grains (especially during glacial conditions), therefore, it is possible that input of material with a preformed neodymium isotopic signature is influencing the record [Rutberg et al. 2000; Bayon et al. 2002; Bayon et al. 2004]. This hypothesis can be tested through the abundance of elements common in terrestrial environments but depleted in open marine settings (e.g. Ti, Zr, Pb) [M. Gutjahr, pers. comm.]. None of these elements show correlation with either Nd/Ca or ε_{Nd}, and the samples with high concentrations of Zr, Pb and Ti exhibit low Nd/Ca values (figure 3.4). Therefore, it does not appear that terrestrial contamination significantly influences the neodymium isotopic data presented here.

3.6.1.2 Volcanic ash

The influence of volcanic ash on the fidelity of neodymium isotope reconstructions of bottom water chemistry is a significant concern in the North Atlantic [e.g. Elmore et al. 2011]. Volcanic material has a very radiogenic isotopic signature [e.g. Jeandel et al.

2007; Sarbas and Nohl 2008], and hence has the potential to significantly modify the neodymium isotopic signatures of sediment components.

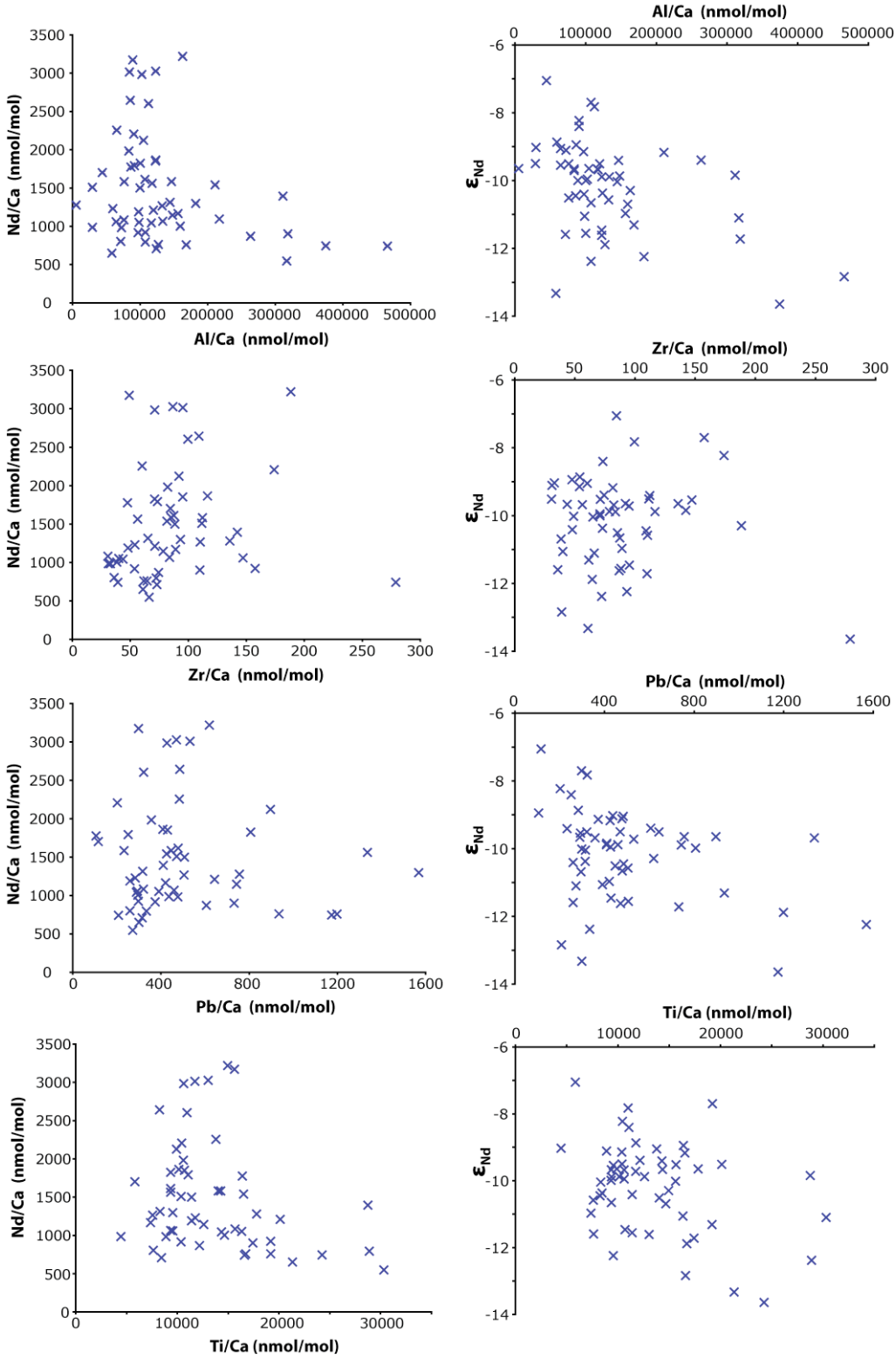

Figure 3.4: Cross-plots to assess the extent of lithogenic contamination on the neodymium concentrations (left) and neodymium isotope signatures (right) of mixed planktonic foraminifera samples. Elements used to assess degree of contamination are, from top to bottom: aluminium, zirconium, lead and titanium.

A strong influence of easily leacheable, radiogenic volcanic material on sediment leachate ε_{Nd} values has been documented in the North Atlantic, most notably in close proximity to Iceland [Elmore et al. 2011]. Site 980 is located approximately 1000 km from Iceland, just outside the affected zone of core top material identified by Elmore et al. [2011]. Therefore, the data presented here could potentially be affected during intervals of high volcanic output, or under different patterns in atmospheric or oceanic circulation, which resulted in the transport a higher proportion of ash towards the site. To test this hypothesis, the multi-substrate neodymium isotope reconstructions were compared to counts of igneous grains >150 μm from ODP Site 980 (presented in chapter 2) and to the occurrence of ash layers documented in other regional climate archives (illustrated in figure 3.5).

The presence or absence of ash in the sediment does not appear to be the dominant control on the neodymium isotopic signature of either the sediment leachate, foraminiferal or fish debris records (illustrated in figure 3.5), with no clear relationship between the ages of documented ash layers and ε_{Nd} values at Site 980. The absence of ash throughout much of the Holocene also suggests that the offset between the foraminiferal and sediment leachate records through this interval is not caused by leaching of increased levels of ash. Small excursions to more radiogenic values in the foraminiferal ε_{Nd} record occur either at, or close to, three of the four major ash layers, giving values as (or sometimes slightly more) radiogenic than the sediment leachates. This raises the possibility either that the foraminiferal signal is modified by interaction with young volcanic material at times of major ash input, as previously observed on the Iceland margin [Elmore et al. 2011] or that samples contain small residual amounts of fine material, despite the clay removal step in their preparation. Trace element concentrations do not suggest any abnormally high levels of contamination by either clays or terrestrial material in the affected samples. It should be also noted that two of

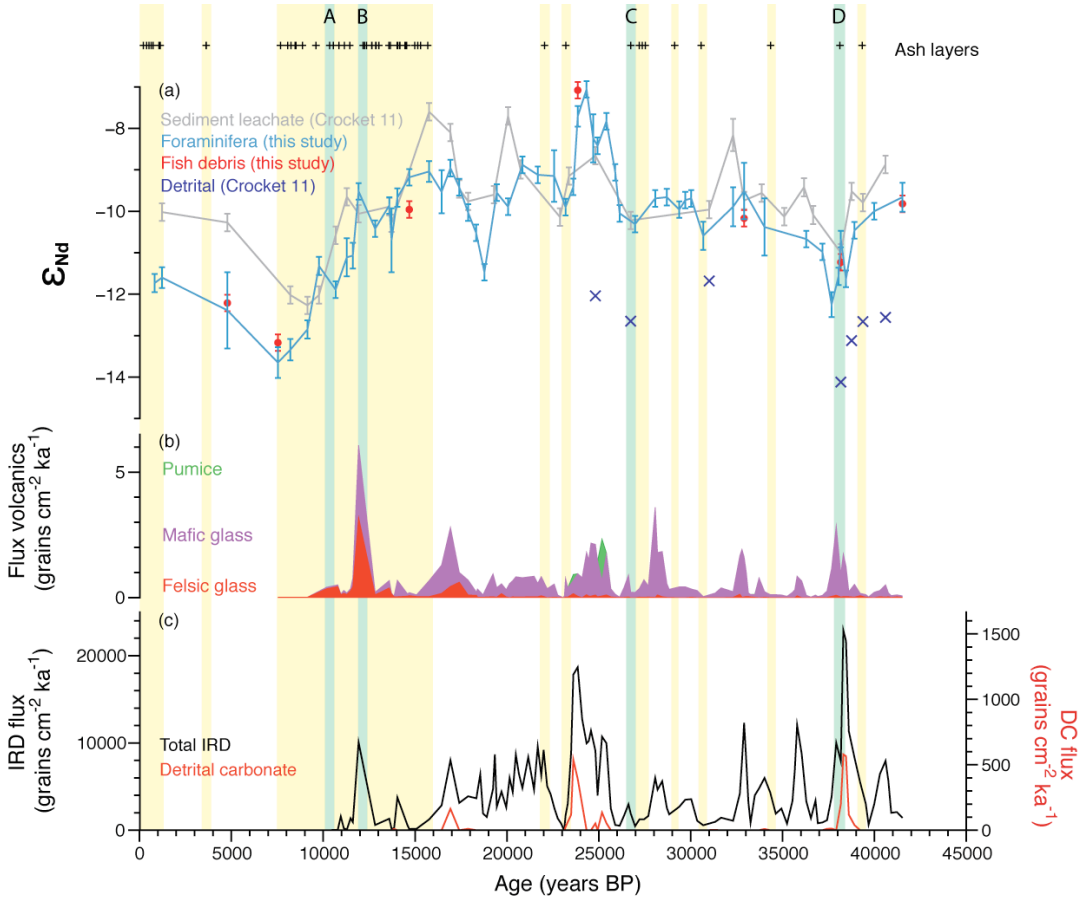

Figure 3.5: Assessment of the impact of volcanic input on multi-substrate neodymium isotope reconstructions. Vertical yellow bands highlight the time intervals when ash layers have been previously documented in the North Atlantic region, with black plus signs (+) marking the age of each individual ash layer [Wastegård et al. 2006; Lowe et al. 2008; Thornalley et al. 2011; Abbott and Davies 2012; Davies et al. 2012, and references therein]. The four major ash horizons of the last 40,000 years in the North Atlantic are highlighted in green (A: Saksunarvatn Ash, B: Vedde Ash, C: Faeroe-Marine Ash Zone II – Fugloyarbanki tephra, D: Faeroe-Marine Ash Zone III) [e.g. Davies et al. 2012]. (a) Down core neodymium isotopic signature of bulk sediment leachates (grey) [Crocket et al. 2011], mixed planktonic foraminifera (blue), fish debris (red), and the detrital fraction of the sediment (black crosses) [Crocket et al. 2011], all from ODP Site 980. Error bars indicate either internal or external error (whichever is larger). (b) Fluxes of volcanic grains in the >150 μm size fraction from Site 980, with colour shading indicating lithologies (red: felsic volcanic glass, purple: mafic volcanic glass and green: pumice. (c) Fluxes of ice-rafted debris (black) and detrital carbonate grains (red) in the >150 μm size fraction, from Site 980.

these three radiogenic excursions coincide with proposed climatic events (with the Younger Dryas and Heinrich event 4 approximately coincident with the Saksunarvatn Ash and Faeroe-Marine Ash Zone III respectively). Therefore, it seems plausible that water mass changes may be responsible for these observed neodymium isotope excursions, however, the influence of ash on foraminiferal neodymium isotopes (possibly through modification of pore/bottom water chemistry) is worthy of further investigation.

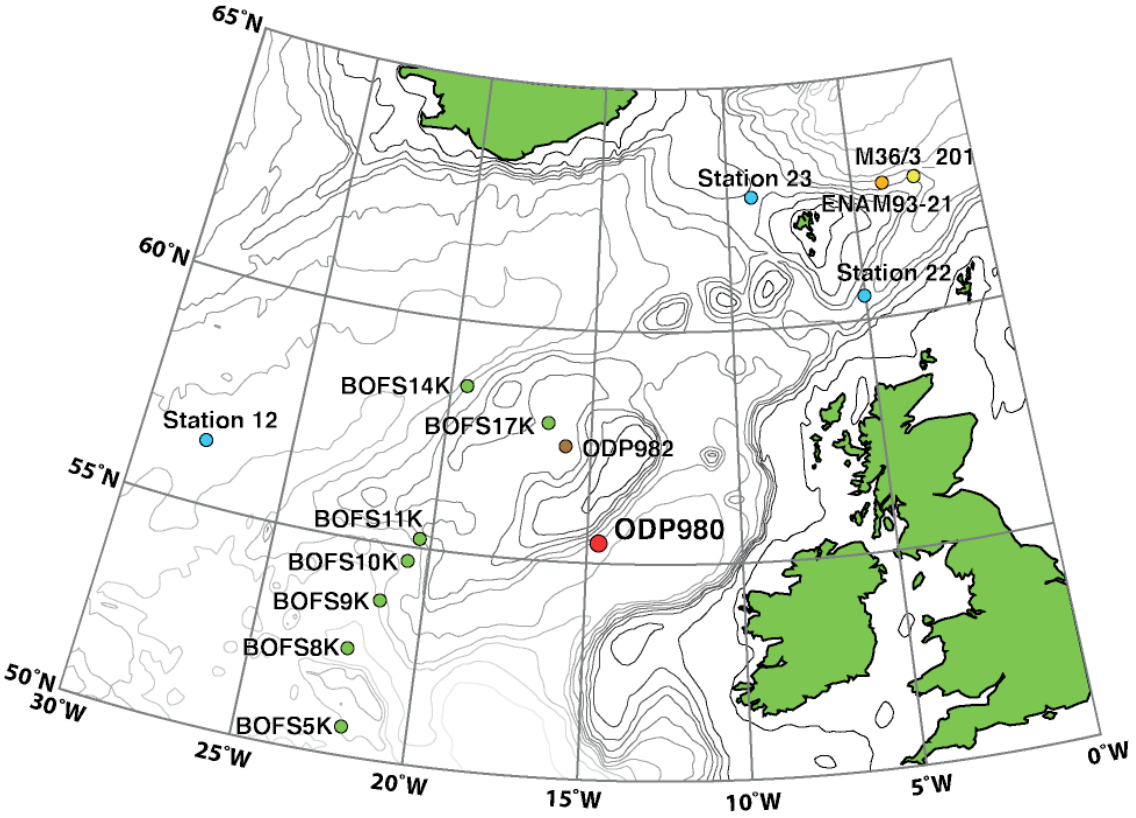

Figure 3.6: Location of sites referred to in discussion. Red: ODP Site 980 [Shipboard Scientific Party 1996], blue: water column data [Lacan and Jeandel 2004b; Lacan and Jeandel 2005a], green: % total organic carbon [Lowry et al. 1994], yellow: pore water chemistry [Sauter 1997], orange: ENAM93-21 for sedimentation rate comparison [e.g. Rasmussen et al. 1996] and brown: neodymium isotopes of fish teeth [Martin et al. 2010]. Figure created using Ocean Data View [Schlitzer 2013], plotted on an orthographic (North Pole) projection

3.6.2 Rare earth element distributions

3.6.2.1 Distribution of rare earth elements associated with foraminifera

The distribution of rare earth elements recorded in a foraminiferal sample can shed light on the phases with which they are associated. Numerous phases have been proposed as REE carriers associated with foraminiferal tests, including the calcite lattice and ferromanganese coatings (discussed in more detail in section 3.2.3). The nature of the REE carrying phases has important implications for how the REE become associated with the planktonic foraminifera, and hence the environmental conditions that they record. The relative influence of surface and bottom/pore water chemistry on planktonic foraminiferal neodymium isotopic signatures is particularly strongly debated [e.g. Vance and Burton 1999; Pomiès et al. 2002; Vance et al. 2004; Haley et al. 2005; Martìnez-Botì et al. 2009; Roberts et al. 2012]. In this study, no attempt has been made to separate the geochemical signatures of the different REE carrying phases associated with planktonic foraminifera. Figure 3.7 compares the Site 980 foraminiferal samples to published estimates of separated lattice and coating REE distributions from Palmer [1985] and Bayon et al. [2004]. Foraminifera from both zone I and zone II (as defined in section 3.5.2) of the core are much more similar to the estimates based on coatings, with the enrichment of HREE over the MREE in the lattice phase not seen in our samples. This supports previous suggestions that the majority of the neodymium associated with sedimentary planktonic foraminifera is in phases other than the primary calcite [e.g. Palmer 1985; Roberts et al. 2012; Tachikawa et al. 2013].

It should be noted, however, that the depletion of the HREE relative to the MREE observed in the zone II samples is not seen in zone I, which, coupled with the lower total rare earth element concentrations, may suggest a greater proportional contribution of the lattice phase to the total foraminferal rare earth concentrations in the upper section of the core. The zone I samples fit the estimated coating composition of Bayon et al. [2004] more closely, while in zone II, there is a better match to Palmer [1985]. This is most likely due to the different techniques used to estimate the coating signature. Bayon et al.

[2004] analysed whole, uncleaned foraminifera and assumed that all of the rare earths were contained within the coatings, so their quoted coating rare earth distributions are actually whole foraminifera and likely contain a component of lattice-bound REEs. In contrast, Palmer [1985] measured the lattice rare earth distribution after the coatings had been removed and subtracted these values from the total foraminiferal signal to obtain the coating composition. The zone II samples therefore likely contain a higher proportion of authigenic REEs, with lattice-bound REEs less significant, hence a better fit to the pure coating signal is observed. This is supported by the increased Nd/Ca ratios of the zone II samples (figure 3.2).

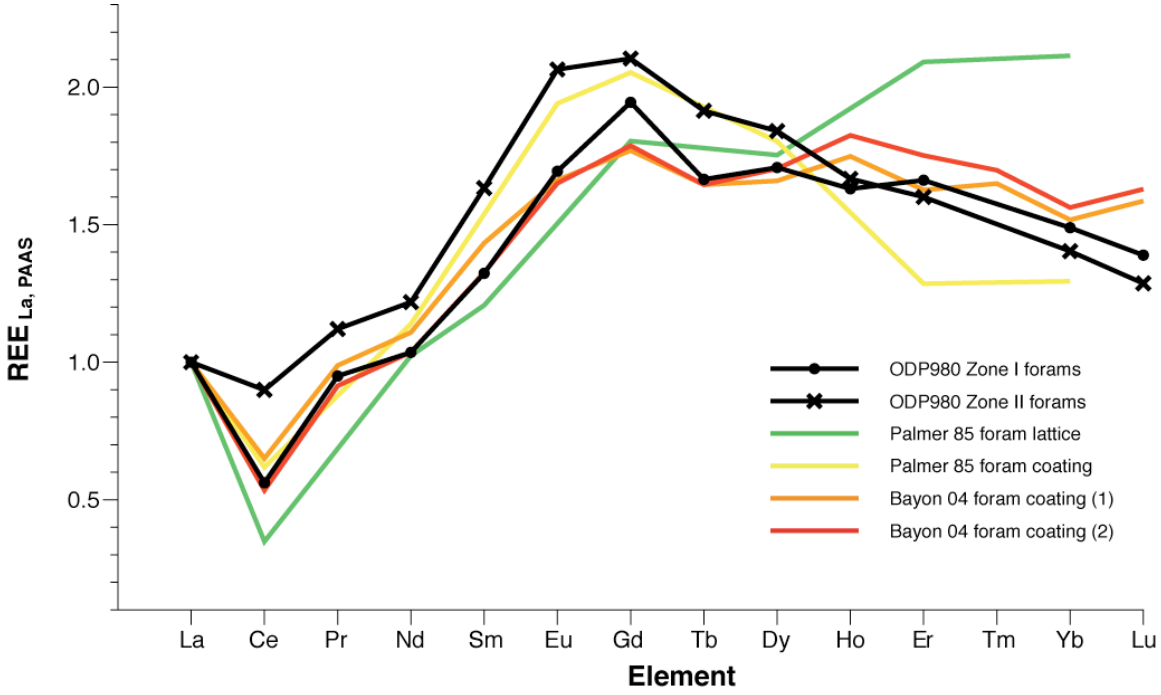

Figure 3.7: Rare earth element profiles, with values normalised to PAAS and La = 1. Mixed planktonic foraminifera from ODP Site 980 (black) are compared to a core top foraminiferal lattice signature (green) [Palmer 1985], core top foraminiferal coatings (yellow) [Palmer 1985] and estimates of foraminiferal coating from the core top and 46 cm depth at two different sites in the Cape Basin (orange and red respectively) [Bayon et al. 2004].

The issue of whether foraminiferal coatings preserve a seawater or pore water neodymium isotopic signal, or a combination of the two is still debated [e.g. Palmer 1985; Pomiès et al. 2002; Vance et al. 2004; Haley et al. 2005; Martìnez-Botì et al. 2009; Roberts et al. 2010]. Rare earth element distributions can help to distinguish between the two regimes. In figure 3.8, the neodymium isotopic signature of foraminifera presented here is compared to seawater samples from three oceanographically similar sites to ODP Site 980 (locations shown on figure 3.6). Station 12 is located in the Iceland Basin, with a sample taken at 2020 m water depth, situated between the Labrador Sea Water (LSW) and North East Atlantic Deep Water (NEADW) layers [Lacan and Jeandel 2005a], the same water masses bathing Site 980 (see section 1.4).

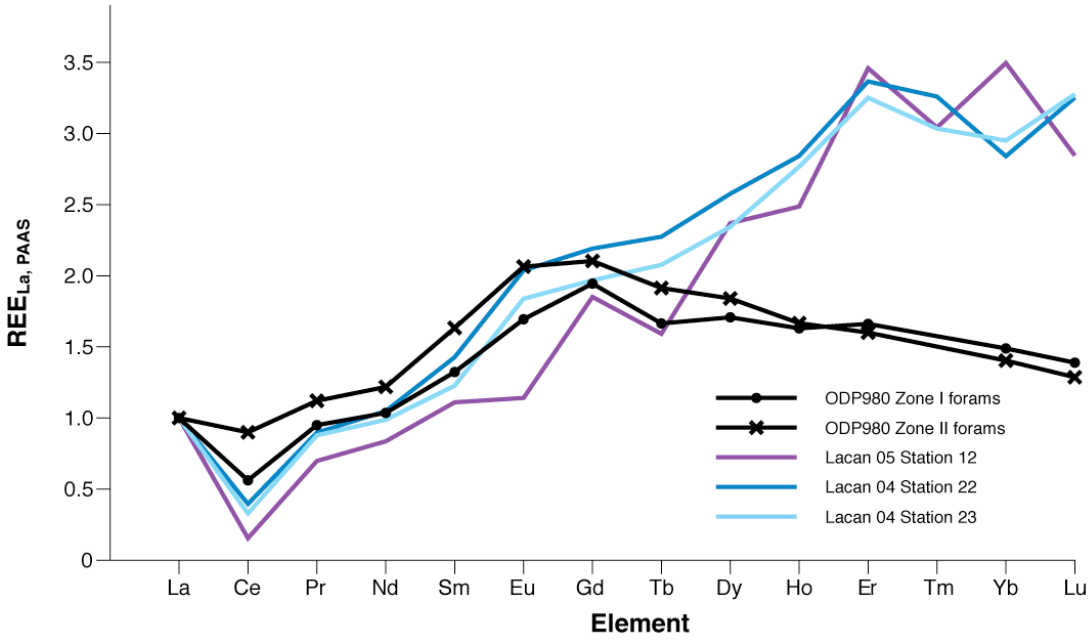

Figure 3.8: Rare earth element profiles (with concentrations normalised to PAAS and La = 1) of mixed planktonic foraminifera from ODP Site 980 (black) compared with seawater chemistry. Purple: 2020 m water depth at Station 12, from the Iceland Basin [Lacan and Jeandel 2005a], dark blue: 483 m water depth at Station 22, Faroe-Shetland Channel [Lacan and Jeandel 2004b], light blue: 988 m water depth at Station 23, Faroe-Shetland Channel [Lacan and Jeandel 2004b]. Station locations are shown on figure 3.6.

As Site 980 may also be influenced by overflow waters from the Nordic Seas, bottom water signatures at Stations 22 and 23 from the Faroe-Shetland Channel [Lacan and

Jeandel 2004b] have also been included for comparison. All three seawater REE profiles are very similar to each other, with steady increasing PAAS-normalised REE concentrations as atomic mass increases and a strong negative cerium anomaly. Shale-normalised HREE concentrations are enriched by approximately a factor of 3 over the LREEs, which is a significantly greater enrichment than observed in any of the foraminiferal samples. Therefore, it seems that the rare earth element signature of foraminifera is strongly fractionated from seawater and/or modified within the sediment.

There is a much better match between the foraminiferal REE distribution and that documented in pore waters (illustrated in figure 3.9). Haley et al. [2004] identify three distinct patterns in the REE distribution of shallow pore waters under a range of redox conditions (figure 3.9), with similar pore water REE distributions recorded by Sholkovitz et al. [1989]. The "linear" pattern is the most common of the three, and has been linked to the degradation of particulate organic carbon (POC). The second pattern has a distinctive "MREE bulge". This signal in pore waters has been associated with the dissolution of iron oxides under anoxic conditions [e.g. Froelich et al. 1979; Aller and Barry 1980; Stumm and Sulzberger 1992; Burdige 1993; Johannesson and Zhou 1999; Haley et al. 2004]. A third "HREE enriched" pattern has only been observed at the sediment surface [Haley et al. 2004], and hence is a poor match for the Site 980 record, where the shallowest sample was taken at 5–7 cm below the sediment surface.

There is a much closer correspondence of the foraminiferal records presented here with both the "linear" and "MREE bulge" patterns in pore waters than there is to the seawater patterns shown in figure 3.8. This suggests that the rare earth element signature of foraminifera is acquired at shallow depths within the sediment, and hence the chemistry of pore waters rather than bottom water chemistry is preserved, most likely in authigenic phases rather than being incorporated into the calcite lattice of the foraminifera.

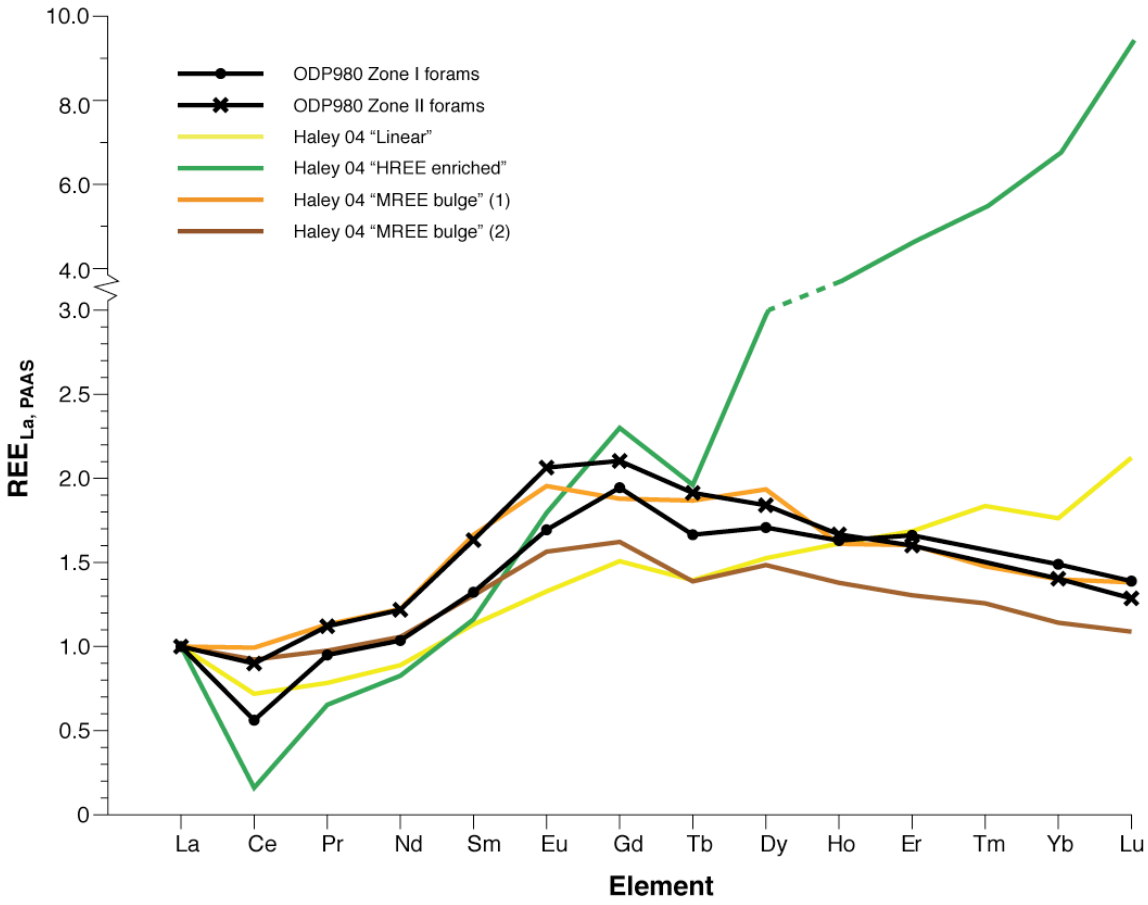

Figure 3.9: Rare earth element profiles (with concentrations normalised to PAAS and La = 1) of mixed planktonic foraminifera from ODP Site 980 (black) compared with examples of the three types of pore water profiles identified by Haley et al. [2004]. All data from Haley et al. [2004] with yellow: Station 9, 1.47 cm depth ("Linear" profile), green: Station MC64, 1.18 cm depth ("HREE enriched" profile), orange: Station 8, 17.83 cm depth ("MREE bulge") and brown: Station 10, 5.33 cm depth ("MREE bulge").

3.6.2.2 Comparison with the REE signature of fish debris

Fragments of fish debris were analysed at various depths downcore to provide an additional check on the fidelity of the planktonic foraminifera rare earth element and neodymium isotope records. A clear similarity between the rare earth element profiles of foraminifera and fish debris from the same depth horizons can be seen throughout the record. The fish debris samples also show a distinct difference between the zone I and zone II sections of the core, with profiles very similar to those recorded in foraminifera

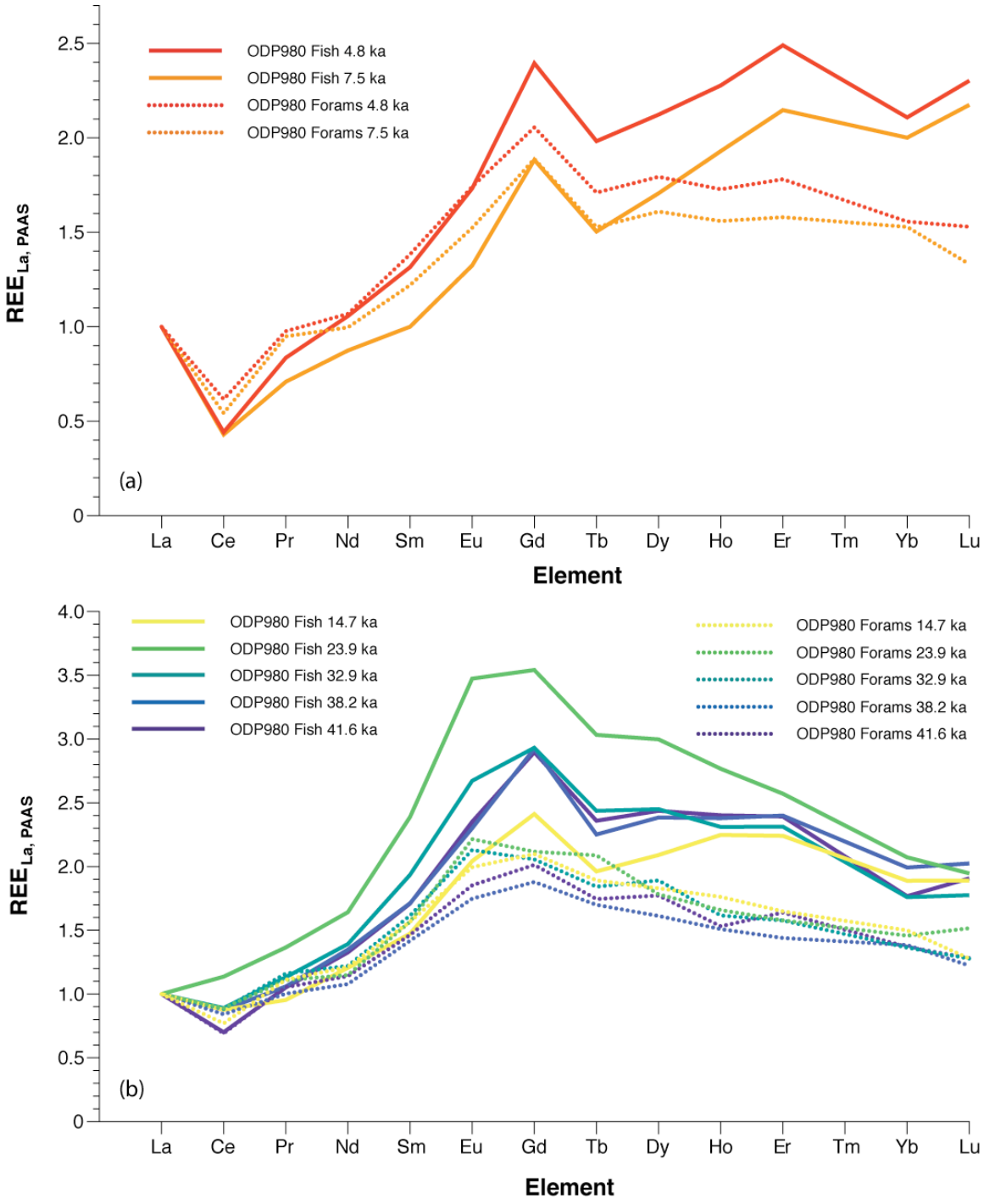

Figure 3.10: Comparison of REE profiles of fish debris and mixed planktonic foraminifera (normalised to PAAS and La = 1), from the same depth horizons in ODP Site 980. Solid lines indicate fish debris samples while foraminifera are plotted with dotted lines. Samples of equal depth within the sediment are shown in the same colour.

(illustrated in figure 3.10). In the upper part of the core (zone I), both substrates show a strong cerium anomaly, with MREE and HREE enriched over the LREE (with a slightly greater HREE enrichment in the fish). The fish debris samples from zone II show a strong MREE bulge, with similar profile shapes to the foraminifera, except for a lower proportion of LREE in the PAAS-normalised fish debris. The negative cerium anomaly is much less pronounced in both substrates in zone II than zone I. The similarity in the REE profiles of fish and foraminifera suggests that the processes controlling the rare earth distributions influence both substrates to a similar extent.

Different mechanisms have been invoked to explain the association of rare earth elements with fish debris and foraminifera. REEs are adsorbed to the surface of biogenic apatite during early diagenesis, with little fractionation or exchange with detrital material. REE concentrations increase by several orders of magnitude over unaltered apatite, hence any in vivo signature is almost completely obscured [Wright et al. 1984; Shaw and Wasserburg 1985; Elderfield and Pagett 1986; Grandjean et al. 1987; Grandjean and Albarède 1989; Trueman and Tuross 2002]. This signal is relatively resistant to diagenesis, with substitution of rare earth elements into the crystal lattice occurring only under more extreme conditions, resulting in a distinctive bell-shaped REE profile [Staudigel et al. 1985; Keto and Jacobsen 1987; Reynard et al. 1999; Armstrong et al. 2001; Martin and Scher 2004]. This bell-shaped profile is not seen in any of the samples presented here, suggesting that a shallow pore water signature is preserved by the fish debris. Therefore, the fish debris samples support the interpretation of the foraminiferal REE profiles presented in section 3.6.2.1, which suggest that planktonic foraminifera without their ferromanganese coatings removed preserve a shallow pore water signature rather than a seawater profile.

3.6.2.3 Explaining the changing downcore REE distributions

The rare earth element profiles of both planktonic foraminifera and fish debris at ODP Site 980 are clearly divided into two different regimes, which have been labelled zone I (the upper section of the core) and zone II (illustrated in figure 3.2). The cerium anomaly

is much lower in the zone 1 samples than those in zone II (figure 3.2), which suggests that more oxic conditions are recorded in the upper part of the core. An offset between the sediment leachate values and the other substrates is recorded in zone I but not zone II, which raises the possibility of a link between the processes controlling the shift in REE distributions and those determining the offset of one or more of the substrates from seawater ε_{Nd} values. Understanding the cause of the change in REE behaviour, therefore, has important implications for the fidelity of neodymium isotopic reconstruction of bottom water chemistry. Three potential explanations for these changes are explored here: a lithologic control, an active redox front in the sediment or preserved differences between glacial and interglacial conditions.

Lithology has been shown to have a strong control over the rare earth signature of bulk sediment [e.g. Thomson et al. 1984; Sholkovitz 1988; Sholkovitz 1990; Dubinin and Rozanov 2001]. However, the detrital fraction is typically unreactive (as evidenced by its extraction procedure) [Jones et al. 1994; Bayon et al. 2002], and REE concentrations are much lower than in the oxyhydroxide fraction [Gutjahr et al. 2007], hence the detrital influence on the REE signature of planktonic foraminifera is expected to be weak. Comparison of the fish debris, foraminifera and sediment leachate data with the bulk sediment neodymium isotopic record from Site 980 of Crocket et al. [2011] also argues against significant exchange of the REEs between the foraminifera and the sediments (illustrated in figure 3.5). Both H2 and H4 show unradiogenic bulk sediment signatures, while the foraminiferal record gives excursions in opposite directions at these two events. Therefore, significant exchange with the detrital fraction of the sediments can be ruled out.

An alternative explanation of the change in character of the REE profiles between zones I and II is that there is an active redox front in the sediment, resulting in a remobilisation and redistribution of the rare earth elements. In sediments, organic matter is gradually oxidised via a sequence of reactions involving progressively less energetically favourable terminal electron acceptors as each species is sequentially consumed with increasing depth below the sediment-water interface [e.g. Froelich et al. 1979; Burdige

1993; Calvert et al. 2007]. This sequence is illustrated in figure 3.11. As part of this succession, first manganese, and then iron are reduced to soluble ions (Mn^{2+} and Fe^{2+} respectively), leading to the dissolution of foraminiferal ferromanganese coatings and remobilisation of the associated rare earth elements [Palmer and Elderfield 1986; Burdige 1993; Roberts et al. 2012]. Unfortunately, the published pore water data for Site 980 is of too low resolution to establish the depth of these transitions [Shipboard Scientific Party 1996], but in figure 3.11, data from Greenland-Scotland Ridge site M36/3_201 [Sauter 1997] is shown for comparison with the model of Froelich et al. [1979]. Similar sedimentation rates to Site 980 have been recorded at site ENAM93-21, which is only 200 m deeper and 80 km west of M36/3_201 [Rasmussen et al. 1996], suggesting that M36_201 is a suitable analogue for Site 980. Pore water Mn^{2+} concentrations rapidly increase from 6 cm depth within the sediment at site M36/3_201, suggesting that oxygen concentrations are close to zero by this depth. Similar oxygen penetration depths to have been recorded at sites in and around the Rockall Trough with comparable water depths to Site 980 [Black et al. 2001; Papadimitriou et al. 2004]. The transition in rare earth element distributions at Site 980 occurs at ca. 2.9 m depth below the sea floor, therefore, active remobilisation of manganese coatings cannot be responsible for the shift in rare earth element distributions at this depth. The existence of significant iron reduction influencing the record is more difficult to determine. Although nitrate concentrations do not reach zero within the top 0.17 m of the core, they do drop significantly, so the presence of iron reduction cannot be completely ruled out.

In suboxic and anoxic sediments, if Mn^{2+} concentrations and carbonate alkalinity are sufficiently high, manganese may precipitate out as carbonates [e.g. Grill 1978; Pedersen and Price 1982; Middelburg et al. 1987; Burdige 1993]. This typically occurs on the order of tens of centimetres below the active Mn redox boundary [Pedersen and Price 1982; Burdige 1993], which is a better fit to the depth transition between zones I and II at Site 980. The precipitation of diagenetic manganese carbonates associating with foraminifera has the potential to alter their rare earth signature, particularly because these phases cannot be easily removed in the cleaning process [Palmer and Elderfield 1986; Roberts et al. 2012], although questions remain regarding the significance of the

association of rare earth elements with manganese carbonates [Tachikawa et al. 2013]. An alternative source of rare earth association with foraminifera comes through adsorption to the surface of iron sulphides under sulphate reducing conditions, which have been documented deeper within the sediment at ODP Site 980 [Shipboard Scientific Party 1996].

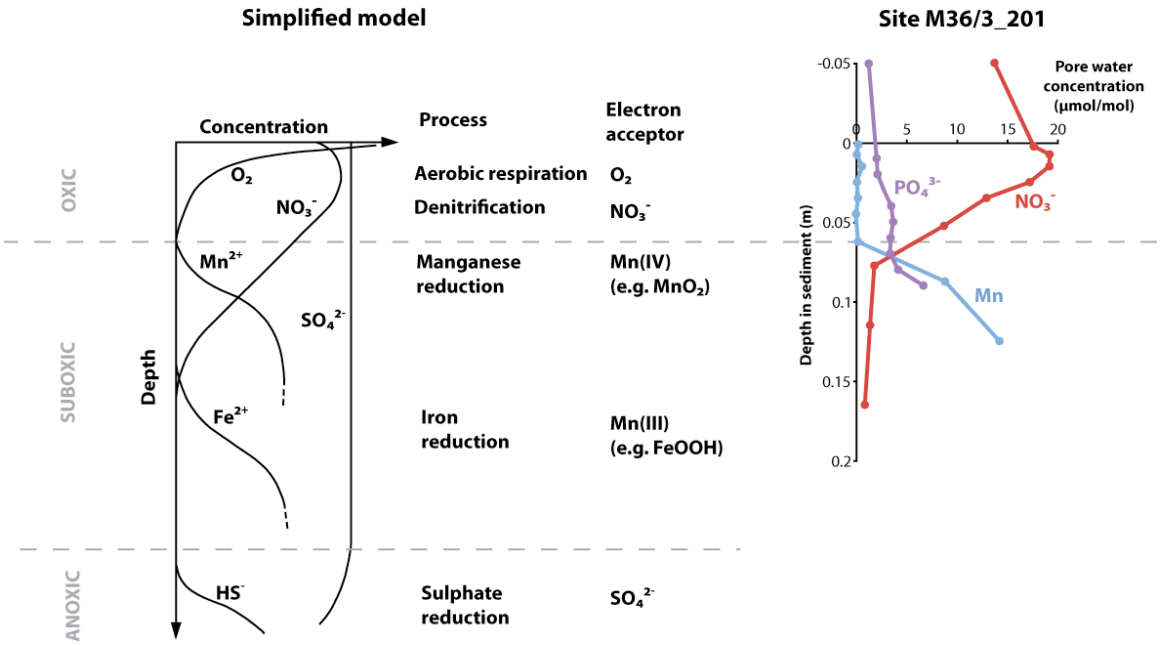

Figure 3.11: Comparison of pore water chemistry of Site M36/3_201 (right) with the model of Froelich et al. [1979] (left). Schematic depth profile of concentrations of main species in redox chemistry redrawn from Burdige [2006]. Site M36/3_201 data from Sauter [1997]. The onset of manganese reduction is clearly visible at 0.06 m depth, however the presence of iron reduction is less clearly identifiable.

Uncertainties in the pore water chemistry at depth make it difficult to fully evaluate the possibility of an active redox front driving the observed trends in REE chemistry. Manganese reduction can be ruled out, but iron reduction, manganese carbonate precipitation and/or pyritisation could all potentially be involved. Barite has also been proposed as a rare earth element carrier associated with foraminifera [Bayon 2002; Haley and Klinkhammer 2002], however pore water studies suggest that barium cycling

is dominant at depths shallower than manganese cycling [Haley et al. 2004], hence this is unlikely to be driving the observed changes at ODP Site 980.

The coincidence of the shift in REE distribution of foraminifera with the climatic transition into the Holocene raises the possibility that differences between glacial and interglacial conditions have been preserved and are responsible for the changes observed between zone I and zone II samples. Glacial-interglacial differences in the degree of oxygenation of shallow sediments have been documented in a number of studies [e.g. Mangini et al. 1990; Thomson et al. 1996; Mangini et al. 2001; Reitz et al. 2004], including Roberts et al. [2012] who observe similar changes in foraminifera REE concentrations and cerium anomalies from a site on the Bermuda Rise with a water depth of 4.5 km. These changes are dated to within ca. 1000 years of the similar transition observed at Site 980. A combination of oxygen-poor southern-sourced water reaching the site during the glacial interval and increased sedimentation rates leading to increased organic carbon burial allowing the development of suboxic conditions during the glacial have been proposed to explain the differences to the oxic Holocene conditions [Roberts et al. 2012]. However, these explanations cannot simply be invoked at Site 980 for three main reasons. First, the site is much shallower than the Bermuda Rise site studied by Roberts et al. [2012], with minimal influence of southern sourced waters during the glacial [e.g. Boyle and Keigwin 1987; Curry and Oppo 2005; Yu et al. 2008, and chapter 4 of this study]. Second, sedimentation rates at Site 980 were generally higher in the Holocene than during the glacial interval (see chapter 2). Third, there is no evidence of increased carbon burial during the glacial interval at this site. There is no dramatic change in total organic carbon (TOC) contents at the nearby BOFS cores, with generally slightly lower concentrations under glacial conditions than in the Holocene (illustrated in figure 3.12) [Lowry et al. 1994]. However, the occurrence of a transition to more reducing conditions at approximately the same age at two sites thousands of kilometres apart despite differences in sedimentation rate, bottom waters and trace metal cycling is suggestive of a common driving force.

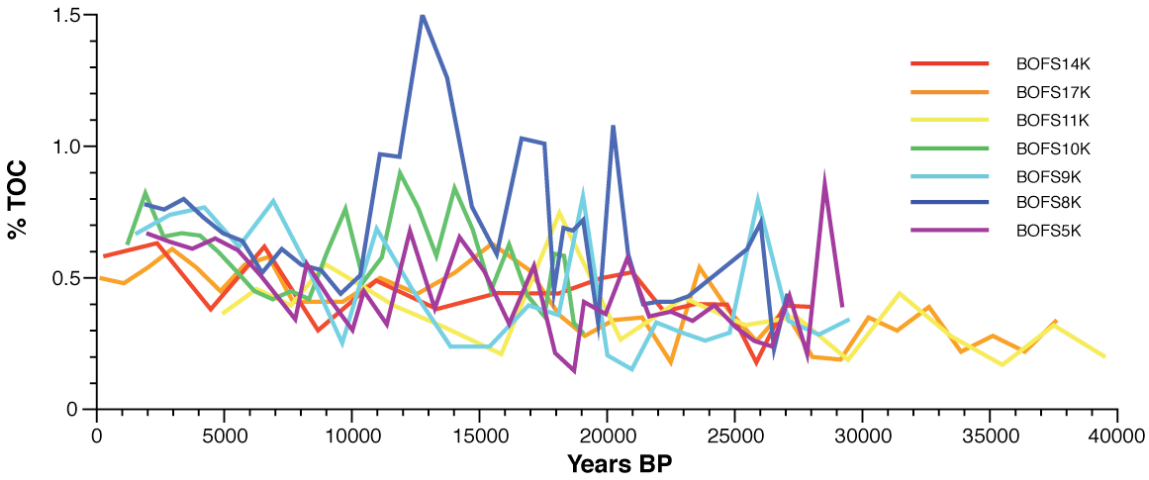

Figure 3.12: Percentage of organic carbon (% TOC) in sediments from BOFS cores [Lowry et al. 1994]. Sites are ordered by latitude, with BOFS14K the most northerly and BOFS5K the furthest south (exact locations shown in figure 5). Chronology for all BOFS cores from Manighetti et al. [1995].

The absence of southern-sourced waters bathing Site 980 does not necessarily preclude a reduction in bottom water oxygen content. Decreased oxygen content during the glacial interval is much more widespread than simply following the extent of southern sourced bottom waters [Murphy and Thomas 2010; Jaccard and Galbraith 2012], and has been documented on the Portuguese Margin at equal water depths to Site 980 [Baas et al. 1998; Schönfeld et al. 2003]. Increased alkalinity of the glacial ocean may also contribute to the glacial-interglacial differences [Sanyal et al. 1995; Yu et al. 2008; Rickaby et al. 2010, T. Chalk unpublished data], particularly if the rare earth elements are primarily associated with authigenic carbonates, as their formation is promoted by high pore water alkalinity [Grill 1978; Pedersen and Price 1982; Boyle 1983; Middelburg et al. 1987].

The preservation of a glacial shallow pore water signature without significant modification by later diagenetic processes by both the foraminifera and fish debris in the zone II samples is supported by comparing the data presented here with published REE distributions of fish teeth of Miocene age from nearby ODP Site 982 (location shown on figure 3.6) [Martin et al. 2010]. Although slightly flatter, the Miocene samples generally

exhibit very similar REE profiles to the samples presented here (figure 3.13). One of the most noticeable features is the preservation of a distinct negative cerium anomaly in all of the Miocene samples. The redox behaviour of cerium is thought to be very similar to that of manganese [Elderfield et al. 1988], hence reduction of Ce (IV) to Ce (III) (releasing Ce^{3+} ions into the pore waters) is expected to occur at shallow depths within the sediment, reducing the distinct negative cerium anomaly [e.g. Haley et al. 2004]. If the original, strong negative anomaly of the glacial samples from Site 980 had been reset by diagenetic processes deeper within the sediment, then it might be expected that the same would be true of the much older samples at Site 982. However, this is not the case. The similarity between the fish and foraminiferal signatures presented here suggests that foraminifera also preserve a near surface pore water signature.

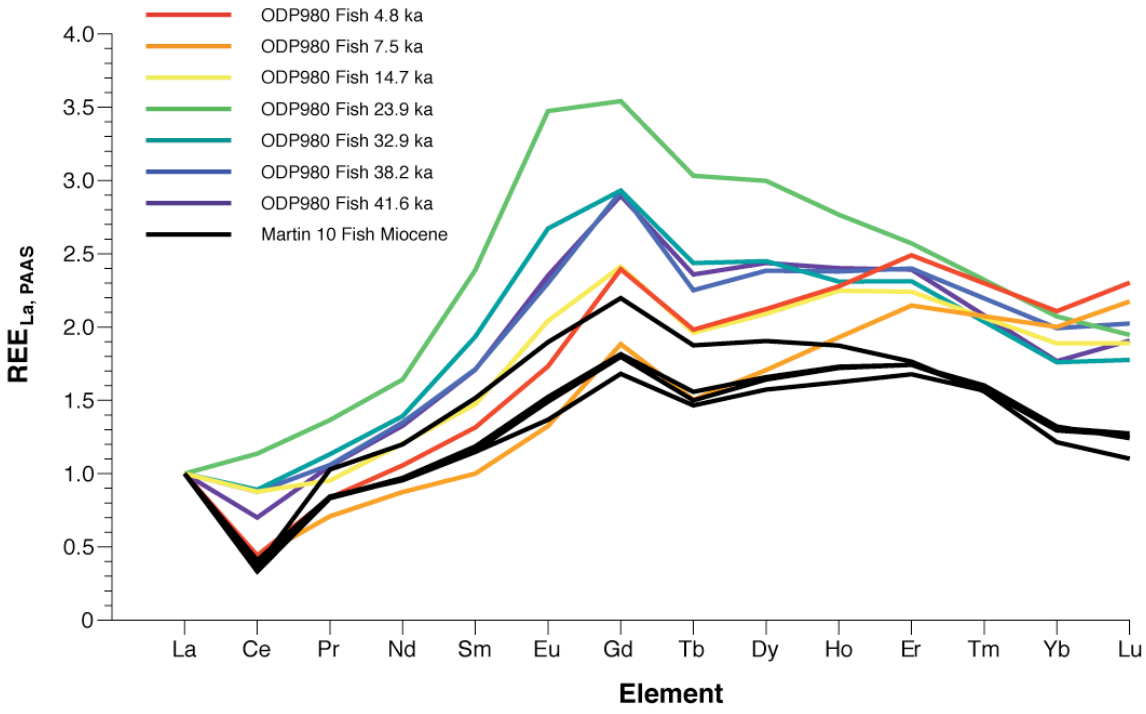

Figure 3.13: Rare earth element distribution of fish debris from ODP Site 980 (normalised to PAAS and La = 1), with colour indicating age of the samples, compared to Miocene age fish teeth from ODP Site 982 (black), published by Martin et al. [2010].

It therefore seems most probable that the changes in rare earth element distributions between the upper and lower sections of the core (zones I and II) are recording a change in the degree of shallow pore water oxygenation between the glacial and Holocene. It does not appear that diagenetic processes are resetting the rare earth element signature of either fish debris or planktonic foraminifera that is acquired in the top few centimetres of the sediment column, hence shallow pore water signals are preserved. Therefore, diagenetic remobilisation of the rare earth elements associated with planktonic foraminifera cannot explain why there is only agreement with the bulk sediment neodymium isotopic signatures in the deeper part of the core (zone II). Alternative hypotheses are explored in section 3.6.3.

3.6.3 Explaining the differences between the neodymium isotopic signatures of different substrates

Three different substrates have been used to reconstruct changes in the neodymium isotopic composition of seawater over the past 40,000 years at ODP Site 980: fish debris, mixed planktonic foraminifera (without coatings removed) and bulk sediment leachates (presented by Crocket et al. [2011]). Throughout the record, the agreement between the fish debris and planktonic foraminifera is either within error or close to it, with most of the record also showing good agreement with the sediment leachate record. However, there are some significant differences between the leachate and foraminiferal records, which fall into two categories. Firstly, there are several short radiogenic excursions recorded in the leachate record not supported by the other substrates (e.g. at 16 ka, 20 ka and 32 ka). Secondly, the leachates show a sustained radiogenic offset from both the foraminifera and the fish debris throughout the last 11.5 ka (zone I), which is concurrent with the change in REE distributions discussed in section 3.6.2.

The major discrepancies between the ε_{Nd} records at 16 ka, 20 ka and 32 ka do not seem to correlate with any major changes in bottom water properties as indicated by other proxies (see chapter 4), nor do they have any distinctive signal in the coarse lithic inputs or magnetic susceptibility suggestive of changes in sediment sourcing (chapter 2).

Therefore, it seems unlikely that these short-term differences between the neodymium substrates are caused by a primary climatic or oceanographic feature. There is also no clear increase in either the documented occurrence of ash layers or the concentration of coarse volcanic grains in the core at the main intervals of more radiogenic sediment leachate values (figure 3.5) to suggest that increased volcanic input is the cause of the offsets. The extraction of a neodymium isotopic signature from sedimentary material has been shown to be a delicate procedure, highly sensitive to the reagents used, solid-solution ratios and leaching time [Gutjahr et al. 2007; Piotrowski et al. 2012; Wilson et al. 2013]. The partial incorporation of a detrital signal into the sediment leachate may therefore be a more complex process than the simple presence of volcanic ash (or other easily leachable material) in the sediment, and could be responsible for these sporadic offsets between the substrates.

The second type of offset between the sediment leachates and foraminiferal neodymium isotope records is a 1–2 ε_{Nd} unit increasingly radiogenic signature preserved by the leachates throughout the uppermost 11.5 ka of the record (zone I), when compared to both foraminifera and fish debris. Unfortunately, the neodymium isotopic signature of modern bottom water at ODP Site 980 has not been directly measured to assess which of the substrates is recording bottom water chemistry accurately. However, the signatures of the individual water masses influencing the site (discussed in greater detail in sections 1.4 and 4.2.2) can be used to estimate the modern bottom water signature. Site 980 sits close to the boundary of Labrador Sea Water ($\varepsilon_{Nd} = -13.9 \pm 0.4$) and North East Atlantic Deep Water ($\varepsilon_{Nd} = -12.8 \pm 0.2$) [Lacan and Jeandel 2005a], with a possible influence of the Wyville-Thomson Overflow Waters ($\varepsilon_{Nd} = -11.4$ +2.4/–1.5, appendix 4). Therefore, the core top sediment leachate neodymium isotope values of $\varepsilon_{Nd} = -10.2 \pm 0.3$ [Crocket et al. 2011] are too radiogenic to be accurately recording bottom water values, unless the site is bathed by pure overflow waters, which is not supported by modern oceanographic observations [e.g. Ellett and Martin 1973; New and Smythe-Wright 2001; Sherwin and Turrell 2005; Johnson et al. 2010; McGrath et al. 2012]. The foraminiferal and fish debris values are more plausible estimates of bottom water chemistry. Therefore, the

sediment leachates must be influenced by an additional source of radiogenic neodymium in zone I, but not in zone II.

Offsets between sediment leachate and foraminiferal neodymium isotopes in core top samples have previously been recorded at numerous sites across the North Atlantic during the Holocene and attributed to the influence of easily leachable volcanic ash [Elmore et al. 2011]. However, there is no evidence for increased or sustained volcanic activity throughout the Holocene, corresponding to zone I (see figure 3.5). Instead, ash layers are much more widespread during the deglaciation, the early part of which shows a very good agreement between the foraminifera and fish records. Therefore, airborne volcanic ash cannot easily be invoked to explain the observed offset between the substrates.

In section 3.6.2.3, glacial-interglacial oceanographic changes were proposed as the most likely cause of the changing REE distributions recorded by fish and foraminifera between zones I and II. Therefore, variations in oceanography may explain the offsets between neodymium isotopic compositions of the substrates in the Holocene.

ODP Site 980 is located within one of the major North Atlantic sediment drifts (the Feni Drift), which means that sedimentation rates are enhanced by the deposition of fine-grained material transported by bottom current activity. Bottom currents were much stronger in the Holocene than the glacial in the Atlantic [Manighetti and McCave 1995; McCave et al. 1995; Innocent et al. 1997; McManus et al. 2004; McIntyre and Howe 2009], likely resulting in an increased accumulation of this fine material. The variable transport of fine titanomagentite grains from the Greenland-Scotland Ridge has been documented in a number of sites on the southern side of the ridge, particularly at sites in the path of the overflow waters [Kissel et al. 1999; Kissel 2005; Ballini et al. 2006]. This material likely has a radiogenic neodymium isotopic signature, sourced from the young igneous rocks of the Greenland-Scotland Ridge. Therefore, increased transport of leachable fine material from upstream during the stronger bottom current regime of the Holocene relative to the glacial is a plausible explanation for the more radiogenic

signature recorded by sediment leachates compared to fish debris and foraminifera during the Holocene. This explanation is supported by evidence for more radiogenic leachate values compared to other substrates in drift deposits from the Bermuda Rise [Roberts et al. 2010] and North Atlantic site BOFS8K during the Holocene [Piotrowski et al. 2012]. The pattern of sites showing unreasonably radiogenic sediment leachate ε_{Nd} values identified by Elmore et al. [2011] agrees well with the major modern Nordic Overflow water pathways [e.g. Hansen and Østerhus 2000]. Very radiogenic leachate values can be seen extending along the eastern side of the Reykjanes Ridge and around the southern tip of Greenland, while the raised Rockall Plateau (which is too shallow to be influenced by overflow waters) remains unaffected. Therefore, the influence of fine material transported by bottom currents appears to be the most likely explanation of anomalously radiogenic sediment leachate values recorded at Site 980 during the Holocene, casting doubt on the use of bulk sediment leachates to reconstruct bottom water chemistry at sediment drift sites.

3.6.4 The validity of neodymium isotopes as a bottom water proxy

The rare earth element profiles and multi-substrate neodymium isotopic reconstructions presented in this chapter allow the use of neodymium isotopes in planktonic foraminifera, bulk sediment leachates and fish debris to be reassessed. Although this study has only focussed on a single location (ODP Site 980), the implications are likely to be much wider ranging. One of the most significant results presented here is that bulk sediment leachate data from sediment drift sites should be treated with caution. Although sediment leachates have advantages over foraminifera and fish debris in that they are faster to process and often can be used to give much higher resolution records, the neodymium isotope values of the leachates are the least reliable of the three phases as a bottom water proxy. Therefore, if sediment leachates are to be used, the record should be supplemented by a second substrate (although not necessarily at the same resolution) to strengthen confidence in the leachate ε_{Nd} estimates, particularly in environments with a high, fine grained, easily leachable lithic input, such as volcanic ash, glacial flour or current-transported fine fraction from basaltic provinces.

Neodymium isotope values of foraminifera should also be carefully monitored in environments with high levels of volcanic ash, as there is a suggestion of increasingly radiogenic values coincident with times of increased ash delivery to the sediment, although this effect is difficult to disentangle from water mass changes at Site 980 (section 3.6.1.2).

The difference in rare earth element profiles between the foraminiferal samples and the bottom waters does not necessarily imply that the neodymium isotope signature preserved by foraminifera is unrepresentative of bottom water chemistry. Multiple studies have shown good agreement between bottom water and core top/shallow foraminifera ε_{Nd} values [e.g. Palmer and Elderfield 1985; Roberts et al. 2010; Elmore et al. 2011; Piotrowski et al. 2012]. The cycling of rare earth elements at shallow depths within the sediment involves release from phases that form within the water column, including ferromanganese oxides and organic matter [e.g. de Baar et al. 1985; de Baar et al. 1988; Sholkovitz et al. 1989; Jeandel et al. 1995; Haley et al. 2004; Roberts et al. 2012]. Fractionation between the rare earth elements is much greater than between isotopes hence phases with differing rare earth element signatures can still preserve a seawater isotopic ratio [Palmer and Elderfield 1986; Martin and Haley 2000; Martin et al. 2010; Tütken et al. 2011]. The sharpness of the excursions presented in the neodymium isotope record suggest that any smoothing only occurs over short distances (a maximum of ca. 10 cm), comparable to the scale of bioturbation, and in agreement with Roberts et al. [2012]. The excursions in ε_{Nd} preserved in the Site 980 record (for example, at H4 and H2) are not represented in the REE distributions, suggesting that they are not driven by diagenetic processes. Therefore, excursions in the neodymium isotopic signature recorded by foraminfera and fish debris are attributed to changes in bottom water chemistry (which is determined by the origin and transport history of the water mass), and hence provides a useful source of palaeoceanographic information for climatic reconstructions.

3.7 Summary and conclusions

Neodymium isotopic signatures of mixed planktonic foraminifera, fish debris and bulk sediment leachates from a single open ocean site are presented here to assess the accuracy and fidelity of bottom water ε_{Nd} values reconstructed by three commonly used techniques. In general, there is good agreement between the substrates, particularly the fish debris and planktonic foraminfera. However, there is a large discrepancy in the Holocene, with bulk sediment leachates preserving consistently more radiogenic neodymium isotope values than both fish debris and foraminifera. This observation cannot easily be explained by increased concentrations of easily leachable volcanic ash. Instead, the offset is attributed to the sensitivity of the bulk sediment leaching procedure to increased transport of fine titanomagnetite grains from upstream locations (including the Greenland-Scotland Ridge) under the stronger bottom current regime of the Holocene. Sediment leachate values in the Holocene are significantly offset from the estimated modern bottom water neodymium isotopic signature, casting significant doubt on the accuracy by which bottom water ε_{Nd} signatures can be reconstructed from bulk sediment leachates at sites with a high influx of easily leachable fine material, such as sediment drift deposits.

The distribution of rare earth elements preserved by both foraminifera and fish debris is much closer to pore water profiles than seawater samples, suggesting that their rare earth signature is dominantly acquired at shallow depths within the sediment column. There is a distinct shift in the rare earth element distribution of both foraminifera and fish debris approximately coincident with the glacial-interglacial transition in the sediment. This change in REE chemistry is attributed to more oxic conditions prevailing in the shallow sediment during the Holocene than under glacial conditions. An alternative hypothesis is the existence of a redox horizon approximately 3 m below the sediment-water interface, resulting in a diagenetic redistribution of the rare earth elements. This hypothesis cannot be completely discounted without pore water data. However, the presence of distinct negative cerium anomalies in much older fish debris samples at a nearby site [Martin et al. 2010], similar to those recorded in the Holocene but not the glacial at Site 980 argues against the influence of a strong diagenetic overprint on the records. This is supported by the sharpness of the neodymium isotopic excursions preserved during certain Heinrich

events at the site, arguing against significant smoothing of the signal as a result of REE remobilisation at depth. Therefore, a shallow pore water signal of rare earth elements appears to be preserved by both planktonic foraminifera and fish debris throughout the upper 8 m of the sediment column at Site 980, supporting the use of both of these substrates in palaeoceanographic reconstructions.

3.8 Acknowledgements

A large amount of gratitude goes to Matt Cooper for assistance developing the methodology used in this chapter, with invaluable support for the neodymium isotope work from Marcus Gutjahr and Dave Lang. Andy Milton, Marcus Gutjahr and Agnes Michalik provided vital analytical and technical support, making this work possible. Megan Spencer helped to pick some of the foraminiferal samples. Marcus Gutjahr, Paul Wilson, Tom Chalk, Joe Stewart and Heiko Pälike are thanked for very productive discussions, with useful feedback on this chapter provided by Paul Wilson and Heiko Pälike. Thanks also go to Dan Murphy and Wendy Kordesch for assistance identifying fish debris.

3.9 References

Abbott, P. M., and Davies, S. M., 2012, Volcanism and the Greenland Ice-cores: The Tephra Record: Earth-Science Reviews.

Aller, R. C., and Barry, S., 1980, Diagenetic Processes Near the Sediment-Water Interface of Long Island Sound. II. Fe and Mn, Advances in Geophysics, Elsevier, p. 351-415.

Armstrong, H. A., Pearson, D. G., and Griselin, M., 2001, Thermal effects on rare earth element and strontium isotope chemistry in single conodont elements: Geochimica et Cosmochimica Acta, v. 65, p. 435-441.

Arsouze, T., Dutay, J. C., Lacan, F., and Jeandel, C., 2009, Reconstructing the Nd oceanic cycle using a coupled dynamical-biogeochemical model: Biogeosciences, v. 6, p. 2829-2846.

Baas, J. H., Schönfeld, J., and Zahn, R., 1998, Mid-depth oxygen drawdown during Heinrich events: evidence from benthic foraminiferal community structure, trace-fossil tiering, and benthic δ13C at the Portuguese Margin: Marine Geology, v. 152, p. 25-55.

Ballini, M., Kissel, C., Colin, C., and Richter, T., 2006, Deep-water mass source and dynamic associated with rapid climatic variations during the last glacial stage in the North Atlantic: A multiproxy investigation of the detrital fraction of deep-sea sediments: Geochem. Geophys. Geosyst., v. 7, p. Q02N01.

Bayon, G., 2002, An Investigation Into Nd and Sr Isotopes in Marine Sediments and their Application to Paleoceanography, University of Southampton 211 p.

Bayon, G., German, C. R., Boella, R. M., Milton, J. A., Taylor, R. N., and Nesbitt, R. W., 2002, An improved method for extracting marine sediment fractions and its application to Sr and Nd isotopic analysis: Chemical Geology, v. 187, p. 179-199.

Bayon, G., German, C. R., Burton, K. W., Nesbitt, R. W., and Rogers, N., 2004, Sedimentary Fe-Mn oxyhydroxides as paleoceanographic archives and the role of aeolian flux in regulating oceanic dissolved REE: Earth and Planetary Science Letters, v. 224, p. 477-492.

Bertram, C. J., and Elderfield, H., 1993, The geochemical balance of the rare earth elements and neodymium isotopes in the oceans: Geochimica et Cosmochimica Acta, v. 57, p. 1957-1986.

Black, K. S., Fones, G. R., Peppe, O. C., Kennedy, H. A., and Bentaleb, I., 2001, An autonomous benthic lander: preliminary observations from the UK BENBO thematic programme: Continental Shelf Research, v. 21, p. 859-877.

Boyle, E. A., 1983, Manganese carbonate overgrowths on foraminifera tests: Geochimica et Cosmochimica Acta, v. 47, p. 1815-1819.

Boyle, E. A., and Keigwin, L., 1987, North Atlantic thermohaline circulation during the past 20,000 years linked to high-latitude surface temperature: Nature, v. 330, p. 35-40.

Broecker, S. W., and Peng, T.-H., 1982, Tracers in the Sea, Eldigo Press, Palisades, NY, 690 p.

Burdige, D. J., 1993, The biogeochemistry of manganese and iron reduction in marine sediments: Earth-Science Reviews, v. 35, p. 249-284.

—, 2006, Geochemistry of Marine Sediments, v. 398, Princeton University Press, Princeton.

Burton, K. W., and Vance, D., 2000, Glacial-interglacial variations in the neodymium isotope composition of seawater in the Bay of Bengal recorded by planktonic foraminifera: Earth and Planetary Science Letters, v. 176, p. 425-441.

Byrne, R. H., and Kim, K.-H., 1990, Rare earth element scavenging in seawater: Geochimica et Cosmochimica Acta, v. 54, p. 2645-2656.

Calvert, S. E., Pedersen, T. F., Hillaire-Marcel, C., and De Vernal, A., 2007, Chapter Fourteen Elemental Proxies for Palaeoclimatic and Palaeoceanographic Variability in Marine Sediments: Interpretation and Application, Developments in Marine Geology, Elsevier, p. 567-644.

Cantrell, K. J., and Byrne, R. H., 1987, Rare earth element complexation by carbonate and oxalate ions: Geochimica et Cosmochimica Acta, v. 51, p. 597-605.

Chaillou, G., Anschutz, P., Lavaux, G., and Blanc, G., 2006, Rare earth elements in the modern sediments of the Bay of Biscay (France): Marine Chemistry, v. 100, p. 39-52.

Cohen, A. S., O'Nions, R. K., Siegenthaler, R., and Griffin, W. L., 1988, Chronology of the pressure-temperature history recorded by a granulite terrain: Contributions to Mineralogy and Petrology, v. 98, p. 303-311.

Colin, C., Frank, N., Copard, K., and Douville, E., 2010, Neodymium isotopic composition of deep-sea corals from the NE Atlantic: implications for past hydrological changes during the Holocene: Quaternary Science Reviews, v. 29, p. 2509-2517.

Copard, K., Colin, C., Douville, E., Freiwald, A., Gudmundsson, G., De Mol, B., and Frank, N., 2010, Nd isotopes in deep-sea corals in the North-eastern Atlantic: Quaternary Science Reviews, v. 29, p. 2499-2508.

Crocket, K. C., Vance, D., Gutjahr, M., Foster, G. L., and Richards, D. A., 2011, Persistent Nordic deep-water overflow to the glacial North Atlantic: Geology, v. 39, p. 515-518.

Curry, W. B., and Oppo, D. W., 2005, Glacial water mass geometry and the distribution of δ13C of ΣCO2 in the western Atlantic Ocean: Paleoceanography, v. 20, p. PA1017.

Davies, S. M., Abbott, P. M., Pearce, N. J. G., Wastegård, S., and Blockley, S. P. E., 2012, Integrating the INTIMATE records using tephrochronology: rising to the challenge: Quaternary Science Reviews, v. 36, p. 11-27.

de Baar, H. J. W., Bacon, M. P., Brewer, P. G., and Bruland, K. W., 1985, Rare earth elements in the Pacific and Atlantic Oceans: Geochimica et Cosmochimica Acta, v. 49, p. 1943-1959.

de Baar, H. J. W., German, C. R., Elderfield, H., and van Gaans, P., 1988, Rare earth element distributions in anoxic waters of the Cariaco Trench: Geochimica et Cosmochimica Acta, v. 52, p. 1203-1219.

DePaolo, D. J., and Wasserburg, G. J., 1977, The sources of island arcs as indicated by Nd and Sr isotopic studies: Geophysical Research Letters, v. 4, p. 465-468.

Dubinin, A. V., 2004, Geochemistry of Rare Earth Elements in the Ocean: Lithology and Mineral Resources, v. 39, p. 289-307.

Dubinin, A. V., and Rozanov, A. G., 2001, Geochemistry of Rare Earth Elements and Thorium in Sediments and Ferromanganese Nodules of the Atlantic Ocean: Lithology and Mineral Resources, v. 36, p. 268-279.

Elderfield, H., and Greaves, M. J., 1982, The rare earth elements in seawater: Nature, v. 296, p. 214-219.

Elderfield, H., and Pagett, R., 1986, Rare earth elements in ichthyoliths: Variations with redox conditions and depositional environment: Science of The Total Environment, v. 49, p. 175-197.

Elderfield, H., Whitfield, M., Burton, J. D., Bacon, M. P., and Liss, P. S., 1988, The Oceanic Chemistry of the Rare-Earth Elements: Philosophical Transactions of the Royal Society of London. Series A, Mathematical and Physical Sciences, v. 325, p. 105-126.

Ellett, D. J., and Martin, J. H. A., 1973, The physical and chemical oceanography of the Rockall channel: Deep Sea Research and Oceanographic Abstracts, v. 20, p. 585-625.

Elmore, A. C., Piotrowski, A. M., Wright, J. D., and Scrivner, A. E., 2011, Testing the extraction of past seawater Nd isotopic composition from North Atlantic deep sea sediments and foraminifera: Geochem. Geophys. Geosyst., v. 12, p. Q09008.

Frank, M., 2002, Radiogenic Isotopes: Tracers of Past Ocean Circulation and Erosional Input: Reviews of Geophysics, v. 40, p. 1-38.

Froelich, P. N., Klinkhammer, G. P., Bender, M. L., Luedtke, N. A., Heath, G. R., Cullen, D., Dauphin, P., Hammond, D., Hartman, B., and Maynard, V., 1979, Early oxidation of organic matter in pelagic sediments of the eastern equatorial Atlantic: suboxic diagenesis: Geochimica et Cosmochimica Acta, v. 43, p. 1075-1090.

Garrison, T., 2011, Essentials of oceanography, Thomson Brooks/Cole, Cengage Learing, Inc.

Goldberg, E. D., Koide, M., Schmitt, R. A., and Smith, R. H., 1963, Rare-Earth distributions in the marine environment: Journal of Geophysical Research, v. 68, p. 4209-4217.

Goldstein, S. L., and O'Nions, R. K., 1981, Nd and Sr isotopic relationships in pelagic clays and ferromanganese deposits: Nature, v. 292, p. 324-327.

Goldstein, S. L., O'Nions, R. K., and Hamilton, P. J., 1984, A Sm-Nd isotopic study of atmospheric dusts and particulates from major river systems: Earth and Planetary Science Letters, v. 70, p. 221-236.

Grandjean, P., and Albarède, F., 1989, Ion probe measurement of rare earth elements in biogenic phosphates: Geochimica et Cosmochimica Acta, v. 53, p. 3179-3183.

Grandjean, P., Cappetta, H., Michard, A., and Albarède, F., 1987, The assessment of REE patterns and 143Nd/144Nd ratios in fish remains: Earth and Planetary Science Letters, v. 84, p. 181-196.

Grill, E. V., 1978, The effect of sediment-water exchange on manganese deposition and nodule growth in Jervis Inlet, British Columbia: Geochimica et Cosmochimica Acta, v. 42, p. 485-494.

Gromet, L. P., Haskin, L. A., Korotev, R. L., and Dymek, R. F., 1984, The "North American shale composite": Its compilation, major and trace element characteristics: Geochimica et Cosmochimica Acta, v. 48, p. 2469-2482.

Grousset, F. E., Biscaye, P. E., Revel, M., Petit, J.-R., Pye, K., Joussaume, S., and Jouzel, J., 1992, Antarctic (Dome C) ice-core dust at 18 k.y. B.P.: Isotopic constraints on origins: Earth and Planetary Science Letters, v. 111, p. 175-182.

Gutjahr, M., Frank, M., Stirling, C. H., Klemm, V., van de Flierdt, T., and Halliday, A. N., 2007, Reliable extraction of a deepwater trace metal isotope signal from Fe-Mn oxyhydroxide coatings of marine sediments: Chemical Geology, v. 242, p. 351-370.

Haley, B. A., and Klinkhammer, G. P., 2002, Development of a flow-through system for cleaning and dissolving foraminiferal tests: Chemical Geology, v. 185, p. 51-69.

Haley, B. A., Klinkhammer, G. P., and McManus, J., 2004, Rare earth elements in pore waters of marine sediments: Geochimica et Cosmochimica Acta, v. 68, p. 1265-1279.

Haley, B. A., Klinkhammer, G. P., and Mix, A. C., 2005, Revisiting the rare earth elements in foraminiferal tests: Earth and Planetary Science Letters, v. 239, p. 79-97.

Hansen, B., and Østerhus, S., 2000, North Atlantic-Nordic Seas exchanges: Progress In Oceanography, v. 45, p. 109-208.

Hartmann, M., Müller, P. J., Suess, E., and van der Weijden, C. H., 1973, Oxidation of organic matter in recent marine sediments: Meteor Forschungsergebnisse, Deutsche Forschungsgemeinschaft, Reihe C Geologie und Geophysik, Gebrüder Bornträger, Berlin, Stuttgart, v. C12, p. 74-86.

Haskin, M. A., and Haskin, L. A., 1966, Rare Earths in European Shales: A Redetermination: Science, v. 154, p. 507-509.

Innocent, C., Fagel, N., Stevenson, R. K., and Hillaire-Marcel, C., 1997, Sm–Nd signature of modern and late Quaternary sediments from the northwest North Atlantic: Implications for deep current changes since the Last Glacial Maximum: Earth and Planetary Science Letters, v. 146, p. 607-625.

Jaccard, S. L., and Galbraith, E. D., 2012, Large climate-driven changes of oceanic oxygen concentrations during the last deglaciation: Nature Geosci, v. 5, p. 151-156.

Jacobsen, S. B., and Wasserburg, G. J., 1980, Sm-Nd isotopic evolution of chondrites: Earth and Planetary Science Letters, v. 50, p. 139-155.

Jeandel, C., Arsouze, T., Lacan, F., Téchiné, P., and Dutay, J. C., 2007, Isotopic Nd compositions and concentrations of the lithogenic inputs into the ocean: A compilation, with an emphasis on the margins: Chemical Geology, v. 239, p. 156-164.

Jeandel, C., Bishop, J. K., and Zindler, A., 1995, Exchange of neodymium and its isotopes between seawater and small and large particles in the Sargasso Sea: Geochimica et Cosmochimica Acta, v. 59, p. 535-547.

Jeandel, C., Thouron, D. l., and Fieux, M. l., 1998, Concentrations and isotopic compositions of neodymium in the eastern Indian Ocean and Indonesian straits: Geochimica et Cosmochimica Acta, v. 62, p. 2597-2607.

Johannesson, K. H., and Zhou, X., 1999, Origin of middle rare earth element enrichments in acid waters of a Canadian High Arctic lake: Geochimica et Cosmochimica Acta, v. 63, p. 153-165.

Johnson, C., Sherwin, T., Smythe-Wright, D., Shimmield, T., and Turrell, W., 2010, Wyville Thomson Ridge Overflow Water: Spatial and temporal distribution in the Rockall Trough: Deep Sea Research Part I: Oceanographic Research Papers, v. 57, p. 1153-1162.

Jones, C. E., Halliday, A. N., Rea, D. K., and Owen, R. M., 1994, Neodymium isotopic variations in North Pacific modern silicate sediment and the insignificance of detrital REE contributions to seawater: Earth and Planetary Science Letters, v. 127, p. 55-66.

Keto, L. S., and Jacobsen, S. B., 1987, Nd and Sr isotopic variations of Early Paleozoic oceans: Earth and Planetary Science Letters, v. 84, p. 27-41.

Kidd, R. B., and Hill, P. R., 1986, Sedimentation on Feni and Gardar Sediment Drifts, *in* Ruddiman, W. F., Kidd, R. B., Thomas, E., and et al, eds., Init. Repts. DSDP 94, Washington (U.S. Govt. Printing Office).

Kissel, C., 2005, Magnetic signature of rapid climatic variations in glacial North Atlantic, a review: Comptes Rendus Geoscience, v. 337, p. 908-918.

Kissel, C., Laj, C., Labeyrie, L., Dokken, T., Voelker, A., and Blamart, D., 1999, Rapid climatic variations during marine isotopic stage 3: magnetic analysis of sediments from Nordic Seas and North Atlantic: Earth and Planetary Science Letters, v. 171, p. 489-502.

Lacan, F., and Jeandel, C., 2004a, Denmark Strait water circulation traced by heterogeneity in neodymium isotopic compositions: Deep Sea Research Part I: Oceanographic Research Papers, v. 51, p. 71-82.

—, 2004b, Neodymium isotopic composition and rare earth element concentrations in the deep and intermediate Nordic Seas: Constraints on the Iceland Scotland Overflow Water signature: Geochem. Geophys. Geosyst., v. 5, p. Q11006.

—, 2005a, Acquisition of the neodymium isotopic composition of the North Atlantic Deep Water: Geochem. Geophys. Geosyst., v. 6, p. Q12008.

—, 2005b, Neodymium isotopes as a new tool for quantifying exchange fluxes at the continent–ocean interface: Earth and Planetary Science Letters, v. 232, p. 245-257.

Lacan, F., Tachikawa, K., and Jeandel, C., 2012, Neodymium isotopic composition of the oceans: a compilation of seawater data: Chemical Geology, v. 300-301, p. 177-184.

Lowe, J. J., Rasmussen, S. O., Björck, S., Hoek, W. Z., Steffensen, J. P., Walker, M. J. C., and Yu, Z. C., 2008, Synchronisation of palaeoenvironmental events in the North Atlantic region during the Last Termination: a revised protocol recommended by the INTIMATE group: Quaternary Science Reviews, v. 27, p. 6-17.

Lowry, R. K., Machin, P., and Cramer, R. N., 1994, BOFS North Atlantic Data Set. Oceanographic data collected during the North Atlantic cruises of the NERC Biogeochemical Ocean Flux Study (1989-1991): a UK contribution of JGOFS, Natural Environmental Research Council, British Oceanographic Data Centre, Merseyside, United Kingdom.

Mangini, A., Eisenhauer, A., and Walter, P., 1990, Response of manganese in the ocean to the climatic cycles in the Quaternary: Paleoceanography, v. 5, p. 811-821.

Mangini, A., Jung, M., and Laukenmann, S., 2001, What do we learn from peaks of uranium and of manganese in deep sea sediments?: Marine Geology, v. 177, p. 63-78.

Manighetti, B., and McCave, I. N., 1995, Late Glacial and Holocene Palaeocurrents Around Rockall Bank, NE Atlantic Ocean: Paleoceanography, v. 10, p. 611-626.

Manighetti, B., McCave, I. N., Maslin, M., and Shackleton, N. J., 1995, Chronology for climate change: Developing age models for the biogeochemical ocean flux study cores: Paleoceanography, v. 10, p. 513-525.

Martin, E. E., Blair, S. W., Kamenov, G. D., Scher, H. D., Bourbon, E., Basak, C., and Newkirk, D. N., 2010, Extraction of Nd isotopes from bulk deep sea sediments for paleoceanographic studies on Cenozoic time scales: Chemical Geology, v. 269, p. 414-431.

Martin, E. E., and Haley, B. A., 2000, Fossil fish teeth as proxies for seawater Sr and Nd isotopes: Geochimica et Cosmochimica Acta, v. 64, p. 835-847.

Martin, E. E., and Scher, H. D., 2004, Preservation of seawater Sr and Nd isotopes in fossil fish teeth: bad news and good news: Earth and Planetary Science Letters, v. 220, p. 25-39.

Martìnez-Botì, M. A., Vance, D., and Mortyn, P. G., 2009, Nd/Ca ratios in plankton-towed and core top foraminifera: Confirmation of the water column acquisition of Nd: Geochem. Geophys. Geosyst., v. 10, p. Q08018.

McCave, I. N., 2002, A Poisoned Chalice?: Science, v. 298, p. 1186-1187.

McCave, I. N., Manighetti, B., and Beveridge, N. A. S., 1995, Circulation in the glacial North Atlantic inferred from grain-size measurements: Nature, v. 374, p. 149-152.

McGrath, T., Nolan, G., and McGovern, E., 2012, Chemical characteristics of water masses in the Rockall Trough: Deep Sea Research Part I: Oceanographic Research Papers.

McIntyre, K. L., and Howe, J. A., 2009, Bottom-current variability during the last glacial-deglacial transition, Northern Rockall Trough and Faroe Bank Channel, NE Atlantic: Scottish Journal of Geology, v. 45, p. 43-57.

McLennan, S. M., 1989, Rare earth elements in sedimentary rocks; influence of provenance and sedimentary processes: Reviews in Mineralogy and Geochemistry, v. 21, p. 169-200.

McManus, J. F., Francois, R., Gherardi, J. M., Keigwin, L. D., and Brown-Leger, S., 2004, Collapse and rapid resumption of Atlantic meridional circulation linked to deglacial climate changes: Nature, v. 428, p. 834-837.

Mearns, E. W., 1988, A samarium-neodymium isotopic survey of modern river sediments from Northern Britain: Chemical Geology: Isotope Geoscience section, v. 73, p. 1-13.

Middelburg, J. J., De Lange, G. J., and van Der Weijden, C. H., 1987, Manganese solubility control in marine pore waters: Geochimica et Cosmochimica Acta, v. 51, p. 759-763.

Murphy, D. P., and Thomas, D. J., 2010, The negligible role of intermediate water circulation in stadial–interstadial oxygenation variations along the southern California margin: Evidence from Nd isotopes: Quaternary Science Reviews, v. 29, p. 2442-2450.

New, A. L., and Smythe-Wright, D., 2001, Aspects of the circulation in the Rockall Trough: Continental Shelf Research, v. 21, p. 777-810.

O'Nions, R. K., Carter, S. R., Cohen, R. S., Evensen, N. M., and Hamilton, P. J., 1978, Pb, Nd and Sr isotopes in oceanic ferromanganese deposits and ocean floor basalts: Nature, v. 273, p. 435-438.

Palmer, M. R., 1985, Rare earth elements in foraminifera tests: Earth and Planetary Science Letters, v. 73, p. 285-298.

Palmer, M. R., and Elderfield, H., 1985, Variations in the Nd isotopic composition of foraminifera from Atlantic Ocean sediments: Earth and Planetary Science Letters, v. 73, p. 299-305.

—, 1986, Rare earth elements and neodymium isotopes in ferromanganese oxide coatings of Cenozoic foraminifera from the Atlantic Ocean: Geochimica et Cosmochimica Acta, v. 50, p. 409-417.

Papadimitriou, S., Kennedy, H., and Thomas, D. N., 2004, Rates of organic carbon oxidation in deep sea sediments in the eastern North Atlantic from pore water profiles of O2 and the δ13C of dissolved inorganic carbon: Marine Geology, v. 212, p. 97-111.

Pearce, C. R., Jones, M. T., Oelkers, E. H., Pradoux, C., and Jeandel, C., 2013, The effect of particulate dissolution on the neodymium (Nd) isotope and Rare Earth Element (REE) composition of seawater: Earth and Planetary Science Letters.

Pedersen, T. F., and Price, N. B., 1982, The geochemistry of manganese carbonate in Panama Basin sediments: Geochimica et Cosmochimica Acta, v. 46, p. 59-68.

Pena, L. D., Cacho, I., Calvo, E., Pelejero, C., Eggins, S., and Sadekov, A., 2008, Characterization of contaminant phases in foraminifera carbonates by electron microprobe mapping: Geochemistry, Geophysics, Geosystems, v. 9, p. Q07012.

Pena, L. D., Calvo, E., Cacho, I., Eggins, S., and Pelejero, C., 2005, Identification and removal of Mn-Mg-rich contaminant phases on foraminiferal tests: Implications for Mg/Ca past temperature reconstructions: Geochemistry, Geophysics, Geosystems, v. 6, p. Q09P02.

Piepgras, D. J., and Wasserburg, G. J., 1987, Rare earth element transport in the western North Atlantic inferred from Nd isotopic observations: Geochimica et Cosmochimica Acta, v. 51, p. 1257-1271.

Piepgras, D. J., Wasserburg, G. J., and Dasch, E. J., 1979, The isotopic composition of Nd in different ocean masses: Earth and Planetary Science Letters, v. 45, p. 223-236.

Pin, C., and Zalduegui, J. F. S., 1997, Sequential separation of light rare-earth elements, thorium and uranium by miniaturized extraction chromatography: Application to isotopic analyses of silicate rocks: Analytica Chimica Acta, v. 339, p. 79-89.

Piotrowski, A. M., Galy, A., Nicholl, J. A. L., Roberts, N., Wilson, D. J., Clegg, J. A., and Yu, J., 2012, Reconstructing deglacial North and South Atlantic deep water sourcing using foraminiferal Nd isotopes: Earth and Planetary Science Letters, v. 357-358, p. 289-297.

Piotrowski, A. M., Goldstein, S. L., Hemming, S. R., and Fairbanks, R. G., 2004, Intensification and variability of ocean thermohaline circulation through the last deglaciation: Earth and Planetary Science Letters, v. 225, p. 205-220.

Pomiès, C., Davies, G. R., and Conan, S. M. H., 2002, Neodymium in modern foraminifera from the Indian Ocean: implications for the use of foraminiferal Nd isotope compositions in paleo-oceanography: Earth and Planetary Science Letters, v. 203, p. 1031-1045.

Rasmussen, T. L., Thomsen, E., Labeyrie, L., and van Weering, T. C. E., 1996, Circulation changes in the Faeroe-Shetland Channel correlating with cold events during the last glacial period (58-10 ka): Geology, v. 24, p. 937-940.

Reitz, A., Hensen, C., Kasten, S., Funk, J. A., and de Lange, G. J., 2004, A combined geochemical and rock-magnetic investigation of a redox horizon at the last glacial/interglacial transition: Physics and Chemistry of the Earth, Parts A/B/C, v. 29, p. 921-931.

Reynard, B., Lécuyer, C., and Grandjean, P., 1999, Crystal-chemical controls on rare-earth element concentrations in fossil biogenic apatites and implications for paleoenvironmental reconstructions: Chemical Geology, v. 155, p. 233-241.

Richards, F. A., 1965, Anoxic basins and fjords, *in* Ripley, J. P., and Skirrow, G., eds., Chemical Oceanography, London, Academic Press, p. 611-643.

Rickaby, R. E. M., Elderfield, H., Roberts, N., Hillenbrand, C. D., and Mackensen, A., 2010, Evidence for elevated alkalinity in the glacial Southern Ocean: Paleoceanography, v. 25, p. PA1209.

Roberts, N. L., Piotrowski, A. M., Elderfield, H., Eglinton, T. I., and Lomas, M. W., 2012, Rare earth element association with foraminifera: Geochimica et Cosmochimica Acta, v. 94, p. 57-71.

Roberts, N. L., Piotrowski, A. M., McManus, J. F., and Keigwin, L. D., 2010, Synchronous Deglacial Overturning and Water Mass Source Changes: Science, v. 327, p. 75-78.

Robinson, L. F., and van de Flierdt, T., 2009, Southern Ocean evidence for reduced export of North Atlantic Deep Water during Heinrich event 1: Geology, v. 37, p. 195-198.

Rutberg, R. L., Hemming, S. R., and Goldstein, S. L., 2000, Reduced North Atlantic Deep Water flux to the glacial Southern Ocean inferred from neodymium isotope ratios: Nature, v. 405, p. 935-938.

Sanyal, A., Hemming, N. G., Hanson, G. N., and Broecker, W. S., 1995, Evidence for a higher pH in the glacial ocean from boron isotopes in foraminifera: Nature, v. 373, p. 234-236.

Sarbas, B., and Nohl, U., 2008, The GEOROC database as part of a growing geoinformatics network, 2008 Geoinformatics conference.

Sarmiento, J. L., and Gruber, N., 2004, Ocean Biogeochemical Dynamics: Princeton, NJ, Princeton University Press, 526 p.

Sauter, E., 1997, Eintrag, Akkumulation und Überlieferung von organischem Kohlenstoff in Oberflächensedimenten des Europäischen Nordmeeres: Berichte aus dem Sonderforschungsbereich 313, Veränderungen der Umwelt - Der Nördliche Nordatlantik, v. 71, p. 1-84.

Schlitzer, R., 2013, Ocean Data View, http://odv.awi.de.

Schönfeld, J., Zahn, R., and de Abreu, L., 2003, Surface and deep water response to rapid climate changes at the Western Iberian Margin: Global and Planetary Change, v. 36, p. 237-264.

Scrivner, A. E., Vance, D., and Rohling, E. J., 2004, New neodymium isotope data quantify Nile involvement in Mediterranean anoxic episodes: Geology, v. 32, p. 565-568.

Shaw, H. F., and Wasserburg, G. J., 1985, Sm-Nd in marine carbonates and phosphates: Implications for Nd isotopes in seawater and crustal ages: Geochimica et Cosmochimica Acta, v. 49, p. 503-518.

Sherwin, T. J., and Turrell, W. R., 2005, Mixing and advection of a cold water cascade over the Wyville Thomson Ridge: Deep Sea Research Part I: Oceanographic Research Papers, v. 52, p. 1392-1413.

Shipboard Scientific Party, 1996, Sites 980/981, *in* Jansen, E., Raymo, M. E., and Blum P. et al., eds., Proceedings of the Ocean Drilling Program, Initial Reports, College station, TX, p. 49-90.

Sholkovitz, E. R., 1988, Rare earth elements in the sediments of the North Atlantic Ocean, Amazon Delta, and East China Sea; reinterpretation of terrigenous input patterns to the oceans: American Journal of Science, v. 288, p. 236-281.

—, 1990, Rare-earth elements in marine sediments and geochemical standards: Chemical Geology, v. 88, p. 333-347.

Sholkovitz, E. R., Landing, W. M., and Lewis, B. L., 1994, Ocean particle chemistry: The fractionation of rare earth elements between suspended particles and seawater: Geochimica et Cosmochimica Acta, v. 58, p. 1567-1579.

Sholkovitz, E. R., Piepgras, D. J., and Jacobsen, S. B., 1989, The pore water chemistry of rare earth elements in Buzzards Bay sediments: Geochimica et Cosmochimica Acta, v. 53, p. 2847-2856.

Sholkovitz, E. R., Shaw, T. J., and Schneider, D. L., 1992, The geochemistry of rare earth elements in the seasonally anoxic water column and porewaters of Chesapeake Bay: Geochimica et Cosmochimica Acta, v. 56, p. 3389-3402.

Siddall, M., Khatiwala, S., van de Flierdt, T., Jones, K., Goldstein, S. L., Hemming, S., and Anderson, R. F., 2008, Towards explaining the Nd paradox using reversible scavenging in an ocean general circulation model: Earth and Planetary Science Letters, v. 274, p. 448-461.

Staudigel, H., Doyle, P., and Zindler, A., 1985, Sr and Nd isotope systematics in fish teeth: Earth and Planetary Science Letters, v. 76, p. 45-56.

Stille, P., 1992, Nd-Sr isotope evidence for dramatic changes of paleocurrents in the Atlantic Ocean during the past 80 m.y: Geology, v. 20, p. 387-390.

Stille, P., and Fischer, H., 1990, Secular variation in the isotopic composition of Nd in Tethys seawater: Geochimica et Cosmochimica Acta, v. 54, p. 3139-3145.

Stordal, M. C., and Wasserburg, G. J., 1986, Neodymium isotopic study of Baffin Bay water: sources of REE from very old terranes: Earth and Planetary Science Letters, v. 77, p. 259-272.

Stumm, W., and Sulzberger, B., 1992, The cycling of iron in natural environments: Considerations based on laboratory studies of heterogeneous redox processes: Geochimica et Cosmochimica Acta, v. 56, p. 3233-3257.

Tachikawa, K., Athias, V., and Jeandel, C., 2003, Neodymium budget in the modern ocean and paleo-oceanographic implications: J. Geophys. Res., v. 108, p. 3254.

Tachikawa, K., Jeandel, C., and Roy-Barman, M., 1999, A new approach to the Nd residence time in the ocean: the role of atmospheric inputs: Earth and Planetary Science Letters, v. 170, p. 433-446.

Tachikawa, K., Toyofuku, T., Basile-Doelsch, I., and Delhaye, T., 2013, Microscale neodymium distribution in sedimentary planktonic foraminiferal tests and associated mineral phases: Geochimica et Cosmochimica Acta, v. 100, p. 11-23.

Tanaka, T., Togashi, S., Kamioka, H., Amakawa, H., Kagami, H., Hamamoto, T., Yuhara, M., Orihashi, Y., Yoneda, S., Shimizu, H., Kunimaru, T., Takahashi, K., Yanagi, T., Nakano, T., Fujimaki, H., Shinjo, R., Asahara, Y., Tanimizu, M., and Dragusanu, C., 2000, JNdi-1: a neodymium isotopic reference in consistency with LaJolla neodymium: Chemical Geology, v. 168, p. 279-281.

Taylor, S. R., and McLennan, S. M., 1985, The continental crust: its composition and evolution: Oxford, Blackwell, 312 p.

Thomas, D. J., Bralower, T. J., and Jones, C. E., 2003, Neodymium isotopic reconstruction of late Paleocene–early Eocene thermohaline circulation: Earth and Planetary Science Letters, v. 209, p. 309-322.

Thomson, J., Carpenter, M. S. N., Colley, S., Wilson, T. R. S., Elderfield, H., and Kennedy, H., 1984, Metal accumulation rates in northwest Atlantic pelagic sediments: Geochimica et Cosmochimica Acta, v. 48, p. 1935-1948.

Thomson, J., Higgs, N. C., and Colley, S., 1996, Diagenetic redistributions of redox-sensitive elements in northeast Atlantic glacial/interglacial transition sediments: Earth and Planetary Science Letters, v. 139, p. 365-377.

Thornalley, D. J. R., McCave, I. N., and Elderfield, H., 2011, Tephra in deglacial ocean sediments south of Iceland: Stratigraphy, geochemistry and oceanic reservoir ages: Journal of Quaternary Science, v. 26, p. 190-198.

Trueman, C. N., and Tuross, N., 2002, Trace elements in recent and fossil bone apatite: Reviews in mineralogy and geochemistry, v. 48, p. 489-521.

Tütken, T., Vennemann, T. W., and Pfretzschner, H.-U., 2011, Nd and Sr isotope compositions in modern and fossil bones – Proxies for vertebrate provenance and taphonomy: Geochimica et Cosmochimica Acta, v. 75, p. 5951-5970.

van de Flierdt, T., Robinson, L. F., Adkins, J. F., Hemming, S. R., and Goldstein, S. L., 2006, Temporal stability of the neodymium isotope signature of the Holocene to glacial North Atlantic: Paleoceanography, v. 21, p. PA4102.

Vance, D., and Burton, K., 1999, Neodymium isotopes in planktonic foraminifera: a record of the response of continental weathering and ocean circulation rates to climate change: Earth and Planetary Science Letters, v. 173, p. 365-379.

Vance, D., Scrivner, A. E., Beney, P., Staubwasser, M., Henderson, G. M., and Slowey, N. C., 2004, The use of foraminifera as a record of the past neodymium isotope composition of seawater: Paleoceanography, v. 19, p. PA2009.

Vance, D., and Thirlwall, M., 2002, An assessment of mass discrimination in MC-ICPMS using Nd isotopes: Chemical Geology, v. 185, p. 227-240.

Wastegård, S., Rasmussen, T. L., Kuijpers, A., Nielsen, T., and van Weering, T. C. E., 2006, Composition and origin of ash zones from Marine Isotope Stages 3 and 2 in the North Atlantic: Quaternary Science Reviews, v. 25, p. 2409-2419.

Wilson, D. J., Piotrowski, A. M., and Galy, A., 2009, Deglacial changes in neodymium isotopes in the western Indian Ocean: Geochimica et Cosmochimica Acta Supplement, v. 73, p. 1446.

Wilson, D. J., Piotrowski, A. M., Galy, A., and Clegg, J. A., 2013, Reactivity of neodymium carriers in deep sea sediments: implications for boundary exchange and paleoceanography: Geochimica et Cosmochimica Acta, v. 109, p. 197-221.

Wilson, D. J., Piotrowski, A. M., Galy, A., and McCave, I. N., 2012, A boundary exchange influence on deglacial neodymium isotope records from the deep western Indian Ocean: Earth and Planetary Science Letters, v. 341–344, p. 35-47.

Wright, J., Seymour, R. S., and Shaw, H. F., 1984, REE and Nd isotopes in conodont apatite: Variations with geological age and depositional environment: Geological Society of America Special Papers, v. 196, p. 325-340.

Yu, J., Elderfield, H., and Piotrowski, A. M., 2008, Seawater carbonate ion-δ13C systematics and application to glacial-interglacial North Atlantic ocean circulation: Earth and Planetary Science Letters, v. 271, p. 209-220.

Chapter 4

Distinct Differences in Mid-Depth North Atlantic Circulation Between Heinrich Events

4.1 Abstract

Predictions of the anthropogenic influence on future climate suggest that melting of ice sheets during the coming centuries will result in increased input of fresh water to the oceans. Addition of cold, low salinity water changes the ocean density structure and hence has the potential to significantly modify oceanic overturning thermohaline circulation. The Heinrich (H-) events of the last glacial provide natural experiments to explore these processes, with rapid ice sheet destabilisations during Heinrich events resulting in the addition of large amounts of fresh water to the North Atlantic. Proxy records and modelling experiments have suggested that this fresh water addition resulted in a near complete shutdown of the Atlantic meridional overturning circulation (AMOC), allowing southern sourced waters to penetrate much further into the North Atlantic. It has not yet been well established, however, whether the same degree of disruption to the AMOC occurred during each of the Heinrich events. Multi-proxy reconstructions of bottom water properties from ODP Site 980 are presented here, including the first paired neodymium and stable isotopic data from the North Atlantic of sufficient resolution to clearly resolve the Heinrich events of the last 40,000 years. It can clearly be seen that each Heinrich event shows a unique bottom water signature, demonstrating that they are not simple, repeating phenomena. Southern sourced waters do not influence Site 980 during H4 and H3, but their impact can potentially be seen during H1 and H2. North Atlantic circulation is therefore highly sensitive to subtle differences between the events, which include the amount, rate and location of fresh water input and the surface water properties prior to the Heinrich event at sites of deep water formation. A complete shutdown of the overturning circulation at Heinrich events, with an expansion of the range of southern sourced waters into the North Atlantic

appears too simplistic a model to explain the response of the thermohaline circulation to freshwater addition.

4.2 Introduction

4.2.1 Modern, glacial and Heinrich overturning circulation modes

Palaeoceanographic reconstructions and the results of numerical modelling experiments of the ocean suggest that the pattern of ocean currents observed in the Atlantic basin today did not persist throughout the last glacial cycle. Three main modes of overturning circulation have been widely identified: 'modern', 'glacial' and 'Heinrich' or 'melt water' circulation states (alternatively 'warm', 'cold' and 'off') [Stommel 1961; Broecker et al. 1985; Sarnthein et al. 1994; Alley and Clark 1999; Ganopolski and Rahmstorf 2001; Rahmstorf 2002]. Simplified illustrations of these three modes are shown in figure 4.1.

The circulation of the modern Atlantic Ocean is dominated by strong deep water formation in the Nordic and Labrador Seas. The waters produced are relatively cold and dense and sink upon entering the main Atlantic basin, forming North Atlantic Deep Water (NADW) [e.g. Dickson and Brown 1994; Schmitz 1996; Marshall and Schott 1999, and references therein]. Southern sourced Antarctic Bottom Water (AABW) is generally confined to depths below 4 km [Kroopnick 1985] (figure 4.1(a)).

Atlantic Ocean circulation during the Last Glacial Maximum (LGM) was very different to the modern ocean. The strength of the Atlantic meridional overturning circulation (AMOC) was weaker than present [Lynch-Stieglitz et al. 2007], with less vigorous deep water formation in the North Atlantic generating Glacial North Atlantic Intermediate Water (GNAIW). The main locus of deep water formation may have moved to the south of the Greenland-Scotland Ridge [Duplessy et al. 1975; Duplessy et al. 1980; Curry and Lohmann 1982; Curry and Lohmann 1983; Labeyrie et al. 1992; Oppo and Lehman 1993]. The presence of southern sourced bottom waters has been inferred at shallower

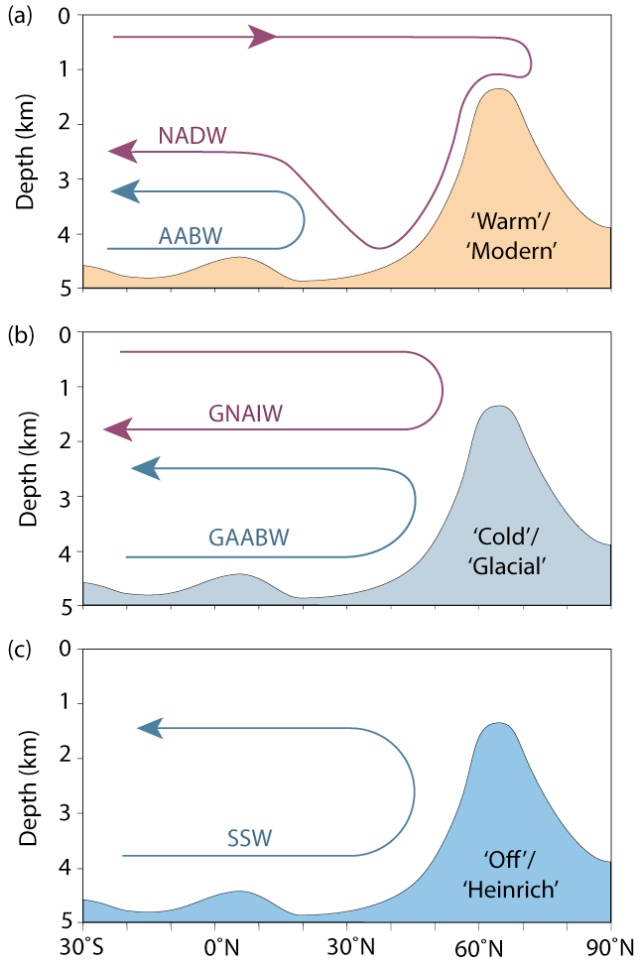

Figure 4.1: Simplified circulation modes of the North Atlantic Ocean, from Rahmstorf [2002], also based upon Alley et al. [1999]. (a) 'Warm' or 'Modern' mode, with North Atlantic Deep Water (NADW) formed in the Nordic Seas overflowing the Greenland-Scotland Ridge. Northwards flowing Antarctic Bottom Water (AABW) is confined to deeper depths only. (b) 'Cold' or 'Glacial' mode, with sinking of surface waters moved south of the Greenland-Scotland Ridge. The resulting Glacial North Atlantic Intermediate Water (GNAIW) only reaches shallower depths, allowing a shoaling of Glacial Antarctic Bottom Water (GAABW). (c) 'Off' or 'Heinrich' mode, with minimal deep water formation in the North Atlantic, resulting in the dominance of Southern Sourced Waters (SSW) in the North Atlantic Ocean.

depths and more northerly latitudes (illustrated in figure 4.1(b)) [Boyle and Keigwin 1982; Oppo and Fairbanks 1987; Curry et al. 1988; Duplessy et al. 1988; Oppo and Horowitz 2000; Curry and Oppo 2005]. However, this view has more recently been challenged, with the suggestion that a significant component of glacial "southern

sourced" waters were ventilated in the North Atlantic rather than the Southern Ocean [Kwon et al. 2012]. A sustained contribution of overflow waters from the Nordic Seas during the last glacial has also been proposed [Yu et al. 2008; Crocket et al. 2011].

More extreme shifts in AMOC have been invoked when melt water is rapidly added to the North Atlantic during Heinrich events (figure 4.1(c)). A drastic disruption of overturning circulation is indicated by numerous proxy records, which reflect change in the chemistry of bottom waters and/or current velocities [e.g. Keigwin and Lehman 1994; Sarnthein et al. 1994; Zahn et al. 1997; Cortijo et al. 2000; Rasmussen et al. 2003; McManus et al. 2004; Piotrowski et al. 2008; Robinson and van de Flierdt 2009]. Significantly weaker deep water formation at Heinrich events compared to background glacial conditions is also predicted by the results of ocean modelling studies [e.g. Stocker and Wright 1991; Manabe and Stouffer 1995; Rahmstorf 1995; Seidov et al. 1996; Seidov and Maslin 1999]. Increased penetration of southern sourced waters to more northerly latitudes and shallower depths in the Atlantic basin has been linked to a reduction in the strength of the meridional overturning circulation at Heinrich events [e.g. Vidal et al. 1997; Alley et al. 1999; Willamowski and Zahn 2000; Elliot et al. 2002]. However, a stronger signature of overflow waters from the Nordic Seas has also been proposed at Heinrich events [Meland et al. 2008; Thornalley et al. 2010; Crocket et al. 2011].

4.2.2 Fingerprinting water masses

Numerous different palaeoceanographic proxies have been employed to reconstruct the changing state of the global thermohaline circulation throughout the last glacial cycle. Different proxies have different strengths and weaknesses, and also respond to different aspects of the climate system. One approach to reconstruct changes in the strength of overturning circulation uses proxies sensitive to current velocities. These include the mean sediment grain sizes of the terrigenous 10–63 μm size fraction [e.g. Manighetti and McCave 1995; McCave et al. 1995a; McCave et al. 1995b] and the $^{231}Pa/^{230}Th$ ratio of sediments [e.g. Yu et al. 1996; Marchal et al. 2000; McManus et al. 2004].

Alternative approaches to estimate the strength of the AMOC use the chemical and biological properties of bottom water masses to infer the extent of ocean ventilation. The nutrient content of deep waters is determined by the both nutrient content of the surface waters from which they form (preformed nutrients) and nutrients released by the remineralisation of organic matter in the deep ocean (regenerated nutrients), which accumulate the longer a water mass is out of contact with the surface ocean [e.g. Deuser and Hunt 1969; Kroopnick 1985; Sigman et al. 2010]. The most commonly used deep water nutrient tracer is the carbon isotope ratio of benthic foraminiferal calcite (usually expressed as $\delta^{13}C$). The regeneration of organic matter at depth releases a higher proportion of the lighter isotope of carbon, ^{12}C, into the water column, which accumulates over time, hence "old" water masses have lighter $\delta^{13}C$ signatures [e.g. Broecker 1982; Curry and Lohmann 1982; Kroopnick 1985; Venz et al. 1999; Curry and Oppo 2005]. However, the carbon isotope signal is also influenced by numerous other factors, including air-sea exchange, export productivity, and vital and microhabitat effects of the foraminifera recording the signal [e.g. Grossman 1984; Wefer and Berger 1991; Lynch-Stieglitz and Fairbanks 1994; Mackensen et al. 2000; Cooke and Rohling 2001; Mackensen 2008]. Additional proxies used to reconstruct the nutrient content of bottom water masses include the Cd/Ca [Boyle and Keigwin 1982; Boyle 1988; Bertram et al. 1995; Rickaby and Elderfield 2005], Ba/Ca [Lea and Boyle 1990; Martin and Lea 1998; Hall and Chan 2004] and Zn/Ca [Marchitto et al. 2000; Marchitto et al. 2002; Bryan and Marchitto 2010] ratios of the tests of benthic foraminifera. Another method of estimating the "age" of a water mass (the time that it has been isolated from interacting with the atmosphere) comes through the use of radiocarbon dating [Broecker et al. 1960], either of paired planktonic and benthic foraminiferal samples [Andrée et al. 1985; Shackleton et al. 1988; Duplessy et al. 1989], or of uranium-thorium and radiocarbon dating of deep sea corals [Adkins et al. 1998; Mangini et al. 1998; Robinson et al. 2005].

Another property of a water mass that can be used to further constrain its origin is its carbonate ion concentration, which is determined by a number of processes including air-sea exchange, alkalinity and biology [Yu et al. 2008]. Many reconstructions of

carbonate ion concentration have been based upon the principle of increased dissolution at lower carbonate ion concentrations [e.g. Farrell and Prell 1989; Howard and Prell 1994; Broecker and Clark 2001; Anderson and Archer 2002; Barker and Elderfield 2002]. In addition, boron isotope ratios in planktonic and benthic foraminifera have been shown to correlate with seawater pH [e.g. Sanyal et al. 1995; Hönisch and Hemming 2004; Foster 2008; Rae et al. 2010; Yu et al. 2010], with the ratio of boron to calcium in benthic foraminifera empirically shown to correlate with the carbonate ion concentration the ambient water mass [e.g. Yu and Elderfield 2007; Yu et al. 2008].

Not all water mass tracers are influenced by biological activity. The neodymium isotopic signature of deep waters (recorded by various substrates including bulk sediments, foraminifera and fish debris) is determined by the source area of the water mass, and modified both by interaction with sediments and by mixing with other water masses along its path [Piepgras et al. 1979; Palmer and Elderfield 1985; Staudigel et al. 1985; Rutberg et al. 2000; van de Flierdt and Frank 2010; Elmore et al. 2011]. Neodymium isotopes therefore complement carbon isotopic data well as both provide different information about the transport history of a water mass. The neodymium isotope signature of the major water masses in the modern North Atlantic is given in table 4.1.

The oxygen isotopic signature of benthic foraminifera is one of the most widely used proxies of bottom water chemistry, and is influenced by both global and local signals. A strong response to changes in the global ice volume over glacial-interglacial timescales allows oxygen isotope records to provide a useful correlative tool between sedimentary records [e.g. Duplessy et al. 1970; Shackleton et al. 1977; Shackleton 1987; Waelbroeck et al. 2002; Lisiecki and Raymo 2005]. However, foraminiferal oxygen isotopes may also show local variations, for example, due to the input of isotopically light melt waters [e.g. Veum et al. 1992; Rasmussen et al. 1996b; Vidal et al. 1998; Dokken and Jansen 1999; Meland et al. 2008; Thornalley et al. 2010], with a temperature response also well documented [e.g. Urey 1947; Epstein et al. 1951; Epstein et al. 1953; Shackleton 1974; Grossman and Ku 1986; Bemis et al. 1998].

Water mass	Full name	ε_{Nd}	Reference(s)
SPMW*	Subpolar Mode Water	-13.5 +1.9/-1.3	(7), (8)
MOW	Mediterranean Overflow Water	-9.4 ± 0.4	(2), (8), (9)
LSW	Labrador Sea Water	-13.9 ± 0.4	(8)
pISOW	Pure Iceland-Scotland Overflow Water	-8.2 ± 0.6	(3), (6)
DSOW	Denmark Strait Overflow Water	-8.4 ± 1.4	(3), (5)
WTOW†	Wyville-Thomson Ridge Overflow Water	-11.4 +2.4/-1.5	Appendix 4
NSAIW	Norwegian Sea Intermediate Water	~ -8.1	(6)
NSDW	Norwegian Sea Deep Water	~ -8.2	(6)
NEADW	North East Atlantic Deep Water	-12.8 ± 0.2	(8)
NADW	North Atlantic Deep Water	-13.5 ± 0.5	(3), (8)
AAIW	Antarctic Intermediate Water	-8.2 ± 1	(3), (4), (8)
AABW	Antarctic Bottom Water	-8.5 ± 0.3	(1), (4), (8), (9)

*Table 4.1: Modern neodymium isotopic composition of the major water masses found in the northeast Atlantic Ocean. References: (1) Piepgras and Wasserburg [1982], (2) Piepgras and Wasserburg [1983], (3) Piepgras and Wasserburg [1987], (4) Jeandel [1993], (5) Lacan and Jeandel [2004a], (6) Lacan and Jeandel [2004b], (7) Lacan and Jeandel [2004c] (8) Lacan and Jeandel [2005a; Meland et al. 2008], (9) Rickli et al. [2009]. *SPMW has highly spatially variable ε_{Nd} values [Lacan and Jeandel 2004c], so the value quoted is a best estimate for the signature at ODP Site 980. †WTOW estimate describes the property of the water mass as found in the Rockall Trough, where near surface waters have been entrained by the overflowing NSDW. Details of the estimation of the WTOW ε_{Nd} signature can be found in appendix 4.*

As each proxy in the palaeoceanographer's toolkit has its own strengths and weaknesses and may be influenced by numerous biotic and abiotic factors, combining evidence from multiple proxies, each a function of different variables, can help to identify the processes responsible for driving the observed variability in palaeoclimatic recontructions. Therefore, it is important to consider multiple proxy records when interpreting past oceanographic changes.

4.3 Aims

The main aims of this chapter are as follows:

- To reconstruct changes in the bottom water chemistry of ODP Site 980 over the past 40,000 years by producing the first co-registered neodymium and stable isotopic records from the North Atlantic with sufficient resolution to resolve Heinrich events.
- To link these changes in properties to source areas of intermediate and deep water masses in the North Atlantic to better understand the circulation changes occurring as a result of fresh water input to the ocean.
- To determine whether southern sourced waters penetrate to the mid-depth northeast Atlantic during Heinrich events.
- To establish the phasing of any thermohaline circulation changes at Heinrich events through comparison to co-registered records of climate evolution in the cryosphere and surface ocean at Site 980.
- To use these relationships to gain a better understanding of the mechanisms responsible for the generation of Heinrich events.
- To assess the extent of variability amongst Heinrich events.
- To evaluate the degree of thermohaline circulation shutdown at Heinrich events.

4.4 Methods

Between one and four specimens of the benthic foraminifera *Cibicides wuellerstorfi* (Schwager, 1866) were picked from the >212 μm size fraction for stable isotope analysis (corresponding to a carbonate mass of 60–100 μg). Oxygen and carbon isotopic compositions of this carbonate were analysed using a Europa Geo–2020 mass spectrometer in the Palaeoceanography and Palaeoclimate research group, School of Ocean and Earth Sciences, University of Southampton. Measurements were corrected for instrumental drift using linear extrapolation between reference standards at the start and end of the run. All sample values are expressed in delta notation, relative to the Vienna Peedee Belemnite standard (VPBD), as given by equation 4.1:

$$\delta^{18}O = \left(\frac{\left(\frac{^{18}O}{^{16}O}\right)_{sample}}{\left(\frac{^{18}O}{^{16}O}\right)_{VPDB}} - 1 \right) \times 1000\ ‰ \qquad \text{Equation 4.1}$$

External reproducibility (measured on a blind standard) is better than 0.053 ‰ for $\delta^{18}O$ and 0.027 ‰ for $\delta^{13}C$. *C. wuellerstorfi* $\delta^{18}O$ values were adjusted for species-specific disequilibrium from seawater values by applying a correction factor of +0.64 ‰ [Shackleton and Opdyke 1973].

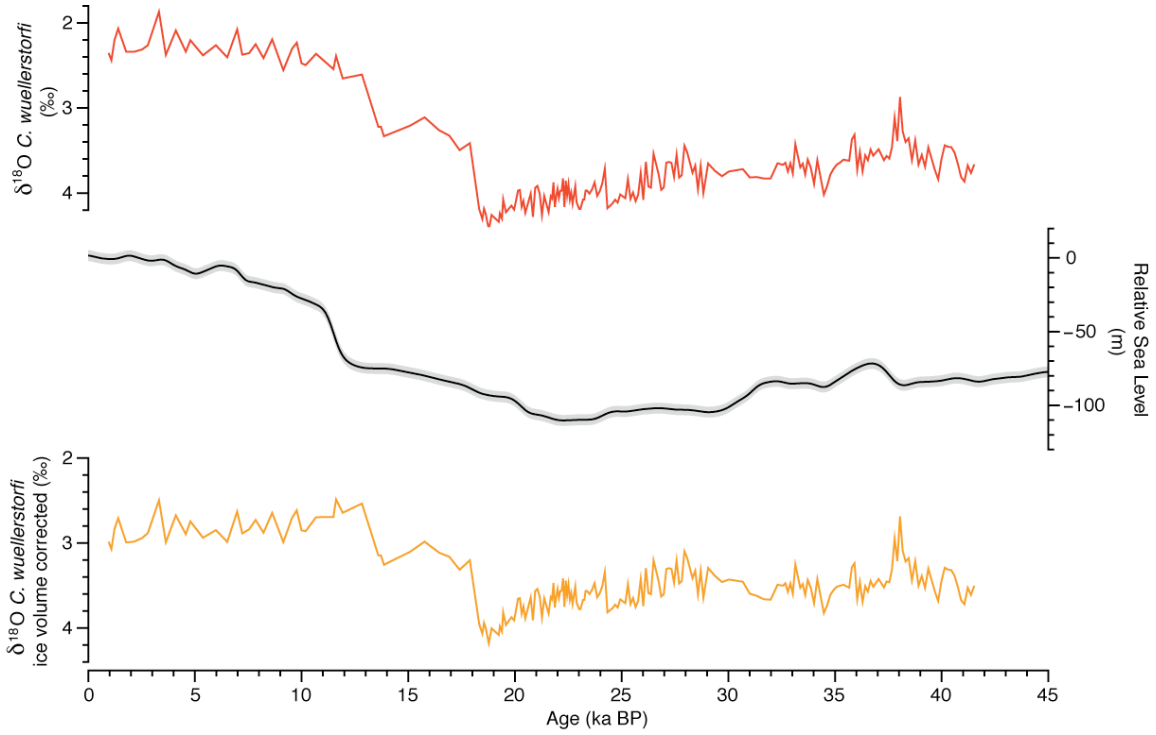

Figure 4.2: Adjustment of benthic foraminiferal $\delta^{18}O$ values for changes in global ice volume. Top: uncorrected C. wuellerstorfi *$\delta^{18}O$ values. Middle: most probable values of Red Sea relative sea level reconstruction of Siddall et al. [2003] and Rohling et al. [2009] (assumed to be globally representative), plotted on the chronology of Grant et al. [2012], with shading indicating ±2SE (standard errors). Bottom:* C. wuellerstorfi *$\delta^{18}O$ values corrected for ice volume changes and species offset (procedure described in section 4.4).*

To compare data among Heinrich events, oxygen isotope values were further adjusted for changes in sea level resulting from variations in the global ice sheet volume. These adjusted oxygen isotope compositions are expressed as $\delta^{18}O_{ivc}$ (ice volume corrected). Sea level reconstructions from the Red Sea (based upon combined oxygen isotope reconstructions and hydraulic modelling) [Siddall et al. 2003; Rohling et al. 2009; Grant et al. 2012] were used to correct the foraminiferal oxygen isotope values. Good correlation has been observed between the Red Sea records and sea level estimates obtained by corals, modelling and foraminifera [Chappell et al. 1996; Lea et al. 2002; Waelbroeck et al. 2002; Peltier and Fairbanks 2006], suggesting that the site is globally representative. A glacial-interglacial global oxygen isotope shift of 1.05 ‰ was assumed to correspond to the total sea level shift of 110 m observed across this time interval [e.g. McManus et al. 1999; Duplessy et al. 2002; Meland et al. 2008]. The sea level record from the Red Sea [Siddall et al. 2003; Rohling et al. 2009], plotted on the chronology of Grant et al. [2012] is illustrated in figure 4.2, with both the corrected and uncorrected oxygen isotope records from ODP Site 980.

4.5 Results and discussion

4.5.1 Glacial-interglacial differences

Modern oceanographic observations show that ODP Site 980 is bathed by a mixture of North East Atlantic Deep Water (NEADW) and Labrador Sea Water (LSW), with a possible influence of Wyville-Thompson Overflow Waters (WTOW) [e.g. Ellett and Martin 1973; Ellett and Roberts 1973; New and Smythe-Wright 2001; Johnson et al. 2010; McGrath et al. 2012]. However, the proxy records presented here suggest that a water mass with different properties bathed the site during the last glacial interval. (proxy reconstructions illustrated in figure 4.3). Glacial bottom waters are marked by a more radiogenic neodymium isotope signal recorded by planktonic foraminifera ($\varepsilon_{Nd} \sim -9.5$ units compared to a late Holocene value of $\varepsilon_{Nd} = -11.7$), heavier *C. wuellerstorfi* $\delta^{18}O_{ivc}$ (~ 2.9 ‰ compared to 2.2 ‰ in the Holocene) and slightly lighter $\delta^{13}C$ (0.7 ‰ compared to 0.9 ‰).

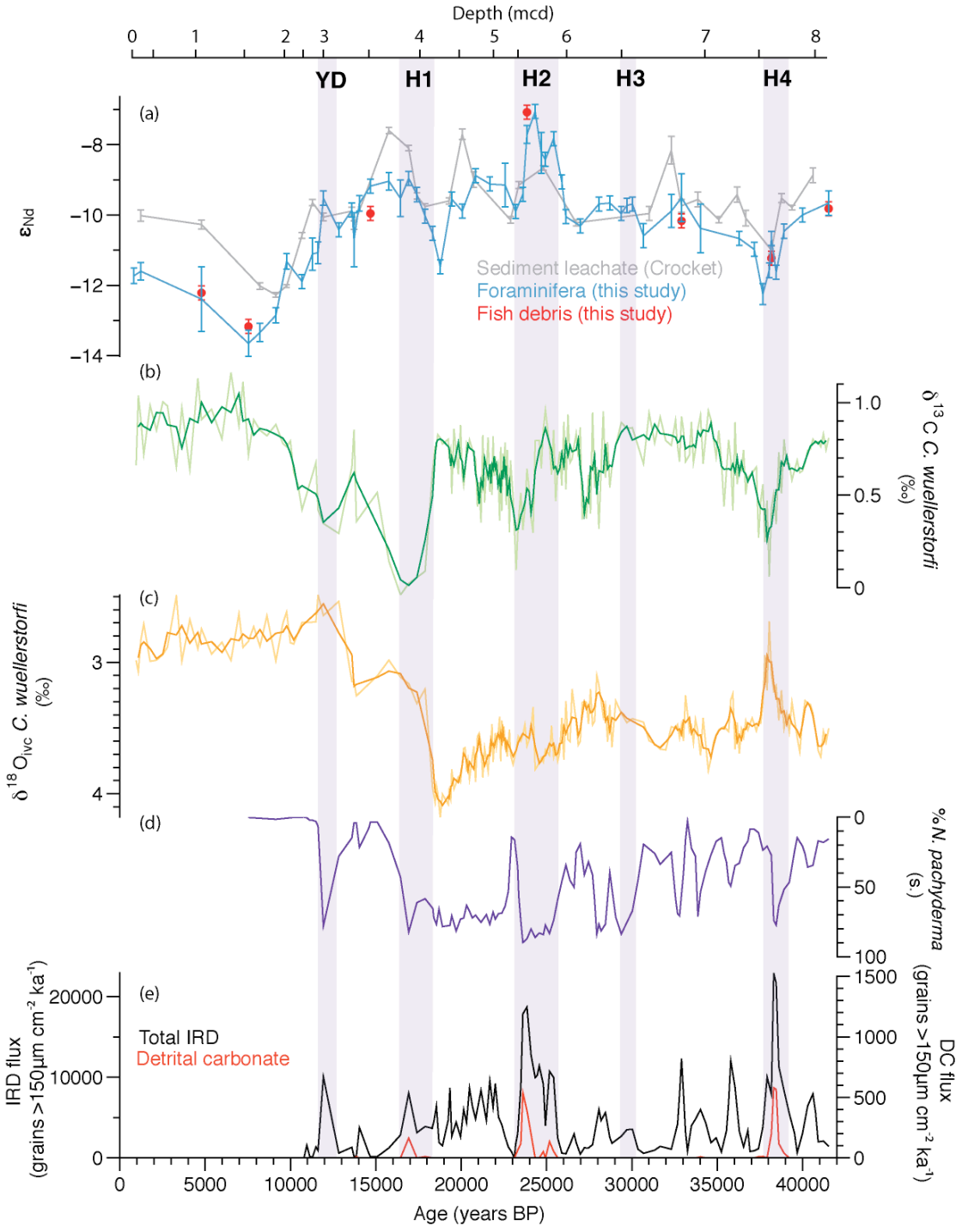

Figure 4.3: Compilation of palaeoceanographic proxy data from ODP Site 980. Purple bands mark the position of the Heinrich events and Younger Dryas. (a) Neodymium isotope ratios of bulk sediment leachates from Crocket et al. [2011] (in grey), planktonic foraminifera with ferromanganese coatings not removed (blue) and

reductively cleaned fish debris (red). (b) $\delta^{13}C$ of benthic foraminifera C. wuellerstorfi, with darker line colour marking the three-point running mean. (c) $\delta^{18}O$ of C. wuellerstorfi, adjusted for global ice volume changes and species offset from seawater, with darker line colour marking the three-point running mean. (d) Percentage of polar species N. pachyderma (s.) as a proportion of the total number of planktonic foraminifera. (e) Fluxes of ice-rafted debris (black) and detrital carbonate clasts (red).

There are three main water mass source regions in the modern North Atlantic which could have contributed a radiogenic neodymium isotope signal to the Feni Drift during the last glacial: the Southern Ocean, overflows from the Nordic Seas and the Mediterranean Sea (figure 4.4) [e.g. Jeandel 1993; Lacan and Jeandel 2004a; Lacan and Jeandel 2004b; Tachikawa et al. 2004; Lacan et al. 2012]. Previous studies have concluded that Mediterranean outflow has a heavy carbon isotope signature and was reduced in volume during the last glacial interval [Zahn et al. 1997], hence this is the least likely candidate to explain the observed glacial water mass signal at Site 980.

A shoaling of southern sourced water in the North Atlantic during the glacial interval has been widely supported in the literature [e.g. Streeter and Shackleton 1979; Curry and Lohmann 1982; Curry and Lohmann 1990; Oppo and Lehman 1993; Bertram et al. 1995]. Low carbon isotope values are typically associated with older, nutrient-rich southern-sourced waters [Kroopnick 1985; Curry and Oppo 2005], with the Nordic Seas characterised by slightly heavier $\delta^{13}C$ values [Veum et al. 1992; Meland et al. 2008]. Therefore, the $\delta^{13}C$ signal recorded at Site 980 would appear to support an increased contribution from the Southern Ocean. However, highly variable benthic carbon isotope signals have been reported in the glacial Nordic Seas, which have been attributed to the influence of factors such as brine rejection, freshwater input, productivity and sea ice cover [Dokken and Jansen 1999; Raymo et al. 2004; Meland et al. 2008; Thornalley et al. 2010]. An increased proportion of northern-sourced waters cannot, therefore, be ruled out on the basis of carbon isotopes alone [Lynch-Stieglitz and Fairbanks 1994; Yu et al. 2008].

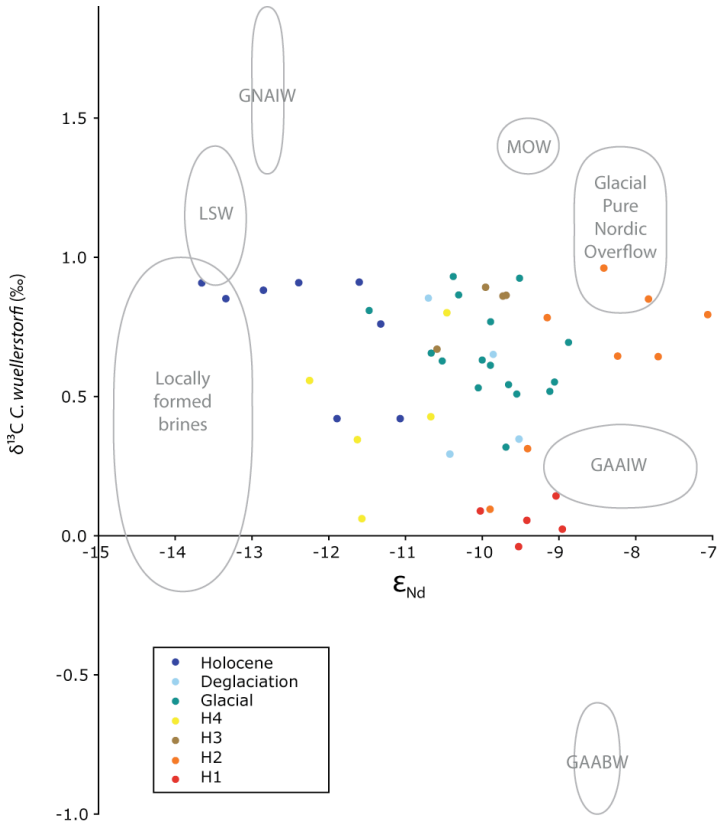

Figure 4.4: Cross-plot of $\delta^{13}C$ (C. wuellerstorfi) and ε_{Nd} (planktonic foraminifera) values of ODP Site 980 samples. Grey ovals mark estimates of local water mass chemistry. Carbon isotope values plotted are estimated glacial compositions, with the exception of LSW (modern values used as glacial composition not well constrained) [Bertram et al. 1995; Curry and Oppo 2005; Voelker et al. 2006; Meland et al. 2008; Olsen and Ninnemann 2010; Thornalley et al. 2010]. All ε_{Nd} estimates represent modern water mass chemistry, as glacial end member compositions are not well defined [data from Lacan and Jeandel 2004b; Lacan and Jeandel 2004c; Lacan and Jeandel 2005a]. Although ε_{Nd} values are not influenced by glacial-interglacial fluctuations in productivity, temporally variable amounts of mixing may influence glacial water mass signatures [Piotrowski et al. 2008]. Glacial pure Nordic overflow water estimates assume no entrainment of surface waters, and hence are based upon Norwegian Sea intermediate/deep waters. GAABW: Glacial Antarctic Bottom Water; GAAIW: Glacial Antarctic Intermediate Water; MOW: Mediterranean Overflow Water; LSW: Labrador Sea Water (Holocene value); GNAIW: Glacial North Atlantic Intermediate Water.

Water masses from the South Atlantic and Nordic Seas have very different carbonate ion concentrations, hence this property can be used to distinguish between the two source areas. Southern sourced waters have relatively low [CO_3^{2-}] (compared to LSW, NEADW and WTOW influencing the site today), and were likely even lower during the last glacial interval [Howard and Prell 1994; Hodell et al. 2001; Yu et al. 2008], while northern component waters have much higher carbonate ion concentration, and may have been even higher during the glacial than today [Barker and Elderfield 2002; Hönisch and Hemming 2005; Yu et al. 2008]. If there was an increase in the proportion of southern sourced water reaching Site 980, lower glacial B/Ca values would be expected. New unpublished data from Site 980, however, indicates increased glacial B/Ca [Chalk et al. 2013]. The difference in bottom water chemistry between the glacial and Holocene in this study is therefore most consistent with a stronger influence of overflow waters sourced from the Nordic Seas at Site 980 under glacial conditions.

4.5.2 Heinrich events

Two main source areas have previously been invoked to explain the changes in bottom water properties recorded in the North Atlantic during Heinrich events: southern sourced waters [e.g. Rahmstorf 1994; Vidal et al. 1997; Willamowski and Zahn 2000; Rickaby and Elderfield 2005; Gutjahr et al. 2010; Thornalley et al. 2011a] and overflows from the Nordic Seas [e.g. Meland et al. 2008; Thornalley et al. 2010; Crocket et al. 2011]. However, the multi-proxy reconstructions of bottom water chemistry presented here (figures 4.3 – 4.9) strongly suggest that mid-depth circulation changes during Heinrich events are more complex than can be simply explained by the repeated presence of either of these two water masses. Sections 4.5.2.1–4.5.2.4 explore the water mass changes at each Heinrich event in more detail.

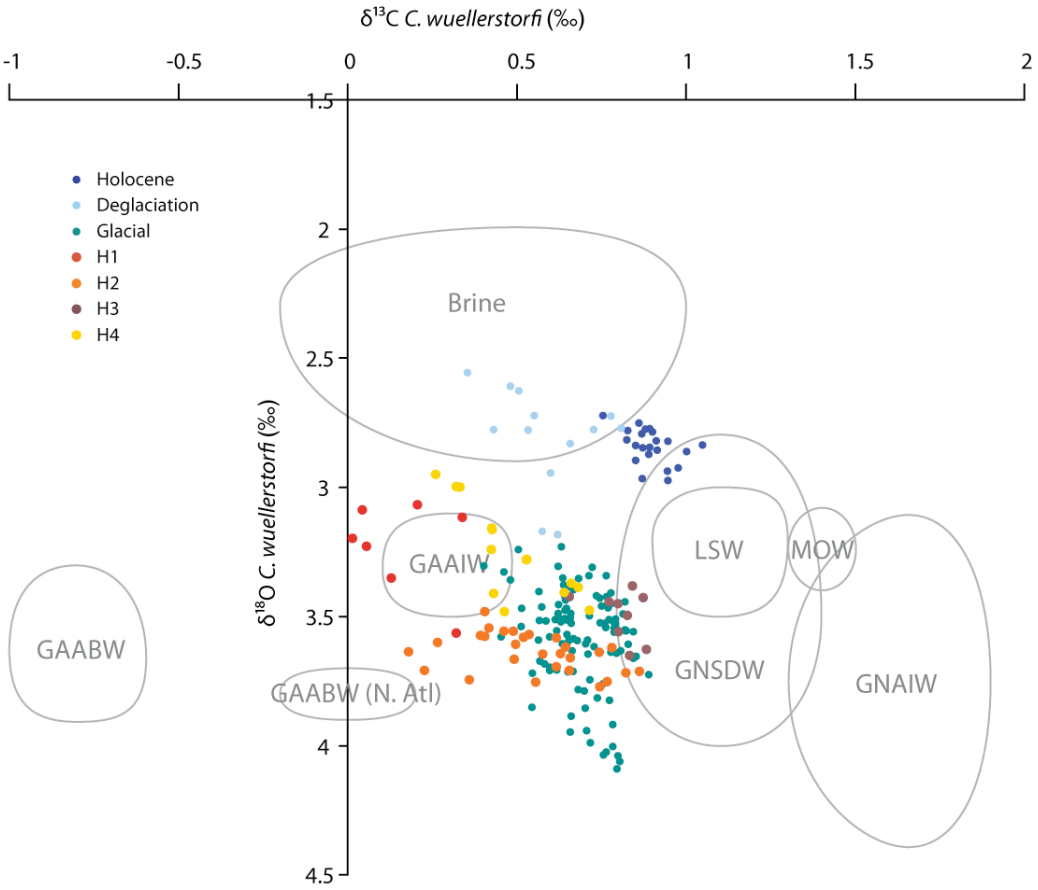

Figure 4.5: Cross-plot of co-measured oxygen and carbon isotopes of C. wuellerstorfi from ODP Site 980. All values are smoothed (3-point running mean), with $\delta^{18}O$ values adjusted for global ice volume changes, as explained in section 4.4. Estimated water mass compositions shown in grey, based upon Bertram et al. [1995], Voelker et al. [2006], Meland et al. [2008] and Thornalley et al. [2010]. Water masses as figure 4.5, with GAABW (N. Atl): Glacial Antarctic Bottom Water as found in the North Atlantic; GNSDW: Glacial Norwegian Sea Deep Water. Note that the isotopic composition of brines is highly variable.

4.5.2.1 Heinrich event 4

Heinrich event 4 is unique in the record presented here in that it is the only Heinrich event to clearly show a shift towards unradiogenic neodymium isotope values and a decrease in benthic oxygen isotopes, clearly indicating a change in the provenance of the bottom waters bathing ODP Site 980 when compared to background glacial conditions

(illustrated in figure 4.6). A strong influence of southern sourced waters during H4 can be discounted by the observed shift of ~ 2 ε_{Nd} units towards less radiogenic values (reaching a minimum of ε_{Nd} = –12.2), as modern southern sourced waters have a signature of ε_{Nd} = –7 to –10, with values as high as ε_{Nd} = –6 reached during the last glacial [e.g. Jeandel 1993; Piotrowski et al. 2004; Piotrowski et al. 2008; Lacan et al. 2012]. Low oxygen isotope values are also not typically associated with southern sourced water masses. Light carbon and oxygen isotope signatures instead suggest an increased influence of brines on the site (figures 4.4 and 4.5). A strong brine influence has previously been attributed to a Nordic Sea overflow signature [Meland et al. 2008], however, this is not supported by the observed reduction in ε_{Nd}. Estimated isotopic compositions for modern Wyville-Thomson overflow waters range from ε_{Nd} = –9 to –11.6 (see appendix 4). Decreased Pacific input to the Norwegian-Greenland Seas (via the Arctic Ocean) due to the closure of the Bering Strait under glacial conditions [Shaffer and Bendtsen 1994; Hu et al. 2010] might be expected to shift the overflow signature towards more unradiogenic values, matching that recorded at Site 980 during H4. However, there is limited variation in the neodymium isotope signature in the Arctic Ocean through the dramatic sea level variations of the last deglaciation [Jang et al. 2013], hence variable Pacific input is unlikely to have significantly influenced the overflow water signature through the last 40,000 years.

The neodymium isotopic composition of WTOW is extremely sensitive to the composition and degree of mixing of unradiogenic Subpolar Mode Waters (SPMW) with pure overflow waters as they descend on the southern flank of the ridge, shifting their composition towards less radiogenic values (see appendix 4) [Lacan and Jeandel 2004c; Sherwin and Turrell 2005]. There is significant variation in upper water column neodymium isotope values in the North Atlantic today [Lacan and Jeandel 2004c], and surface circulation was likely very different during the last glacial interval (particularly during Heinrich events) [see Sarnthein et al. 1995; Seidov et al. 1996; Death et al. 2006; Bigg et al. 2010, and discussion in section 2.7.4.5]. Mixing of overflows with less radiogenic SPMW (with an increased signal from the northwest Atlantic) and/or increased entrainment of the upper water column, therefore, cannot be ruled out at H4.

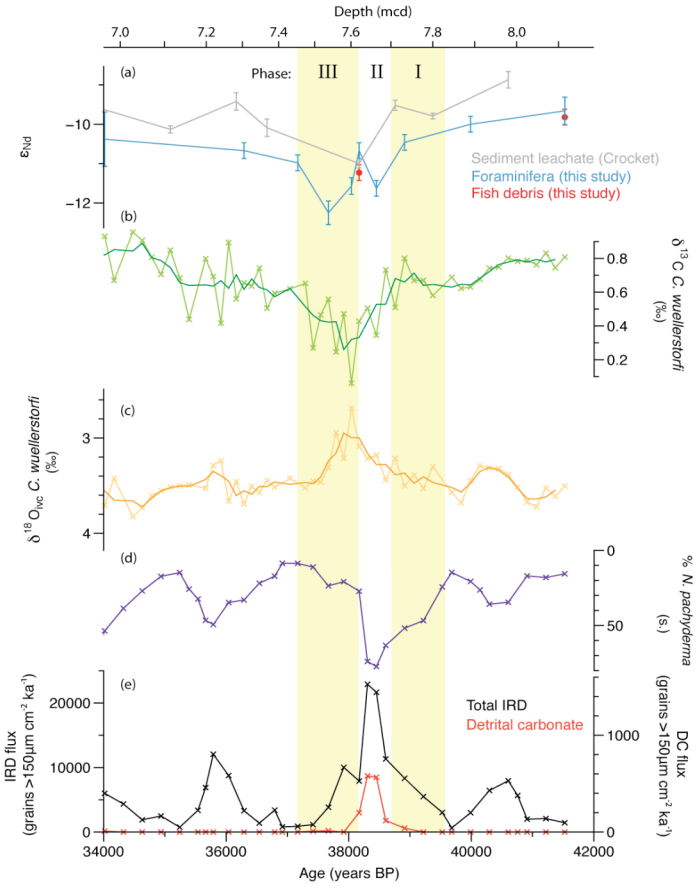

Figure 4.6: Heinrich event 4 recorded at ODP Site 980, with (a) to (e) as figure 4.3. Shading indicates three main phases to the event. I: Cooling of sea surface temperatures and increasing flux of IRD. II: Detrital carbonate deposition occurs with maxima in total IRD flux and % N. pachyderma (s.). Start of significant change in bottom water chemistry in $\delta^{13}C$, $\delta^{18}O$ and ε_{Nd} records. III: Warm sea surface temperatures and low IRD fluxes indicate return to interstadial conditions while bottom water proxies indicate maximal perturbations before recovering to pre-event values.

Also, although well documented [e.g. Jeandel et al. 1995; Tachikawa et al. 1999; Lacan and Jeandel 2001; Lacan and Jeandel 2004a; Amakawa et al. 2009; Wilson et al. 2012], the influence of boundary exchange processes on seawater neodymium isotope signatures is not fully understood [Lacan and Jeandel 2005b; Wilson et al. 2013]. Modern overflow waters become significantly more radiogenic as they cross the Greenland-Scotland Ridge due to interaction with the young basaltic crust [Lacan and

Jeandel 2004b; Lacan and Jeandel 2004a]. If, this interaction was weaker for any reason (e.g. current velocity), a less radiogenic WTOW composition would be recorded.

The above uncertainties mean that an increased contribution from the Nordic Seas cannot entirely be ruled out, however, other source areas for waters with isotopically light carbon, oxygen and neodymium isotope signatures should be considered. Although waters with light oxygen and carbon isotope values in the North Atlantic have previously been attributed to overflows from the Nordic Seas [e.g. Meland et al. 2008], the same processes inferred to export low stable isotopic signatures to depth in the Nordic Seas may also be occurring in other locations [e.g. Thornalley et al. 2010].

The mechanisms by which low oxygen isotope signatures are transferred to intermediate and deep waters are subject to ongoing debate (see reviews by Bauch and Bauch [2001] and Stanford et al. [2011]). One of the more commonly invoked hypotheses is the sinking of isotopically light brines, produced during sea ice formation [e.g. Jansen and Veum 1990; Veum et al. 1992; Dokken and Jansen 1999], possibly in conjunction with the addition of water of initially meteoric origin to the surface ocean [Rozanski et al. 1993; Macdonald et al. 1995; Melling and Moore 1995; Bauch and Bauch 2001]. Melting below an ice sheet can also produce isotopically light waters, with surface water masses becoming cooler and denser due to brine release [Weiss et al. 1979; Schlosser et al. 1990; Weppernig et al. 1996]. Alternatively, the delivery of isotopically light waters to the deep ocean in sediment-laden hyperpycnal plumes may play a significant role [Mulder and Syvitski 1995; Mulder et al. 2003; Stanford et al. 2011], with deposits linked to hyperpycnal flow activity during the last glacial interval documented in the Norwegian-Greenland Seas [Lekens et al. 2005], Labrador Sea [Hesse et al. 2004] and North Atlantic [Zaragosi et al. 2001; Zaragosi et al. 2006; Toucanne et al. 2009; Toucanne et al. 2010], suggesting that inputs of isotopically light water may have been widespread. Bottom water warming has also been proposed explain the light oxygen isotope excursions observed at Heinrich events [Rasmussen et al. 1996b; Bauch and Bauch 2001; Rasmussen and Thomsen 2004; Marcott et al. 2011], however, doubts have been raised about the density of a warm subsurface water mass [Meland et al. 2008;

Stanford et al. 2011], and warming alone cannot explain the observed excursions in carbon and neodymium isotopes at Site 980. Many of the other mechanisms proposed to explain the light oxygen isotope excursion, however, can result in an increased proportion of light carbon, with brine formation [Millo et al. 2006; Dickson et al. 2008; Meland et al. 2008; Thornalley et al. 2010] and riverine input [Spielhagen and Erlenkeuser 1994; Finlay 2001; Bauch et al. 2002] both linked with a depleted $\delta^{13}C$ signal. This range of processes invoked to export isotopically light waters to depth would not have been confined to the Nordic Seas, particularly during the cold surface conditions during Heinrich stadials. Two alternative sites of deep water formation (or of fresh water input) during H4 which are more compatible with an unradiogenic neodymium signature are therefore proposed below.

The Labrador Sea is a major site of deepwater formation in the modern ocean, with Labrador Sea Water (LSW) found in the Rockall Trough from 1500–2000 m depth, and as a constituent of Northeast Atlantic Deep Water (NEADW) [Talley and McCartney 1982; Dickson and Brown 1994; Marshall and Schott 1999; Lacan and Jeandel 2005a; McGrath et al. 2012]. Waters sourced from the Labrador Sea region therefore exert a strong influence at Site 980 today. Models and proxy-based reconstructions have both suggested that LSW formation was either severely reduced or completely stopped at the last glacial maximum [de Vernal and Hillaire-Marcel 2000; Hillaire-Marcel and Bilodeau 2000; Hillaire-Marcel et al. 2001; de Vernal et al. 2002; Cottet-Puinel et al. 2004]. However, there is some evidence to suggest that surface conditions may have been more favourable for LSW formation during some Heinrich events than background glacial conditions, with increased surface density, increased brine formation and faster deepwater currents [Clarke and Gascard 1983; Hillaire-Marcel et al. 2001; Weber et al. 2001; Hillaire-Marcel and de Vernal 2008; Hillaire-Marcel et al. 2011]. The Labrador Sea is the main source of unradiogenic neodymium to the North Atlantic due to the old, cratonic rocks in the surrounding area [Piepgras and Wasserburg 1987; Lacan and Jeandel 2005a; Jeandel et al. 2007; Lacan et al. 2012]. Therefore, a small increase in the proportion of LSW exported to the North East Atlantic could significantly modify the neodymium isotopic signature recorded at Site 980.

Alternatively, the observed proxy signals at H4 may have been a result of deep water formation south of the Greenland-Scotland Ridge, possibly in close proximity to Site 980. Local surface waters have neodymium isotopes of ε_{Nd} = –13 to –14 [Lacan and Jeandel 2004c; Lacan and Jeandel 2004b], hence an increased proportion of this water transported to intermediate/deep depths, for example, due to brine rejection, could result in the observed isotopic signal. Several studies have suggested that deep water formation occurred south of the Greenland-Scotland Ridge during the last glacial interval [Duplessy et al. 1980; Duplessy et al. 1988; Labeyrie et al. 1992; Rasmussen et al. 2003; Millo et al. 2006]. However, as Heinrich events are marked by large decreases in sea surface density in the NE Atlantic [Maslin et al. 1995], with the North Atlantic Drift not penetrating north of 40-50^{o}N at H4 [Cortijo et al. 2005], and a sustained offset in the isotopic signatures of surface and subsurface dwelling planktonic foraminifera [Peck et al. 2008], it seems unlikely that there was increased open ocean convection at these times. Instead, isotopically light waters may have been more continental in origin; either attributable to brine formation on the European and/or Icelandic margins, Rockall Plateau or Greenland-Scotland Ridge [Meland et al. 2008; Thornalley et al. 2010], or via hyperpycnal flows from Europe [Zaragosi et al. 2006; Eynaud et al. 2007; Toucanne et al. 2009; Toucanne et al. 2010].

In summary, the low benthic stable isotope and unradiogenic neodymium isotope signatures observed at Site 980 during H4 therefore cannot be easily attributed to a single source area or process. A significant influence of southern sourced waters can, however, be excluded. Overflowing brines from the Nordic Seas are also unlikely to be the main contributor. Instead, an increased contribution of Labrador Sea Water (relative to typical stadial/interstadial conditions), or from waters sourced from the south of the Greenland-Scotland Ridge seems plausible.

4.5.2.2 Heinrich event 3

The records presented here show no significant change in either oxygen, carbon or neodymium isotope isotopic signatures during Heinrich event 3. This suggests that there were no major changes in the bottom water masses directly overlying Site 980 (illustrated in figure 4.7). An absence of significant change in bottom water chemistry during Heinrich event 3 is a relatively common feature in the North Atlantic [e.g. Vidal et al. 1997; Zahn et al. 1997; Peck et al. 2007; Skinner et al. 2007], although there is evidence of a drop in bottom current velocity at this time [Kissel 2005].

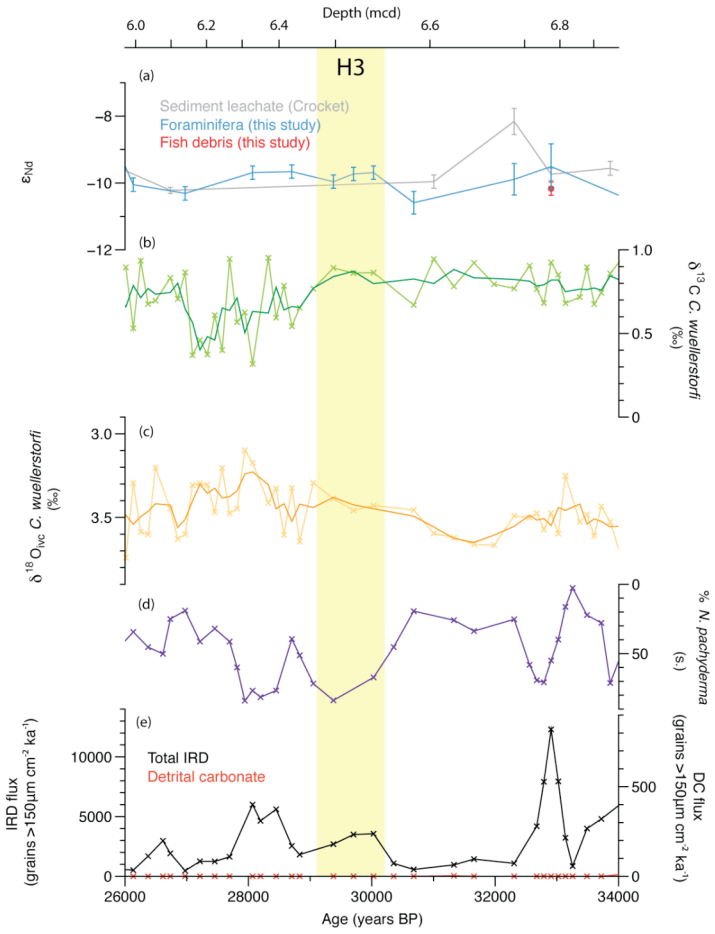

Figure 4.7: Heinrich event 3 recorded at ODP Site 980, with (a) to (e) as figure 4.3. Shading indicates position of the IRD layer. There is no evidence of associated changes in bottom water properties.

It should be noted that if the alternative age model described in section 2.5 is adopted, a shallower IRD peak (at 6.3–6.4 mcd) is identified as corresponding to Heinrich event 3.

Small excursions towards lighter benthic carbon and oxygen isotopes (by ~0.3 ‰ and 0.2 ‰ respectively) can be seen postdating the peak in IRD, hence if the alternative age model is correct, an influence of brines on the site may be seen following deposition of the H3 IRD layer. However, due to the mis-match between the ages of a peak in the concentration of volcanic ash in this section of the core (figure 2.9) and the Fugloyarbanki/Faeroe Marine Ash Zone II (as discussed in section 2.5), the small excursion in bottom water properties at 6.1–6.4 mcd may not be directly related to a Heinrich event.

4.5.2.3 Heinrich event 2

Major shifts in bottom water properties are recorded during Heinrich event 2 (illustrated in figure 4.8). Neodymium isotope values reach the most radiogenic values of the entire record ($\varepsilon_{Nd} = -7.1$), with a ~ 0.5 ‰ decrease in carbon isotope values. Unlike the other Heinrich events recorded at ODP Site 980, variations in the different bottom water proxy records are not synchronous with one another. Much of the interval with high IRD fluxes and cold sea surface temperatures (high % *N. pachyderma* (s.)) is marked by a shift towards very radiogenic neodymium isotope values, with little change in carbon or oxygen isotope values (figure 4.8). The carbon isotope excursion is significantly delayed, occurring only as neodymium isotope values recover to pre-event values (figure 4.8). This asynchroneity will be discussed further in section 4.6.5.2.

There are three main ways to explain an excursion towards more radiogenic neodymium isotopic values at Site 980 under glacial conditions: an increased signal Mediterranean Outflow signature, greater interaction with the basaltic Greenland-Scotland Ridge (most likely attributable to overflow waters from the Nordic Seas) or increased input of water from the Southern Ocean. The plausibility of each of these scenarios is discussed in the following section.

Waters of the Mediterranean Sea exhibit relatively radiogenic isotope signatures ($\varepsilon_{Nd} = -4$ to -12) [Piepgras and Wasserburg 1983; Spivack and Wasserburg 1988; Henry et al.

1994; Tachikawa et al. 2004; Lacan et al. 2012]. It has been suggested, however, that Mediterranean outflows only have the potential to influence the North Atlantic by a maximum of approximately 1 ε_{Nd} unit, due to the relatively small flux of neodymium out of the Mediterranean Sea [Spivack and Wasserburg 1988]. Therefore, Mediterranean overflow waters cannot easily be invoked to explain an excursion of >2 ε_{Nd} units

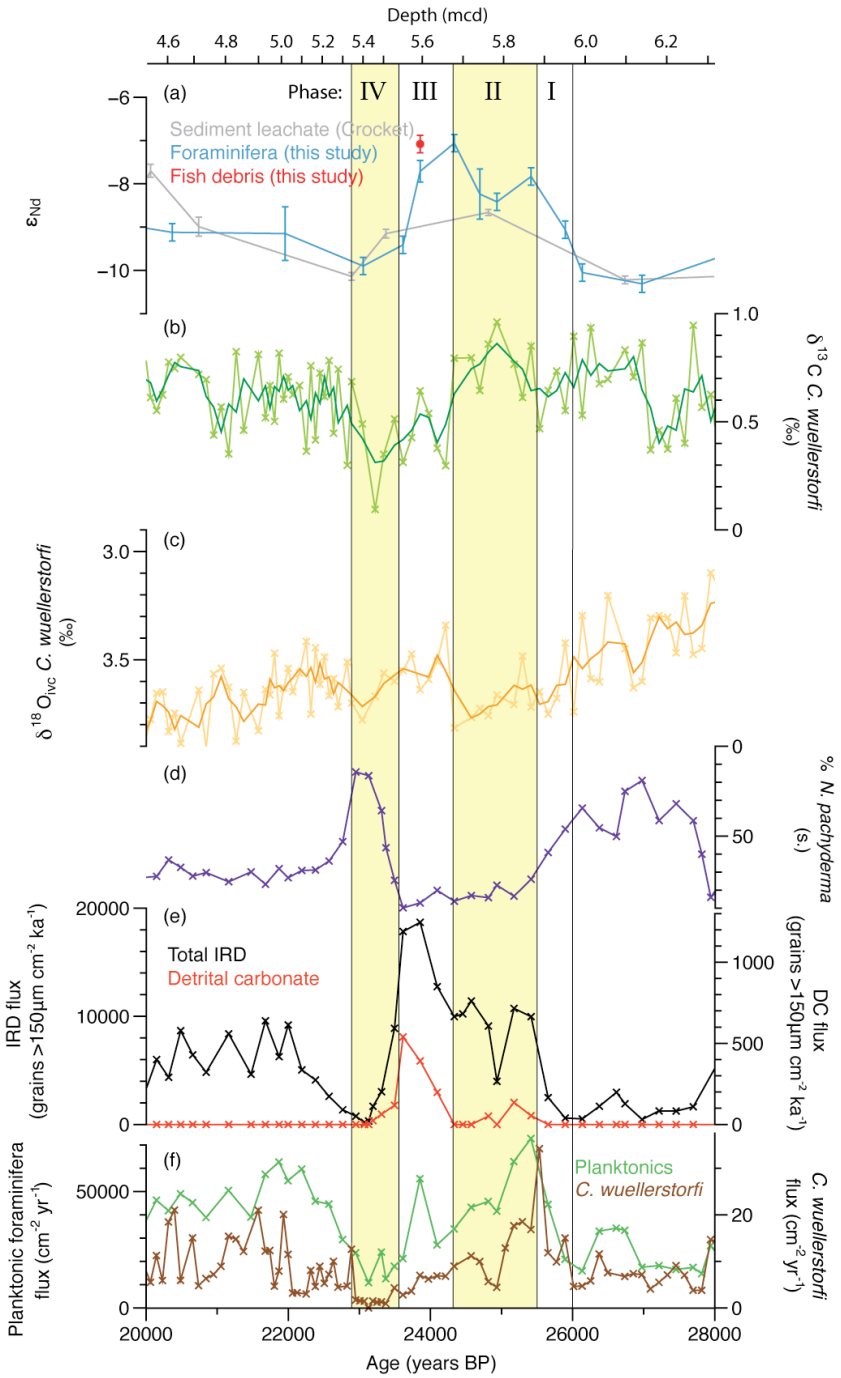

Figure 4.8: Heinrich event 2 recorded at ODP Site 980, with (a) to (e) as figure 4.3. (f) Fluxes of total planktonic foraminifera (green) and benthic foraminifera (brown) (see section 2.6.1). Shading indicates four main phases to the event. I: Early shift in neodymium isotope values associated with decreasing sea surface temperatures. II: IRD fluxes increase to moderate values with high % N. pachyderma (s.) and radiogenic neodymium isotope values. III: Main detrital carbonate layer with maximum IRD fluxes. Carbon isotope values start to shift towards lighter values as neodymium isotope signature returns to pre-event values. IV: Minima in carbon isotope values associated with low IRD and foraminiferal fluxes and % N. pachyderma (s.) values indicating a return to stadial conditions.

observed during H2 (figure 4.8). Also, as discussed in section 4.5.1, Mediterranean outflow waters have a heavy $\delta^{13}C$ signature and were likely reduced in volume during the last glacial [Zahn et al. 1997]. Increased Mediterranean Outflow has been observed associated with Heinrich events but only delayed by ~740 years after meltwater input [Voelker et al. 2006]. At Site 980, the shift towards radiogenic neodymium isotopes is recorded during the early stages of H2 (potentially even preceding increased IRD input; figure 4.8), hence a strong Mediterranean influence on Site 980 can be discounted.

A second possible explanation of the radiogenic neodymium isotopic signal at Site 980 is strengthened overflow from the Nordic Seas. Pure overflow waters crossing the Greenland-Scotland Ridge have a neodymium isotope signature of $\varepsilon_{Nd} = -8$, close to the most radiogenic values recorded at Site 980 during H2. However, in the modern ocean, these waters are highly temporally variable [Sherwin et al. 2008; Johnson et al. 2010] and diluted by a factor of three or more through mixing with other water masses as they descend on the southern side of the ridge [Ellett and Roberts 1973; Swift 1984; Holliday et al. 2000; Sherwin and Turrell 2005; Hansen and Østerhus 2007]. The degree of entrainment strongly depends upon the overflow dynamics and water column density structure [e.g. Price and O'Neil Baringer 1994; Nielsen et al. 2004; Sherwin and Turrell 2005]. The existence of a more stratified glacial water column in the North Atlantic [e.g. Bertram et al. 1995; Curry and Oppo 2005; Yu et al. 2008] therefore may have influenced the degree of mixing/entrainment of other water masses by the overflows. It

is also possible that interaction of overflow waters with the radiogenic Greenland-Scotland Ridge by boundary exchange processes was stronger. Although the average neodymium isotopic signal of the overflow waters is approximately $\varepsilon_{Nd} = -8$, values as high as $\varepsilon_{Nd} = -3.9$ have been recorded in modern bottom waters, where neodymium concentrations are approximately double [Lacan and Jeandel 2004b]. Thus if the water mass bathing Site 980 during H2 is sourced from the Nordic Seas, it would require either close to a pure overflow signal reaching the site, or greater interaction of the overflows with the basaltic Greenland-Scotland Ridge.

If a more concentrated overflow water signal is recorded at Site 980 during H2, similarities with the chemistry of overflow source region in the Nordic Seas would be expected [Meland et al. 2008; Yu et al. 2008; Thornalley et al. 2010]. Excursions towards lower $\delta^{18}O$ and $\delta^{13}C$ values are documented in the Nordic Seas during Heinrich events, although H2 is less pronounced, particularly in carbon isotopes [Rasmussen et al. 1996a; Dokken and Jansen 1999]. No excursions in either carbon or oxygen benthic foraminiferal isotopes occurs in phase with the neodymium isotope excursion in the Site 980 record (figure 4.8), which argues against increased overflow waters driving the observed neodymium isotopic signature during H2.

A third potential explanation for the change in radiogenic neodymium isotope signature is that there was an increased incursion of southern-sourced waters to the northeast Atlantic during H2. Incursions of southern sourced waters during Heinrich events have been strongly advocated by benthic foraminiferal Cd/Ca [Willamowski and Zahn 2000; Rickaby and Elderfield 2005] and radiocarbon data [Thornalley et al. 2011a] from the North Atlantic. Shifts towards neodymium isotopic compositions of $\varepsilon_{Nd} = -8$ in the Site 980 data are typical of southern sourced waters [Jeandel 1993; Piotrowski et al. 2004; Piotrowski et al. 2008; Lacan et al. 2012]. Although these values are close to a pure Southern Ocean signal today, the South Atlantic was more radiogenic during the last glacial (especially during stadials and Heinrich events), allowing for some dilution of the signal as the water mass moved northwards [Piotrowski et al. 2008].

Increased northward penetration of southern sourced waters into the North Atlantic during the last glacial interval has been widely associated with a shift towards low carbon isotope values [e.g. Boyle and Keigwin 1982; Curry et al. 1988; Curry and Lohmann 1990; Oppo and Lehman 1993; Willamowski and Zahn 2000; Hoffman and Lund 2012]. Therefore, the absence of an accompanying carbon isotope excursion in the Site 980 *C. wuellerstorfi* data would seem to argue against the presence of southern sourced waters during the early stages of H2 in the mid-depth northeast Atlantic Ocean. However, the Glacial Antarctic Intermediate Water end member (GAAIW) appears to have a much less depleted carbon isotopic signature than Glacial Antarctic Bottom Water (GAABW) due to increased air-sea exchange, with $\delta^{13}C \sim 0.5$ ‰ compared to < -1 ‰ [e.g. Hodell et al. 2003; Curry and Oppo 2005; Thornalley et al. 2011a].

The water mass that therefore appears to best explain the radiogenic neodymium isotopic excursion recorded at Site 980 during H2 is GAAIW. Evidence of southern-sourced intermediate waters has been reported at a number of sites in the North Atlantic during H1, extending to 60°N, and to water depths of 2.3 km [e.g. Adkins et al. 1998; Willamowski and Zahn 2000; Schröder-Ritzrau et al. 2003; Rickaby and Elderfield 2005; Pahnke et al. 2008; Thornalley et al. 2011a]. The data presented here suggests that a similar scenario may have existed during H2. However, this result is at odds with several previous studies which argue against a northward penetration of AAIW during Heinrich events [e.g. Sortor and Lund 2010; Xie et al. 2012], suggesting that this interval is worthy of further investigation.

4.5.2.4 Heinrich event 1

Carbon isotope values reach the lowest values of the entire record during H1, both at Site 980 (figures 4.3 and 4.9) and other nearby sites [e.g. Jung 1996; Vidal et al. 1997]. There is no clear concurrent excursion in oxygen isotopes, although values do become significantly lighter as part of the deglacial trend (figure 4.9). No clear excursion in the neodymium isotopic signature of planktonic foraminifera is recorded during H1,

although radiogenic values are recorded by the bulk sediment leachates [Crocket et al. 2011].

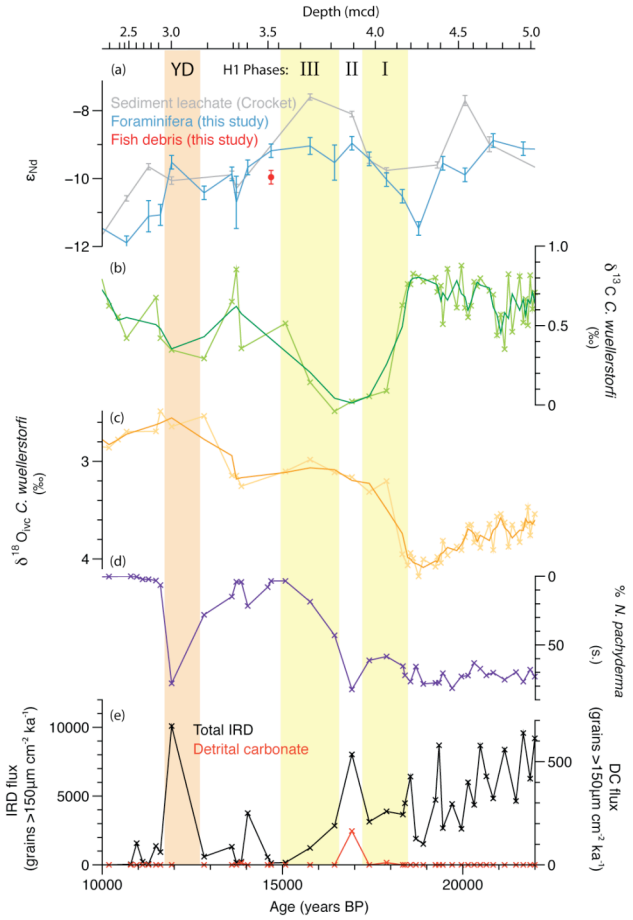

Figure 4.9: Heinrich event 1 recorded at ODP Site 980, with (a) to (e) as figure 4.3. Yellow shading indicates three phases to the event. I: Large shift towards lighter benthic carbon and oxygen isotopes. II: Detrital carbonate layer with light benthic isotope signature maintained. III: Decreasing % N. pachyderma (s.) indicating gradual warming of the upper water column associated with gradual recovery of bottom water carbon isotopic signature. The position of the Younger Dryas is marked in orange.

The very low carbon isotope values recorded during H1 could be attributed to waters of either southern or northern origin. An excursion towards very light values of $\delta^{13}C$ have been documented by the infaunal benthic foraminifera *C. teretis* at site MD95-2010 on the Norwegian margin at this time [Dokken and Jansen 1999], although it should be noted that this excursion is much less prominent at greater depths in the Norwegian

Basin [Bauch et al. 2001], suggesting that deep water generation was spatially variable. An alternative explanation is that waters of southern origin reach ODP Site 980 during H1. A northwards expansion of GAAIW (to latitudes of 60^{o}N and beyond) has been advocated to explain Cd/Ca ratios [e.g. Rickaby and Elderfield 2005], neodymium isotopes [e.g. Pahnke et al. 2008] and radiocarbon data [e.g. Adkins et al. 1998; Schröder-Ritzrau et al. 2003; Thornalley et al. 2011a], with the results of modelling studies supporting this conclusion [e.g. Sijp and England 2006]. Increased northward penetration of waters of Antarctic origin has also been proposed in other ocean basins [Schulte et al. 1999; Pahnke and Zahn 2005]. No clear shift to more radiogenic neodymium isotope values is, however, observed at Site 980 and B/Ca ratios of *C. wuellerstorfi* are much greater than would be expected for pure southern sourced waters (particularly during the early stages of H1) [Chalk et al. 2013]. This raises the possibility that the poorly ventilated water mass identified in previous studies [e.g. Keigwin and Lehman 1994; Adkins et al. 1998; Rickaby and Elderfield 2005] and suggested by light δ^{13}C values at Site 980 may not have originated in the Southern Ocean.

It is plausible that both southern and northern sourced waters influenced ODP Site 980 during H1. In the early part of the light carbon excursion, B/Ca values are high, however, in the later part of the excursion, they decrease significantly [Chalk et al. 2013]. High values are more typical of overflow waters from the Nordic Seas or local deep water formation, while low values are associated with southern sourced waters [Howard and Prell 1994; Yu et al. 2008]. This suggestion is supported by estimates of the age offset between surface and deep waters at the South Iceland Rise at water depths of 1.2–2.3 km [Thornalley et al. 2011a]. This data set shows a brief interval with an influence of very young bottom waters coincident with surface freshening, brine formation and low oxygen and carbon isotope values in the Nordic Seas [Dokken and Jansen 1999; Thornalley et al. 2011b], followed by a dramatic increase in the surface-deep age offset to values of over 3,000 years, which persisted until the Bølling-Allerød interval [Thornalley et al. 2011a]. This sequence of events agrees well with the data from Site 980 and suggests that evolution of mid-depth waters in the North Atlantic

during H1 was complex, as the ocean adjusted to temporally variable fresh water inputs from a number of localities.

4.5.3 Dansgaard-Oeschger variability

Different modes of deep water ventilation in the North Atlantic have been proposed to operate during stadials and interstadials, with thermohaline circulation changes suggested driving force of Dansgaard-Oeshger variability [e.g. Broecker et al. 1985; Alley et al. 1999; Ganopolski and Rahmstorf 2001; Clark et al. 2007]. Although rapid and dramatic changes in surface water temperatures have been extremely well documented in the North Atlantic and at a number of other locations globally [Voelker 2002, and references therein], convincing evidence of changes in deeper waters to support their involvement in stadial-interstadial variability has proved much rarer [see Charles et al. 1996; Jung 1996; Rasmussen et al. 1996a; Keigwin and Boyle 1999; Boyle 2000; van Kreveld et al. 2000; Elliot et al. 2002; Hagen and Hald 2002; Kissel 2005; Ballini et al. 2006; Dickson et al. 2008]. Quantifying the scale of deep water changes has important implications for determining the potential involvement of the thermohaline circulation in Dansgaard-Oeschger variability.

Evidence for mid-depth circulation changes at ODP Site 980 associated with stadial-interstadial variability is not conclusive, however, there is a suggestion of variability in bottom water properties in phase with the surface ocean data. Neodymium isotope values appear slightly less radiogenic (by 0.3–0.7 ε_{Nd} units) during many of the stadials of MIS3, in both the bulk sediment leachate data of Crocket et al. [2011] and the planktonic foramniniferal data presented here, with slightly lower benthic oxygen isotope values often also recorded (illustrated in figure 4.10). It should be noted that the resolution of the neodymium isotope data and the small and variable nature of the oxygen isotope excursions prevent any water mass changes to be stated with complete confidence. However, both the neodymium and oxygen isotope records could indicate the presence of increased brines sourced from the Nordic Seas during stadials, as proposed by Dokken and Jansen [1999] and Dickson et al. [2008]. The weaker signal

compared to site MD95-2006 from the northern part of the Rockall Trough at a very similar water depth [Dickson et al. 2008] may be a result of the dilution of the overflow signal as the waters move southwards into the main Atlantic basin. Increased brine formation to the south of the Greenland-Scotland Ridge may also contribute to the light benthic oxygen isotope signature during stadials [van Kreveld et al. 2000], however, as modern surface waters have ε_{Nd} values of –13 to –14 [Lacan and Jeandel 2004c; Lacan and Jeandel 2004b], local brine formation alone cannot account for the more

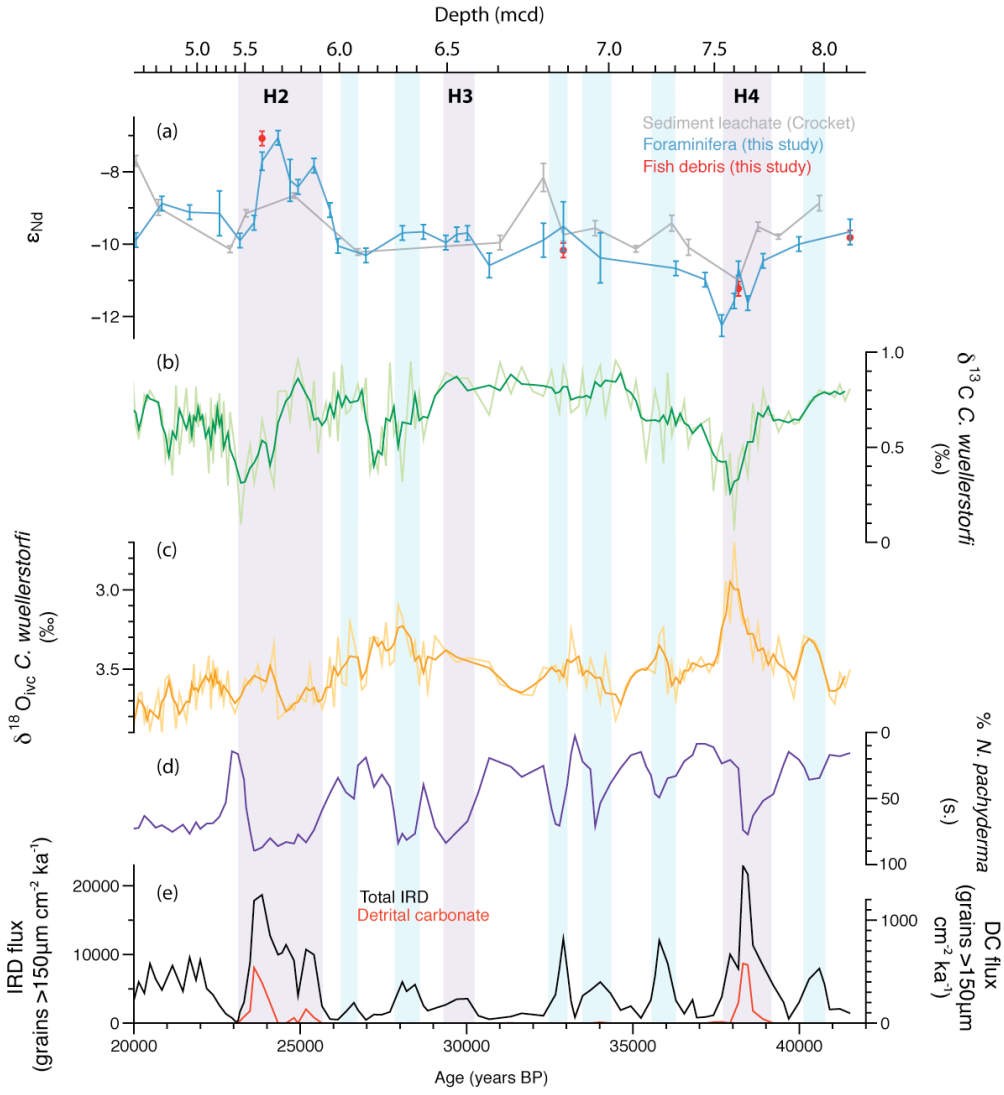

Figure 4.10: Dansgaard-Oeschger variability at ODP Site 980. (a) to (e) as figure 4.3, with pale blue bands marking the position of stadial intervals

radiogenic neodymium isotope signature recorded during stadials. Increased export of brine enriched overflow waters has been previously linked to rapid warming events out of stadial intervals [Kuijpers et al. 1998; Dickson et al. 2008]. Higher resolution neodymium isotope records than those presented here would be needed to clarify this phase relationship.

4.5.4 Younger Dryas and Holocene

The deglaciation is marked by a dramatic decrease in neodymium values to a minimum of $\varepsilon_{Nd} = -13.5$ around 8 ka. This trend is interrupted by an excursion of ~ 1 ε_{Nd} towards more radiogenic values, lasting less than 1000 years and occurring synchronously with the IRD peak identified as the Younger Dryas (figure 4.9). This excursion is accompanied by a lower $\delta^{13}C$ signature of benthic foraminiferal calcite. Oxygen isotope values (corrected for global sea level changes) are low, without displaying a clear excursion. It is possible that the neodymium isotope signature is a result of contamination from the Vedde Ash layer, which is found in the North Atlantic region at this time (12,171 ± 114 years) [Mangerud et al. 1984; Rasmussen et al. 2006]. However, the concurrent excursion in *C. wuellerstorfi* $\delta^{13}C$ strongly suggests that the signal is a result of water mass changes. A decrease in the strength of NADW production has been widely documented in the North Atlantic during the Younger Dryas [e.g. Boyle and Keigwin 1987; Broecker and Denton 1989; Smith et al. 1997; Marchitto et al. 1998; McManus et al. 2004; Praetorius et al. 2008; Elmore and Wright 2011]. A strengthened influence of overflow waters has been suggested by Labeyrie et al. [2005], Meland et al. [2008] and Thornalley et al. [2010]. Radiogenic neodymium isotopes, and low carbon and oxygen isotopic signatures recorded at Site 980 support the influence of Nordic overflows on the mid-depth Atlantic during the Younger Dryas.

The early Holocene is marked by a very unradiogenic neodymium isotope signature, with the lowest values identified from 8.2–7.5 ka (figure 4.3). This phenomenon has been previously documented in the Northeast Atlantic and the Bermuda Rise, at water depths from 750 m to 4500 m [Colin et al. 2010; Roberts et al. 2010; Crocket et al.

2011]. This is coincident with the catastrophic draining of Lake Agassiz [e.g. Klitgaard-Kristensen et al. 1998; Barber et al. 1999; Hillaire-Marcel et al. 2007], which released large amounts of material with an unradiogenic isotopic signature into the North Atlantic [Crocket et al. 2011] and disrupted both surface and deep circulation [Ellison et al. 2006].

Neodymium isotopic signatures gradually return to more radiogenic values from approximately 7 ka, while both oxygen and carbon isotope values stabilise (figure 4.3). Recovery from the input of unradiogenic material from the drainage of Lake Agassiz was gradual, due to the significant residence time of neodymium in the ocean, which is estimated to be 200–1000 years [Tachikawa et al. 1999; Tachikawa et al. 2003; Arsouze et al. 2009]. An increase in the strength of ISOW may also have contributed to the increasingly radiogenic signal observed at Site 980 at this time [Bianchi and McCave 1999; Thornalley et al. 2010]. This could either occur directly, through a stronger WTOW signal, or indirectly, via a greater contribution of Nordic overflow waters to NEADW, as part of a wider reorganisation of North Atlantic circulation during the early Holocene [Hillaire-Marcel et al. 2001; Colin et al. 2010; Hoogakker et al. 2011].

4.5.5 Phasing of changes in the surface and deep ocean at Heinrich events

The classic view of ice sheet destabilisation resulting in fresh water input to the North Ocean and resulting in a shutdown of the AMOC during Heinrich events [e.g. Sarnthein et al. 1994; Seidov et al. 1996] has evolved over the past few decades. A complex sequence of changes in the Nordic Seas has been documented at H1 [Stanford et al. 2011]. A similar sequence of interactions may also have characterised the older Heinrich events, however these are less well studied. Currently, the mechanisms responsible for driving the changes recorded during Heinrich events are still debated [e.g. van Kreveld et al. 2000; Hemming 2004; Clark et al. 2007; Dickson et al. 2008; Gutjahr and Lippold 2011]. Determining the sequence of changes in the cryosphere and ocean can therefore help to assess the plausibility of proposed scenarios.

4.5.5.1 Heinrich event 4

The first indication of a shift in bottom water properties approaching H4 occurs at 40.3 ka, during the preceding stadial interval. The carbon isotopic signature decreases by 0.15 ‰, coincident with a gradual decrease in neodymium isotope values (figure 4.6). Similarly early onsets of thermohaline circulation perturbation have been documented at intermediate depths on the Iberian margin [Zahn et al. 1997], Reykjanes Ridge [Jonkers et al. 2012] and deep western North Atlantic [Hoogakker et al. 2007; Gutjahr et al. 2010]. The first phase of the Heinrich event (in its classic sense, or sensu stricto [Stanford et al. 2011]) occurs when sea surface cooling and IRD deposition both intensify from 39.5 ka (phase I, figure 4.6). The main shift in bottom water properties (as indicated by neodymium isotopes of uncleaned planktonic foraminifera and benthic carbon and oxygen isotopes) began shortly afterwards, and is approximately synchronous with the onset of detrital carbonate deposition at 38.9 ka (phase II). There is a small shift towards more radiogenic neodymium isotopes at 38.2 ka, which may correlate with a perturbation in circulation identified by a bottom water warming in the middle of the carbon isotope excursion on the Iberian Margin [Skinner and Elderfield 2007]. Surface water temperatures increased and IRD concentrations decreased dramatically (marking the end of phase II) before minimum values of carbon and neodymium isotopes were recorded 37.7–38 ka. Carbon, oxygen and neodymium isotopes only recovered to pre-event values at 37 ka (phase III), with a later small shift to heavier $\delta^{13}C$ values at 35 ka.

4.5.5.2 Heinrich event 2

Heinrich event 2 shows a complex structure, and hence has been subdivided here into four phases (illustrated in figure 4.8). The first phase (beginning at 26 ka) consists of a shift towards more radiogenic neodymium isotope values. This is approximately synchronous with an increase in the proportion of *N. pachyderma* (s.), indicating a decrease in sea surface temperature. The second phase is an interval of moderate IRD fluxes and cold, stable SSTs, characterised by a radiogenic bottom water ε_{Nd} signature

throughout. The third phase is marked by significant detrital carbonate deposition (24.1–23.2 ka), with high total IRD fluxes. Carbon isotope values start to decrease during this interval, while neodymium isotopes return to pre-event values. The delayed carbon isotope excursion compared to peak IRD fluxes is a common feature in the Northeast Atlantic [e.g. Zahn et al. 1997; van Kreveld et al. 2000; Peck et al. 2007; Skinner et al. 2007]. During the final (fourth) phase, low percentages of *N. pachyderma* (s.) suggest a return to interstadial conditions, with very low IRD fluxes at this time. This interval is notable, however, due to the very light benthic carbon isotope signature (with a minimum at 23.2 ka) and extremely low fluxes of planktonic foraminifera and *C. wuellerstorfi* (see section 2.7.2).

It appears that a shift in the neodymium isotopic signature marginally leads the change in all other proxies at H2 (figure 4.8). However, not all signals preserved within a single sedimentary horizon would have formed contemporaneously. The stable isotope signature of the epifaunal benthic foraminifera *C. wuellerstorfi* is acquired in bottom waters during its lifetime (assuming no significant later diagenetic modification) [Duplessy et al. 1984; Zahn et al. 1986; Grossman 1987]. The similarity of the foraminiferal rare earth signatures to those of pore waters suggests that the neodymium isotope signature of the mixed planktonic foraminifera is at least partially acquired in the upper few centimetres of sediment column (see chapter 3). Therefore, at any depth within the sediment, the oxygen and carbon isotopic signature is slightly older than the neodymium isotopic signature. The magnitude of the offset is comparable to the scale of mixing of the sediment by bioturbation [Roberts et al. 2012]. It seems unlikely, therefore, that variable depths of redox element cycling can explain the offset between peak excursions in $\delta^{13}C$ and ε_{Nd} during H2, where they are separated by about 40 cm depth in the core. The offset between the ε_{Nd} shift and dramatic IRD increase is 4–8 cm, hence this may also be a primary climatic feature, but is less conclusive. The uncertainties induced by signal smoothing, therefore, mean that the data presented here neither supports nor refutes with confidence the suggestion of Gutjahr and Lippold [2011] that major circulation changes predating H2 may have played a role in ice sheet destabilisation, despite a similar shift towards radiogenic isotope values recorded in both

studies. Evidence of early bottom water circulation changes has been identified at other sites [Zahn et al. 1997; van Kreveld et al. 2000; Hagen and Hald 2002; Gutjahr and Lippold 2011], so it is possible that Site 980 is located too close to the centre of convection to detect early weakening visible elsewhere [Peck et al. 2007].

As the neodymium isotope composition of the bottom water return to their pre-event values, carbon isotopes of *C. wuellerstorfi* start to decrease, reaching a minimum as the IRD flux and percentage of *N. pachyderma* (s.) reach very low values. It was hypothesised in section 2.7.2 that this interval represented an interval of rapid deposition from sediment-laden melt water plumes. However, this cannot easily explain the very low benthic carbon isotope signature, particularly as there is no concurrent excursion in oxygen isotopes, as might be expected for a melt water signal. The absence of an excursion in the neodymium isotope record means that it is difficult to invoke the presence of a water mass with a different source. A pulse of high productivity [Mackensen et al. 1993] also seems unlikely due to the extremely low concentrations of both mixed planktonic foraminifera and the benthic species *C. wuellerstorfi* during this interval, unless the degree of dilution of the foraminifera was extreme. Removal of calcium carbonate foraminiferal tests by dissolution also seems improbable as the site is situated well above the glacial lysocline depth [Archer 1996; Brovkin et al. 2007]. Therefore, a flushing of a stagnant water mass is suggested to explain the light carbon isotope values as the ocean system recovered from Heinrich event 2. Suppressed overturning would have "aged" the bottom water mass as organic matter is oxidised, releasing ^{12}C into the water column. This effect would be particularly noticeable if productivity was elevated along the transport pathway of the water mass. It is possible that the reason this process is only recorded at H2 is due to abnormally high sedimentation rates at this time, linked to input of sediment-laden meltwater plumes (see section 2.7.2), although this explanation may not apply at other North Atlantic sites where a light carbon isotope excursion is also recorded.

4.5.5.3 Heinrich event 1

A distinct shift towards very light carbon isotope values during H1 is identified approximately 1000 years before the main IRD peak, although unfortunately this offset is difficult to date accurately as the isotope shift occurs between samples taken from two different holes (phase I, figure 4.9). Similar early shifts of bottom water properties in intermediate and deep waters have been widely documented across the North Atlantic [e.g. Fagel et al. 1997; Zahn et al. 1997; Lassen et al. 2002; Moros et al. 2002; Schönfeld et al. 2003; Piotrowski et al. 2004; Piotrowski et al. 2005; Voelker et al. 2006; Pahnke et al. 2008; Piotrowski et al. 2012; Stern and Lisiecki 2013], and are also associated with a decrease in the vigour of the meridional overturning circulation [Hall et al. 2006].

Evidence of changing bottom water properties prior to the deposition of IRD from the Laurentide Ice Sheet is more convincing at H1 than the other Heinrich events. This may be due to the influence of increasing solar insolation at this time, which sets it apart from the other Heinrich events in this study [Hays et al. 1976; Raymo 1997; Moros et al. 2002; Huybers and Wunsch 2005; Olsen et al. 2005; Brennan et al. 2013; He et al. 2013]. An early response from some of the more sensitive circum-Atlantic ice sheets released fresh water into the North Atlantic and Nordic Seas, and was likely responsible for the observed perturbation to bottom water circulation [e.g. Grousset et al. 2000; Zaragosi et al. 2001; Darby et al. 2002; Jullien et al. 2006; Ménot et al. 2006; Toucanne et al. 2010; Stanford et al. 2011].

4.5.5.4 Implications for Heinrich event generation

Evidence of circulation changes prior to the deposition of the Heinrich IRD layer is recorded at ODP Site 980 during H4, H2 and H1 (with H3 the exception, as there are no clear changes in bottom water properties). However, the nature of the deep water changes and the confidence that can be placed in the occurrence a precursory shift from the proxy records varies between events. H1 shows by far the most convincing evidence of an early thermohaline circulation perturbation, with a carbon isotope shift of >0.6 ‰ preceding peak IRD by approximately 1000 years. A suggestion of early changes in $\delta^{13}C$ can also be seen at H4, but these are much less distinct, with a shift of 0.15 ‰

approximately 1500 years before the onset of significant detrital carbonate deposition. However, the main excursion in carbon isotopes does not start until elevated IRD fluxes are reached. Whether there is evidence of early circulation changes during H2 at Site 980 depends on the depth within the sediment column at which the neodymium isotope signature of planktonic foraminifera becomes fixed and the scale over which the signal is smoothed. No shift in the $\delta^{13}C$ of *C. wuellerstorfi* is recorded until after high IRD concentrations are reached. Therefore, it is possible that a precursory AMOC slowdown could have played a role in the generation of some (if not all) of the Heinrich events, however, there is no clear repeating sequence of events leading up to the deposition of the Heinrich IRD layer.

Two main mechanisms have been proposed to explain how AMOC slowdown can result in ice sheet destabilisation: subsurface warming of the ocean directly melting ice [e.g. Moros et al. 2002; Shaffer et al. 2004; Olsen et al. 2005; Marcott et al. 2011] and thermal expansion of seawater causing sea levels to rise [e.g. Chappell 2002; Flückiger et al. 2006]. Heinrich event 4 is the only event that shows a clear benthic oxygen isotope excursion (as would be expected if there was a bottom water warming), which occurred after the main IRD peak (see figure 4.6). However, Site 980 may be too deep for a strong warming signal to be seen, with observed bottom water warming recorded at depths of 1–1.3 km [Rasmussen et al. 1996a; Rasmussen and Thomsen 2004; Marcott et al. 2011] and concentrated at 200–2000 m in modelling studies [e.g. Knutti et al. 2004; Rühlemann et al. 2004; Mignot et al. 2007; Marcott et al. 2011].

One pattern that is shared by the sequence of events during H4, H2 and H1 is that recovery of the AMOC (as inferred from bottom water chemistry at Site 980) is delayed until after the cessation of major IRD input. All three events show the lightest benthic carbon isotopic signatures after detrital carbonate deposition has ceased. Rapid warming of sea surface temperatures also occurs before bottom water properties recover. It has been suggested that the deeper ocean plays a key role in driving the rapid surface warming out of stadial intervals, with hypotheses including subsurface warming driving a rapid reduction in sea ice as a result of the collapse of an ice shelf [Gildor and

Tziperman 2003; Li et al. 2005; Li et al. 2010; Petersen et al. 2013], sudden upwelling of deeper warm waters [Rasmussen and Thomsen 2004; Olsen et al. 2005] and reduction of fresh water input and/or iceberg calving to the North Atlantic resulting in a reinvigoration of the overturning circulation and northwards incursion of warm Atlantic waters [Ganopolski and Rahmstorf 2001; Schmittner et al. 2002]. The records here suggest that if changes in the MOC were responsible for the rapid warming out of stadials, either directly or through modulation of ice sheet behaviour, changes must have been concentrated at depths <2000 m, with little influence from the deeper ocean. An alternative suggestion is that circulation was restarted due to enhanced sea ice formation driving brine rejection [Dokken and Jansen 1999; van Kreveld et al. 2000; Dickson et al. 2008]. The records presented here show that at Heinrich events 4 and 2, benthic stable isotopes do show a decrease prior to the rapid warming of sea surface temperatures, however, the lowest values are not reached until significant warming has already occurred, hence deeper circulation changes are unlikely to be the main driver of the transitions to interstadial conditions.

Surface warming likely resulted in the addition of fresh water to the ocean through the melting of ice, suppressing circulation resumption [Schmittner et al. 2002; Clark et al. 2007] and hence could be responsible for the lag in the recovery of AMOC. Whether this process would continue to act for the 500–1000 years required to re-establish pre-event bottom water conditions is unknown. Decreased export of overflow waters from the Nordic Seas, for example, as inferred at H4, may also have played a role, increasing the stability of the reduced AMOC state [Ganopolski and Rahmstorf 2001].

Deep circulation changes are much more distinct at Heinrich events than Dansgaard-Oeschger events in the records from Site 980 and across the North Atlantic, suggesting that there is a significant distinction between the mechanisms responsible for the generation of each type of event. Differences between the bottom water response at Heinrich and Dansgaard-Oeschger events most likely reflect the influence of increased fresh water input to the surface ocean during Heinrich events on the strength of convection [e.g. Stocker and Wright 1991; Manabe and Stouffer 1995; Ganopolski and

Rahmstorf 2001; Olsen et al. 2005]. Evidence of increased freshwater input is provided by decreased salinity of surface waters reconstructed at Heinrich events compared to stadials [e.g. Bond et al. 1992; Maslin et al. 1995; Cortijo et al. 1997; Elliot et al. 1998; Dokken and Jansen 1999; Cortijo et al. 2000]. The location of the fresh water input may also play a role, with IRD records suggesting that the Laurentide ice sheet is significantly more involved at Heinrich events than Dansgaard-Oeschger events [e.g. Andrews and Tedesco 1992; Bond et al. 1992; Bond and Lotti 1995]. The absence of significant change in bottom water properties at the end of non-Heinrich stadials, where sea surface warming is very similar to the end of Heinrich stadials supports the lack of involvement of the deep ocean in driving the rapid warming into interstadial conditions [Petersen et al. 2013].

4.5.6 Explaining the differences between Heinrich events

One of the most eye-catching features of the data presented here is the distinct geochemical signatures of the bottom waters bathing ODP Site 980 during each of the Heinrich events (section 4.5.2). The sequence and nature of changes in the surface and deep ocean also varies between events (section 4.5.5). Site 980 is clearly very sensitive to circulation perturbations under glacial conditions, possibly because it is situated in the path of overflow waters from the Nordic Seas [e.g. Jones et al. 1970; Yu et al. 2008; Johnson et al. 2010; Crocket et al. 2011], and close to the depth of the boundary between northern and southern sourced waters during the glacial [Boyle and Keigwin 1987; Curry et al. 1988; Duplessy et al. 1988; Bertram et al. 1995; Curry and Oppo 2005; Meland et al. 2008; Yu et al. 2008]. Two main groups of hypotheses are put forward here to explain the observed differences mid-depth circulation: variable meltwater input and differing initial conditions prior to each Heinrich event.

Modelling studies have shown that the location of freshwater input to the ocean strongly influences the resulting ocean circulation changes, affecting both the rate of change and timescale of recovery [e.g. Seidov and Maslin 1999; Levine and Bigg 2008; Bigg et al. 2011]. Records of the lithologies of ice-rafted debris from Site 980 suggest differing

involvement of icebergs sourced from the circum-Atlantic ice sheets at each of the Heinrich events (although this signal may also be modified by other factors, as discussed in section 2.7.4.5). Riverine fresh water inputs from different regions also likely varied in association with ice sheet behaviour [e.g. Teller 1990; Brown and Kennett 1998; Marshall and Clarke 1999; Sionneau et al. 2010]. The rate of melt water input also strongly influences ocean circulation [e.g. Rahmstorf 1995; Ganopolski and Rahmstorf 2001; Rind et al. 2001; Meissner and Clark 2006], although changes in this parameter cannot easily be determined in open ocean, far-field sedimentary records.

An alternative explanation for the observed differences in bottom water properties between the Heinrich events is that they are a response to variation in surface water properties. Circulation perturbations are widely attributed to changes in the amount and location of deep water formation in the North Atlantic, and the properties of these deep waters where they form, hence, the density of the surface ocean exerts a strong influence on global thermohaline circulation [Seidov and Maslin 1999; Seidov and Haupt 2003]. % *N. pachyderma* (s.) records from Site 980 (section 2.6.1) suggest that there was a general overall upper ocean cooling trend, from the oldest part of the record (41 ka) until ca. 24 ka (figure 4.3), but only modest differences among Heinrich events. Significant differences in sea surface density, however, have been documented at and between Heinrich events [e.g. Maslin et al. 1995; Sarnthein et al. 1995; Cayre et al. 1999; Dokken and Jansen 1999; Weinelt et al. 2003; Cortijo et al. 2005], suggesting that surface salinity variations are more likely to be the determining factor in explaining the differences in the observed response of the deeper circulation during Heinrich events. Highly variable fluxes of foraminifera (described in section 2.6.3) may be an indicator of variable surface salinity and/or sea ice extent and stability over Site 980. It is the surface ocean properties at the sites of deep water formation (which may include the Rockall Trough region), however, which likely exert the greatest control over the bottom water changes described in this study.

4.6 Summary and conclusions

The location of ODP Site 980 at 2.2 km depth in the western Rockall Trough is close to the boundary of northern and southern sourced water masses during the last glacial interval and in the path of overflow waters from the Nordic Seas. These factors make the site highly sensitive to changes at intermediate/deep depths in the overturning circulation with the addition of freshwater to the North Atlantic at Heinrich events. In this study, a suite of complementary bottom water proxies was used to reconstruct bottom water properties of the mid-depth waters in the northeast Atlantic.

Clear excursions in one or more bottom water proxies ($\delta^{13}C$, $\delta^{18}O$ and ε_{Nd}) can be seen at three of the four Heinrich events in the studied interval. Distinct excursions in the carbon and oxygen isotopes of *C. wuellerstorfi* and the neodymium isotopic signature of planktonic foraminifera (with ferromanganese coatings in tact) clearly show that Site 980 was bathed by a water mass with different properties at each of the Heinrich events of the past 40,000 years (H1–4).

During Heinrich event 4, decreases in both the oxygen and carbon isotopic signatures of *C. wuellerstorfi* suggests the influence of brines on the bottom waters at Site 980, most likely with a source either in the Labrador Sea, or south of the Greenland-Scotland Ridge. In contrast to the other Heinrich events, there is no evidence of a change in bottom water properties from background glacial conditions at H3, with no clear excursion in any of the three bottom water proxy records. Heinrich event 2 shows the most complex structure of the last four Heinrich events. In the early part of the event, a shift to radiogenic neodymium isotopes is most readily explained by a penetration of Glacial Antarctic Intermediate Water into the North Atlantic. This is followed by an interval of very light benthic carbon isotopes, recorded as surface ocean conditions warmed into the following interstadial, possibly indicating the flushing of poorly ventilated waters which formed as a result of reduced circulation vigour during the earlier stages of the event. Heinrich event 1 is marked by the lowest carbon isotope signatures of the entire record, with the influence of northern sourced waters potentially being replaced by those of a southern origin during the interval of low carbon isotope values.

There is evidence, to some extent, of shifts in the bottom water circulation preceding deposition of the ice-rafted debris layer at all three of the Heinrich events that exhibit a bottom water response at Site 980. However, the nature of this precursory change varies strongly between events. Early changes in the intermediate/deep circulation may therefore contribute to the generation of Heinrich IRD layers, however, there is not necessarily a repeating set of triggers for each of the events. Instead, it may be that Heinrich events are a result of the interactions between a number of factors (including internal ice sheet instabilities, sea level changes and subsurface warming), and hence cannot be explained by a singe, simple repeating mechanism.

Rapid warming out of stadial conditions occurs before evidence of recovery in the chemistry of the bottom water masses during all of the Heinrich events studied here (where there is evidence of bottom water perturbation at Site 980). This suggests that changes in the deep ocean are not responsible for driving the rapid warming out of stadial intervals, and hence if oceanic changes are involved, they must be concentrated in the upper 2000 m of the water column. Changes in bottom water chemistry during non-Heinrich stadials are much smaller than at Heinrich events at Site 980, despite a similar degree of warming into the following interstadials, which supports a minimal involvement of the deeper ocean driving Dansgaard-Oeschger variability in this region.

The distinct response of the bottom waters at Site 980 during each of the four Heinrich events studied here highlights the sensitivity of the meridional overturning circulation to the addition of fresh water. The location of fresh water inputs has been suggested as major factor in the oceanic response [Seidov and Maslin 1999; Levine and Bigg 2008; Bigg et al. 2011], with variable patterns in the lithologies of grains of ice-rafted debris recorded at Site 980 (presented in section 2.7.4) pointing to the involvement of different ice sheets at each event (although this IRD signal is also modified by surface ocean conditions). Surface ocean density may also play a key role in modulating the strength of deepwater formation. Although the percentages of the polar planktonic foraminifera *N. pachyderma* (s.) do not vary greatly between the Heinrich events (suggesting little

variation in upper ocean temperatures), the highly variable fluxes of foraminifera could indicate variability in the extent and stability of sea ice over the site. Changes in the properties of the surface ocean in other possible sites of deep water formation also have the potential to influence the reconstructed bottom water chemistry, as Site 980 is influenced by the Labrador and Nordic Seas at the present day, with the potential additional involvement of waters from the Southern Ocean during the last glacial interval.

Understanding how the input of fresh water influences the meridional overturning circulation, particularly close to sites of deepwater formation is of vital importance, with ice sheet melting likely to increase over the coming decades. The contrasting responses of the mid-depth North Atlantic between Heinrich events presented here highlights the sensitivity of deep water circulation to the rates and locations of melt water input and/or the properties of the surface ocean.

4.7 Acknowledgements

Megan Spencer washed ca. 60% of the sediment samples used in this chapter. Tom Chalk generated 18 of the stable isotope data points, and is also thanked for sharing his as yet unpublished benthic foraminiferal B/Ca data. Analytical assistance was provided by Mike Bolshaw and Dave Spanner for the stable isotope data, and by Marcus Gutjahr, Matt Cooper and Andy Milton for the neodymium isotope work. Tom Chalk, Paul Wilson, Ian Bailey, Marcus Gutjahr and Gavin Foster are thanked for many useful discussions on this work, with constructive feedback on this chapter provided by Paul Wilson, Ian Bailey and Heiko Pälike.

4.8 References

Adkins, J. F., Cheng, H., Boyle, E. A., Druffel, E. R. M., and Edwards, R. L., 1998, Deep-Sea Coral Evidence for Rapid Change in Ventilation of the Deep North Atlantic 15,400 Years Ago: Science, v. 280, p. 725-728.

Alley, R. B., and Clark, P. U., 1999, The deglaciation of the northern hemisphere: a global perspective: Annual Review of Earth and Planetary Sciences, v. 27, p. 149-182.

Alley, R. B., Clark, P. U., Keigwin, L. D., and Webb, R. S., 1999, Making sense of millennial-scale climate change: Geophysical Monograph - American Geophysical Union, v. 112, p. 385-394.

Amakawa, H., Sasaki, K., and Ebihara, M., 2009, Nd isotopic composition in the central North Pacific: Geochimica et Cosmochimica Acta, v. 73, p. 4705-4719.

Anderson, D. M., and Archer, D., 2002, Glacial-interglacial stability of ocean pH inferred from foraminifer dissolution rates: Nature, v. 416, p. 70-73.

Andrée, M., Beer, J., Oeschger, H., Mix, A., Broecker, W., Ragano, N., O'Hara, P., Bonani, G., Hofmann, H. J., Morenzoni, E., Nessi, M., Suter, M., and Wölfli, W., 1985, Accelerator radiocarbon ages on foraminifera separated from deep-sea sediments, The Carbon Cycle and Atmospheric CO_2: Natural Variations Archean to Present: Geophys. Monogr. Ser., Washington, DC, AGU, p. 143-153.

Andrews, J. T., and Tedesco, K., 1992, Detrital carbonate-rich sediments, northwestern Labrador Sea: Implications for ice-sheet dynamics and iceberg rafting (Heinrich) events in the North Atlantic: Geology, v. 20, p. 1087-1090.

Archer, D., 1996, A data-driven model of the global calcite lysocline: Global Biogeochemical Cycles, v. 10, p. 511-526.

Arsouze, T., Dutay, J. C., Lacan, F., and Jeandel, C., 2009, Reconstructing the Nd oceanic cycle using a coupled dynamical-biogeochemical model: Biogeosciences, v. 6, p. 2829-2846.

Ballini, M., Kissel, C., Colin, C., and Richter, T., 2006, Deep-water mass source and dynamic associated with rapid climatic variations during the last glacial stage in the North Atlantic: A multiproxy investigation of the detrital fraction of deep-sea sediments: Geochem. Geophys. Geosyst., v. 7, p. Q02N01.

Barber, D. C., Dyke, A., Hillaire-Marcel, C., Jennings, A. E., Andrews, J. T., Kerwin, M. W., Bilodeau, G., McNeely, R., Southon, J., Morehead, M. D., and Gagnon, J. M., 1999, Forcing of the cold event of 8,200 years ago by catastrophic drainage of Laurentide lakes: Nature, v. 400, p. 344-348.

Barker, S., and Elderfield, H., 2002, Foraminiferal Calcification Response to Glacial-Interglacial Changes in Atmospheric CO2: Science, v. 297, p. 833-836.

Bauch, D., and Bauch, H. A., 2001, Last glacial benthic foraminiferal δ18O anomalies in the polar North Atlantic: A modern analogue evaluation: Journal of Geophysical Research: Oceans, v. 106, p. 9135-9143.

Bauch, D., Erlenkeuser, H., Winckler, G., Pavlova, G., and Thiede, J., 2002, Carbon isotopes and habitat of polar planktic foraminifera in the Okhotsk Sea: the 'carbonate ion effect' under natural conditions: Marine Micropaleontology, v. 45, p. 83-99.

Bauch, H. A., Erlenkeuser, H., Spielhagen, R. F., Struck, U., Matthiessen, J., Thiede, J., and Heinemeier, J., 2001, A multiproxy reconstruction of the evolution of deep and surface waters in the subarctic Nordic seas over the last 30,000 yr: Quaternary Science Reviews, v. 20, p. 659-678.

Bemis, B. E., Spero, H. J., Bijma, J., and Lea, D. W., 1998, Reevaluation of the oxygen isotopic composition of planktonic foraminifera: Experimental results and revised paleotemperature equations: Paleoceanography, v. 13, p. 150-160.

Bertram, C. J., Elderfield, H., Shackleton, N. J., and MacDonald, J. A., 1995, Cadmium/Calcium and Carbon Isotope Reconstructions of the Glacial Northeast Atlantic Ocean: Paleoceanography, v. 10, p. 563-578.

Bianchi, G. G., and McCave, I. N., 1999, Holocene periodicity in North Atlantic climate and deep-ocean flow south of Iceland: Nature, v. 397, p. 515-517.

Bigg, G. R., Levine, R. C., Clark, C. D., Greenwood, S. L., Haflidason, H., Hughes, A. L. C., Nygård, A., and Sejrup, H. P., 2010, Last glacial ice-rafted debris off southwestern Europe: the role of the British–Irish Ice Sheet: Journal of Quaternary Science, v. 25, p. 689-699.

Bigg, G. R., Levine, R. C., and Green, C. L., 2011, Modelling abrupt glacial North Atlantic freshening: Rates of change and their implications for Heinrich events: Global and Planetary Change, v. 79, p. 176-192.

Bond, G., Heinrich, H., Broecker, W., Labeyrie, L., McManus, J., Andrews, J., Huon, S., Jantschik, R., Clasen, S., and Simet, C., 1992, Evidence for massive discharges of icebergs into the North Atlantic ocean during the last glacial period: Nature, v. 360, p. 245-249.

Bond, G. C., and Lotti, R., 1995, Iceberg Discharges into the North Atlantic on Millennial Time Scales During the Last Glaciation: Science, v. 267, p. 1005-1010.

Boyle, E. A., 1988, Cadmium: Chemical tracer of deepwater paleoceanography: Paleoceanography, v. 3, p. 471-489.

—, 2000, Is ocean thermohaline circulation linked to abrupt stadial/interstadial transitions?: Quaternary Science Reviews, v. 19, p. 255-272.

Boyle, E. A., and Keigwin, L., 1987, North Atlantic thermohaline circulation during the past 20,000 years linked to high-latitude surface temperature: Nature, v. 330, p. 35-40.

Boyle, E. A., and Keigwin, L. D., 1982, Deep Circulation of the North Atlantic over the Last 200,000 Years: Geochemical Evidence: Science, v. 218, p. 784-787.

Brennan, C. E., Meissner, K. J., Eby, M., Hillaire-Marcel, C., and Weaver, A. J., 2013, Impact of sea ice variability on the oxygen isotope content of seawater under glacial and interglacial conditions: Paleoceanography, In Press.

Broecker, W., and Clark, E., 2001, A dramatic Atlantic dissolution event at the onset of the last glaciation: Geochemistry, Geophysics, Geosystems, v. 2, p. 1065.

Broecker, W. S., 1982, Glacial to interglacial changes in ocean chemistry: Progress in Oceanography, v. 11, p. 151-197.

Broecker, W. S., and Denton, G. H., 1989, The role of ocean-atmosphere reorganizations in glacial cycles: Geochimica et Cosmochimica Acta, v. 53, p. 2465-2501.

Broecker, W. S., Gerard, R., Ewing, M., and Heezen, B. C., 1960, Natural Radiocarbon in the Atlantic Ocean: J. Geophys. Res., v. 65, p. 2903-2931.

Broecker, W. S., Peteet, D. M., and Rind, D., 1985, Does the ocean-atmosphere system have more than one stable mode of operation?: Nature, v. 315, p. 21-26.

Brovkin, V., Ganopolski, A., Archer, D., and Rahmstorf, S., 2007, Lowering of glacial atmospheric CO2 in response to changes in oceanic circulation and marine biogeochemistry: Paleoceanography, v. 22, p. PA4202.

Brown, P. A., and Kennett, J. P., 1998, Megaflood erosion and meltwater plumbing changes during last North American deglaciation recorded in Gulf of Mexico sediments: Geology, v. 26, p. 599-602.

Bryan, S. P., and Marchitto, T. M., 2010, Testing the utility of paleonutrient proxies Cd/Ca and Zn/Ca in benthic foraminifera from thermocline waters: Geochemistry, Geophysics, Geosystems, v. 11, p. Q01005.

Cayre, O., Lancelot, Y., Vincent, E., and Hall, M. A., 1999, Paleoceanographic Reconstructions from Planktonic Foraminifera off the Iberian Margin: Temperature, Salinity, and Heinrich Events: Paleoceanography, v. 14, p. 384-396.

Chalk, T. B., Crocker, A. J., Foster, G. L., Bailey, I., and Wilson, P. A., 2013, Intermediate water dynamics and origins during Heinrich Events in the North Atlantic, 11th International Conference of Paleoceanography, Sitges - Barcelona.

Chappell, J., 2002, Sea level changes forced ice breakouts in the Last Glacial cycle: new results from coral terraces: Quaternary Science Reviews, v. 21, p. 1229-1240.

Chappell, J., Omura, A., Esat, T., McCulloch, M., Pandolfi, J., Ota, Y., and Pillans, B., 1996, Reconciliaion of late Quaternary sea levels derived from coral terraces at Huon

Peninsula with deep sea oxygen isotope records: Earth and Planetary Science Letters, v. 141, p. 227-236.

Charles, C. D., Lynch-Stieglitz, J., Ninnemann, U. S., and Fairbanks, R. G., 1996, Climate connections between the hemisphere revealed by deep sea sediment core/ice core correlations: Earth and Planetary Science Letters, v. 142, p. 19-27.

Clark, P. U., Hostetler, S. W., Pisias, N. G., Schmittner, A., and Meissner, K. J., 2007, Mechanisms for an ~7-kyr climate and sea-level oscillation during marine isotope stage 3, Ocean Circulation: Mechanisms and Impacts—Past and Future Changes of Meridional Overturning: Geophys. Monogr. Ser., Washington, DC, AGU, p. 209-246.

Clarke, R. A., and Gascard, J.-C., 1983, The Formation of Labrador Sea Water. Part I: Large-Scale Processes: Journal of Physical Oceanography, v. 13, p. 1764-1778.

Colin, C., Frank, N., Copard, K., and Douville, E., 2010, Neodymium isotopic composition of deep-sea corals from the NE Atlantic: implications for past hydrological changes during the Holocene: Quaternary Science Reviews, v. 29, p. 2509-2517.

Cooke, S., and Rohling, E. J., 2001, Stable isotopes in foraminiferal carbonate: Southampton Oceanography Centre Internal Document, 72, p. 40.

Cortijo, E., Duplessy, J.-C., Labeyrie, L., Duprat, J., and Paillard, D., 2005, Heinrich events: hydrological impact: Comptes Rendus Geoscience, v. 337, p. 897-907.

Cortijo, E., Labeyrie, L., Elliot, M., Balbon, E., and Tisnerat, N., 2000, Rapid climatic variability of the North Atlantic Ocean and global climate: a focus of the IMAGES program: Quaternary Science Reviews, v. 19, p. 227-241.

Cortijo, E., Labeyrie, L., Vidal, L., Vautravers, M., Chapman, M., Duplessy, J.-C., Elliot, M., Arnold, M., Turon, J.-L., and Auffret, G., 1997, Changes in sea surface hydrology associated with Heinrich event 4 in the North Atlantic Ocean between 40˚ and 60˚N: Earth and Planetary Science Letters, v. 146, p. 29-45.

Cottet-Puinel, M., Weaver, A. J., Hillaire-Marcel, C., de Vernal, A., Clark, P. U., and Eby, M., 2004, Variation of Labrador Sea Water formation over the Last Glacial cycle in a climate model of intermediate complexity: Quaternary Science Reviews, v. 23, p. 449-465.

Crocket, K. C., Vance, D., Gutjahr, M., Foster, G. L., and Richards, D. A., 2011, Persistent Nordic deep-water overflow to the glacial North Atlantic: Geology, v. 39, p. 515-518.

Curry, W. B., Duplessy, J. C., Labeyrie, L. D., and Shackleton, N. J., 1988, Changes in the distribution of δ13C of deep water ΣCO2 between the Last Glaciation and the Holocene: Paleoceanography, v. 3, p. 317-341.

Curry, W. B., and Lohmann, G. P., 1982, Carbon isotopic changes in benthic foraminifera from the western South Atlantic: Reconstruction of glacial abyssal circulation patterns: Quaternary Research, v. 18, p. 218-235.

—, 1983, Reduced advection into Atlantic Ocean deep eastern basins during last glaciation maximum: Nature, v. 306, p. 577-580.

—, 1990, Reconstructing past particle fluxes in the tropical Atlantic Ocean: Paleoceanography, v. 5, p. 487-505.

Curry, W. B., and Oppo, D. W., 2005, Glacial water mass geometry and the distribution of δ13C of ΣCO2 in the western Atlantic Ocean: Paleoceanography, v. 20, p. PA1017.

Darby, D. A., Bischof, J. F., Spielhagen, R. F., Marshall, S. A., and Herman, S. W., 2002, Arctic ice export events and their potential impact on global climate during the late Pleistocene: Paleoceanography, v. 17, p. 1025.

de Vernal, A., and Hillaire-Marcel, C., 2000, Sea-ice cover, sea-surface salinity and halo-/thermocline structure of the northwest North Atlantic: modern versus full glacial conditions: Quaternary Science Reviews, v. 19, p. 65-85.

de Vernal, A., Hillaire-Marcel, C., Peltier, W. R., and Weaver, A. J., 2002, Structure of the upper water column in the northwest North Atlantic: Modern versus Last Glacial Maximum conditions: Paleoceanography, v. 17, p. 2-1–2-15.

Death, R., Siegert, M. J., Bigg, G. R., and Wadley, M. R., 2006, Modelling iceberg trajectories, sedimentation rates and meltwater input to the ocean from the Eurasian Ice Sheet at the Last Glacial Maximum: Palaeogeography, Palaeoclimatology, Palaeoecology, v. 236, p. 135-150.

Deuser, W. G., and Hunt, J. M., 1969, Stable isotope ratios of dissolved inorganic carbon in the Atlantic: Deep Sea Research and Oceanographic Abstracts, v. 16, p. 221-225.

Dickson, A. J., Austin, W. E. N., Hall, I. R., Maslin, M. A., and Kucera, M., 2008, Centennial-scale evolution of Dansgaard-Oeschger events in the northeast Atlantic Ocean between 39.5 and 56.5 ka B.P: Paleoceanography, v. 23, p. PA3206.

Dickson, R. R., and Brown, J., 1994, The production of North Atlantic Deep Water: Sources, rates, and pathways: Journal of Geophysical Research: Oceans, v. 99, p. 12319-12341.

Dokken, T. M., and Jansen, E., 1999, Rapid changes in the mechanism of ocean convection during the last glacial period: Nature, v. 401, p. 458-461.

Duplessy, J.-C., Labeyrie, L., and Waelbroeck, C., 2002, Constraints on the ocean oxygen isotopic enrichment between the Last Glacial Maximum and the Holocene: Paleoceanographic implications: Quaternary Science Reviews, v. 21, p. 315-330.

Duplessy, J.-C., Moyes, J., and Pujol, C., 1980, Deep water formation in the North Atlantic Ocean during the last ice age: Nature, v. 286, p. 479-482.

Duplessy, J.-C., Shackleton, N. J., Matthews, R. K., Prell, W., Ruddiman, W. F., Caralp, M. l., and Hendy, C. H., 1984, 13C Record of benthic foraminifera in the last interglacial ocean: Implications for the carbon cycle and the global deep water circulation: Quaternary Research, v. 21, p. 225-243.

Duplessy, J. C., Arnold, M., Bard, E., Juillet, L. A., Kallel, N., and Labeyrie, L., 1989, AMS ^{14}C study of transient events and of the ventilation rate of the Pacific intermediate water during the last deglaciation: Radiocarbon.

Duplessy, J. C., Chenouard, L., and Vila, F., 1975, Weyl's Theory of Glaciation Supported by Isotopic Study of Norwegian Core K 11: Science, v. 188, p. 1208-1209.

Duplessy, J. C., Lalou, C., and Vinot, A. C., 1970, Differential Isotopic Fractionation in Benthic Foraminifera and Paleotemperatures Reassessed: Science, v. 168, p. 250-251.

Duplessy, J. C., Shackleton, N. J., Fairbanks, R. G., Labeyrie, L., Oppo, D., and Kallel, N., 1988, Deepwater source variations during the last climatic cycle and their impact on the global deepwater circulation: Paleoceanography, v. 3, p. 343-360.

Ellett, D. J., and Martin, J. H. A., 1973, The physical and chemical oceanography of the Rockall channel: Deep Sea Research and Oceanographic Abstracts, v. 20, p. 585-625.

Ellett, D. J., and Roberts, D. G., 1973, The overflow of Norwegian Sea Deep Water across the Wyville-Thomson Ridge: Deep Sea Research and Oceanographic Abstracts, v. 20, p. 819-835.

Elliot, M., Labeyrie, L., Bond, G., Cortijo, E., Turon, J.-L., Tisnerat, N., and Duplessy, J.-C., 1998, Millennial-Scale Iceberg Discharges in the Irminger Basin During the Last Glacial Period: Relationship with the Heinrich Events and Environmental Settings: Paleoceanography, v. 13, p. 433-446.

Elliot, M., Labeyrie, L., and Duplessy, J.-C., 2002, Changes in North Atlantic deep-water formation associated with the Dansgaard-Oeschger temperature oscillations (60-10 ka): Quaternary Science Reviews, v. 21, p. 1153-1165.

Ellison, C. R. W., Chapman, M. R., and Hall, I. R., 2006, Surface and Deep Ocean Interactions During the Cold Climate Event 8200 Years Ago: Science, v. 312, p. 1929-1932.

Elmore, A. C., Piotrowski, A. M., Wright, J. D., and Scrivner, A. E., 2011, Testing the extraction of past seawater Nd isotopic composition from North Atlantic deep sea sediments and foraminifera: Geochem. Geophys. Geosyst., v. 12, p. Q09008.

Elmore, A. C., and Wright, J. D., 2011, North Atlantic Deep Water and climate variability during the Younger Dryas cold period: Geology, v. 39, p. 107-110.

Epstein, S., Buchsbaum, R., Lowenstam, H., and Urey, H. C., 1951, Carbonate-water isotopic temperature scale: Geological Society of America Bulletin, v. 62, p. 417-426.

Epstein, S., Buchsbaum, R., Lowenstam, H. A., and Urey, H. C., 1953, Revised carbonate-water isotopic temperature scale: Geological Society of America Bulletin, v. 64, p. 1315-1326.

Eynaud, F., Zaragosi, S., Scourse, J. D., Mojtahid, M., Bourillet, J. F., Hall, I. R., Penaud, A., Locascio, M., and Reijonen, A., 2007, Deglacial laminated facies on the NW European continental margin: The hydrographic significance of British-Irish Ice Sheet deglaciation and Fleuve Manche paleoriver discharges: Geochem. Geophys. Geosyst., v. 8, p. Q06019.

Fagel, N., Hillaire-Marcel, C., and Robert, C., 1997, Changes in the Western Boundary Undercurrent Outflow Since the Last Glacial Maximum, From Smectite/Illite Ratios in Deep Labrador Sea Sediments: Paleoceanography, v. 12, p. 79-96.

Farrell, J. W., and Prell, W. L., 1989, Climatic change and CaCO3 preservation: An 800,000 year bathymetric Reconstruction from the central equatorial Pacific Ocean: Paleoceanography, v. 4, p. 447-466.

Finlay, J. C., 2001, Stable-Carbon-Isotope Ratios of River Biota: Implications for Energy Flow in Lotic Food Webs: Ecology, v. 82, p. 1052-1064.

Flückiger, J., Knutti, R., and White, J. W. C., 2006, Oceanic processes as potential trigger and amplifying mechanisms for Heinrich events: Paleoceanography, v. 21, p. PA2014.

Foster, G. L., 2008, Seawater pH, pCO2 and [CO_3^{2-}] variations in the Caribbean Sea over the last 130 kyr: A boron isotope and B/Ca study of planktic foraminifera: Earth and Planetary Science Letters, v. 271, p. 254-266.

Ganopolski, A., and Rahmstorf, S., 2001, Rapid changes of glacial climate simulated in a coupled climate model: Nature, v. 409, p. 153-158.

Gildor, H., and Tziperman, E., 2003, Sea-ice switches and abrupt climate change: Philosophical Transactions of the Royal Society of London. Series A: Mathematical, Physical and Engineering Sciences, v. 361, p. 1935-1944.

Grant, K. M., Rohling, E. J., Bar-Matthews, M., Ayalon, A., Medina-Elizalde, M., Ramsey, C. B., Satow, C., and Roberts, A. P., 2012, Rapid coupling between ice volume and polar temperature over the past 150,000 years: Nature, v. 491, p. 744-747.

Grossman, E. L., 1984, Carbon isotopic fractionation in live benthic foraminifera - comparison with inorganic precipitate studies: Geochimica et Cosmochimica Acta, v. 48, p. 1505-1512.

—, 1987, Stable isotopes in modern benthic foraminifera; a study of vital effect: The Journal of Foraminiferal Research, v. 17, p. 48-61.

Grossman, E. L., and Ku, T.-L., 1986, Oxygen and carbon isotope fractionation in biogenic aragonite: Temperature effects: Chemical Geology: Isotope Geoscience section, v. 59, p. 59-74.

Grousset, F. E., Pujol, C., Labeyrie, L., Auffret, G., and Boelaert, A., 2000, Were the North Atlantic Heinrich events triggered by the behavior of the European ice sheets?: Geology, v. 28, p. 123-126.

Gutjahr, M., Hoogakker, B. A. A., Frank, M., and McCave, I. N., 2010, Changes in North Atlantic Deep Water strength and bottom water masses during Marine Isotope Stage 3 (45–35 ka BP): Quaternary Science Reviews, v. 29, p. 2451-2461.

Gutjahr, M., and Lippold, J., 2011, Early arrival of Southern Source Water in the deep North Atlantic prior to Heinrich event 2: Paleoceanography, v. 26, p. PA2101.

Hagen, S., and Hald, M., 2002, Variation in surface and deep water circulation in the Denmark Strait, North Atlantic, during marine isotope stages 3 and 2: Paleoceanography, v. 17, p. 1061.

Hall, I. R., Moran, S. B., Zahn, R., Knutz, P. C., Shen, C. C., and Edwards, R. L., 2006, Accelerated drawdown of meridional overturning in the late-glacial Atlantic triggered by transient pre-H event freshwater perturbation: Geophysical Research Letters, v. 33, p. L16616.

Hall, J. M., and Chan, L. H., 2004, Ba/Ca in benthic foraminifera: Thermocline and middepth circulation in the North Atlantic during the last glaciation: Paleoceanography, v. 19, p. PA4018.

Hansen, B., and Østerhus, S., 2007, Faroe Bank Channel overflow 1995–2005: Progress in Oceanography, v. 75, p. 817-856.

Hays, J. D., Imbrie, J., and Shackleton, N. J., 1976, Variations in the Earth's orbit: pacemaker of the ice ages: Science, v. 194, p. 1121-1132.

He, F., Shakun, J. D., Clark, P. U., Carlson, A. E., Liu, Z., Otto-Bliesner, B. L., and Kutzbach, J. E., 2013, Northern Hemisphere forcing of Southern Hemisphere climate during the last deglaciation: Nature, v. 494, p. 81-85.

Hemming, S. R., 2004, Heinrich events: Massive late Pleistocene detritus layers of the North Atlantic and their global climate imprint: Rev. Geophys., v. 42, p. RG1005.

Henry, F., Jeandel, C., Dupré, B., and Minster, J. F., 1994, Particulate and dissolved Nd in the western Mediterranean Sea: Sources, fate and budget: Marine Chemistry, v. 45, p. 283-305.

Hesse, R., Rashid, H., and Khodabakhsh, S., 2004, Fine-grained sediment lofting from meltwater-generated turbidity currents during Heinrich events: Geology, v. 32, p. 449-452.

Hillaire-Marcel, C., and Bilodeau, G., 2000, Instabilities in the Labrador Sea water mass structure during the last climatic cycle: Canadian Journal of Earth Sciences, v. 37, p. 795-809.

Hillaire-Marcel, C., and de Vernal, A., 2008, Stable isotope clue to episodic sea ice formation in the glacial North Atlantic: Earth and Planetary Science Letters, v. 268, p. 143-150.

Hillaire-Marcel, C., de Vernal, A., Candon, L., Bilodeau, G., and Stoner, J., 2001, Changes of potential density gradients in the northwestern North Atlantic during the last climatic cycle based on a multiproxy approach, The Oceans and Rapid Climate Change: Past, Present, and Future: Geophys. Monogr. Ser., Washington, DC, AGU, p. 83-100.

Hillaire-Marcel, C., de Vernal, A., and McKay, J., 2011, Foraminifer isotope study of the Pleistocene Labrador Sea, northwest North Atlantic (IODP Sites 1302/03 and 1305), with emphasis on paleoceanographical differences between its "inner" and "outer" basins: Marine Geology, v. 279, p. 188-198.

Hillaire-Marcel, C., de Vernal, A., and Piper, D. J. W., 2007, Lake Agassiz Final drainage event in the northwest North Atlantic: Geophysical Research Letters, v. 34, p. L15601.

Hodell, D. A., Charles, C. D., and Sierro, F. J., 2001, Late Pleistocene evolution of the ocean's carbonate system: Earth and Planetary Science Letters, v. 192, p. 109-124.

Hodell, D. A., Venz, K. A., Charles, C. D., and Ninnemann, U. S., 2003, Pleistocene vertical carbon isotope and carbonate gradients in the South Atlantic sector of the Southern Ocean: Geochemistry, Geophysics, Geosystems, v. 4, p. 1004.

Hoffman, J. L., and Lund, D. C., 2012, Refining the stable isotope budget for Antarctic Bottom Water: New foraminiferal data from the abyssal southwest Atlantic: Paleoceanography, v. 27, p. PA1213.

Holliday, P. N., Pollard, R. T., Read, J. F., and Leach, H., 2000, Water mass properties and fluxes in the Rockall Trough, 1975–1998: Deep Sea Research Part I: Oceanographic Research Papers, v. 47, p. 1303-1332.

Hönisch, B., and Hemming, N. G., 2004, Ground-truthing the boron isotope-paleo-pH proxy in planktonic foraminifera shells: Partial dissolution and shell size effects: Paleoceanography, v. 19, p. PA4010.

—, 2005, Surface ocean pH response to variations in pCO2 through two full glacial cycles: Earth and Planetary Science Letters, v. 236, p. 305-314.

Hoogakker, B. A. A., Chapman, M. R., McCave, I. N., Hillaire-Marcel, C., Ellison, C. R. W., Hall, I. R., and Telford, R. J., 2011, Dynamics of North Atlantic Deep Water masses during the Holocene: Paleoceanography, v. 26, p. PA4214.

Hoogakker, B. A. A., McCave, I. N., and Vautravers, M. J., 2007, Antarctic link to deep flow speed variation during Marine Isotope Stage 3 in the western North Atlantic: Earth and Planetary Science Letters, v. 257, p. 463-473.

Howard, W. R., and Prell, W. L., 1994, Late Quaternary CaCO3 production and preservation in the Southern Ocean: Implications for oceanic and atmospheric carbon cycling: Paleoceanography, v. 9, p. 453-482.

Hu, A., Meehl, G. A., Otto-Bliesner, B. L., Waelbroeck, C., Han, W., Loutre, M.-F., Lambeck, K., Mitrovica, J. X., and Rosenbloom, N., 2010, Influence of Bering Strait flow and North Atlantic circulation on glacial sea-level changes: Nature Geosci, v. 3, p. 118-121.

Huybers, P., and Wunsch, C., 2005, Obliquity pacing of the late Pleistocene glacial terminations: Nature, v. 434, p. 491-494.

Jang, K., Han, Y., Huh, Y., Nam, S.-I., Stein, R., Mackensen, A., and Matthiessen, J., 2013, Glacial freshwater discharge events recorded by authigenic neodymium isotopes in sediments from the Mendeleev Ridge, western Arctic Ocean: Earth and Planetary Science Letters.

Jansen, E., and Veum, T., 1990, Evidence for two-step deglaciation and its impact on North Atlantic deep-water circulation: Nature, v. 343, p. 612-616.

Jeandel, C., 1993, Concentration and isotopic composition of Nd in the South Atlantic Ocean: Earth and Planetary Science Letters, v. 117, p. 581-591.

Jeandel, C., Arsouze, T., Lacan, F., Téchiné, P., and Dutay, J. C., 2007, Isotopic Nd compositions and concentrations of the lithogenic inputs into the ocean: A compilation, with an emphasis on the margins: Chemical Geology, v. 239, p. 156-164.

Jeandel, C., Bishop, J. K., and Zindler, A., 1995, Exchange of neodymium and its isotopes between seawater and small and large particles in the Sargasso Sea: Geochimica et Cosmochimica Acta, v. 59, p. 535-547.

Johnson, C., Sherwin, T., Smythe-Wright, D., Shimmield, T., and Turrell, W., 2010, Wyville Thomson Ridge Overflow Water: Spatial and temporal distribution in the Rockall Trough: Deep Sea Research Part I: Oceanographic Research Papers, v. 57, p. 1153-1162.

Jones, E. J. W., Ewing, M., Ewing, J. I., and Eittreim, S. L., 1970, Influences of Norwegian Sea Overflow Water on Sedimentation in the Northern North Atlantic and Labrador Sea: J. Geophys. Res., v. 75, p. 1655-1680.

Jonkers, L., Prins, M. A., Moros, M., Weltje, G. J., Troelstra, S. R., and Brummer, G.-J. A., 2012, Temporal offsets between surface temperature, ice-rafting and bottom flow speed proxies in the glacial (MIS 3) northern North Atlantic: Quaternary Science Reviews, v. 48, p. 43-53.

Jullien, E., Grousset, F. E., Hemming, S. R., Peck, V. L., Hall, I. R., Jeantet, C., and Billy, I., 2006, Contrasting conditions preceding MIS3 and MIS2 Heinrich events: Global and Planetary Change, v. 54, p. 225-238.

Jung, S., 1996, Wassermassenaustausch zwischen NE-Atlantik und Nordmeer während der letzten 300 000/80 000 Jahre im Abbild stabiler O-und C-Isotope: Berichte aus dem Sonderforschungsbereich 313, Christian-Albrechts-Universität, Kiel, v. 61, p. 104.

Keigwin, L. D., and Boyle, E. A., 1999, Surface and deep ocean variability in the northern Sargasso Sea during marine isotope stage 3: Paleoceanography, v. 14, p. 164-170.

Keigwin, L. D., and Lehman, S. J., 1994, Deep Circulation Change Linked to HEINRICH Event 1 and Younger Dryas in a Middepth North Atlantic Core: Paleoceanography, v. 9, p. 185-194.

Kissel, C., 2005, Magnetic signature of rapid climatic variations in glacial North Atlantic, a review: Comptes Rendus Geoscience, v. 337, p. 908-918.

Klitgaard-Kristensen, D., Sejrup, H. P., Haflidason, H., Johnsen, S., and Spurk, M., 1998, A regional 8200 cal. yr BP cooling event in northwest Europe, induced by final stages of the Laurentide ice-sheet deglaciation?: Journal of Quaternary Science, v. 13, p. 165-169.

Knutti, R., Fluckiger, J., Stocker, T. F., and Timmermann, A., 2004, Strong hemispheric coupling of glacial climate through freshwater discharge and ocean circulation: Nature, v. 430, p. 851-856.

Kroopnick, P. M., 1985, The distribution of 13C of ΣCO2 in the world oceans: Deep Sea Research Part A. Oceanographic Research Papers, v. 32, p. 57-84.

Kuijpers, A., Troelstra, S. R., Wisse, M., Heier Nielsen, S., and van Weering, T. C. E., 1998, Norwegian Sea overflow variability and NE Atlantic surface hydrography during the past 150,000 years: Marine Geology, v. 152, p. 75-99.

Kwon, E. Y., Hain, M. P., Sigman, D. M., Galbraith, E. D., Sarmiento, J. L., and Toggweiler, J. R., 2012, North Atlantic ventilation of "southern-sourced" deep water in the glacial ocean: Paleoceanography, v. 27, p. PA2208.

Labeyrie, L., Waelbroeck, C., Cortijo, E., Michel, E., and Duplessy, J.-C., 2005, Changes in deep water hydrology during the Last Deglaciation: Comptes Rendus Geoscience, v. 337, p. 919-927.

Labeyrie, L. D., Duplessy, J.-C., Duprat, J., Juillet-Leclerc, A., Moyes, J., Michel, E., Kallel, N., and Shackleton, N. J., 1992, Changes in the vertical structure of the North Atlantic Ocean between glacial and modern times: Quaternary Science Reviews, v. 11, p. 401-413.

Lacan, F., and Jeandel, C., 2001, Tracing Papua New Guinea imprint on the central Equatorial Pacific Ocean using neodymium isotopic compositions and Rare Earth Element patterns: Earth and Planetary Science Letters, v. 186, p. 497-512.

—, 2004a, Denmark Strait water circulation traced by heterogeneity in neodymium isotopic compositions: Deep Sea Research Part I: Oceanographic Research Papers, v. 51, p. 71-82.

—, 2004b, Neodymium isotopic composition and rare earth element concentrations in the deep and intermediate Nordic Seas: Constraints on the Iceland Scotland Overflow Water signature: Geochem. Geophys. Geosyst., v. 5, p. Q11006.

—, 2004c, Subpolar Mode Water formation traced by neodymium isotopic composition: Geophys. Res. Lett., v. 31, p. L14306.

—, 2005a, Acquisition of the neodymium isotopic composition of the North Atlantic Deep Water: Geochem. Geophys. Geosyst., v. 6, p. Q12008.

—, 2005b, Neodymium isotopes as a new tool for quantifying exchange fluxes at the continent–ocean interface: Earth and Planetary Science Letters, v. 232, p. 245-257.

Lacan, F., Tachikawa, K., and Jeandel, C., 2012, Neodymium isotopic composition of the oceans: a compilation of seawater data: Chemical Geology, v. 300-301, p. 177-184.

Lassen, S., Kuijpers, A., Kunzendorf, H., Lindgren, H., Heinemeier, J., Jansen, E., and Knudsen, K. L., 2002, Intermediate water signal leads surface water response during Northeast Atlantic deglaciation: Global and Planetary Change, v. 32, p. 111-125.

Lea, D. W., and Boyle, E. A., 1990, Foraminiferal reconstruction of barium distributions in water masses of the glacial oceans: Paleoceanography, v. 5, p. 719-742.

Lea, D. W., Martin, P. A., Pak, D. K., and Spero, H. J., 2002, Reconstructing a 350 ky history of sea level using planktonic Mg/Ca and oxygen isotope records from a Cocos Ridge core: Quaternary Science Reviews, v. 21, p. 283-293.

Lekens, W. A. H., Sejrup, H. P., Haflidason, H., Petersen, G. Ø., Hjelstuen, B., and Knorr, G., 2005, Laminated sediments preceding Heinrich event 1 in the Northern North Sea and Southern Norwegian Sea: Origin, processes and regional linkage: Marine Geology, v. 216, p. 27-50.

Levine, R. C., and Bigg, G. R., 2008, Sensitivity of the glacial ocean to Heinrich events from different iceberg sources, as modeled by a coupled atmosphere-iceberg-ocean model: Paleoceanography, v. 23, p. PA4213.

Li, C., Battisti, D. S., and Bitz, C. M., 2010, Can North Atlantic Sea Ice Anomalies Account for Dansgaard–Oeschger Climate Signals?: Journal of Climate, v. 23, p. 5457-5475.

Li, C., Battisti, D. S., Schrag, D. P., and Tziperman, E., 2005, Abrupt climate shifts in Greenland due to displacements of the sea ice edge: Geophysical Research Letters, v. 32, p. L19702.

Lisiecki, L. E., and Raymo, M. E., 2005, A Pliocene-Pleistocene stack of 57 globally distributed benthic $\delta^{18}O$ records: Paleoceanography, v. 20, p. PA1003.

Lynch-Stieglitz, J., Adkins, J. F., Curry, W. B., Dokken, T., Hall, I. R., Herguera, J. C., Hirschi, J. l. J. M., Ivanova, E. V., Kissel, C., Marchal, O., Marchitto, T. M., McCave, I. N., McManus, J. F., Mulitza, S., Ninnemann, U., Peeters, F., Yu, E.-F., and Zahn, R., 2007, Atlantic Meridional Overturning Circulation During the Last Glacial Maximum: Science, v. 316, p. 66-69.

Lynch-Stieglitz, J., and Fairbanks, R. G., 1994, A conservative tracer for glacial ocean circulation from carbon isotope and palaeo-nutrient measurements in benthic foraminifera: Nature, v. 369, p. 308-310.

Macdonald, R. W., Paton, D. W., Carmack, E. C., and Omstedt, A., 1995, The freshwater budget and under-ice spreading of Mackenzie River water in the Canadian Beaufort Sea based on salinity and 18O/16O measurements in water and ice: Journal of Geophysical Research: Oceans, v. 100, p. 895-919.

Mackensen, A., 2008, On the use of benthic foraminiferal δ13C in palaeoceanography: constraints from primary proxy relationships: Geological Society, London, Special Publications, v. 303, p. 121-133.

Mackensen, A., Hubberten, H. W., Bickert, T., Fischer, G., and Fütterer, D. K., 1993, The δ13C in benthic foraminiferal tests of Fontbotia wuellerstorfi (Schwager) Relative to the δ13C of dissolved inorganic carbon in Southern Ocean Deep Water: Implications for glacial ocean circulation models: Paleoceanography, v. 8, p. 587-610.

Mackensen, A., Schumacher, S., Radke, J., and Schmidt, D. N., 2000, Microhabitat preferences and stable carbon isotopes of endobenthic foraminifera: clue to quantitative reconstruction of oceanic new production?: Marine Micropaleontology, v. 40, p. 233-258.

Manabe, S., and Stouffer, R. J., 1995, Simulation of abrupt climate change induced by freshwater input to the North Atlantic Ocean: Nature, v. 378, p. 165-167.

Mangerud, J., Lie, S. E., Furnes, H., Kristiansen, I. L., and Lømo, L., 1984, A Younger Dryas Ash Bed in western Norway, and its possible correlations with tephra in cores from the Norwegian Sea and the North Atlantic: Quaternary Research, v. 21, p. 85-104.

Mangini, A., Lomitschka, M., Eichstadter, R., Frank, N., Vogler, S., Bonani, G., Hajdas, I., and Patzold, J., 1998, Coral provides way to age deep water: Nature, v. 392, p. 347-348.

Manighetti, B., and McCave, I. N., 1995, Late Glacial and Holocene Palaeocurrents Around Rockall Bank, NE Atlantic Ocean: Paleoceanography, v. 10, p. 611-626.

Marchal, O., François, R., Stocker, T. F., and Joos, F., 2000, Ocean thermohaline circulation and sedimentary 231Pa/230Th ratio: Paleoceanography, v. 15, p. 625-641.

Marchitto, T. M., Curry, W. B., and Oppo, D. W., 1998, Millennial-scale changes in North Atlantic circulation since the last glaciation: Nature, v. 393, p. 557-561.

—, 2000, Zinc concentrations in benthic foraminifera reflect seawater chemistry: Paleoceanography, v. 15, p. 299-306.

Marchitto, T. M., Jr., Oppo, D. W., and Curry, W. B., 2002, Paired benthic foraminiferal Cd/Ca and Zn/Ca evidence for a greatly increased presence of Southern Ocean Water in the glacial North Atlantic: Paleoceanography, v. 17, p. 1038.

Marcott, S. A., Clark, P. U., Padman, L., Klinkhammer, G. P., Springer, S. R., Liu, Z., Otto-Bliesner, B. L., Carlson, A. E., Ungerer, A., Padman, J., He, F., Cheng, J., and Schmittner, A., 2011, Ice-shelf collapse from subsurface warming as a trigger for Heinrich events: Proceedings of the National Academy of Sciences, v. 108, p. 13415-13419.

Marshall, J., and Schott, F., 1999, Open-ocean convection: Observations, theory, and models: Reviews of Geophysics, v. 37, p. 1-64.

Marshall, S. J., and Clarke, G. K. C., 1999, Modeling North American Freshwater Runoff through the Last Glacial Cycle: Quaternary Research, v. 52, p. 300-315.

Martin, P. A., and Lea, D. W., 1998, Comparison of water mass changes in the deep tropical Atlantic derived from Cd/Ca and carbon isotope records: Implications for changing Ba composition of Deep Atlantic Water Masses: Paleoceanography, v. 13, p. 572-585.

Maslin, M. A., Shackleton, N. J., and Pflaumann, U., 1995, Surface Water Temperature, Salinity, and Density Changes in the Northeast Atlantic During the Last 45,000 Years: Heinrich Events, Deep Water Formation, and Climatic Rebounds: Paleoceanography, v. 10, p. 527-544.

McCave, I. N., Manighetti, B., and Beveridge, N. A. S., 1995a, Circulation in the glacial North Atlantic inferred from grain-size measurements: Nature, v. 374, p. 149-152.

McCave, I. N., Manighetti, B., and Robinson, S. G., 1995b, Sortable silt and fine sediment size/composition slicing: Parameters for palaeocurrent speed and palaeoceanography: Paleoceanography, v. 10, p. 593-610.

McGrath, T., Nolan, G., and McGovern, E., 2012, Chemical characteristics of water masses in the Rockall Trough: Deep Sea Research Part I: Oceanographic Research Papers.

McManus, J. F., Francois, R., Gherardi, J. M., Keigwin, L. D., and Brown-Leger, S., 2004, Collapse and rapid resumption of Atlantic meridional circulation linked to deglacial climate changes: Nature, v. 428, p. 834-837.

McManus, J. F., Oppo, D. W., and Cullen, J. L., 1999, A 0.5-Million-Year Record of Millennial-Scale Climate Variability in the North Atlantic: Science, v. 283, p. 971-975.

Meissner, K. J., and Clark, P. U., 2006, Impact of floods versus routing events on the thermohaline circulation: Geophysical Research Letters, v. 33, p. L15704.

Meland, M. Y., Dokken, T. M., Jansen, E., and Hevrøy, K., 2008, Water mass properties and exchange between the Nordic seas and the northern North Atlantic during the period 23-6 ka: Benthic oxygen isotopic evidence: Paleoceanography, v. 23, p. PA1210.

Melling, H., and Moore, R. M., 1995, Modification of halocline source waters during freezing on the Beaufort Sea shelf: evidence from oxygen isotopes and dissolved nutrients: Continental Shelf Research, v. 15, p. 89-113.

Ménot, G., Bard, E., Rostek, F., Weijers, J. W. H., Hopmans, E. C., Schouten, S., and Damsté, J. S. S., 2006, Early Reactivation of European Rivers During the Last Deglaciation: Science, v. 313, p. 1623-1625.

Mignot, J., Ganopolski, A., and Levermann, A., 2007, Atlantic Subsurface Temperatures: Response to a Shutdown of the Overturning Circulation and Consequences for Its Recovery: Journal of Climate, v. 20, p. 4884-4898.

Millo, C., Sarnthein, M., Voelker, A., and Erlenkeuser, H., 2006, Variability of the Denmark Strait Overflow during the Last Glacial Maximum: Boreas, v. 35, p. 50-60.

Moros, M., Kuijpers, A., Snowball, I., Lassen, S., Bäckström, D., Gingele, F., and McManus, J., 2002, Were glacial iceberg surges in the North Atlantic triggered by climatic warming?: Marine Geology, v. 192, p. 393-417.

Mulder, T., and Syvitski, J. P. M., 1995, Turbidity currents generated at river mouths during exceptional discharges to the world oceans: The Journal of Geology, p. 285-299.

Mulder, T., Syvitski, J. P. M., Migeon, S., Faugères, J.-C., and Savoye, B., 2003, Marine hyperpycnal flows: initiation, behavior and related deposits. A review: Marine and Petroleum Geology, v. 20, p. 861-882.

New, A. L., and Smythe-Wright, D., 2001, Aspects of the circulation in the Rockall Trough: Continental Shelf Research, v. 21, p. 777-810.

Nielsen, M. H., Pratt, L., and Helfrich, K., 2004, Mixing and entrainment in hydraulically driven stratified sill flows: Journal of Fluid Mechanics, v. 515, p. 415-443.

Olsen, A., and Ninnemann, U., 2010, Large δ13C Gradients in the Preindustrial North Atlantic Revealed: Science, v. 330, p. 658-659.

Olsen, S. M., Shaffer, G., and Bjerrum, C. J., 2005, Ocean oxygen isotope constraints on mechanisms for millennial-scale climate variability: Paleoceanography, v. 20, p. PA1014.

Oppo, D. W., and Fairbanks, R. G., 1987, Variability in the deep and intermediate water circulation of the Atlantic Ocean during the past 25,000 years: Northern Hemisphere modulation of the Southern Ocean: Earth and Planetary Science Letters, v. 86, p. 1-15.

Oppo, D. W., and Horowitz, M., 2000, Glacial deep water geometry: South Atlantic benthic foraminiferal Cd/Ca and δ13C evidence: Paleoceanography, v. 15, p. 147-160.

Oppo, D. W., and Lehman, S. J., 1993, Mid-Depth Circulation of the Subpolar North Atlantic During the Last Glacial Maximum: Science, v. 259, p. 1148-1152.

Pahnke, K., Goldstein, S. L., and Hemming, S. R., 2008, Abrupt changes in Antarctic Intermediate Water circulation over the past 25,000 years: Nature Geosci, v. 1, p. 870-874.

Pahnke, K., and Zahn, R., 2005, Southern Hemisphere Water Mass Conversion Linked with North Atlantic Climate Variability: Science, v. 307, p. 1741-1746.

Palmer, M. R., and Elderfield, H., 1985, Variations in the Nd isotopic composition of foraminifera from Atlantic Ocean sediments: Earth and Planetary Science Letters, v. 73, p. 299-305.

Peck, V. L., Hall, I. R., Zahn, R., and Elderfield, H., 2008, Millennial-scale surface and subsurface paleothermometry from the northeast Atlantic, 55-8 ka BP: Paleoceanography, v. 23, p. PA3221.

Peck, V. L., Hall, I. R., Zahn, R., and Scourse, J. D., 2007, Progressive reduction in NE Atlantic intermediate water ventilation prior to Heinrich events: Response to NW European ice sheet instabilities?: Geochem. Geophys. Geosyst., v. 8, p. Q01N10.

Peltier, W. R., and Fairbanks, R. G., 2006, Global glacial ice volume and Last Glacial Maximum duration from an extended Barbados sea level record: Quaternary Science Reviews, v. 25, p. 3322-3337.

Petersen, S. V., Schrag, D. P., and Clark, P. U., 2013, A new mechanism for Dansgaard-Oeschger cycles: Paleoceanography, v. 28, p. 24-30.

Piepgras, D. J., and Wasserburg, G. J., 1982, Isotopic Composition of Neodymium in Waters from the Drake Passage: Science, v. 217, p. 207-214.

—, 1983, Influence of the Mediterranean Outflow on the Isotopic Composition of Neodymium in Waters of the North Atlantic: J. Geophys. Res., v. 88, p. 5997-6006.

—, 1987, Rare earth element transport in the western North Atlantic inferred from Nd isotopic observations: Geochimica et Cosmochimica Acta, v. 51, p. 1257-1271.

Piepgras, D. J., Wasserburg, G. J., and Dasch, E. J., 1979, The isotopic composition of Nd in different ocean masses: Earth and Planetary Science Letters, v. 45, p. 223-236.

Piotrowski, A. M., Galy, A., Nicholl, J. A. L., Roberts, N., Wilson, D. J., Clegg, J. A., and Yu, J., 2012, Reconstructing deglacial North and South Atlantic deep water sourcing using foraminiferal Nd isotopes: Earth and Planetary Science Letters, v. 357-358, p. 289-297.

Piotrowski, A. M., Goldstein, S. L., Hemming, S. R., and Fairbanks, R. G., 2004, Intensification and variability of ocean thermohaline circulation through the last deglaciation: Earth and Planetary Science Letters, v. 225, p. 205-220.

—, 2005, Temporal Relationships of Carbon Cycling and Ocean Circulation at Glacial Boundaries: Science, v. 307, p. 1933-1938.

Piotrowski, A. M., Goldstein, S. L., R, H. S., Fairbanks, R. G., and Zylberberg, D. R., 2008, Oscillating glacial northern and southern deep water formation from combined neodymium and carbon isotopes: Earth and Planetary Science Letters, v. 272, p. 394-405.

Praetorius, S. K., McManus, J. F., Oppo, D. W., and Curry, W. B., 2008, Episodic reductions in bottom-water currents since the last ice age: Nature Geosci, v. 1, p. 449-452.

Price, J. F., and O'Neil Baringer, M., 1994, Outflows and deep water production by marginal seas: Progress in Oceanography, v. 33, p. 161-200.

Rae, J. W. B., Foster, G. L., Schmidt, D. N., and Elliott, T., 2010, Boron isotopes and B/Ca in benthic foraminifera: Proxies for the deep ocean carbonate system: Earth and Planetary Science Letters, v. 302, p. 403-413.

Rahmstorf, S., 1994, Rapid climate transitions in a coupled ocean-atmosphere model: Nature, v. 372, p. 82-85.

—, 1995, Bifurcations of the Atlantic thermohaline circulation in response to changes in the hydrological cycle: Nature, v. 378, p. 145-149.

—, 2002, Ocean circulation and climate during the past 120,000 years: Nature, v. 419, p. 207-214.

Rasmussen, S. O., Andersen, K. K., Svensson, A. M., Steffensen, J. P., Vinther, B. M., Clausen, H. B., Siggaard-Andersen, M. L., Johnsen, S. J., Larsen, L. B., Dahl-Jensen, D., Bigler, M., Röthlisberger, R., Fischer, H., Goto-Azuma, K., Hansson, M. E., and Ruth, U., 2006, A new Greenland ice core chronology for the last glacial termination: J. Geophys. Res., v. 111, p. D06102.

Rasmussen, T. L., Oppo, D. W., Thomsen, E., and Lehman, S. J., 2003, Deep sea records from the southeast Labrador Sea: Ocean circulation changes and ice-rafting events during the last 160,000 years: Paleoceanography, v. 18, p. 1018.

Rasmussen, T. L., and Thomsen, E., 2004, The role of the North Atlantic Drift in the millennial timescale glacial climate fluctuations: Palaeogeography, Palaeoclimatology, Palaeoecology, v. 210, p. 101-116.

Rasmussen, T. L., Thomsen, E., Labeyrie, L., and van Weering, T. C. E., 1996a, Circulation changes in the Faeroe-Shetland Channel correlating with cold events during the last glacial period (58-10 ka): Geology, v. 24, p. 937-940.

Rasmussen, T. L., Thomsen, E., van Weering, T. C. E., and Labeyrie, L., 1996b, Rapid Changes in Surface and Deep Water Conditions at the Faeroe Margin During the Last 58,000 Years: Paleoceanography, v. 11, p. 757-771.

Raymo, M. E., 1997, The timing of major climate terminations: Paleoceanography, v. 12, p. 577-585.

Raymo, M. E., Oppo, D. W., Flower, B. P., Hodell, D. A., McManus, J. F., Venz, K. A., Kleiven, K. F., and McIntyre, K., 2004, Stability of North Atlantic water masses in face

of pronounced climate variability during the Pleistocene: Paleoceanography, v. 19, p. PA2008.

Rickaby, R. E. M., and Elderfield, H., 2005, Evidence from the high-latitude North Atlantic for variations in Antarctic Intermediate water flow during the last deglaciation: Geochem. Geophys. Geosyst., v. 6, p. Q05001.

Rickli, J., Frank, M., and Halliday, A. N., 2009, The hafnium–neodymium isotopic composition of Atlantic seawater: Earth and Planetary Science Letters, v. 280, p. 118-127.

Rind, D., deMenocal, P., Russell, G., Sheth, S., Collins, D., Schmidt, G., and Teller, J., 2001, Effects of glacial meltwater in the GISS coupled atmosphereocean model: 1. North Atlantic Deep Water response: Journal of Geophysical Research: Atmospheres, v. 106, p. 27335-27353.

Roberts, N. L., Piotrowski, A. M., Elderfield, H., Eglinton, T. I., and Lomas, M. W., 2012, Rare earth element association with foraminifera: Geochimica et Cosmochimica Acta, v. 94, p. 57-71.

Roberts, N. L., Piotrowski, A. M., McManus, J. F., and Keigwin, L. D., 2010, Synchronous Deglacial Overturning and Water Mass Source Changes: Science, v. 327, p. 75-78.

Robinson, L. F., Adkins, J. F., Keigwin, L. D., Southon, J., Fernandez, D. P., Wang, S. L., and Scheirer, D. S., 2005, Radiocarbon Variability in the Western North Atlantic During the Last Deglaciation: Science, v. 310, p. 1469-1473.

Robinson, L. F., and van de Flierdt, T., 2009, Southern Ocean evidence for reduced export of North Atlantic Deep Water during Heinrich event 1: Geology, v. 37, p. 195-198.

Rohling, E. J., Grant, K., Bolshaw, M., Roberts, A. P., Siddall, M., Hemleben, C., and Kucera, M., 2009, Antarctic temperature and global sea level closely coupled over the past five glacial cycles: Nature Geosci, v. 2, p. 500-504.

Rozanski, K., Araguás-Araguás, L., and Gonfiantini, R., 1993, Isotopic patterns in modern global precipitation, *in* Swart P. K. et al., ed., Climate Change in Continental Isotopic Records: Geophys. Monogr. Ser., Washington, DC, AGU, p. 1-36.

Rühlemann, C., Mulitza, S., Lohmann, G., Paul, A., Prange, M., and Wefer, G., 2004, Intermediate depth warming in the tropical Atlantic related to weakened thermohaline circulation: Combining paleoclimate data and modeling results for the last deglaciation: Paleoceanography, v. 19, p. PA1025.

Rutberg, R. L., Hemming, S. R., and Goldstein, S. L., 2000, Reduced North Atlantic Deep Water flux to the glacial Southern Ocean inferred from neodymium isotope ratios: Nature, v. 405, p. 935-938.

Sanyal, A., Hemming, N. G., Hanson, G. N., and Broecker, W. S., 1995, Evidence for a higher pH in the glacial ocean from boron isotopes in foraminifera: Nature, v. 373, p. 234-236.

Sarnthein, M., Jansen, E., Weinelt, M., Arnold, M., Duplessy, J. C., Erlenkeuser, H., Flatøy, A., Johannessen, G., Johannessen, T., Jung, S., Koc, N., Labeyrie, L., Maslin, M., Pflaumann, U., and Schulz, H., 1995, Variations in Atlantic Surface Ocean Paleoceanography, 50º-80ºN: A Time-Slice Record of the Last 30,000 Years: Paleoceanography, v. 10, p. 1063-1094.

Sarnthein, M., Winn, K., Jung, S. J. A., Duplessy, J.-C., Labeyrie, L., Erlenkeuser, H., and Ganssen, G., 1994, Changes in East Atlantic Deepwater Circulation Over the Last 30,000 years: Eight Time Slice Reconstructions: Paleoceanography, v. 9, p. 209-267.

Schlosser, P., Bayer, R., Foldvik, A., Gammelsrød, T., Rohardt, G., and Münnich, K. O., 1990, Oxygen 18 and helium as tracers of ice shelf water and water/ice interaction in the Weddell Sea: Journal of Geophysical Research: Oceans, v. 95, p. 3253-3263.

Schmittner, A., Yoshimori, M., and Weaver, A. J., 2002, Instability of Glacial Climate in a Model of the Ocean-Atmosphere-Cryosphere System: Science, v. 295, p. 1489-1493.

Schmitz, W. J., 1996, On the world ocean circulation. Volume I, some global features/North Atlantic circulation, Woods Hole Oceanographic Institution Technical Report WHOI-96-03, Woods Hole Oceanographic Institution.

Schönfeld, J., Zahn, R., and de Abreu, L., 2003, Surface and deep water response to rapid climate changes at the Western Iberian Margin: Global and Planetary Change, v. 36, p. 237-264.

Schröder-Ritzrau, A., Mangini, A., and Lomitschka, M., 2003, Deep-sea corals evidence periodic reduced ventilation in the North Atlantic during the LGM/Holocene transition: Earth and Planetary Science Letters, v. 216, p. 399-410.

Schulte, S., Rostek, F., Bard, E., Rullkötter, J., and Marchal, O., 1999, Variations of oxygen-minimum and primary productivity recorded in sediments of the Arabian Sea: Earth and Planetary Science Letters, v. 173, p. 205-221.

Seidov, D., and Haupt, B. J., 2003, On sensitivity of ocean circulation to sea surface salinity: Global and Planetary Change, v. 36, p. 99-116.

Seidov, D., and Maslin, M., 1999, North Atlantic deep water circulation collapse during Heinrich events: Geology, v. 27, p. 23-26.

Seidov, D., Sarnthein, M., Stattegger, K., Prien, R., and Weinelt, M., 1996, North Atlantic ocean circulation during the last glacial maximum and subsequent meltwater event: A numerical model: J. Geophys. Res., v. 101, p. 16305-16332.

Shackleton, N. J., 1974, Attainment of isotopic equilibrium between ocean water and the benthonic foraminifera genus Uvigerina: isotopic changes in the ocean during the last glacial: Centre National de la Recherche Scientifique Colloque International, v. 219, p. 203-209.

—, 1987, Oxygen isotopes, ice volume and sea level: Quaternary Science Reviews, v. 6, p. 183-190.

Shackleton, N. J., Duplessy, J. C., Arnold, M., Maurice, P., Hall, M. A., and Cartlidge, J., 1988, Radiocarbon age of last glacial Pacific deep water: Nature, v. 335, p. 708-711.

Shackleton, N. J., Lamb, H. H., Worssam, B. C., Hodgson, J. M., Lord, A. R., Shotton, F. W., Schove, D. J., and Cooper, L. H. N., 1977, The Oxygen Isotope Stratigraphic Record of the Late Pleistocene: Philosophical Transactions of the Royal Society of London. Series B, Biological Sciences, v. 280, p. 169-182.

Shackleton, N. J., and Opdyke, N. D., 1973, Oxygen isotope and palaeomagnetic stratigraphy of Equatorial Pacific core V28-238: Oxygen isotope temperatures and ice volumes on a 105 year and 106 year scale: Quaternary Research, v. 3, p. 39-55.

Shaffer, G., and Bendtsen, J., 1994, Role of the Bering Strait in controlling North Atlantic ocean circulation and climate: Nature, v. 367, p. 354-357.

Shaffer, G., Olsen, S. M., and Bjerrum, C. J., 2004, Ocean subsurface warming as a mechanism for coupling Dansgaard-Oeschger climate cycles and ice-rafting events: Geophysical Research Letters, v. 31, p. L24202.

Sherwin, T. J., Griffiths, C. R., Inall, M. E., and Turrell, W. R., 2008, Quantifying the overflow across the Wyville Thomson Ridge into the Rockall Trough: Deep Sea Research Part I: Oceanographic Research Papers, v. 55, p. 396-404.

Sherwin, T. J., and Turrell, W. R., 2005, Mixing and advection of a cold water cascade over the Wyville Thomson Ridge: Deep Sea Research Part I: Oceanographic Research Papers, v. 52, p. 1392-1413.

Siddall, M., Rohling, E. J., Almogi-Labin, A., Hemleben, C., Meischner, D., Schmelzer, I., and Smeed, D. A., 2003, Sea-level fluctuations during the last glacial cycle: Nature, v. 423, p. 853-858.

Sigman, D. M., Hain, M. P., and Haug, G. H., 2010, The polar ocean and glacial cycles in atmospheric CO2 concentration: Nature, v. 466, p. 47-55.

Sijp, W. P., and England, M. H., 2006, Sensitivity of the Atlantic Thermohaline Circulation and Its Stability to Basin-Scale Variations in Vertical Mixing: Journal of Climate, v. 19, p. 5467-5478.

Sionneau, T., Bout-Roumazeilles, V., Flower, B. P., Bory, A., Tribovillard, N., Kissel, C., Van Vliet-Lanoë, B., and Montero Serrano, J. C., 2010, Provenance of freshwater pulses in the Gulf of Mexico during the last deglaciation: Quaternary Research, v. 74, p. 235-245.

Skinner, L. C., and Elderfield, H., 2007, Rapid fluctuations in the deep North Atlantic heat budget during the last glacial period: Paleoceanography, v. 22, p. PA1205.

Skinner, L. C., Elderfield, H., and Hall, M., 2007, Phasing of millennial climate events and northeast Atlantic deep-water temperature change since 50 ka BP, Ocean Circulation: Mechanisms and Impacts—Past and Future Changes of Meridional Overturning: Geophys. Monogr. Ser., Washington, DC, AGU, p. 197-208.

Smith, J. E., Risk, M. J., Schwarcz, H. P., and McConnaughey, T. A., 1997, Rapid climate change in the North Atlantic during the Younger Dryas recorded by deep-sea corals: Nature, v. 386, p. 818-820.

Sortor, R. N., and Lund, D. C., 2010, No evidence for a deglacial intermediate water δ14C anomaly in the SW Atlantic: Earth and Planetary Science Letters, v. 310, p. 65-72.

Spielhagen, R. F., and Erlenkeuser, H., 1994, Stable oxygen and carbon isotopes in planktic foraminifers from Arctic Ocean surface sediments: Reflection of the low salinity surface water layer: Marine Geology, v. 119, p. 227-250.

Spivack, A. J., and Wasserburg, G. J., 1988, Neodymium isotopic composition of the Mediterranean outflow and the eastern North Atlantic: Geochimica et Cosmochimica Acta, v. 52, p. 2767-2773.

Stanford, J. D., Rohling, E. J., Bacon, S., Roberts, A. P., Grousset, F. E., and Bolshaw, M., 2011, A new concept for the paleoceanographic evolution of Heinrich event 1 in the North Atlantic: Quaternary Science Reviews, v. 30, p. 1047-1066.

Staudigel, H., Doyle, P., and Zindler, A., 1985, Sr and Nd isotope systematics in fish teeth: Earth and Planetary Science Letters, v. 76, p. 45-56.

Stern, J. V., and Lisiecki, L. E., 2013, North Atlantic circulation and reservoir age changes over the past 41,000 years: Geophysical Research Letters, p. n/a-n/a.

Stocker, T. F., and Wright, D. G., 1991, Rapid transitions of the ocean's deep circulation induced by changes in surface water fluxes: Nature, v. 351, p. 729-732.

Stommel, H., 1961, Thermohaline Convection with Two Stable Regimes of Flow: Tellus, v. 13, p. 224-230.

Streeter, S. S., and Shackleton, N. J., 1979, Paleocirculation of the Deep North Atlantic: 150,000-Year Record of Benthic Foraminifera and Oxygen-18: Science, v. 203, p. 168-171.

Swift, J. H., 1984, The circulation of the Denmark Strait and Iceland-Scotland overflow waters in the North Atlantic: Deep Sea Research Part A. Oceanographic Research Papers, v. 31, p. 1339-1355.

Tachikawa, K., Athias, V., and Jeandel, C., 2003, Neodymium budget in the modern ocean and paleo-oceanographic implications: J. Geophys. Res., v. 108, p. 3254.

Tachikawa, K., Jeandel, C., and Roy-Barman, M., 1999, A new approach to the Nd residence time in the ocean: the role of atmospheric inputs: Earth and Planetary Science Letters, v. 170, p. 433-446.

Tachikawa, K., Roy-Barman, M., Michard, A., Thouron, D., Yeghicheyan, D., and Jeandel, C., 2004, Neodymium isotopes in the Mediterranean Sea: comparison between seawater and sediment signals: Geochimica et Cosmochimica Acta, v. 68, p. 3095-3106.

Talley, L. D., and McCartney, M. S., 1982, Distribution and Circulation of Labrador Sea Water: Journal of Physical Oceanography, v. 12, p. 1189-1205.

Teller, J. T., 1990, Volume and routing of late-glacial runoff from the southern Laurentide Ice Sheet: Quaternary Research, v. 34, p. 12-23.

Thornalley, D. J. R., Barker, S., Broecker, W. S., Elderfield, H., and McCave, I. N., 2011a, The Deglacial Evolution of North Atlantic Deep Convection: Science, v. 331, p. 202-205.

Thornalley, D. J. R., Elderfield, H., and McCave, I. N., 2010, Intermediate and deep water paleoceanography of the northern North Atlantic over the past 21,000 years: Paleoceanography, v. 25, p. PA1211.

—, 2011b, Reconstructing North Atlantic deglacial surface hydrography and its link to the Atlantic overturning circulation: Global and Planetary Change, v. 79, p. 163-175.

Toucanne, S., Zaragosi, S., Bourillet, J.-F., Marieu, V., Cremer, M., Kageyama, M., Van Vliet-Lanoë, B., Eynaud, F., Turon, J.-L., and Gibbard, P. L., 2010, The first estimation of Fleuve Manche palaeoriver discharge during the last deglaciation: Evidence for Fennoscandian ice sheet meltwater flow in the English Channel ca 20–18 ka ago: Earth and Planetary Science Letters, v. 290, p. 459-473.

Toucanne, S., Zaragosi, S., Bourillet, J. F., Cremer, M., Eynaud, F., Van Vliet-Lanoë, B., Penaud, A., Fontanier, C., Turon, J. L., Cortijo, E., and Gibbard, P. L., 2009, Timing of massive 'Fleuve Manche' discharges over the last 350 kyr: insights into the European ice-sheet oscillations and the European drainage network from MIS 10 to 2: Quaternary Science Reviews, v. 28, p. 1238-1256.

Urey, H. C., 1947, The thermodynamic properties of isotopic substances: Journal of the Chemical Society (Resumed), p. 562-581.

van de Flierdt, T., and Frank, M., 2010, Neodymium isotopes in paleoceanography: Quaternary Science Reviews, v. 29, p. 2439-2441.

van Kreveld, S., Sarnthein, M., Erlenkeuser, H., Grootes, P., Jung, S., Nadeau, M. J., Pflaumann, U., and Voelker, A., 2000, Potential Links Between Surging Ice Sheets, Circulation Changes, and the Dansgaard-Oeschger Cycles in the Irminger Sea, 60-18 Kyr: Paleoceanography, v. 15, p. 425-442.

Venz, K. A., Hodell, D. A., Stanton, C., and Warnke, D. A., 1999, A 1.0 Myr Record of Glacial North Atlantic Intermediate Water Variability from ODP Site 982 in the Northeast Atlantic: Paleoceanography, v. 14, p. 42-52.

Veum, T., Jansen, E., Arnold, M., Beyer, I., and Duplessy, J.-C., 1992, Water mass exchange between the North Atlantic and the Norwegian Sea during the past 28,000 years: Nature, v. 356, p. 783-785.

Vidal, L., Labeyrie, L., Cortijo, E., Arnold, M., Duplessy, J. C., Michel, E., Becqué, S., and van Weering, T. C. E., 1997, Evidence for changes in the North Atlantic Deep Water linked to meltwater surges during the Heinrich events: Earth and Planetary Science Letters, v. 146, p. 13-27.

Vidal, L., Labeyrie, L., and van Weering, T. C. E., 1998, Benthic δ18O Records in the North Atlantic Over the Last Glacial Period (60-10 kyr): Evidence for Brine Formation: Paleoceanography, v. 13, p. 245-251.

Voelker, A. H. L., 2002, Global distribution of centennial-scale records for Marine Isotope Stage (MIS) 3: a database: Quaternary Science Reviews, v. 21, p. 1185-1212.

Voelker, A. H. L., Lebreiro, S. M., Schönfeld, J., Cacho, I., Erlenkeuser, H., and Abrantes, F., 2006, Mediterranean outflow strengthening during northern hemisphere coolings: A salt source for the glacial Atlantic?: Earth and Planetary Science Letters, v. 245, p. 39-55.

Waelbroeck, C., Labeyrie, L., Michel, E., Duplessy, J. C., McManus, J. F., Lambeck, K., Balbon, E., and Labracherie, M., 2002, Sea-level and deep water temperature changes derived from benthic foraminifera isotopic records: Quaternary Science Reviews, v. 21, p. 295-305.

Weber, M. E., Mayer, L. A., Hillaire-Marcel, C., Bilodeau, G., Rack, F., Hiscott, R. N., and Aksu, A. E., 2001, Derivation of δ18O from Sediment Core Log Data: Implications for Millennial-Scale Climate Change in the Labrador Sea: Paleoceanography, v. 16, p. 503-514.

Wefer, G., and Berger, W. H., 1991, Isotope paleontology: growth and composition of extant calcareous species: Marine Geology, v. 100, p. 207-248.

Weinelt, M., Vogelsang, E., Kucera, M., Pflaumann, U., Sarnthein, M., Voelker, A., Erlenkeuser, H., and Malmgren, B. A., 2003, Variability of North Atlantic heat transfer during MIS 2: Paleoceanography, v. 18, p. 1071.

Weiss, R. F., Östlund, H. G., and Craig, H., 1979, Geochemical studies of the Weddell sea: Deep Sea Research Part A. Oceanographic Research Papers, v. 26, p. 1093-1120.

Weppernig, R., Schlosser, P., Khatiwala, S., and Fairbanks, R. G., 1996, Isotope data from Ice Station Weddell: Implications for deep water formation in the Weddell Sea: Journal of Geophysical Research: Oceans, v. 101, p. 25723-25739.

Willamowski, C., and Zahn, R., 2000, Upper ocean circulation in the glacial North Atlantic from benthic foraminiferal isotope and trace element fingerprinting: Paleoceanography, v. 15, p. 515-527.

Wilson, D. J., Piotrowski, A. M., Galy, A., and Clegg, J. A., 2013, Reactivity of neodymium carriers in deep sea sediments: implications for boundary exchange and paleoceanography: Geochimica et Cosmochimica Acta, v. 109, p. 197-221.

Wilson, D. J., Piotrowski, A. M., Galy, A., and McCave, I. N., 2012, A boundary exchange influence on deglacial neodymium isotope records from the deep western Indian Ocean: Earth and Planetary Science Letters, v. 341–344, p. 35-47.

Xie, R. C., Marcantonio, F., and Schmidt, M. W., 2012, Deglacial variability of Antarctic Intermediate Water penetration into the North Atlantic from authigenic neodymium isotope ratios: Paleoceanography, v. 27, p. PA3221.

Yu, E.-F., Francois, R., and Bacon, M. P., 1996, Similar rates of modern and last-glacial ocean thermohaline circulation inferred from radiochemical data: Nature, v. 379, p. 689-694.

Yu, J., and Elderfield, H., 2007, Benthic foraminiferal B/Ca ratios reflect deep water carbonate saturation state: Earth and Planetary Science Letters, v. 258, p. 73-86.

Yu, J., Elderfield, H., and Piotrowski, A. M., 2008, Seawater carbonate ion-δ13C systematics and application to glacial-interglacial North Atlantic ocean circulation: Earth and Planetary Science Letters, v. 271, p. 209-220.

Yu, J., Foster, G. L., Elderfield, H., Broecker, W. S., and Clark, E., 2010, An evaluation of benthic foraminiferal B/Ca and $\delta^{11}B$ for deep ocean carbonate ion and pH reconstructions: Earth and Planetary Science Letters, v. 293, p. 114-120.

Zahn, R., Schönfeld, J., Kudrass, H.-R., Park, M.-H., Erlenkeuser, H., and Grootes, P., 1997, Thermohaline Instability in the North Atlantic During Meltwater Events: Stable Isotope and Ice-Rafted Detritus Records from Core SO75-26KL, Portuguese Margin: Paleoceanography, v. 12, p. 696-710.

Zahn, R., Winn, K., and Sarnthein, M., 1986, Benthic foraminiferal δ13C and accumulation rates of organic carbon: Uvigerina Peregrina group and Cibicidoides Wuellerstorfi: Paleoceanography, v. 1, p. 27-42.

Zaragosi, S., Bourillet, J.-F., Eynaud, F., Toucanne, S., Denhard, B., Van Toer, A., and Lanfumey, V., 2006, The impact of the last European deglaciation on the deep-sea turbidite systems of the Celtic-Armorican margin (Bay of Biscay): Geo-Marine Letters, v. 26, p. 317-329.

Zaragosi, S., Eynaud, F., Pujol, C., Auffret, G. A., Turon, J. L., and Garlan, T., 2001, Initiation of the European deglaciation as recorded in the northwestern Bay of Biscay slope environments (Meriadzek Terrace and Trevelyan Escarpment): a multi-proxy approach: Earth and Planetary Science Letters, v. 188, p. 493-507.

Chapter 5

Conclusions

5.1 Summary of thesis

ODP Site 980 and its partner site ODP Site 981 provide an extremely valuable archive of North Atlantic climate variability stretching back into the Pliocene. In this study, the millennial scale variability of the last glacial interval in both the surface and deep ocean has been resolved for the first time at Site 980.

Chapter 2 focusses on reconstruction of the expression of the millennial scale variability in the cryosphere and surface ocean. The position of the Heinrich IRD layers during the last glacial interval are unambiguously identified for the first time at Site 980, and used in conjunction with the percentages of *N. pachyderma* (s.) polar planktonic foraminifera and recalibrated previously published radiocarbon dates [Oppo et al. 2003; Benway et al. 2010] to produce a new age model for the site. Comparison of temporal changes in the lithologies of ice-rafted debris with other nearby sites demonstrates how spatially variable the patterns of iceberg transport are even over relatively small distances, with surface ocean currents and properties likely influencing the flux of IRD to the sediment. This observation therefore cautions against the use of the temporal variation in IRD lithologies at any single site to deduce phasing in ice sheet behaviour. Differences in the sequence of ice-rafted debris lithologies recorded between Heinrich events are not indicative of a simple, repeating sequence of changes in the cryosphere and/or surface ocean for each of the Heinrich events studied.

Chapter 3 assesses the suitability of neodymium isotopes as a proxy for bottom water chemistry by combining multi-substrate isotopic reconstructions with rare earth element profiles. New data from planktonic foraminifera (uncleaned of their ferromanganese coatings) and fish debris shows that both of these substrates record a shallow pore water rare earth element signature that does not undergo significant diagenetic modification as

sediments become more deeply buried. Previously published sediment leachate values [Crocket et al. 2011] are strongly offset from both fish debris and foraminferal ε_{Nd} values throughout the Holocene, however, all substrates generally show good agreement during glacial conditions. Increased deposition of airborne volcanic ash cannot explain the abnormally radiogenic sediment leachate values in the Holocene. Instead, the influence of strengthened bottom current driven transport of fine, radiogenic material (potentially from the Greenland-Scotland Ridge) on the sediment leachates is suggested as the cause of this offset between substrates. Thus, planktonic foraminifera and fish debris appear to be more reliable recorders of bottom water neodymium isotopic compositions than bulk sediment leachates at drift sites.

Chapter 4 reconstructs the changes in the mid-depth North Atlantic Ocean water masses by presenting co-registered records of neodymium, carbon and oxygen isotope ratios. Different geochemical signatures are seen in the bottom waters bathing the site at each of the Heinrich events. A possible influence of southern sourced waters on Site 980 is recorded at H1 and H2, but not seen at H3 or H4. This finding argues against a complete shutdown of the overturning circulation as a response to freshwater inputs at Heinrich events, resulting in an increased northwards extension and shoaling of southern sourced waters. Evidence of changes in bottom water circulation are seen to predate IRD deposition for during H1, H2 and H4. This result is consistent with the suggestion that the thermohaline circulation plays a role in ice sheet destabilisation, however the nature of precursory changes strongly varies between events, arguing against any simple, repeating trigger mechanism. The recovery of bottom water properties is delayed until after surface waters warm, implying that changes in the deep ocean are not responsible for driving the rapid warming out of stadial conditions.

One of the strongest conclusions to be drawn based upon the work presented in this thesis is to highlight the individuality of each of the Heinrich events. Differences are seen in the origin of icebergs reaching ODP Site 980, the sequence of precursory changes in the surface and intermediate/deep ocean prior to the destabilisation of the Laurentide Ice Sheet and the disruption to the thermohaline circulation in the northeast

Atlantic. Any suggestion of a complete shutdown of the overturning circulation as a result of fresh water input to the North Atlantic at Heinrich events appears too simplistic. The range of response observed in bottom water chemistry to differences in the initial state of the ocean and/or the nature of the freshwater forcing illustrates just how sensitive the Atlantic meridional overturning circulation is to perturbation, hence making Heinrich events a vital target for future research.

5.2 Suggestions for future research

Synchroneity of late glacial warming

Chapter 2 raised concerns about the synchroneity of warming of the atmosphere and surface ocean across the North Atlantic after Heinrich event 1, and hence whether this warming can be used as a tie-point in the construction of sediment core chronologies in this region. Unfortunately, the relative timing of warming between sites is not easy to test, particularly in the absence of major tephra layers around H1 to provide independent tie-points aiding correlation between records. One possible approach is to make paired measurements of the radiocarbon age of terrestrial organic matter and marine carbonates from the same shallow marine core. This technique has been used to study the Holocene and Younger Dryas, but no records currently exist extending further back in time [e.g. Bard et al. 1994; Austin et al. 1995; Bondevik et al. 1999; Reimer et al. 2002; Bondevik et al. 2006].

Fidelity of REE profiles as a palaeoredox indicator

In chapter 3, it was concluded that a distinct shift in the rare earth element profiles of planktonic foraminifera and fish debris, occurring at approximately three metres depth in the sediment (coincident with the last deglaciation) is more likely to be a result of glacial-interglacial differences in the degree of oxygenation of bottom waters than a modern redox horizon in the sediment. Reconstructions of REE profiles though previous terminations could provide a test of this hypothesis. This is an important issue because diagenetic remobilisation within the sediment column has the potential to strongly affect the fidelity of down core neodymium isotope reconstructions. If the changes in REE

distributions observed through the last deglaciation are a result of temporal variation in bottom water properties, a similar pattern of change might be expected at previous glacial terminations. However, if the shift in REE patterns is the result of an active redox front in the sediment, no changes would be expected through earlier deglaciations.

Dansgaard-Oeschger variability in water mass provenance

A suggestion of stadial-interstadial variability in the neodymium isotopic composition of mid-depth waters of the North Atlantic was presented in chapter 4. This is a potentially important result if confirmed with a higher resolution study. Neodymium isotopic signatures are not directly influenced by productivity and meltwater addition/sea ice formation in the surface ocean, unlike previously documented carbon and oxygen isotope evidence for stadial-interstadial variability in the northeast Atlantic. Therefore, neodymium isotopes could be used to provide an independent test as to whether changes in the pattern of intermediate/deep circulation in the North Atlantic occured during Dansgaard-Oeschger events.

Reconstruction of sea ice extent

Changes in sea ice extent have been hypothesised to play a major role in both deep water formation [Vidal et al. 1998; Dokken and Jansen 1999] and driving of Dansgaard-Oeschger atmospheric and sea surface temperature variability [Gildor and Tziperman 2003; Li et al. 2005; Li et al. 2010; Petersen et al. 2013]. Knowledge of sea ice extent also provides an important constraint for climate models, influencing both the albedo and the extent of evaporation and air-sea exchange [e.g. Gildor and Tziperman 2003; Sarnthein et al. 2003]. A number of proxies have shown promise in reconstructing sea ice extent including organic biomarkers [e.g. Belt et al. 2007; Belt and Müller 2013], foraminiferal stable isotopes [e.g. Hillaire-Marcel and de Vernal 2008] and faunal assemblages of dinocysts [e.g. de Vernal et al. 1997; de Vernal et al. 2013], foraminifera [e.g. de Vernal et al. 1997; Sarnthein et al. 2003; Scott et al. 2009; Seidenkrantz 2013], diatoms [e.g. Crosta et al. 1998; Gersonde et al. 2005] and ostracodes [Cronin et al. 2010]. However, variability in the sea ice extent in the North Atlantic through the last glacial interval is currently very poorly constrained. Published records of glacial sea ice

extent are dominated by snapshot reconstructions of the North Atlantic at the last glacial maximum [e.g. Sarnthein et al. 2003; de Vernal et al. 2005] with time series only covering the Arctic [e.g. Spielhagen et al. 2004; Müller et al. 2009; Cronin et al. 2010; Müller et al. 2011] and northwest Atlantic [e.g. de Vernal and Hillaire-Marcel 2000; Hillaire-Marcel and de Vernal 2008]. Site 980 provides an excellent target for sea ice reconstructions because it is located close to the reconstructed position of the polar front at the last glacial maximum [Sarnthein et al. 2003; de Vernal et al. 2005] and hence would be sensitive to fluctuations in the sea ice extent. It is also in close proximity to a number of potential deep water formation regions with shallower water depths (e.g. Rockall Plateau, British/Irish margin, Greenland-Scotland Ridge) and hence can assess the likelihood of deep water formation via brine rejection occurring south of the Nordic Seas. Sites in the southern Nordic Seas and in suggested brine formation regions (e.g. the North Sea) would also make good targets for sea ice reconstructions.

Strength of Labrador Sea outflow

One of the major contributors to the formation of modern North Atlantic Deep Water is outflow from the Labrador Sea, however, the strength of Labrador Sea outflow through the last glacial interval is not yet well constrained. A depth transect of cores located in the path of these outflows (for example, at Orphan Knoll or the Newfoundland margin) could help to better constrain the history of this important aspect of North Atlantic palaeoceanography. Evidence of decreased circulation vigour at Heinrich events in the southeast Labrador Sea has been presented based upon benthic carbon isotopes and foraminiferal assemblages [Rasmussen et al. 2003]. Neodymium isotopic studies could greatly enrich previous work, because the highly unradiogenic signature of the Labrador Sea makes the strength of LSW export easy to determine. Another advantage of studying the southeast Labrador Sea is that it is located on the major pathway of southward export of North Atlantic waters. Therefore, results from this region can be used to constrain the geochemical signature of NADW exported from the North Atlantic, and hence are vital in determining the extent of a North Atlantic influence at more far-field sites.

5.3 References

Austin, W. N., Hunt, J. B., Kroon, D., and Peacock, J. D., 1995, The 14C age of the Icelandic Vedde Ash: implications for Younger Dryas marine reservoir age corrections: Radiocarbon, v. 37, p. 53-62.

Bard, E., Arnold, M., Mangerud, J., Paterne, M., Labeyrie, L., Duprat, J., Mélières, M.-A., Sønstegaard, E., and Duplessy, J.-C., 1994, The North Atlantic atmosphere-sea surface 14C gradient during the Younger Dryas climatic event: Earth and Planetary Science Letters, v. 126, p. 275-287.

Belt, S. T., Massé, G., Rowland, S. J., Poulin, M., Michel, C., and LeBlanc, B., 2007, A novel chemical fossil of palaeo sea ice: IP25: Organic Geochemistry, v. 38, p. 16-27.

Belt, S. T., and Müller, J., 2013, The Arctic sea ice biomarker IP25: a review of current understanding, recommendations for future research and applications in palaeo sea ice reconstructions: Quaternary Science Reviews.

Benway, H. M., McManus, J. F., Oppo, D. W., and Cullen, J. L., 2010, Hydrographic changes in the eastern subpolar North Atlantic during the last deglaciation: Quaternary Science Reviews, v. 29, p. 3336-3345.

Bondevik, S., Birks, H. H., Gulliksen, S., and Mangerud, J., 1999, Late Weichselian Marine 14C Reservoir Ages at the Western Coast of Norway: Quaternary Research, v. 52, p. 104-114.

Bondevik, S., Mangerud, J., Birks, H. H., Gulliksen, S., and Reimer, P., 2006, Changes in North Atlantic Radiocarbon Reservoir Ages During the Allerod and Younger Dryas: Science, v. 312, p. 1514-1517.

Crocket, K. C., Vance, D., Gutjahr, M., Foster, G. L., and Richards, D. A., 2011, Persistent Nordic deep-water overflow to the glacial North Atlantic: Geology, v. 39, p. 515-518.

Cronin, T. M., Gemery, L., Briggs Jr, W. M., Jakobsson, M., Polyak, L., and Brouwers, E. M., 2010, Quaternary Sea-ice history in the Arctic Ocean based on a new Ostracode sea-ice proxy: Quaternary Science Reviews, v. 29, p. 3415-3429.

Crosta, X., Pichon, J. J., and Burckle, L. H., 1998, Application of modern analog technique to marine Antarctic diatoms: Reconstruction of maximum sea-ice extent at the Last Glacial Maximum: Paleoceanography, v. 13, p. 284-297.

de Vernal, A., Eynaud, F., Henry, M., Hillaire-Marcel, C., Londeix, L., Mangin, S., Matthiessen, J., Marret, F., Radi, T., Rochon, A., Solignac, S., and Turon, J. L., 2005, Reconstruction of sea-surface conditions at middle to high latitudes of the Northern Hemisphere during the Last Glacial Maximum (LGM) based on dinoflagellate cyst assemblages: Quaternary Science Reviews, v. 24, p. 897-924.

de Vernal, A., and Hillaire-Marcel, C., 2000, Sea-ice cover, sea-surface salinity and halo-/thermocline structure of the northwest North Atlantic: modern versus full glacial conditions: Quaternary Science Reviews, v. 19, p. 65-85.

de Vernal, A., Rochon, A., Fréchette, B., Henry, M., Radi, T., and Solignac, S., 2013, Reconstructing past sea ice cover of the Northern Hemisphere from dinocyst assemblages: status of the approach: Quaternary Science Reviews.

de Vernal, A., Rochon, A., Turon, J.-L., and Matthiessen, J., 1997, Organic-walled dinoflagellate cysts: Palynological tracers of sea-surface conditions in middle to high latitude marine environments: Geobios, v. 30, p. 905-920.

Dickson, A. J., Austin, W. E. N., Hall, I. R., Maslin, M. A., and Kucera, M., 2008, Centennial-scale evolution of Dansgaard-Oeschger events in the northeast Atlantic Ocean between 39.5 and 56.5 ka B.P: Paleoceanography, v. 23, p. PA3206.

Dokken, T. M., and Jansen, E., 1999, Rapid changes in the mechanism of ocean convection during the last glacial period: Nature, v. 401, p. 458-461.

Gersonde, R., Crosta, X., Abelmann, A., and Armand, L., 2005, Sea-surface temperature and sea ice distribution of the Southern Ocean at the EPILOG Last Glacial Maximum—a circum-Antarctic view based on siliceous microfossil records: Quaternary Science Reviews, v. 24, p. 869-896.

Gildor, H., and Tziperman, E., 2003, Sea-ice switches and abrupt climate change: Philosophical Transactions of the Royal Society of London. Series A: Mathematical, Physical and Engineering Sciences, v. 361, p. 1935-1944.

Hillaire-Marcel, C., and de Vernal, A., 2008, Stable isotope clue to episodic sea ice formation in the glacial North Atlantic: Earth and Planetary Science Letters, v. 268, p. 143-150.

Keigwin, L. D., and Boyle, E. A., 1999, Surface and deep ocean variability in the northern Sargasso Sea during marine isotope stage 3: Paleoceanography, v. 14, p. 164-170.

Kissel, C., Laj, C., Labeyrie, L., Dokken, T., Voelker, A., and Blamart, D., 1999, Rapid climatic variations during marine isotopic stage 3: magnetic analysis of sediments from Nordic Seas and North Atlantic: Earth and Planetary Science Letters, v. 171, p. 489-502.

Li, C., Battisti, D. S., and Bitz, C. M., 2010, Can North Atlantic Sea Ice Anomalies Account for Dansgaard–Oeschger Climate Signals?: Journal of Climate, v. 23, p. 5457-5475.

Li, C., Battisti, D. S., Schrag, D. P., and Tziperman, E., 2005, Abrupt climate shifts in Greenland due to displacements of the sea ice edge: Geophysical Research Letters, v. 32, p. L19702.

Müller, J., Masse, G., Stein, R., and Belt, S. T., 2009, Variability of sea-ice conditions in the Fram Strait over the past 30,000 years: Nature Geosci, v. 2, p. 772-776.

Müller, J., Wagner, A., Fahl, K., Stein, R., Prange, M., and Lohmann, G., 2011, Towards quantitative sea ice reconstructions in the northern North Atlantic: A combined biomarker and numerical modelling approach: Earth and Planetary Science Letters, v. 306, p. 137-148.

Oppo, D. W., McManus, J. F., and Cullen, J. L., 2003, Palaeo-oceanography: Deepwater variability in the Holocene epoch: Nature, v. 422, p. 277-277.

Petersen, S. V., Schrag, D. P., and Clark, P. U., 2013, A new mechanism for Dansgaard-Oeschger cycles: Paleoceanography, v. 28, p. 24-30.

Rasmussen, T. L., Oppo, D. W., Thomsen, E., and Lehman, S. J., 2003, Deep sea records from the southeast Labrador Sea: Ocean circulation changes and ice-rafting events during the last 160,000 years: Paleoceanography, v. 18, p. 1018.

Rasmussen, T. L., Thomsen, E., Labeyrie, L., and van Weering, T. C. E., 1996, Circulation changes in the Faeroe-Shetland Channel correlating with cold events during the last glacial period (58-10 ka): Geology, v. 24, p. 937-940.

Reimer, P. J., McCormac, F. G., Moore, J., McCormick, F., and Murray, E. V., 2002, Marine radiocarbon reservoir corrections for the midto late Holocene in the eastern subpolar North Atlantic: The Holocene, v. 12, p. 129-135.

Sarnthein, M., Pflaumann, U., and Weinelt, M., 2003, Past extent of sea ice in the northern North Atlantic inferred from foraminiferal paleotemperature estimates: Paleoceanography, v. 18, p. 1047.

Scott, D. B., Schell, T., St-Onge, G., Rochon, A., and Blasco, S., 2009, Foraminiferal assemblage changes over the last 15,000 years on the Mackenzie-Beaufort Sea Slope and Amundsen Gulf, Canada: Implications for past sea ice conditions: Paleoceanography, v. 24, p. PA2219.

Seidenkrantz, M.-S., 2013, Benthic foraminifera as palaeo sea-ice indicators in the subarctic realm — examples from the Labrador Sea—Baffin Bay region: Quaternary Science Reviews.

Spielhagen, R. F., Baumann, K.-H., Erlenkeuser, H., Nowaczyk, N. R., Nørgaard-Pedersen, N., Vogt, C., and Weiel, D., 2004, Arctic Ocean deep-sea record of northern Eurasian ice sheet history: Quaternary Science Reviews, v. 23, p. 1455-1483.

van Kreveld, S., Sarnthein, M., Erlenkeuser, H., Grootes, P., Jung, S., Nadeau, M. J., Pflaumann, U., and Voelker, A., 2000, Potential Links Between Surging Ice Sheets, Circulation Changes, and the Dansgaard-Oeschger Cycles in the Irminger Sea, 60-18 Kyr: Paleoceanography, v. 15, p. 425-442.

Vidal, L., Labeyrie, L., and van Weering, T. C. E., 1998, Benthic δ18O Records in the North Atlantic Over the Last Glacial Period (60-10 kyr): Evidence for Brine Formation: Paleoceanography, v. 13, p. 245-251.

Appendix 1

Splice correlation

In order to be able to place samples from the different holes at Site 980 onto a single age scale, the depth scale for each hole was converted from metres below seafloor (mbsf) to metres composite depth (mcd). This combines all samples onto a single continuous spliced record, constructed from different parts of the record of each of the three holes [Shipboard Scientific Party 1996a]. The top 3.92 metres of our studied interval from Hole 980B form the uppermost part of the spliced record, hence the mbsf and mcd values are identical. For the rest of the record, the individual records were tuned to the splice by their magnetic susceptibility records (illustrated in figure A1.1), as these show excellent agreement between the holes [Shipboard Scientific Party 1996a]. This tuning was carried out using the Analyseries software of Paillard et al. [1996]. Tie-points are listed in table A1.1.

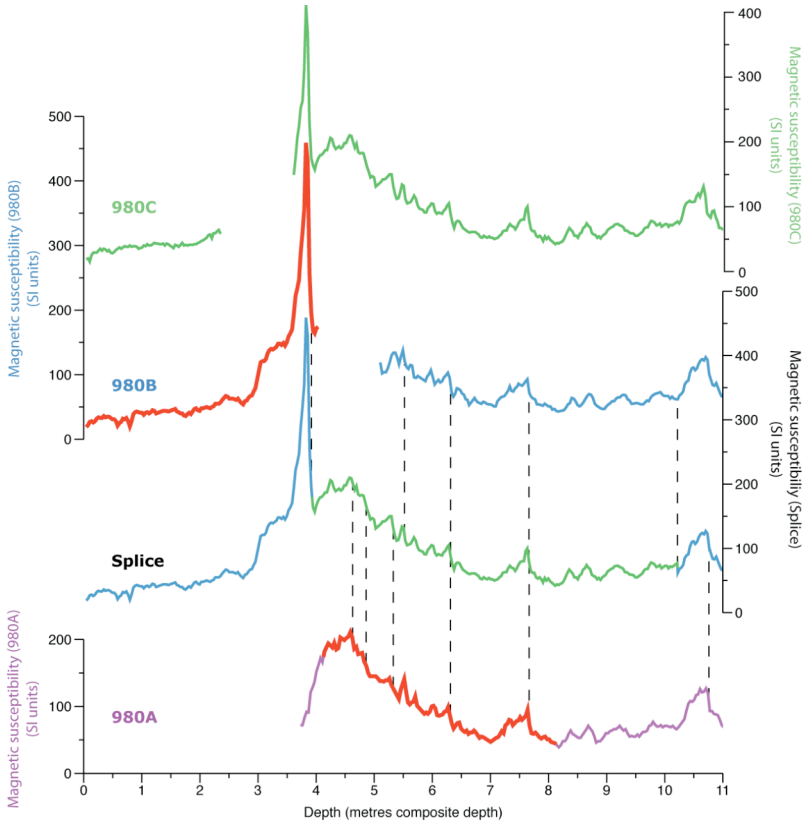

Figure A1.1: Correlation of individual core magnetic susceptibilities with the spliced record. All data is plotted on the metres composite depth scale, with dashed lines marking the tie-points used to correlate the records. Core sections used in this study are highlighted in red. The remaining record is coloured as follows: purple - hole A, blue - hole B, green - hole C. Data from Jansen et al. [Shipboard Scientific Party 1996b].

Depth 980A (mbsf)	Depth 980 splice (mcd)	Age (years before 2000)
0.83	4.63	18863
1.03	4.86	20047
1.45	5.33	22435
2.40	6.31	27979
3.67	7.67	38459
6.42	10.76	59601

Table A1.1: New tie-points for the correlation of Hole 980A magnetic susceptibility with the published Site 980 splice [Shipboard Scientific Party 1996c], with ages on the new age model (presented in section 2.5).

References

Paillard, D., Labeyrie, L., and Yiou, P., 1996, Macintosh program performs time-series analysis: Eos. Trans. AGU, v. 77.

Shipboard Scientific Party, 1996a, Explanatory Notes, *in* Jansen, E., Raymo, M. E., and Blum P. et al., eds., Proceedings of the Ocean Drilling Program, Initial Reports, College station, TX, p. 21-45.

—, 1996b, Proceedings of the Ocean Drilling Program, Initial Reports, Volume 162, College station, TX.

—, 1996c, Sites 980/981, *in* Jansen, E., Raymo, M. E., and Blum P. et al., eds., Proceedings of the Ocean Drilling Program, Initial Reports, College station, TX, p. 49-90.

Appendix 2

Calculation of dry bulk density

In order to calculate changes in the flux of various sediment components, an estimate of sediment density is needed. Unfortunately, a misalignment of the source-sensor apparatus used to measure the gamma-ray attenuation porosity evaluator (GRAPE) wet bulk density during Leg 162 led to a systematic error of approximately 10% in the measurements. Therefore, alternative techniques are needed to estimate the sediment bulk density at ODP Site 980.

An attempt to correct for this offset in the GRAPE density was made by cross-plotting the GRAPE density estimates from Hole 980A with estimates of the wet bulk density of discrete samples from the same depth within the core [Jansen et al. 1996]. Although a strong positive correlation is visible, there is significant scatter in the data. Even with some of the more anomalous data points excluded, the R^2 value for the correlation is only 0.55 (see figure A2.1).

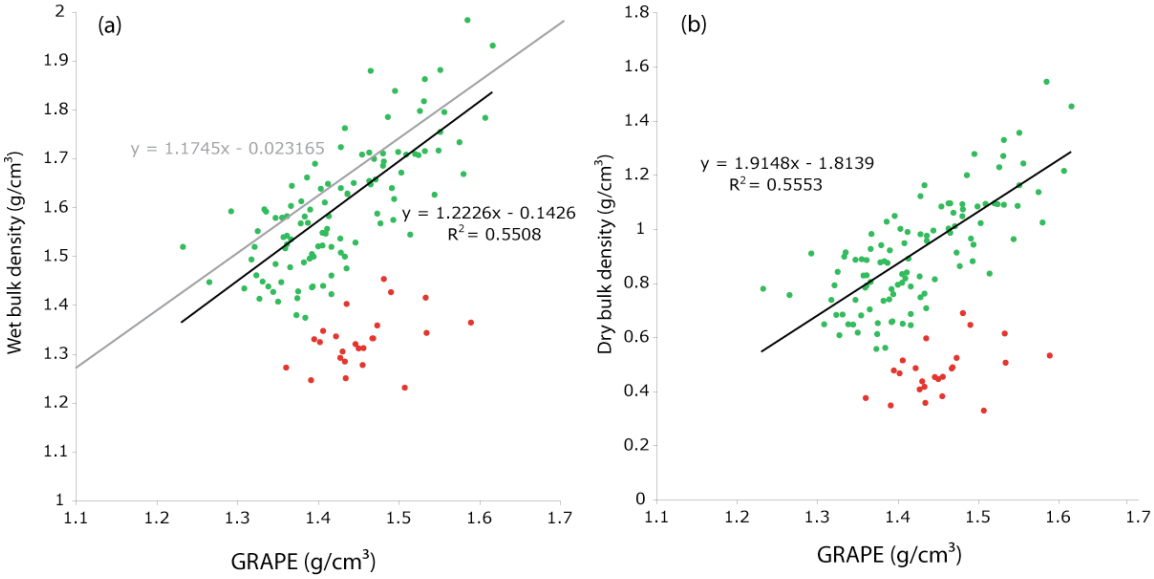

Figure A2.1: Cross-plot of GRAPE density against (a) wet and (b) dry bulk density for equivalent depths in Hole 980A. The best-fit line (calculated by linear regression) is shown in black with green points included and red points excluded from the calculation. The equation and

R^2 value of this best fit line are shown on each plot. The grey line and associated equation on plot (a) show the estimated correction for the Leg 162 GRAPE values of Jansen et al. [2000], based upon the relationship between the GRAPE density values at ODP Site 907 which was originally drilled on Leg 151 (when the MST logger was correctly calibrated) and then re-occupied on Leg 162.

An alternative method of estimating the sample density is from the wet and dry bulk masses of each sample (based upon the same principles as the moisture and density (MAD) estimates outlined in the explanatory notes of Leg 162 Initial Reports [Shipboard Scientific Party 1996]).The mass of pure water in each sample (M_w) was calculated from the difference between the bulk wet sample mass (M_b) and the dried sample mass (M_d):

$$M_w = M_b - M_d$$

The mass of salt remaining from the evaporated pore water (M_{salt}) can then be calculated, assuming a salinity s = 0.035:

$$M_{salt} = \frac{s}{(1-s)} M_w$$

The total pore water mass (M_{pw}) and volume (V_{pw}) are given by the following equations, with a estimated pore water density ρ_{sw} = 1.024 g/cm^3:

$$M_{pw} = M_w + M_{salt}$$

$$M_{pw} = \frac{M_w}{(1-s)}$$

$$V_{pw} = \frac{M_{pw}}{\rho_{sw}}$$

The mass (M_s) and volume (V_s) of the solid component can then be calculated, assuming a salt density (ρ_{salt}) of 2.257 g/cm^3 and a solid grain density (ρ_s) of 2.65 g/cm^3:

$$M_s = M_d - M_{salt}$$

$$V_s = \frac{M_s}{\rho_s}$$

The bulk wet volume of the sample (V_b) is given by:

$$V_b = V_s + V_{pw}$$

The dry bulk density (ρ_d) can then be calculated as follows:

$$\rho_d = \frac{M_s}{V_b}$$

It is important to note that these estimates are likely to be overestimates, as the sediment will have dried out by an unknown amount in the time since the core was drilled. All samples are expected to be affected to a similar extent, so although the absolute flux estimates are may be overestimates, the observed trends are not affected.

References

Jansen, E., Fronval, T., Rack, F., and Channell, J. E. T., 2000, Pliocene-Pleistocene Ice Rafting History and Cyclicity in the Nordic Seas During the Last 3.5 Myr: Paleoceanography, v. 15, p. 709-721.

Jansen, E., Raymo, M. E., and Blum P. et al., 1996, Proceedings of the Ocean Drilling Program, Initial Reports, Volume 162, College station, TX.

Shipboard Scientific Party, 1996, Explanatory Notes, *in* Jansen, E., Raymo, M. E., and Blum P. et al., eds., Proceedings of the Ocean Drilling Program, Initial Reports, College station, TX, p. 21-45.

Appendix 3

Neodymium separation procedure

Unless otherwise stated, all fluid should be allowed to drain through the column between each stage.

Cation exchange columns

Check column resin height is 2.2 cm

Condition column:

Load 1 ml H_2O_{MQ}

Load 0.5 ml 1.75 M HCl

Load 0.5 ml 1.75 M HCl

Load sample

Wash sample in:

Load 0.1 ml 1.75 M HCl

Load 0.1 ml 1.75 M HCl

Load 0.1 ml 1.75 M HCl

Strip waste:

Load 5.5 ml 1.75 M HCl

Load 2.5 ml 2 M HNO_3

Collect REE (into a Teflon vial):

Load 2 ml 6 M HNO_3

Remove Teflon and dry down on hotplate at 140^{o}C

Clean column:

Fill to brim with 6 M HCl

Fill to brim with H_2O_{MQ}

LnSpec exchange columns

Dissolve sample in 0.3 ml 0.2 M HCl when cooled from hotplate

Condition column:

Load 0.5 ml 0.2 M HCl

Load 1 ml 0.2 M HCl

Load sample

Wash sample in:

Load 0.1 ml 0.2 M HCl

Load 0.1 ml 0.2 M HCl

Load 0.1 ml 0.2 M HCl

Strip waste:

Load 2 ml 0.2 M HCl

Collect Nd (into a Teflon vial):

Load 4 ml 0.2 M HCl

Remove Teflon and dry down on hotplate at 140oC

Strip waste:

Load 1 ml 0.4 M HCl

Collect Sm (into vial for storage)

Load 2 ml 0.4 M HCl

Clean column:

Fill to brim with 6 M HCl

Fill to brim with 6 M HCl

Fill to brim with H_2O_{MQ}

Appendix 4

Estimation of the neodymium isotopic signature of Wyville-Thomson Overflow Water

Wyville-Thomson overflow water (WTOW) forms as intermediate/deep waters from the Nordic Sea Overflow Waters (NSOW) cross the Wyville-Thomson ridge, and entrain Eastern North Atlantic Waters (ENAW) as they descend. Therefore, the resulting WTOW ε_{Nd} signature is determined by the neodymium concentration and isotopic composition of its constituent water masses, and the ratio by which they mix. Here, WTOW formation is assumed to form by mixing between two endmembers: NSOW and ENAW, and hence its neodymium isotopic signature can be estimated by the following equation:

$$\varepsilon_{Nd,WTOW} = \frac{f_{nsow} * [Nd]_{NSOW} * \varepsilon_{Nd,NSOW} + (1 - f_{NSOW}) * [Nd]_{SPMW} * \varepsilon_{Nd,SPMW}}{0.5([Nd]_{NSOW} + [Nd]_{SPMW})}$$

where f_{NSOW} is the fraction of the WTOW formed which consists of NSOW.

	Max	Ref	Min	Ref	Best	Reference/Notes
NSOW %	33.3	(5),(6)	10	(1),(2)	20	(10)
ε_{Nd} ENAW	-11.6	(7)	-13	(4)	-12.3	Midpoint (midway between sites)
ε_{Nd} NSOW	-7.3	(3)	-9.1	(3)	-8.2	pISOW signature (3)
[Nd] ENAW	2.26	(7)	2.4	(4)	2.3	Midpoint
[Nd] NSOW	3.54	(3)	2.87	(3)	2.88	(3)
WTOW ε_{Nd} estimate	**-9.0**		**-11.6**		**-10.6**	

Table A4.1: Calculation of a maximum, minimum and best estimate for WTOW ε_{Nd}. Note that maximum and minimum table headings refer to the calculated ε_{Nd} values, rather than the maximum/minimum value of each component parameter [Nd] measured in pg/g. References (ref): (1) Swift [1984], (2) Holliday et al. [2000], (3) Lacan and Jeandel [2004a], (4) Lacan and Jeandel [2004b], (5)

Sherwin and Turrell [2005], (6) Sherwin et al. [2008], (7) Rickli et al. [2009], (8) Johnson [2012].

References

Holliday, P. N., Pollard, R. T., Read, J. F., and Leach, H., 2000, Water mass properties and fluxes in the Rockall Trough, 1975–1998: Deep Sea Research Part I: Oceanographic Research Papers, v. 47, p. 1303-1332.

Johnson, C., 2012, Wyville Thomson Ridge Overflow Water: a temporally and spatially persistent water mass in the Rockall Trough, POC seminar series, NOC Southampton.

Lacan, F., and Jeandel, C., 2004a, Neodymium isotopic composition and rare earth element concentrations in the deep and intermediate Nordic Seas: Constraints on the Iceland Scotland Overflow Water signature: Geochem. Geophys. Geosyst., v. 5, p. Q11006.

—, 2004b, Subpolar Mode Water formation traced by neodymium isotopic composition: Geophys. Res. Lett., v. 31, p. L14306.

Rickli, J., Frank, M., and Halliday, A. N., 2009, The hafnium–neodymium isotopic composition of Atlantic seawater: Earth and Planetary Science Letters, v. 280, p. 118-127.

Sherwin, T. J., Griffiths, C. R., Inall, M. E., and Turrell, W. R., 2008, Quantifying the overflow across the Wyville Thomson Ridge into the Rockall Trough: Deep Sea Research Part I: Oceanographic Research Papers, v. 55, p. 396-404.

Sherwin, T. J., and Turrell, W. R., 2005, Mixing and advection of a cold water cascade over the Wyville Thomson Ridge: Deep Sea Research Part I: Oceanographic Research Papers, v. 52, p. 1392-1413.

Swift, J. H., 1984, The circulation of the Denmark Strait and Iceland-Scotland overflow waters in the North Atlantic: Deep Sea Research Part A. Oceanographic Research Papers, v. 31, p. 1339-1355.